ABSTRACT

KING, MARK HARLEY. Determination of Dynamic Moduli in Uniaxial Compression for North Carolina Hot Mix Asphalt Concrete. (Under the direction of Dr. Y. Richard Kim).

This thesis presents results from an experimental study on the dynamic modulus testing of hot mix asphalts (HMAs) commonly used in North Carolina in uniaxial compression mode. Forty two mixtures with varying aggregate sources, aggregate gradations, asphalt sources, asphalt grades, and asphalt contents are included in this study. With the dynamic modulus database developed, several issues are investigated in this research. Effects of confining pressure on the dynamic modulus are evaluated by comparing results from uniaxial and triaxial compression tests. A modified dynamic modulus test protocol is developed by reducing the required testing time using more frequencies and fewer temperatures based on the time-temperature superposition principle. Hirsch and Witczak predictive models are evaluated. During this analysis a case study was conducted to determine how much pavement performance changes due to the predictive errors. Finally, effects of different mixture variables on dynamic modulus of asphalt concrete are evaluated.

Determination of Dynamic Moduli in Uniaxial Compression for North Carolina Hot Mix Asphalt Concrete

by

MARK HARLEY KING

A thesis submitted to the Graduate Faculty of
North Carolina State University
in partial fulfillment of the
requirements for the Degree of
Master of Science

CIVIL, CONSTRUCTION, AND ENVIRONMENTAL ENGINEERING

Raleigh
2004

APPROVED BY:

_____ _____

_____

Chair of Advisory Committee

November 1, 2004

DEDICATION

It is with great honor that I dedicate this thesis to my parents for their unfailing love, support, and encouragement.

BIOGRAPHY

Mark King was born in Haywood County, North Carolina where he lived there with his parents for 17 years. While there, he attended and graduated from Pisgah High School in June 1999. That fall he enrolled at North Carolina State University where he graduated in December 2002 with a Bachelor of Science degree in Construction Engineering and Management. During his final year of undergraduate work he worked as an undergraduate research assistant under the supervision of Y. Richard Kim. Following graduation, he continued this work while pursuing a Master of Science degree in civil engineering. This document is the culmination of this research.

ACKNOWLEDGEMENTS

"By the word of the LORD the heavens were made, And by the breath of His mouth all their host. He gathers the waters of the sea together as a heap; He lays up the deeps in storehouses. Let all the earth fear the LORD; Let all the inhabitants of the world stand in awe of Him." -- Psalm 33:6-8

God created the world and imparted knowledge to his creation and by doing so made this work possible. God deserves all the credit. I am thankful to Him for the privilege of seeing a glimpse of his amazing power and grand design through my research.

I would like to thank my advisory committee and all the research group members for their help and guidance throughout my work. Specifically, I would like to thank my advisor, Dr. Y. Richard Kim, for his support, encouragement, advice, and friendship during my educational stay. A special thanks goes to Dr. Ghassan Chehab for his help and friendship. I could not have completed this work without the help of my partner and friend, Mostafa Momen. I would also like to thank my friend, Shane Underwood, who provided technical and experimental assistance unselfishly. Many others contributed to my work in encouraging or practical ways. They include: Dr. Youngguk Seo, Dr. Sugjoon Lee, Sangyum Lee, Jusang Lee, Liza Runey, Omar El-Haggan, Jaeseok Lee, and Dr. Moreshwar Kulkarni.

TABLE OF CONTENTS

LIST OF TABLES

LIST OF FIGURES

1. INTRODUCTION

1.1 Research Needs

The NCHRP 1-37A Mechanistic-Empirical Pavement Design Guide is based on mechanistic-empirical principles in which the prediction of pavement responses and performance requires fundamental properties of layer materials. The most important property, but a relatively new concept to state highway agencies, is the dynamic modulus of asphalt concrete. This property represents the temperature and frequency (therefore time) dependent stiffness characteristics of the material.

While the significance of dynamic modulus of asphalt concrete has been known to some researchers since the 1960s (*1 -15*), the use of the dynamic modulus by state highway agencies has not been widespread. This is also true in North Carolina; indeed, there is little information on dynamic moduli for the asphalt concrete mixes used in North Carolina. This lack of experience in testing and inadequate knowledge of dynamic moduli values of local materials constitute major obstacles for the North Carolina Department of Transportation's (NCDOT's) implementation of the NCHRP 1-37A Design Guide.

Based on the lack of experience and knowledge, the NCDOT funded a research project in which the dynamic moduli of local mixtures were to be measured, the variability of mixtures were evaluated, and the accuracy of available predictive models were determined.

1.2 Research Objective and Significance

Recognizing the importance of dynamic modulus testing in the pavement industry, several issues needed to be evaluated. These issues include sensitivity associated with dynamic modulus testing and predictability of moduli values from mixture and material properties. Also of interest is the effect of these issues on the overall pavement performance. These factors were investigated through an analytical/experimental study presented herein. The results may serve as a guideline for how material characterization is handled in the future. The research presented herein was conducted as part of the NCDOT research project HWY 2003-09 entitled "Typical Dynamic Moduli for North Carolina Asphalt Concrete Mixes."

1.3 Thesis Organization

This report is composed of five chapters. Chapter 1 presents the needs and the objectives to be achieved. Literature review is presented in Chapter 2. Chapter 3 includes the specimen preparation and experimental program. Chapter 4 shows uniaxial dynamic moduli data compared to predictive models, compared to tests in confinement, compared to tests performed at differing temperature histories, and evaluated with different mixture variables. Chapter 5 presents the conclusions of this research.

2. LITERATURE REVIEW

2.1 Dynamic Modulus Determination

Stiffness is an important property for design of any structure. In the case of asphalt concrete this stiffness changes with temperature and frequency. Thus when designing a pavement structure the stiffness (moduli) values must be accurately represented at any and all desired temperature–frequency combinations. Development of a "mastercurve" allows the modulus to be determined at any reasonable temperature-frequency combination.

In axial compression under constant confining pressure the modulus is determined by dividing stress by strain. For viscoelastic materials, such as asphalt concrete, the complex modulus (E*) is often used to represent the stiffness of the material. The complex modulus has an elastic or storage component and a loss component. The storage (elastic) component is related to the material's ability to store energy whereas the loss component is responsible for the damping and energy loss in the system. Just like the overall modulus, the storage modulus (E') and the loss modulus (E") change with temperature and rate of loading. For purely elastic materials, there is no damping loss and thus the elastic component is equal to the overall modulus. Complex modulus is related to loss and storage moduli via Eq. 2.1.

$$E^* = E' + iE'' \tag{2.1}$$

where E' = storage modulus;

E" = loss modulus; and

$i = \sqrt{-1}$.

The magnitude of E*, so-called dynamic modulus, is represented by |E*| and can be obtained from:

$$|E^*| = \sqrt{E'^2 + E''^2} \tag{2.2}$$

The phase angle, ϕ, is defined as:

$$\tan\phi = \frac{E''}{E'} \tag{2.3}$$

These relationships can be shown graphically as in Figure 2.1.

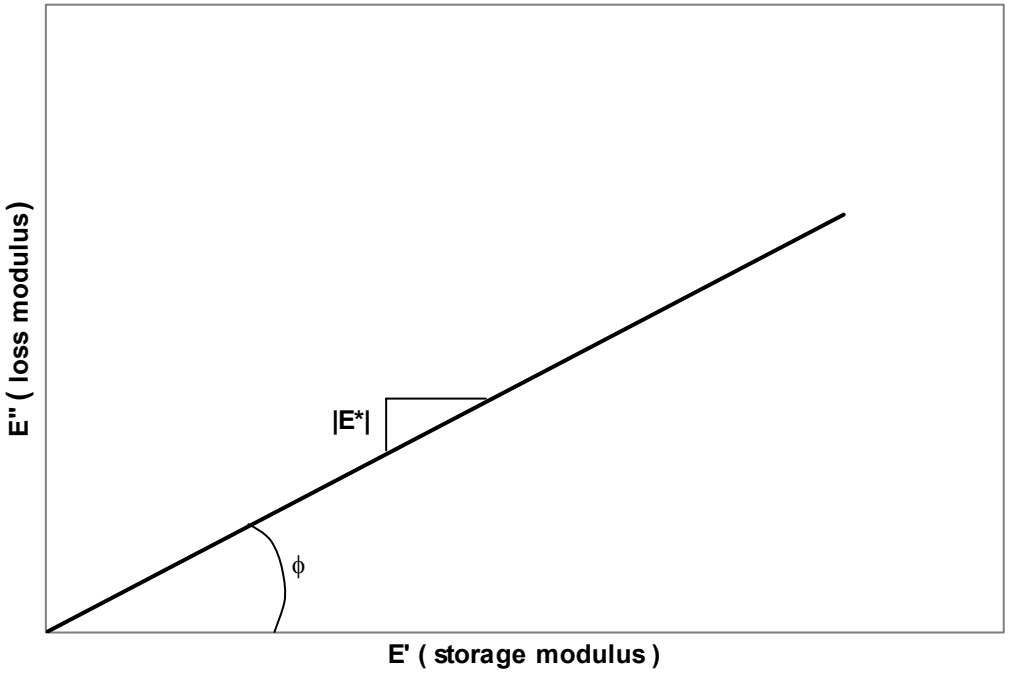

Figure 2.1 Complex modulus relationship

Dynamic modulus and phase angle are determined from uniaxial compression test using a sinusoidal loading history. In uniaxial compression, axial stress (σ) is determined from:

$$\sigma = \frac{P}{A} \tag{2.4}$$

where P = load; and

A = cross-sectional area.

$$\varepsilon = \frac{\Delta}{GL} \tag{2.5}$$

where Δ = change in displacement; and

GL = gauge length.

Figure 2.2 shows typical load and displacement data from uniaxial compression dynamic modulus testing. Figure 2.3 shows the stress and strain data converted from Figure 2.2. The dynamic modulus is determined from:

$$|E^*| = \frac{\sigma_0}{\varepsilon_0} \tag{2.6}$$

where σ_0 = the stress amplitude; and

ε_0 = the strain amplitude.

The phase angle is determined from:

$\phi = 2\pi f \Delta t$

where f = loading frequency in Hz; and

Δt = time delay between the stress and strain cycles.

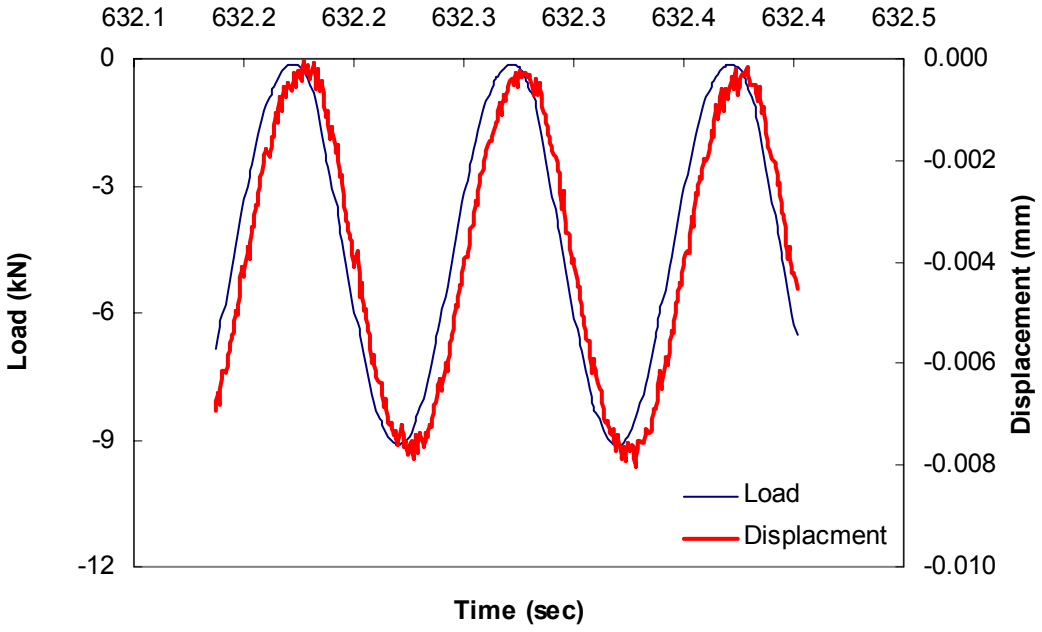

Figure 2.2 Phase lag shown through load and displacement curves

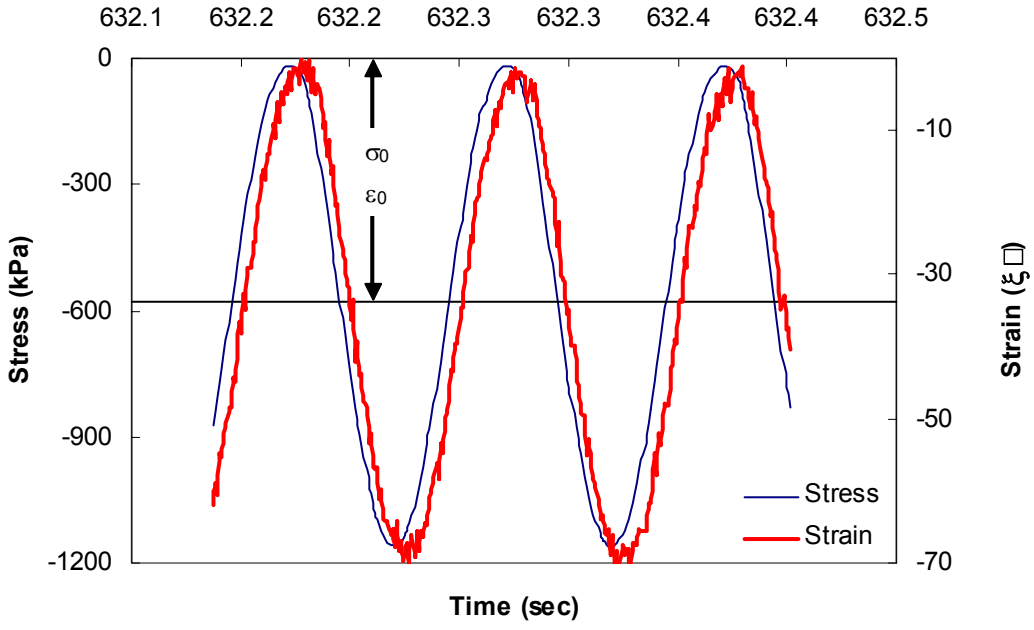

Figure 2.3 Phase lag shown through stress and strain curves

The underlying principle behind the development of the dynamic modulus mastercurve and the testing procedure is time-temperature superposition. According to this principle, the dynamic modulus is solely dependent on the reduced frequency, which is a function of temperature and frequency. Therefore, the effect on the dynamic modulus of altering the temperature can be reproduced by testing at different frequencies.

In the dynamic modulus test, a single specimen is used for all testing temperatures and all frequencies. Although the dynamic modulus test is supposed to be nondestructive, the stress-controlled mode used in the compression dynamic modulus test causes an increase in the mean strain as the test proceeds. Therefore, the testing method needs to be designed so that the testing at the temperature and frequency used in the early sequence in the temperature-frequency sweep has the least effect on the subsequent testing temperatures and frequencies. This consideration is reflected in AASHTO's protocol for dynamic modulus testing (16), TP62-03, by beginning the test at the lowest temperature and proceeding to the highest temperature. Also, at a given temperature, testing begins at the highest frequency and goes to the lowest frequency. This sequence is intuitive because asphalt concrete becomes stiffer at low temperatures and high frequencies.

2.2 Witczak's Predictive Equation

Witczak's predictive equation is the relationship developed between the dynamic modulus and mixture properties from data accumulated over the last 30 years by Witczak (7, 8, 10 and 17). The most recent version of the predictive equation is based on data from more than 200 different asphalt mixes, including a wide range of modified asphalts. The predictive relationship is:

$$\log|E^*| = -1.249937 + 0.029232 \cdot p_{200} - 0.001767 \cdot (p_{200})^2 - 0.002841 \cdot p_4$$
$$- 0.058097 \cdot V_a - 0.802208 \cdot \frac{Vb_{eff}}{(Vb_{eff} + V_a)} \qquad (2.7)$$
$$+ \frac{3.871977 - 0.0021 \cdot p_4 + 0.003958 \cdot p_{38} - 0.000017 \cdot (p_{38})^2 + 0.005470 \cdot p_{34}}{1 + e^{(-0.603313 - 0.313351 \cdot \log(f) - 0.393532 \cdot \log(\eta))}}$$

where |E*| = asphalt mix dynamic modulus in 10^5 psi;

η = bitumen viscosity in 10^6 poise (at any temperature, degree of aging);

f = load frequency in Hz;

V_a = % air voids in the mix, by volume;

Vb_{eff} = % effective bitumen content, by volume;

P_{34} = % retained on the ¾ inch sieve, by total aggregate weight (cumulative);

P_{38} = % retained on the 3/8 inch sieve, by total aggregate weight (cumulative);

P_4 = % retained on the No. 4 sieve, by total aggregate weight (cumulative); and

P_{200} = % passing the No. 200 sieve, by total aggregate weight.

2.3 Hirsch Model

This model was developed by Christensen et al. (18) to estimate the dynamic modulus of asphalt concrete using the binder modulus and volumetric properties of the mixture (VMA and VFA). The model is based upon a widely used model for predicting properties of composite materials, the law of mixtures. The law of mixtures, in its general form, represents the mechanical response of two phases in parallel:

$$E_C = v_1 E_1 + v_2 E_2 \qquad (2.8)$$

where E refers to the material property and ν refers to the volume fraction of a given phase, the subscript c refers to the composite, and the subscripts 1 and 2 refer to different

phases present in the composite. Another form of the law of mixtures can be obtained for phases in series:

$$1/E_C = v_1/E_1 + v_2/E_2 \tag{2.9}$$

The Hirsch model combines both phases in parallel and in series arrangements:

$$1/E_C = v_{1s}/E_1 + v_{2s}/E_2 + \left(v_{1P} + v_{2P}\right)^2 / \left(v_{1P}E_1 + v_{2P}E_2\right) \tag{2.10}$$

Christensen et al. (18) used Eq. (2.10) to develop the following model for predicting the asphalt concrete dynamic modulus from the binder modulus and volumetric properties:

$$E^* = P_c\left[4200000\left(1 - VMA/100\right) + 3\left|G^*\right|\left(\frac{VFA \times VMA}{10000}\right)\right] + \left(1 - P_c\right)\left[\frac{1 - VMA/100}{4200000} + \frac{VMA}{3VFA\left|G^*\right|}\right]^{-1} \tag{2.11}$$

where

$$P_c = \frac{\left(20 + \frac{VFA \times 3\left|G^*\right|}{VMA}\right)^{0.58}}{650 + \left(\frac{VFA \times 3\left|G^*\right|}{VMA}\right)^{0.58}} \tag{2.12}$$

where P_c is referred to as the aggregate contact volume.

3. SPECIMEN PREPARATION AND EXPERIMENTAL PROGRAM

This chapter presents the procedures used for dynamic modulus testing, dynamic shear rheometer testing, and binder shear modulus determination. As a part of each of these testing protocols are methods for specimen preparation, load application, measurement of displacement response, and interpretation of data.

3.1 Dynamic Modulus Testing

This section provides a description for preparing test specimens and performing dynamic modulus tests. Included in this section are the mixtures selected for testing, the procedure for fabrication and preparation of specimens, and uniaxial testing of the asphalt concrete specimens.

3.1.1 Specimen Preparation

3.1.1.1 Asphalt Concrete Mixtures

Forty two asphalt mixtures were tested in this project. Table 3.1 summarizes some key parameters for each mixture. A wide variety of aggregate sources were utilized from the mountains to the coast of North Carolina. The mixtures included 32 designs using granite and 10 using limestone aggregate sources. In these mixtures, there were seven primary aggregate sources used. Also, eight binders with PG grades of 64-22, 70-22 and 76-22 were used in making these mixtures.

Table 3.1 – Summary of Mixture Characteristics

Mix Type	Gradation	Aggregate Type	Primary Aggregate Location	Binder Grade	Asphalt Source	% AC Content
S[a]9.5[b]A[c]	Coarse	Granite	Morganton, NC	PG 64-22	Inman, SC	5.8
S9.5A	Fine	Granite	Charlotte, NC	PG 64-22	Wilmington, NC	6.4
S9.5A	Fine	Limestone	Castle Hayne, NC	PG 64-22	Wilmington, NC	6.7
S9.5B	Coarse	Granite	Haw River, NC	PG 64-22	Wilmington, NC	5.9
S9.5B0[d]	Fine	Granite	Morganton, NC	PG 64-22	Inman, SC	6.3
S9.5B1[d]	Fine	Granite	Charlotte, NC	PG 64-22	Wilmington, NC	5.8
S9.5B2[d]	Fine	Granite	Garner, NC	PG 64-22	Wilmington, NC	5.5
S9.5B3[d]	Fine	Granite	Garner, NC	PG 64-22	Wilmington, NC	5.6
S9.5B4[d]	Fine	Granite	Garner, NC	PG 64-22	Wilmington, NC	5.7
S9.5B	Fine	Limestone	Castle Hayne, NC	PG 64-22	Wilmington, NC	6.2
S9.5C	Coarse	Granite	Holly Springs, NC	PG 70-22	Wilmington, NC	5.3
S9.5C0[d]	Fine	Granite	Garner, NC	PG 70-22	Wilmington, NC	5.0
S9.5C1[d]	Fine	Granite	Garner, NC	PG 70-22	Wilmington, NC	5.0
S9.5C2[d]	Fine	Granite	Garner, NC	PG 70-22	Wilmington, NC	5.2
S9.5C3[d]	Fine	Granite	Garner, NC	PG 64-22	Wilmington, NC	5.9
S9.5C	Fine	Limestone	Castle Hayne, NC	PG 70-22	Wilmington, NC	6.7
S12.5B	Coarse	Granite	Haw River, NC	PG 64-22	Wilmington, NC	5.5
S12.5B	Fine	Granite	Holly Springs, NC	PG 64-22	Wilmington, NC	5.3
S12.5C	Coarse	Granite	Morganton, NC	PG 70-22	Inman, SC	4.6
S12.5C	Fine	Granite	Concord, NC	PG 70-22	Wilmington, NC	5.0
S12.5C	Fine	Limestone	Castle Hayne, NC	PG 70-22	Wilmington, NC	6.7
S12.5D	Coarse	Granite	Concord, NC	PG 70-22	Wilmington, NC	5.0
S12.5D	Fine	Granite	Concord, NC	PG 76-22	Salisbury, NC	4.7
I19.0B	Coarse	Granite	Haw River, NC	PG 64-22	Apex, NC	5.0
I19.0B	Coarse	Limestone	Castle Hayne, NC	PG 64-22	Wilmington, NC	5.2
I19.0B0[d]	Fine	Granite	Garner, NC	PG 64-22	Wilmington, NC	5.4
I19.0B1[d]	Fine	Granite	Charlotte, NC	PG 64-22	Wilmington, NC	4.3
I19.0B2[d]	Fine	Granite	Garner, NC	PG 64-22	Wilmington, NC	4.4
I19.0B3[d]	Fine	Granite	Garner, NC	PG 64-22	Wilmington, NC	4.5
I19.0B	Fine	Limestone	Castle Hayne, NC	PG 64-22	Wilmington, NC	5.1
I19.0C	Coarse	Granite	Garner, NC	PG 64-22	Wilmington, NC	4.7
I19.0C	Fine	Granite	Concord, NC	PG 64-22	Charlotte, NC	4.8
I19.0C	Fine	Limestone	Castle Hayne, NC	PG 64-22	Wilmington, NC	4.9
I19.0D	Coarse	Granite	Charlotte, NC	PG 70-22	Wilmington, NC	4.3
I19.0D	Fine	Granite	Concord, NC	PG 70-22	Salisbury, NC	4.1
B25.0B	Coarse	Granite	Holly Springs, NC	PG 64-22	Wilmington, NC	4.5
B25.0B	Coarse	Limestone	Castle Hayne, NC	PG 64-22	Wilmington, NC	4.2
B25.0B	Fine	Granite	Garner, NC	PG 64-22	Wilmington, NC	4.2
B25.0B	Fine	Limestone	Castle Hayne, NC	PG 64-22	Wilmington, NC	5.0
B25.0C	Coarse	Granite	Haw River, NC	PG 64-22	Wilmington, NC	4.0
B25.0C	Fine	Granite	Concord, NC	PG 64-22	Charlotte, NC	4.4
B25.0C	Fine	Limestone	Castle Hayne, NC	PG 64-22	Wilmington, NC	5.1

Note: [a]S for surface mix, I for intermediate mix, and B for base mix
[b]Nominal Maximum Aggregate Size (in mm)
[c]Traffic volume indicator
[d]Differentiates mixtures with the same designation

3.1.1.2 Maximum Specific Gravity Determination

Maximum specific gravity (G_{mm}) tests were performed on all mixtures in accordance with AASHTO T209 (19). Three batches of each mixture were made and tested. The maximum specific gravity results from the three batches provided the variation in gravities between any two test specimens did not exceed 0.011. If variation exceeded this limit then additional replicates were fabricated. The specimen that varied was easily identified and removed from the average after additional testing was completed.

3.1.1.3 Specimen Fabrication for Dynamic Modulus Tests

Asphalt mixtures were mixed and compacted at temperatures that were in accordance with the requirements for each binder. All mixtures were aged at 135°C for four hours (i.e., short-term oven aging) before compaction.

The mixtures were compacted into gyratory plugs of 150 mm in diameter by 178 mm in height. Later, they were cut and cored to cylindrical specimens with dimensions of 100 mm in diameter and 150 mm in height. Both ends were cut to ensure a more consistent air void distribution along the height of the test specimens. The mass of hot mix added used to make the gyratory plugs was adjusted so that the air void content in the final test specimens would fall within 4% ± 0.5%.

For each of the forty two mixtures there were three replicates of each tested. During fabrication or testing, if errors were made or densities were not met, then the specimen was discarded and an additional specimen was manufactured and tested.

3.1.1.4 Target Air Voids

The air voids for all mixtures was 4% ± 0.5%. In order to achieve this density, the target air voids for the gyratory plug had to be higher than that of the cut and cored specimen. The requirement for different target air voids occurs because of density variations throughout the height and diameter of the compacted specimen. The center of the gyratory plug is most dense with the least dense areas on the outer surfaces. The difference between the target for the gyratory plug and the cut and cored specimen typically increased as the nominal maximum size aggregate increased. More information on this can be found in the paper by Chehab et al. (20).

Air voids were measured using the Corelok vacuum sealing device. Specifications provided in ASTM D6752-03 (21) were followed in performing this measurement and making this calculation. Appropriate adjustments were made to the density of water when measurements were made at temperatures other than 25°C.

3.1.2 Testing Systems

This section will provide information on testing equipment, measurement instrumentation, and data acquisition systems.

3.1.2.1 Testing Equipment

Testing was performed using a closed-loop servo-hydraulic machine, manufactured by MTS. This machine is capable of applying loads, up to 20 kips, over a wide range of frequencies (25 to 0.01 Hz).

3.1.2.2 Temperature Control

A temperature chamber, cooled by liquid nitrogen, was used to control the test temperatures. The system was capable of applying temperatures between -10°C and

55°C, which were the lowest and highest temperatures, respectively, of interest in this research. Dummy specimens with thermocouples embedded in the middle of the specimen were used to monitor the temperature to which the specimens were subjected.

3.1.2.3 Measurement System

The measurement control system was completely computer controlled. This system was capable of acquiring signals from up to 16 channels simultaneously. Of these 16 channels only 6 were used in the testing described herein. One channel was dedicated to the load cell on the machine, one to the actuator LVDT (linear variable differential transducer), and four to the on-specimen, vertical LVDT's.

3.1.2.3.1 Data Acquisition

Data acquisition was controlled though a 16 bit board manufactured by National Instruments. Also, LabView software produced by National Instruments was used to interface with the board. Several programs were developed, using this software, to control data acquisition. In this research, sinusoidal loading was exclusively used and data was collected at 100 points per cycle.

3.1.2.3.2 Deflection Measurement

Vertical deformations were measured using LVDTs. Four loose-core, CD type, LVDTs measured deformations at 90° radial intervals. Targets were glued to the specimen face and the LVDTs were mounted to the targets. The LVDTs were mounted to measure the deformation in the middle two-thirds of the specimen (100 mm). For consistency in measurements a gluing device was used to maintain consistent spacing between the LVDT targets. One of the tested specimens is shown in Figure 3.1 with the LVDTs mounted.

Figure 3.1 LVDT mounting and spacing

3.1.2.3.3 Load Measurement

The MTS loading machine was capable of applying loads up to 20,000 lbs. For all testing in this project a 5 kip load cell was utilized, as the maximum applied load was about 4 kip.

3.1.3 Test Methods

Complex modulus testing was performed in this research. More specifically, this test was performed in uniaxial compression. The complex modulus test is performed in a stress controlled manner and is designed to measure the viscoelastic response of asphalt concrete. In order to measure this response, the stress applied to the specimen must not exceed linear viscoelastic limit or the specimen must not reach a damaged state. In this research, 75 microstrain was used as the limit of viscoelastic behavior. Since the material is temperature and frequency dependent the load applied was adjusted at each

combination of frequency and temperature to ensure that the strain did not exceed 75με. Utilizing a shift factor approach that is discussed in a Section 3.5, the data is shifted to form a mastercurve of moduli values.

Testing was performed by applying sinusoidal loadings at different frequencies and temperatures. Each specimen was subjected to testing frequencies of 25, 10, 5, 1, 0.5, 0.1, 0.05, and 0.01 Hz. Also, prior to applying the first frequency at each temperature, there was a preconditioning cycle applied. This is consistent with previous research and the AASTHO protocol for obtaining higher quality load and deformation data during the test. The preconditioning cycles were applied at 25 Hz and one-half the normal load applied at 25 Hz.

Also, the mixtures were subjected to a temperature sweep. At each temperature, loads were applied at the above mentioned frequencies. Approximately the first half of the mixtures were tested at -10°, 10°, and 35°C. Additional data were desired as testing progressed, so the remaining mixtures were also tested at 54°C.

Following each loading frequency a five minute rest period was allowed before the next frequency was applied. More details on the testing sequence can be found in Table 3.2. The standard guide for testing was AASHTO TP-62, which can be found in Appendix B.

Table 3.2 – Specimen Loading Information

Frequency (Hz)	Number of Loading Cycles
25 – pre	200
25	200
10	200
5	100
1	20
0.5	15

0.1	15
0.05	10
0.01	8

3.2 Dynamic Shear Rheometer Testing

A Dynamic Shear Rheometer (DSR) was used to determine the dynamic shear modulus (G*) of Rolling Thin Film Oven (RTFO) aged asphalt binders. G* was determined, using plate test geometry, by conducting a temperature-frequency sweep. This test method is applicable to asphalt binders with G* values in the range of 100 Pa to 10 MPa. This range of modulus values is typically obtained between 5° and 85°C.

3.2.1 Specimen Preparation for DSR Testing

Testing on seven performance graded binders was performed in this research. These binders include PG64-22, PG70-22, and PG76-22. A summary of these binders can be found in Table 3.3.

Table 3.3 – Asphalt Binders Tested

Binder Type	Refinery – Source	Testing Temperatures °C
PG 64-22	Associated Asphalt - Inman, SC	16,22,28,34
PG 64-22	Citgo – Wilmington, NC	16,22,28,40,54
PG 64-22	El Paso MEP – Charlotte, NC	16,22,28,40,54
PG 64-22	El Paso MEP - Apex, NC	16,22,28,40,54
PG 70-22	Citgo – Wilmington, NC	16,22,28,40,54
PG 70-22	Associated Asphalt - Salisbury, NC	16,22,28,40,54
PG 76-22	Associated Asphalt - Salisbury, NC	16,22,28,40,54

Each binder was RTFO aged by the North Carolina Department of Transportation Materials and Test Unit. RTFO aged binders were heated in closed cans until they became sufficiently fluid to pour the required specimens. The samples were stirred

occasionally to remove any trapped air and to ensure homogeneity. PG 64-22 binders were heated to a temperature of 125°C and PG 70-22 and PG 76-22 binders were heated to 135°C.

Three replicates of each binder type were poured into a silicone rubber mold to form a pellet with a diameter of 25 mm and a height of approximately 1.5 mm. The best two replicates were selected for testing and the third replicate was discarded. The silicon mold was allowed to cool to room temperature. The specimen was then carefully removed from the mold and centered on the lower plate of the DSR. Binder preparation and testing was performed by Mostafa Momen.

3.2.2 Testing Systems

This section will provide information on the DSR testing equipment, measurement instrumentation, and data acquisition systems.

3.2.2.1 Testing Equipment

The DSR test system was manufactured by Bohlin Instruments and consists of parallel metal plates, an environmental chamber, a loading device, and a control and data acquisition system. A metal base plate with a smooth polished surface and a diameter of 25 mm was used as the lower plate. A metal spindle with the same diameter and surface conditions was mounted to the rotating part of the apparatus.

3.2.2.2 Temperature Control

An environmental water bath was used to maintain a constant specimen temperature. That is, the temperature in the chamber was controlled by the circulation of water around the test specimen. The environmental chamber controlled the temperature

of the test specimen to an accuracy of ± 0.1°C and was capable of maintaining this consistency across the temperatures of interest (Table 3.3).

3.2.3 Test Methods

A base plate and the spindle were mounted on the DSR device and tightened firmly. A zero gap level was established by manually spinning the spindle. While the spindle was spinning, the gap was closed until the spindle touched the base plate. The base plate and the spindle were then moved apart, and a gap setting of 1 mm plus 0.05 mm was established. The specimen was placed at the center of the base plate. The spindle was moved downward to compress the sample until the gap between the plates equaled the gap setting. The specimen was trimmed by carefully removing the extra asphalt around the entire perimeter using a heated trimming tool. After trimming the perimeter of the specimen, the gap between the plates was decreased by 0.05 mm to the desired testing gap of 1 mm.

The frame, detectors, and fixtures in the DSR change dimensions as the temperature changes, thus causing the zero gap to change. Therefore, the gap between the plates was set at the middle of the expected range of test temperatures to minimize that error. The test was conducted in a strain control mode where the target strain value was set to 5% as per AASHTO TP-1.

Machine control and data acquisition are both controlled via computer. The software was programmed to test at 15, 10, 5, 1, 0.5, 0.1, 0.05, and 0.01 Hz at each of the temperatures shown in Table 3.3. After reaching the each of the desired testing temperatures, the software was programmed to wait for 10 minutes to ensure that the specimen had also reached that temperature. After the rest period the machine would

perform preconditioning cycles for 10 seconds before starting the test. Testing started from the lowest temperature to the highest, and at each temperature the test progressed from the highest frequency to the lowest.

3.3 Binder Shear Modulus Determination

Binder shear modulus is determined the same way as complex modulus is for asphalt concrete mixtures (see Section 2.1). G* is used to denote binder shear modulus whereas E* is used to denote dynamic modulus of asphalt concrete.

3.4 Software

For time-saving and consistency purposes it was determined that software was needed to analyze the dynamic modulus test data. The analysis program was written using a graphical programming language, LabView. The software would read in the raw data and detect the last five cycles of data for each temperature and frequency combination as per AASHTO TP-62. The last five cycles of data were analyzed and fitted according to the following functional form:

$$f(t) = a + bt + c\cos(\omega t + \phi) \tag{3.1}$$

where *f(t)* is load or deformation time history;

a, *b*, and *c* are regression coefficients;

ϕ is the phase angle; and

ω is the angular frequency.

Coefficient *c* represents the amplitude of the sinusoidal waveform, and the dynamic modulus is then calculated from the ratio of these coefficients from load and deformation

histories. The difference in the phase angles from the load and deformation analyses represent the phase angle of the material. This program uses the Levenberg-Marquardt algorithm which is a least squares approach to curve fitting. This software was developed at North Carolina State University. Credit for the most recent updates to this software, which were used in this research, goes to Shane Underwood.

3.5 Mastercurve Construction

The method outlined below is applicable for binders and asphalt concrete mixtures. Since the majority of the testing was performed on asphalt mixtures, this will be the focus of the text. However, this can also be applied to binders.

3.5.1 Dynamic Modulus

To construct a mastercurve, the dynamic moduli versus frequency curves at various temperatures (Figure 3.2) are horizontally shifted along the frequency axis in a logarithmic scale to form a single curve (Figure 3.3) at a predetermined reference temperature. The reference temperature selected in this research was 10°C. The first step involved in the determination of shift factors was to determine what frequency-temperature combinations yielded the same moduli values. Since the horizontal shift was performed in a logarithmic scale, the shift factor was determined by calculating the ratio of the frequency at the reference temperature to the frequency at the temperature in question. After the horizontal shift, the frequency at the reference temperature is called *reduced frequency*. More details concerning this shift can be found in the AASHTO TP-62 standard that is in Appendix B. In order to accomplish this shift, a difference of squares technique was used in order to minimize the error between the sigmoidal fitting

function and the shifted data. The sigmoidal function is the fit recommended in AASHTO TP-62 and the form that provided the best fit across the entire reduced frequency spectrum. This functional form is presented in Eq. 3.2. An example of the fit between the shifted data and the sigmoidal fit is shown in Figure 3.3. Error minimization was accomplished using the Solver module within Excel. The coefficients (a, b, d, and e) presented in Eq. 3.2 and the shift factors for each temperature other than the reference temperature were simultaneously determined.

$$\log|E^*| = a + \frac{b}{1 + \frac{1}{\exp^{d+e(\log f_R)}}} \tag{3.2}$$

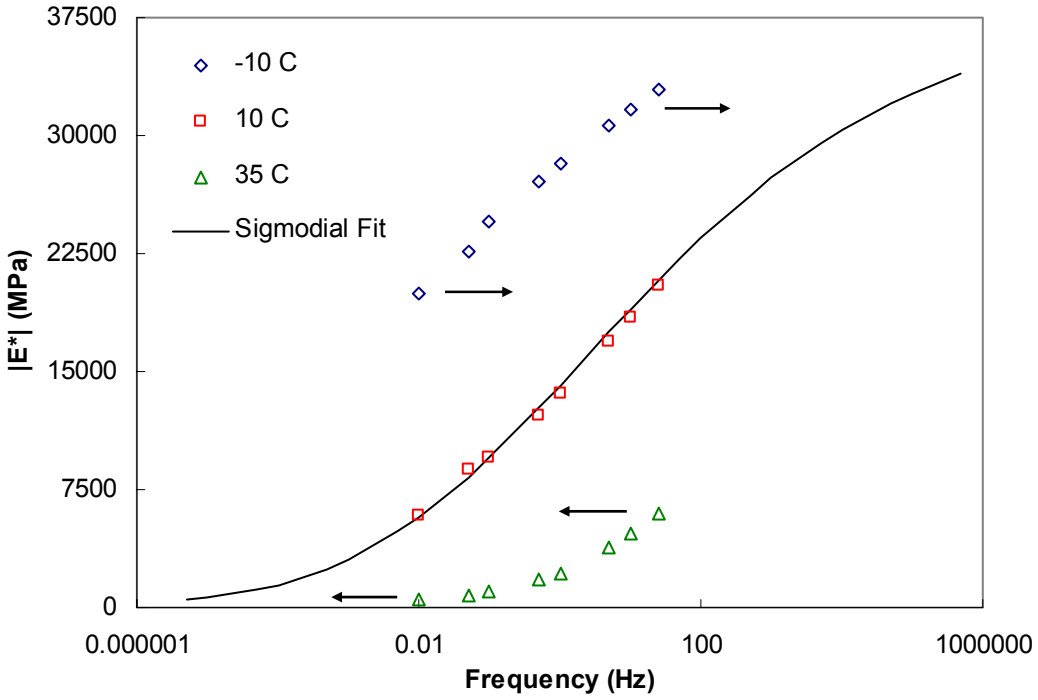

Figure 3.2 Mastercurve development before shifting

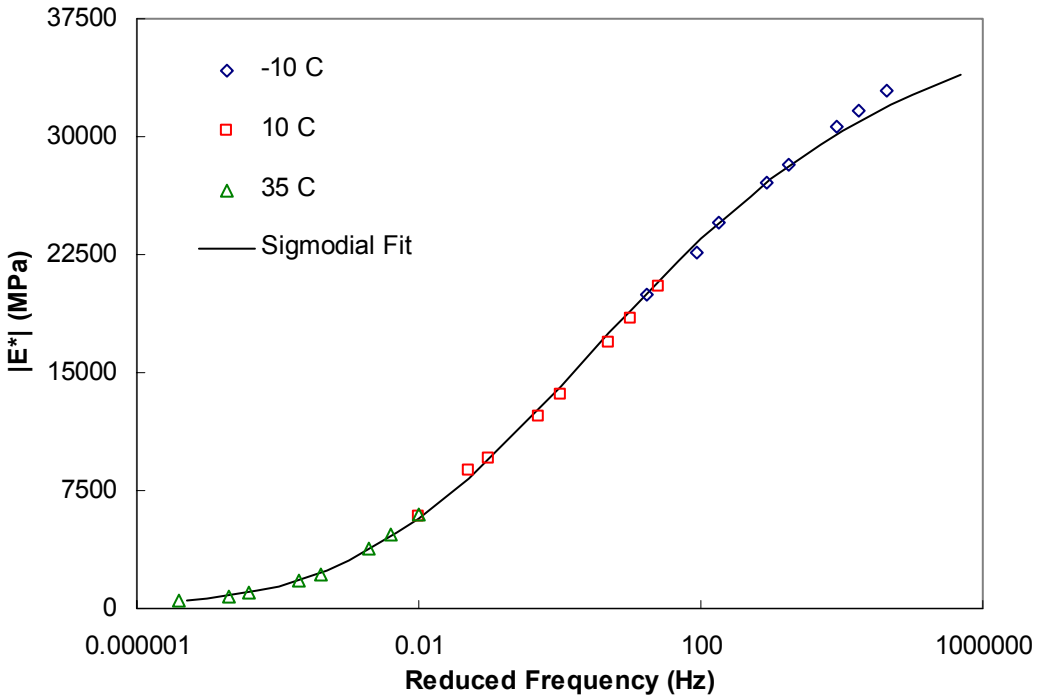

Figure 3.3 Mastercurve development after shifting

The mastercurve was constructed using the averaged dynamic modulus values from the three replicates tested for each mixture. A detailed procedure is outlined in Section 3.5.1.1 to calculate dynamic modulus for any of the mixtures tested in this study using the sigmoidal function and the shift factor formula.

3.5.1.1 Predicting Dynamic Moduli from Sigmoidal Fit

This section presents the procedure to calculate dynamic modulus for all of the 42 mixtures tested in this project between -10°C and 54.4°C. An extrapolated |E*| value could be still determined outside of the given temperature range, but the accuracy of the result could be questionable as discussed in Section 4.2.

The following steps are used to calculate the dynamic modulus at any temperature and frequency. Table 3.4 provides a list of coefficients determined from testing each of

the 42 mixtures. These coefficients define the shape of the sigmoidal curve and also determine the shape of the shift factor versus temperature relationship. The procedure is as follows:

1. Identify the mixture where |E*| needs to be calculated.
2. Determine the frequency (f) in Hz and temperature in degrees Celsius at which |E*| is to be computed.
3. Determine the shift factor coefficients from Table 3.4.
4. Substitute coefficients into the following equation, where T is the temperature and a_T is the shift factor:

$$Log(a_T) = \alpha_1 T^2 + \alpha_2 T + \alpha_3 \quad (3.3)$$

5. Compute the shift factor.
6. Compute the reduced frequency ($f_R = f \times a_T$).
7. Determine the sigmoidal function regression coefficients a, b, d, and e from Table 3.4.
8. Substitute the regression coefficients and f_R into the sigmoidal function Eq. (3.2) to determine the dynamic modulus in MPa.

Table 3.4 – Coefficients to Predict |E*| at Any Temperature and Frequency

Mixture			Shift Function Coefficients			Sigmoidal Coefficients			
			$\alpha 1$	$\alpha 2$	$\alpha 3$	a	b	d	e
S[a]9.5[b]A[c]	Coarse	Granite	0.00060	-0.16543	1.58849	1.38724	3.19616	1.75945	0.43460
S9.5A	Fine	Granite	0.00077	-0.15993	1.52679	1.41656	3.10378	1.46310	0.46369
S9.5A	Fine	Limestone	0.00074	-0.16339	1.55956	1.74392	2.67903	1.64762	0.48697
S9.5B	Coarse	Granite	0.00067	-0.14940	1.49840	1.32570	3.21009	1.54126	0.49085
S9.5B0[d]	Fine	Granite	0.00054	-0.15949	1.56317	0.86302	3.61944	1.76263	0.39345
S9.5B1[d]	Fine	Granite	0.00063	-0.15509	1.48742	1.80806	2.70608	1.49166	0.51246
S9.5B2[d]	Fine	Granite	0.00063	-0.16281	1.56548	1.78184	2.68257	1.72191	0.44429
S9.5B3[d]	Fine	Granite	0.00070	-0.16292	1.55952	1.61112	2.87367	1.71602	0.46512
S9.5B4[d]	Fine	Granite	0.00070	-0.15916	1.52175	1.51435	2.99846	1.67175	0.49359
S9.5B	Fine	Limestone	0.00057	-0.15964	1.53926	2.08083	2.39349	1.73194	0.46166
S9.5C	Coarse	Granite	0.00039	-0.15556	1.49484	1.11690	3.42690	1.96297	0.39558
S9.5C0[d]	Fine	Granite	0.00055	-0.16239	1.60396	0.95234	3.63149	1.99680	0.38857
S9.5C1[d]	Fine	Granite	0.00063	-0.16165	1.55359	1.80725	2.70330	1.78576	0.44931
S9.5C2[d]	Fine	Granite	0.00067	-0.15938	1.52689	1.84010	2.67905	1.84852	0.49910
S9.5C3[d]	Fine	Granite	0.00067	-0.15752	1.50795	1.62218	2.90129	1.65725	0.52524
S9.5C	Fine	Limestone	0.00061	-0.15655	1.50481	2.04012	2.36898	1.91150	0.51392
S12.5B	Coarse	Granite	0.00088	-0.16096	1.56637	1.34244	3.19566	1.63643	0.49564
S12.5B	Fine	Granite	0.00080	-0.16273	1.54227	0.93381	3.60575	1.83115	0.43273
S12.5C	Coarse	Granite	0.00060	-0.16543	1.58849	1.83404	2.75875	1.49861	0.38100
S12.5C	Fine	Granite	0.00043	-0.15267	1.51253	1.48148	3.13354	1.85892	0.41490
S12.5C	Fine	Limestone	0.00053	-0.14935	1.44096	2.31749	2.08901	1.77606	0.56767
S12.5D	Coarse	Granite	0.00060	-0.16045	1.54420	1.26038	3.36417	1.84298	0.40654
S12.5D	Fine	Granite	0.00051	-0.16232	1.56174	0.40363	4.21000	2.18061	0.33868
I19.0B	Coarse	Granite	0.00075	-0.15933	1.51615	1.36605	3.19382	1.56800	0.44184
I19.0B	Coarse	Limestone	0.00078	-0.16068	1.52856	2.02687	2.45922	1.94798	0.57696
I19.0B0[d]	Fine	Granite	0.00080	-0.16009	1.52354	1.08285	3.48199	1.73573	0.48212
I19.0B1[d]	Fine	Granite	0.00053	-0.14952	1.44195	2.32327	2.24418	1.66214	0.60812
I19.0B2[d]	Fine	Granite	0.00067	-0.16039	1.53712	1.67495	2.82577	1.82171	0.44801
I19.0B3[d]	Fine	Granite	0.00070	-0.16099	1.53979	1.78992	2.76709	1.69042	0.44607
I19.0B	Fine	Limestone	0.00076	-0.15876	1.51184	2.16441	2.29710	1.78711	0.53901
I19.0C	Coarse	Granite	-0.00015	-0.11840	1.19400	1.49981	3.13154	2.39859	0.45451
I19.0C	Fine	Granite	0.00052	-0.16137	1.55206	1.02532	3.52729	1.74412	0.36155
I19.0C	Fine	Limestone	0.00060	-0.15756	1.51529	1.87048	2.61784	1.99850	0.47320
I19.0D	Coarse	Granite	0.00047	-0.14957	1.48837	1.63555	2.94731	1.73702	0.45052
I19.0D	Fine	Granite	0.00060	-0.16355	1.60230	1.16137	3.42986	2.09133	0.40324
B25.0B	Coarse	Granite	0.00087	-0.15998	1.51815	1.25921	3.26262	1.71818	0.48357
B25.0B	Coarse	Limestone	0.00066	-0.15704	1.50427	2.03745	2.48150	2.09873	0.57232
B25.0B	Fine	Granite	0.00064	-0.15563	1.49960	1.17188	3.43787	1.91881	0.46299
B25.0B	Fine	Limestone	0.00059	-0.15705	1.51098	2.20753	2.29394	1.80533	0.53732
B25.0C	Coarse	Granite	0.00071	-0.15434	1.46972	1.85690	2.75864	1.63312	0.57629
B25.0C	Fine	Granite	0.00060	-0.16543	1.58849	1.18143	3.35734	1.79427	0.38735
B25.0C	Fine	Limestone	0.00064	-0.15256	1.46207	2.19797	2.22560	1.84270	0.58489

Note: [a]S for surface mix, I for intermediate mix, and B for base mix
[b]Nominal Maximum Aggregate Size (in mm)
[c]Traffic volume indicator
[d]Differentiates mixtures with the same designation

3.5.2 Laboratory Illustration

In this section, typical results from S9.5C–Fine mixture is presented for demonstration purposes, while the results for the remaining 41 mixtures are presented in Appendix A in a graphical format plotted with axial compression data. As mentioned before, three replicates were tested for each mixture and plotted against reduced frequency after shifting the data. Figure 4.2 presents dynamic modulus mastercurves of the three replicates tested. The dynamic modulus values from each replicate were averaged and a single mastercurve representing the mixture was plotted in Figure 4.3. The reference temperature that was used as the basis for shifting the data was 10°C. A quadratic equation was used to fit the three shift factor values obtained. Figure 4.4 shows a shift factor plot against temperature.

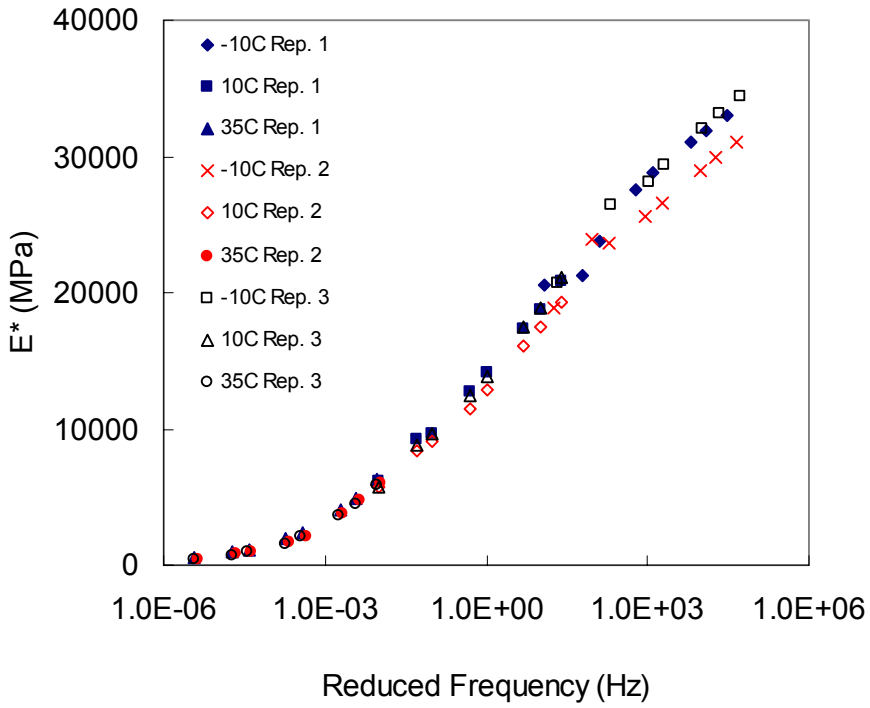

Figure 3.4 S9.5C–Fine mixture mastercurves

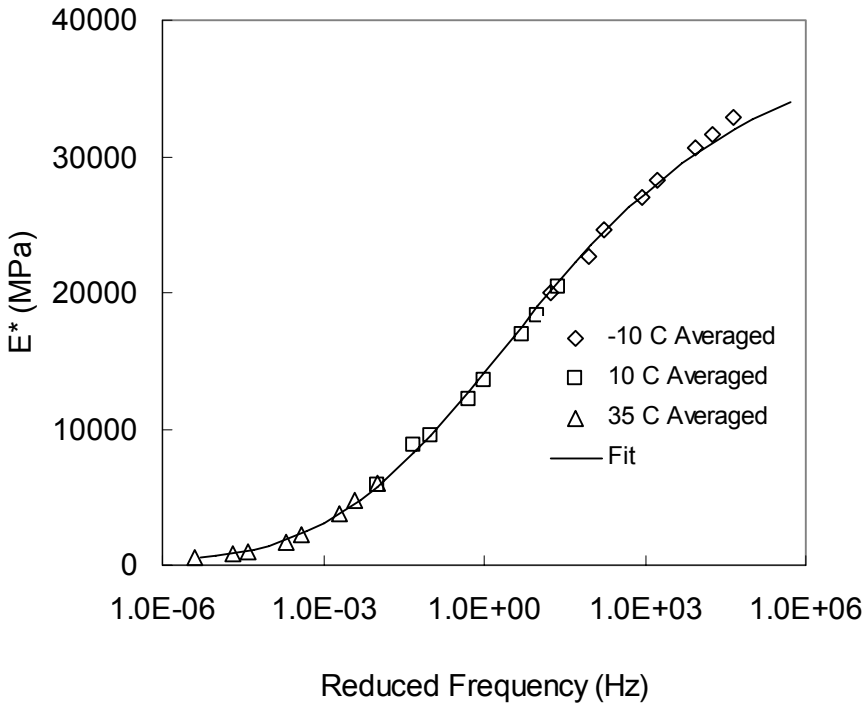

Figure 3.5 S9.5C–Fine mixture dynamic modulus mastercurve

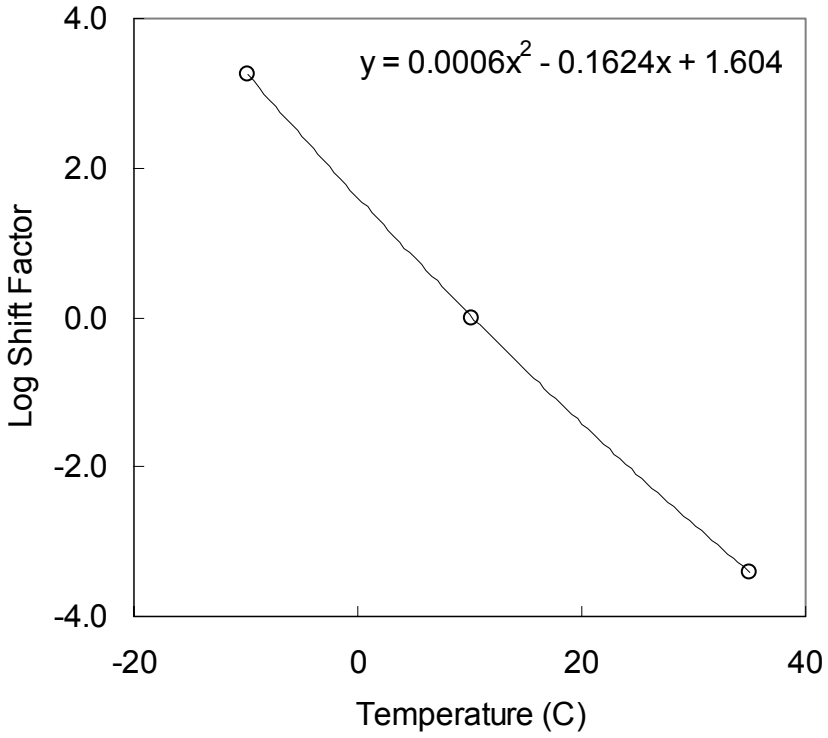

Figure 3.6 S9.5C–Fine shift factor–temperature relationship

4. DISCUSSION OF RESULTS

In this chapter an effect on confining pressure is evaluated for two mixtures evaluated in uniaxial compression. Also evaluated, is the effect of modifying the testing temperatures to save time and add consistency to testing. The effects of mixtures variables are discussed. Finally, the prediction of |E*| using Hirsch and Witczak's models in conjunction with performance predictions are used to evaluate the effect of moduli variability on performance life.

4.1 Effect of Confining Pressure on |E|*

Dynamic moduli of the mixtures determined from unconfined and confined axial compression tests are compared in this section. The comparison for an S9.5C–Fine granite mixture is presented in Figures 4.1 and 4.2.

Figure 4.1 displays the dynamic moduli of S9.5C–Fine mixture determined from uniaxial and triaxial tests in semi-log scale. Although the effect of confinement seems to be insignificant in this figure, further analysis is necessary because the normal scale used in this figure for the dynamic modulus axis suppresses the information at the lower reduced frequencies. Therefore, the same data were plotted in log-log scale in Figure 4.2. The effect of confinement is found to be significant at low reduced frequencies (i.e., high temperature and/or low loading frequency). This observation is also supported by Figures 4.3 – 4.5 where uniaxial and triaxial dynamic moduli of S9.5C–Fine mixture at low, medium, and high reduced frequencies are presented for various air void contents. The dynamic modulus versus air void content relationships are essentially the same between the uniaxial and triaxial data for 10,000 and 1 Hz, whereas at 0.0005 Hz the uniaxial

dynamic moduli are smaller than those determined from triaxial compression. This finding is somewhat expected because, as the temperature increases or loading frequency decreases, asphalt binder becomes softer and the effect of confinement on aggregate structure becomes more significant. The confinement makes the asphalt-aggregate mixture more resistant to stress in these conditions, and thus the triaxial test yields greater dynamic modulus than the uniaxial test.

The dynamic moduli of I19.0C mixture at the three reduced frequencies are plotted in Figures 4.6 – 4.8. Different from Figures 4.3 – 4.5 for the S9.5C mixture, the triaxial dynamic moduli are in general greater than those from the uniaxial test. The difference is much greater at 0.0005 Hz. This observation is different from the one made from the S9.5C data. It is probably due to the fact that I19C has larger aggregate particles and therefore the effect of confinement becomes greater. The reduction in dynamic modulus as the AV% increases is greater (the slope is steeper) in the triaxial data than in the uniaxial data.

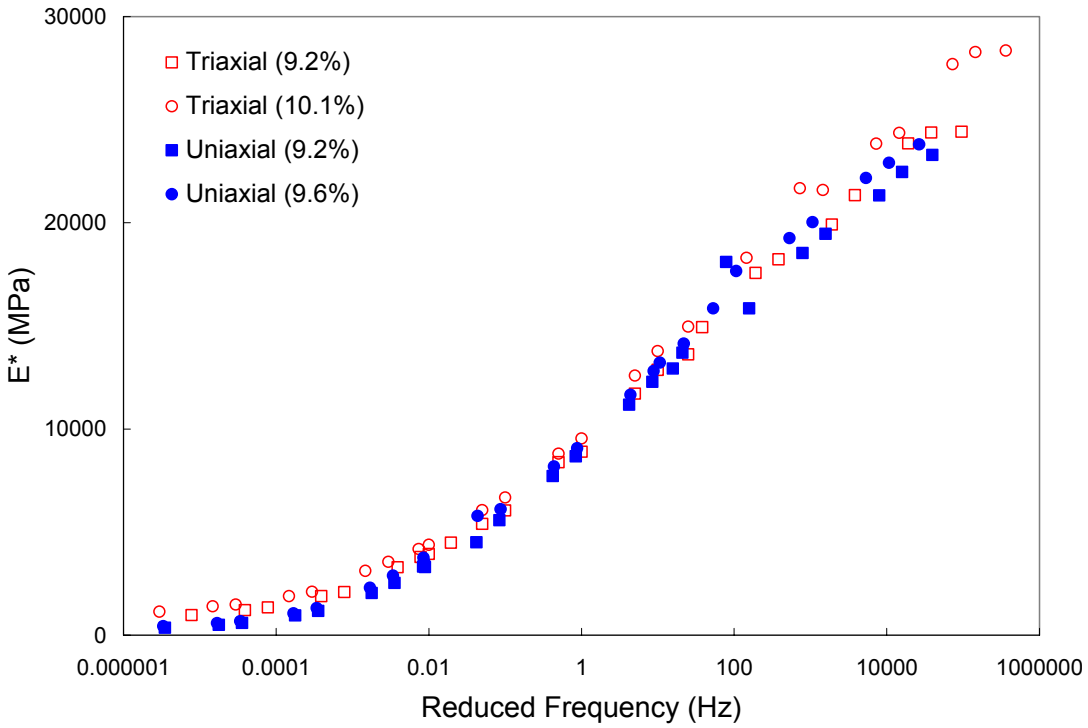

Figure 4.1 lE*l comparison between triaxial and uniaxial tests in semi-log scale for S9.5C–Fine mixture

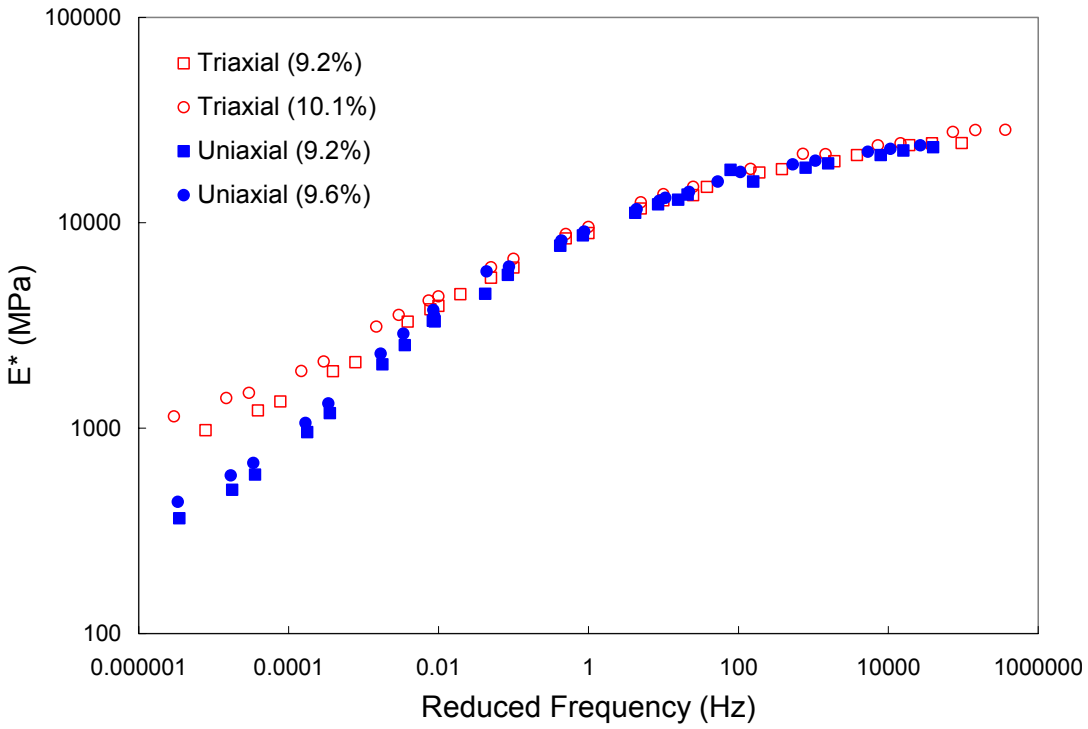

Figure 4.2 |E*| comparison between triaxial and uniaxial tests in log-log scale for S9.5C–Fine mixture

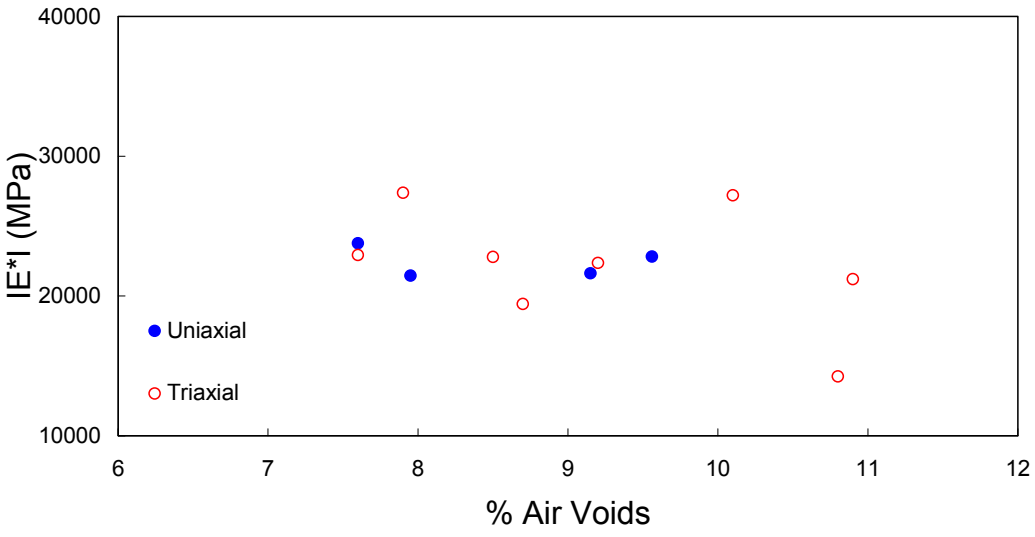

Figure 4.3 |E*| versus % AV at 10,000 Hz for S9.5C–Fine mixture

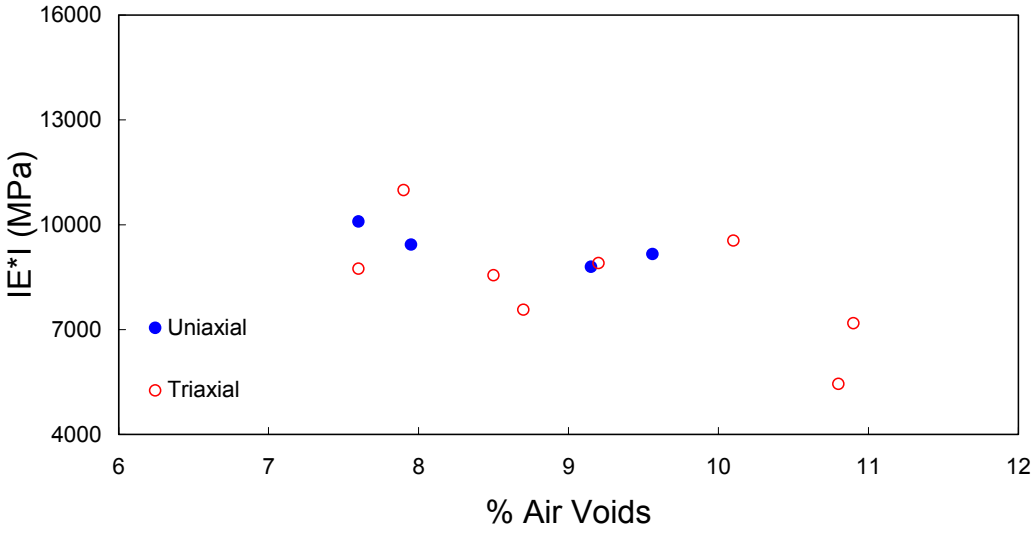

Figure 4.4 |E*| versus % AV at 1 Hz for S9.5C–Fine mixture

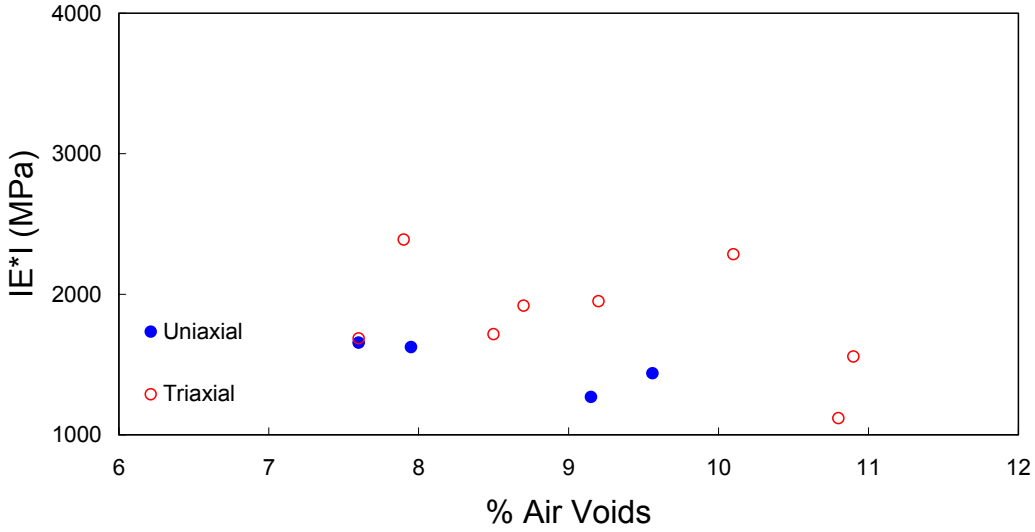

Figure 4.5 |E*| versus % AV at 0.0005 Hz for S9.5C Mix

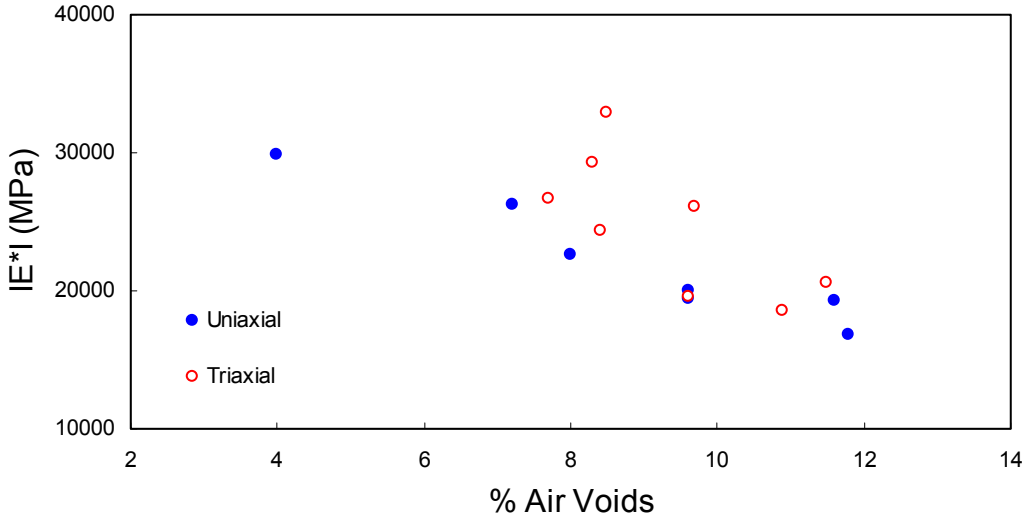

Figure 4.6 |E*| versus % AV at 10,000 Hz for I19.0C–Coarse mixture

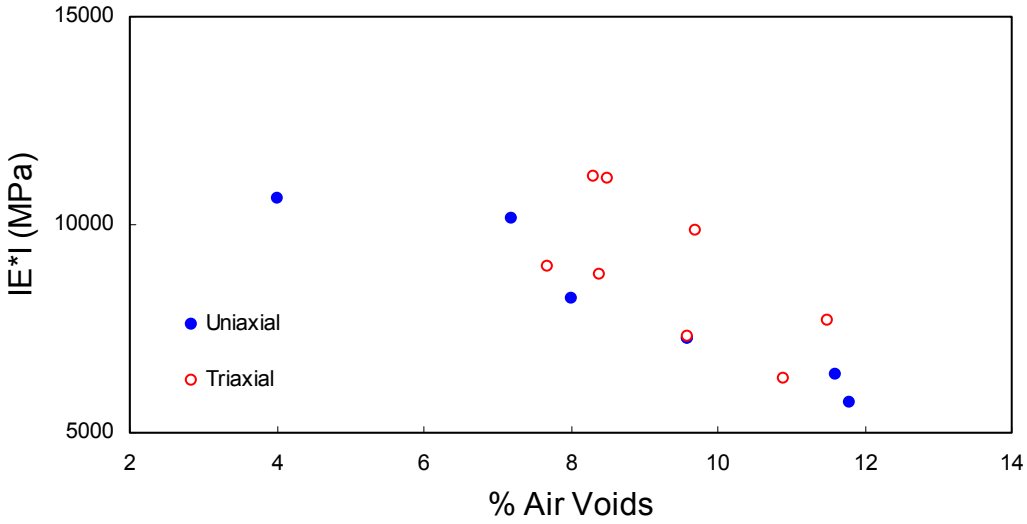

Figure 4.7 |E*| versus % AV at 1 Hz for I19.0C–Coarse mixture

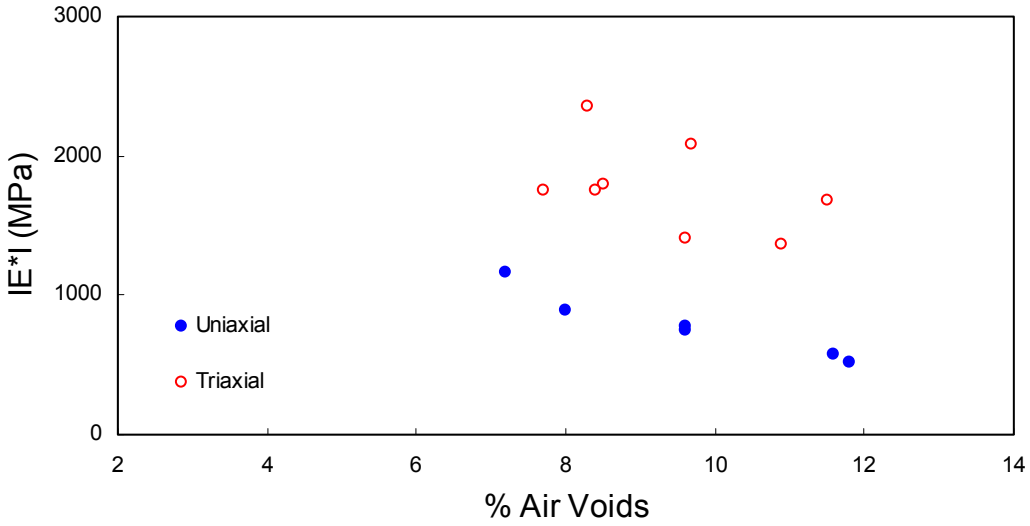

Figure 4.8 |E*| versus % AV at 0.0005 Hz for I19.0C–Coarse mixture

4.2 Test Protocol Modification

Since much emphasis has been placed on dynamic modulus testing, resulting partially from the mechanistic-empirical design guide, it is necessary to understand how varying testing conditions affect the results. One factor evaluated in this research is the number and values of the testing temperatures. The main interest in this evaluation was whether testing at a reduced number of temperatures with an increased number of frequencies would yield the same results (i.e. same mastercurve). Should the evaluation prove positive, this would mean an approximate time savings of 3 hours per test using the environmental chamber and temperature conditioning system (liquid nitrogen) at NCSU. See Table 4.1 for a summary of the current (AASHTO TP62 protocol) versus the proposed (NCSU Modified protocol) for a summary of testing frequencies and temperatures.

Table 4.1 – Comparison of the current and proposed test protocols

Test Protocol	*No. of Temperatures*	*Testing Temperatures (°C)*	*No. of Frequencies*	*Testing Frequencies (Hz)*	*Total Testing Time (hrs)*
Proposed	**3**	-10, 10, and 35	**8**	25, 10, 5, 1, 0.5, 0.1, 0.05, 0.01	**9**
Current	**5**	-10, 4.4, 21.1, 37.8, 54.4	**6**	25, 10, 5, 1, 0.5, 0.1	**12**

The underlying principle behind the development of the dynamic modulus mastercurve is the time-temperature superposition. According to this principle, the dynamic modulus is solely dependent on the reduced frequency, which is a function of temperature and frequency. Therefore, the effect on the dynamic modulus of altering the temperatures can be reproduced by testing at different frequencies.

In the dynamic modulus test, a single specimen is used for all testing temperatures and all frequencies. Although the dynamic modulus test is supposed to be nondestructive, the stress-controlled mode used in the compression dynamic modulus test causes an increase in the mean strain as the test proceeds. Therefore as described in Chapter 3, the testing method needs to be designed so that the testing at the temperature and frequency used in the early sequence in the temperature-frequency sweep has the least effect on the subsequent testing temperatures and frequencies. This consideration is reflected in the current dynamic modulus test protocol by beginning the test at the lowest temperature and proceeding to the highest temperature. Also, at a given temperature, testing begins at the fastest frequency and goes to the slowest frequency. This sequence is intuitive because asphalt concrete deforms the least at low temperatures and high frequencies.

4.2.1 Current Protocol and Testing

One key requirement in developing a dynamic modulus mastercurve is to have an overlap of dynamic modulus versus frequency curves between adjacent testing temperatures. Figure 4.9 illustrates mastercurve development for a mixture based on the current protocol of five testing temperatures. To develop this curve, the dynamic moduli versus frequency curves at various temperatures are horizontally shifted along the frequency axis in a logarithmic scale to form a single curve at a reference temperature. The first step involved in the determination of shift factors is to determine the frequencies at the reference temperature and the temperature in question that yield the same dynamic modulus values. Since the horizontal shift is performed on the logarithmic scale, the shift factor is then determined by calculating the ratio of the frequency at the reference temperature to the frequency at the temperature in question. After the horizontal shift, the frequency at the reference temperature is called *reduced frequency*. Therefore, to find the frequencies at two temperatures that yield the same dynamic modulus values, it is desirable to have data overlap.

This overlap can be seen in Figure 4.9 using the current protocol, which was developed by the NCHRP 9-19 research team and used in the round robin testing coordinated by the Connecticut Transportation Institute (22). However, notice that extra duplication of data exists at the lowest modulus or highest temperature values. The aim of this study is to eliminate excessive duplication in the overlap while maintaining sufficient data for the shift analysis.

4.2.2 Background for Modification of the Current Protocol

Since the mastercurve development combines the effect of testing frequency and temperature into one variable called reduced frequency, it is possible to modify the range of frequencies in each temperature to compensate for the modification in the number of test temperatures. This theoretical justification allows the increase in the number of frequencies and the decrease in the number of testing temperatures, as shown in Table 4.1. This modification is attractive to this research and the practitioner alike because the current protocol takes 12 hours to finish the entire temperature-frequency sweep whereas the modified protocol reduces the testing time to 8 hours, i.e., within one working day. The ability to finish the dynamic modulus testing of a mixture within one working day instead of two provides some major benefits in quality control of test data, over and beyond the benefit of timesaving.

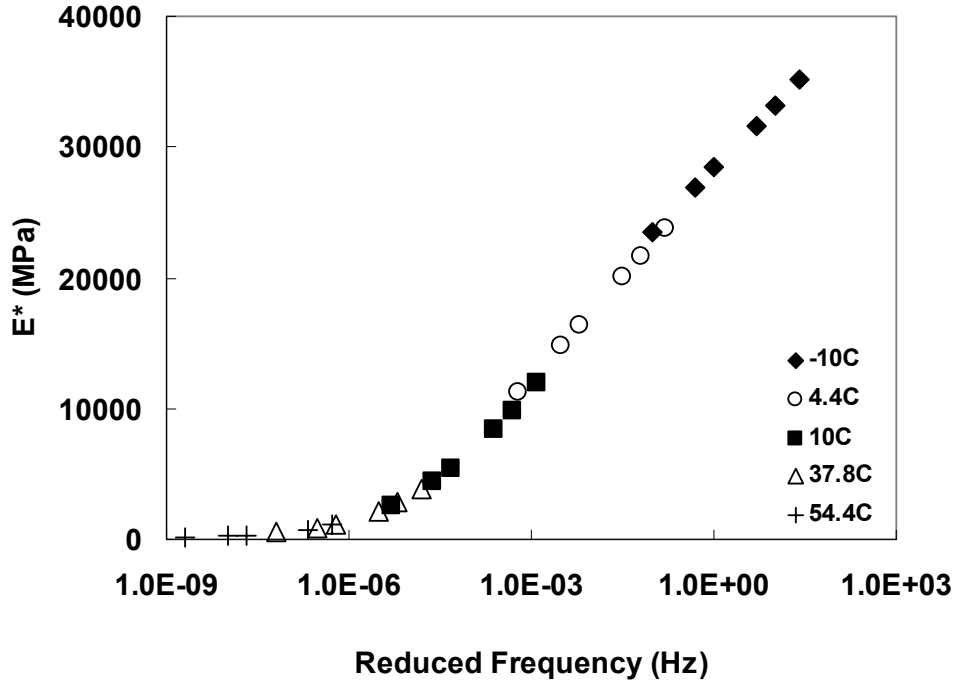

Figure 4.9 Overlapping of dynamic modulus curves from the five-temperature testing

4.2.3 Results from Current and Modified Protocols

As mentioned previously, overlap is desirable in mastercurve development. Figure 4.10 shows the overlap between dynamic modulus curves using the temperatures proposed in the new protocol. It can be seen from Figure 4.10 that, by adding two low frequencies (i.e., 0.05 and 0.01 Hz), enough overlap is experienced to cover the reduction in the number of testing temperatures. The overlap is similar to that seen in five-temperature testing between -10° and 4.4°C or 4.4° and 21.1°C. Some of the extra replication at the higher temperatures does not exist in the three-temperature test data, which does not affect the quality of the overlap because enough data still exist to create overlap.

Another important factor to consider in this comparison is the similarity between dynamic modulus mastercurves from the two protocols. In Figure 4.11 the results from both tests are combined so that, graphically, the similarities can be seen. Each curve in Figure 4.11 represents the average of three replicates. When the average curves are compared in this figure, some discrepancies are seen at higher reduced frequencies (i.e., lower temperatures and/or higher frequencies). It is noted that both the three- and five-temperature tests use -10°C as the first test temperature. Also, it is noted that at a given temperature the test proceeds from the highest to lowest frequency. From Table 4.1, it can be seen that the difference in procedures is adding 0.05 and 0.01 Hz to the three-temperature test. In other words, the testing procedure for both tests is identical until the additional frequencies are added and higher temperatures are used.

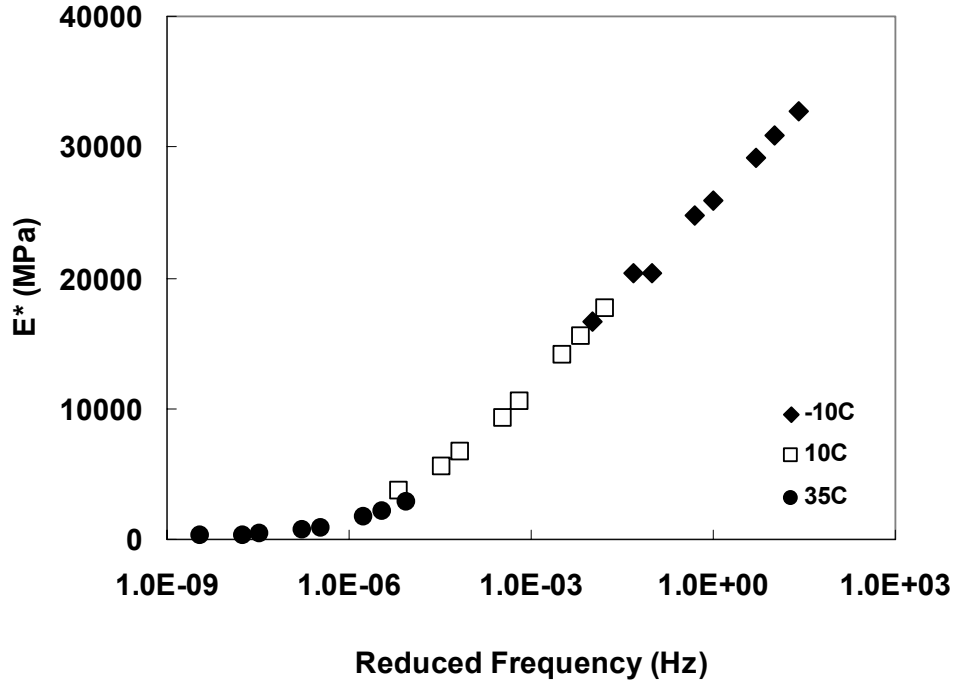

Figure 4.10 Overlapping of dynamic modulus curves from the three-temperature testing

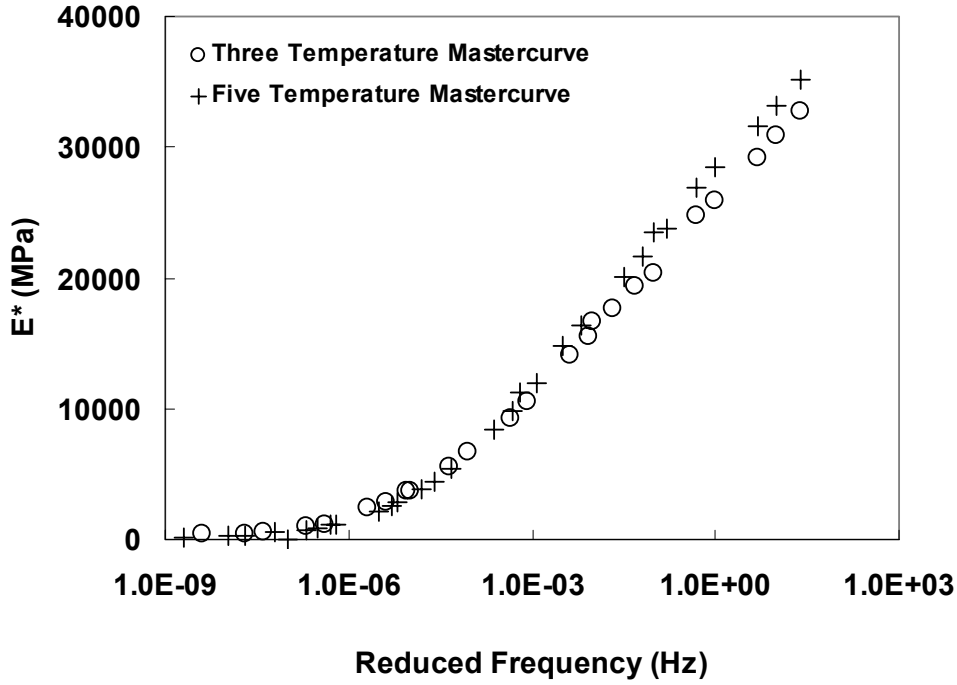

Figure 4.11 Comparison of mastercurves between three- and five-temperature testing

The variation at low temperatures and high frequencies shown in Figure 4.11 is counterintuitive because the loading and temperature histories, initially, are identical, but as testing progresses these histories become different, and the difference becomes less. For this reason, the discrepancy observed in Figure 4.11 may be due to a factor other than the new testing procedure. Since these are virgin specimens made at the same time and tested, at least initially, under the same procedure, the results at -10°C should be the same if the specimen-to-specimen variation is minimal.

Since there are multiple specimens involved in each of the curves shown in Figure 4.11, a statistical analysis is necessary to check if the average is indeed different. Since each test did not have the same reduced frequency, comparison was accomplished by using the actual data at a given reduced frequency for the five-temperature data and comparing this to the sigmoidal fit from the three-temperature data.

A t-test on two means was conducted at a significance level of α=0.05 for all the reduced frequencies at each of the five testing temperatures. The hypothesis test was constructed with the following parameters:

H_o: = $\mu 1 - \mu 2 = 0$

H_1: = $\mu 1 - \mu 2 \neq 0$

The null hypothesis was not rejected except in two instances (0.5 and 1 Hz at -10°C). When the null is not rejected there is not enough evidence that the mean values are different for the two testing protocols. Although the null hypothesis was statistically rejected in those two frequencies, the visual comparison of the data from these two frequencies with the data from other frequencies in Figure 4.11 and the fact that at 26

other frequencies the difference was statistically insignificant suggest that the difference caused by changing the test protocol is minimal.

This method of testing was adopted early on in the research. In the initial analysis there did not appear to be any problems with the protocol. As other researchers attempted to use the three temperature protocol, an issue began to emerge. The mastercurves appear to be the same and statistics support this assumption. However, the shift factor relationships required to obtain the mastercurves are not the same between the differing protocols. There are a couple reasons why the shift factor relationships are different. First, the reduced test procedure did not encompass the full range of temperatures that the original procedure did. As a result, data at temperatures greater than 35°C were extrapolated. Second, the number of points defining the shift factor relationship in the reduced temperature protocol was less than the five temperature protocol. Figure 4.12 shows the shift factor relationship for both testing schemes for the mixture presented previously. The three temperature curve has been extrapolated to show the difference at 54.4°C.

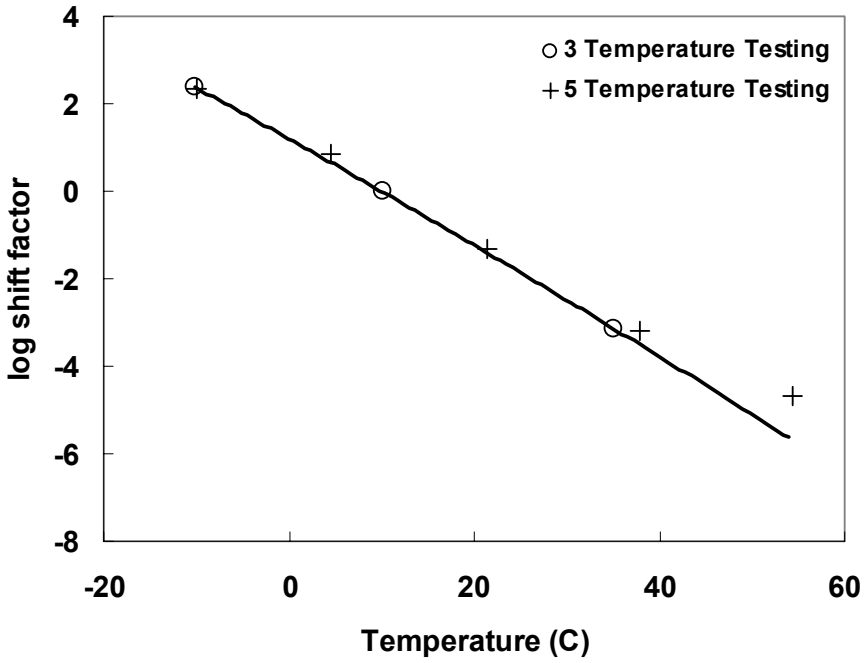

Figure 4.12 – Shift factor difference between the number of testing temperatures

4.2.4 Conclusion

Based on the findings from above, the three- and five-temperature protocols produce statistically the same dynamic modulus mastercurves. However, it was found that there is dissimilarity in the shift factor relationship. Since this was not evident until approximately halfway through the testing, a drastic change to the testing program could not be made. As a result, a couple of items were addressed. The dissimilarity could be addressed in the remaining mixtures by adding 54.4°C to the list of testing temperatures. This modification would add a test temperature that would follow the previous testing temperatures. By doing this an additional point is added to the shift factor curve and the full range of temperatures from TP62 are included in the protocol. In the last half of the mixtures tested, this approach was used. It was felt that reverting back to the original 5 temperature testing setup during the middle of the experimental work could cause

problems in comparison between mixtures tested under different temperature conditions. The addition of 54°C to the dynamic modulus test resulted in a four-temperature protocol. This protocol achieved the results desired from the three-temperature testing which was a shorter testing time. The five-temperature protocol provided testing over a wider range of temperatures and defined the temperature and shift factor relationship more accurately. With the four-temperature protocol, both of these items were accomplished. The testing time was shorter than the original protocol states (~10.5 versus 12 hours) and the temperature and shift factor relationship was developed using the full range of temperatures as given in TP62.

4.3 Variation in Pavement Performance Using Witczak and Hirsch Models in Place of Laboratory Measurements

4.3.1 Predictive Model Comparison

Dynamic moduli predicted by the Hirsch and Witczak's models were compared to the measured data to determine the quality of each model. Witzak's model was developed over the range of temperatures and air voids. However, the Hirsch model was developed within the temperature range between 4° and 38°C. That is, the measured data at -10° and 54.4°C in this research were outside the range of temperatures used to develop the model. Also, the lowest temperature the DSR could handle in this research was 16°C, so the binder data for the Hirsch model at 10°C were extrapolated. As a result, data for 10°, 35°, and 54.4°C are presented for the Hirsch model, but only 35°C fits the input requirements for the model. Also, the air voids under which the Hirsch model was developed are 5.6% to 11.2%, whereas all the data in this report have air voids of 4% ± 0.5%.

In order to determine the accuracy of the models, the % error approach was utilized at each frequency and temperature combination, in which the % error was determined by dividing the difference in the dynamic modulus between the measured and the predicted values by the measured dynamic modulus. This resulted in large quantities of data that had to be summarized. The % error calculations were averaged for differing frequencies at the same temperature for each mixture. Following this, the data were grouped by ranges of % error. The ranges selected include <5, 5<x<15, 15<x<25, 25<x<35, 35<x<45, and >45 % error. After grouping, the percentage of the total number of mixtures that fell within each range was calculated and plotted against the test temperature. Figure 4.13(a) provides a summary for the Witczak prediction, and Figure 4.13(b) provides the data for the Hirsch prediction.

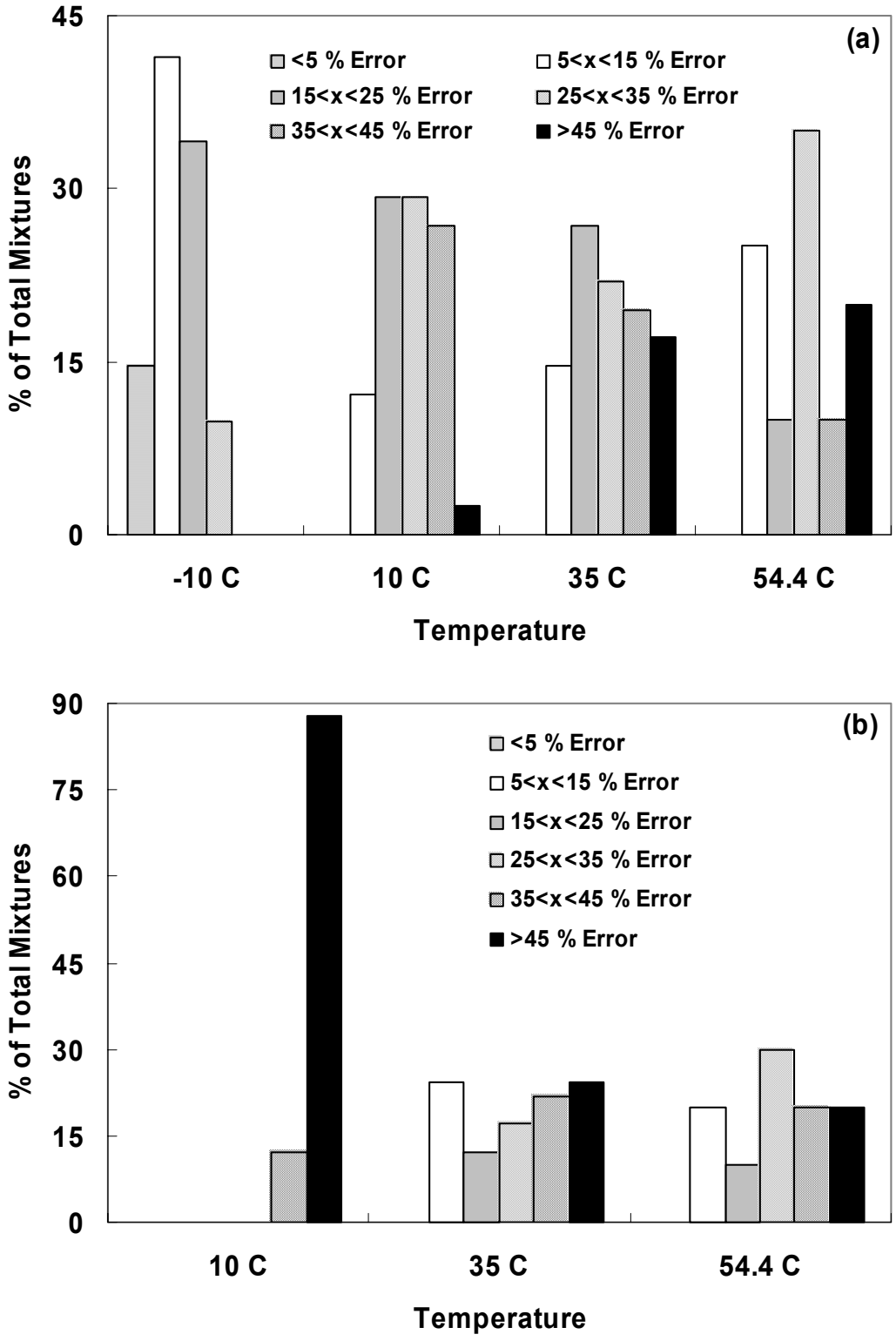

Figure 4.13 – (a) Summary of percent error in dynamic moduli for Witczak's prediction; (b) Summary of percent error in dynamic moduli for Hirsch prediction.

First, it needs to be noted that the scales used in Figures 4.13(a) and 4.13(b) are different. From Figure 4.13(a) it seems that Witczak's prediction at cooler temperatures is better than at warmer temperatures. Also, the Hirsch model, as shown in Figure 4.13(b), performs very poorly at 10°C and approximately the same as Witczak's model at the remaining temperatures. The poorer prediction of the Hirsch model at 10°C could be due to the fact that the binder data at this temperature were extrapolated.

In addition to the prediction summaries shown in Figure 4.13, it is likewise beneficial to see the prediction accuracies of the two models using graphs, as shown in Figures 4.14 to 4.16. In each of these graphs, open symbols are used to represent Hirsch predictions, black symbols Witczak prediction, and gray symbols the measured data. Each of the figures attempts to illustrate a relatively good prediction using Witczak's model in the (a) and (b) graphs, whereas the (c) and (d) graphs show a mixture with a poor prediction. The mixture with a good prediction is S9.5B–Fine replicate 3 and the one with a poor prediction is I19.0B–Fine replicate 1. Multiple plots are presented to allow various comparisons. Similar results are seen with the Hirsch data at 10°C as were seen in the other evaluation. Figure 4.16 shows the line of equality between Witczak and Hirsch and the measured data.

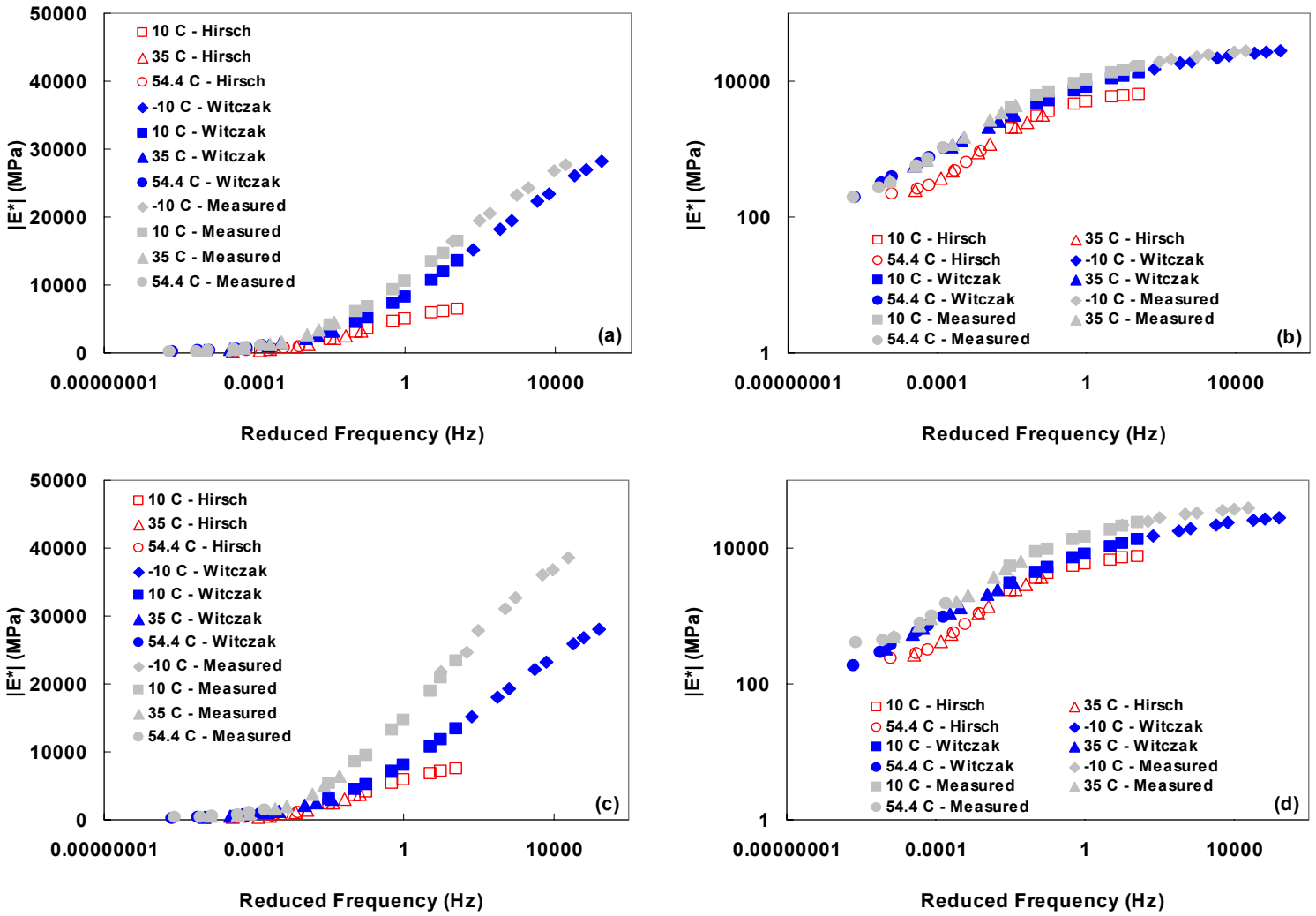

Figure 4.14 – Mastercurves of measured moduli compared to predicted moduli yielding a relatively good prediction for S9.5B–Fine replicate 3 in figures (a) and (b) and a relatively poor prediction for I19.0B–Fine replicate 1 in figures (c) and (d).

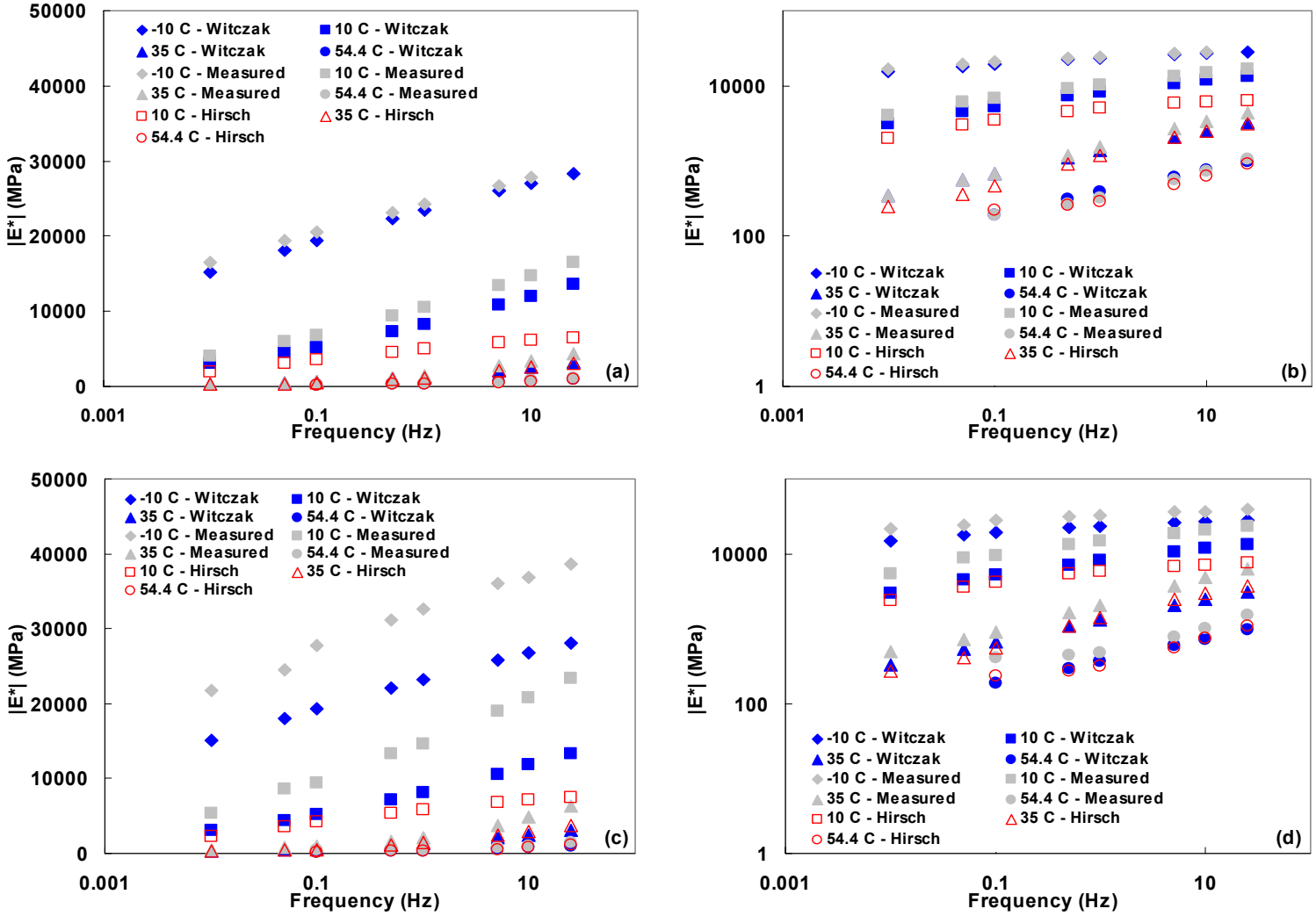

Figure 4.15 – Unshifted measured moduli compared to unshifted predicted moduli yielding a relatively good prediction for S9.5B–Fine replicate 3 in figures (a) and (b) and a relatively poor prediction for I19.0B–Fine replicate 1 in figures (c) and (d).

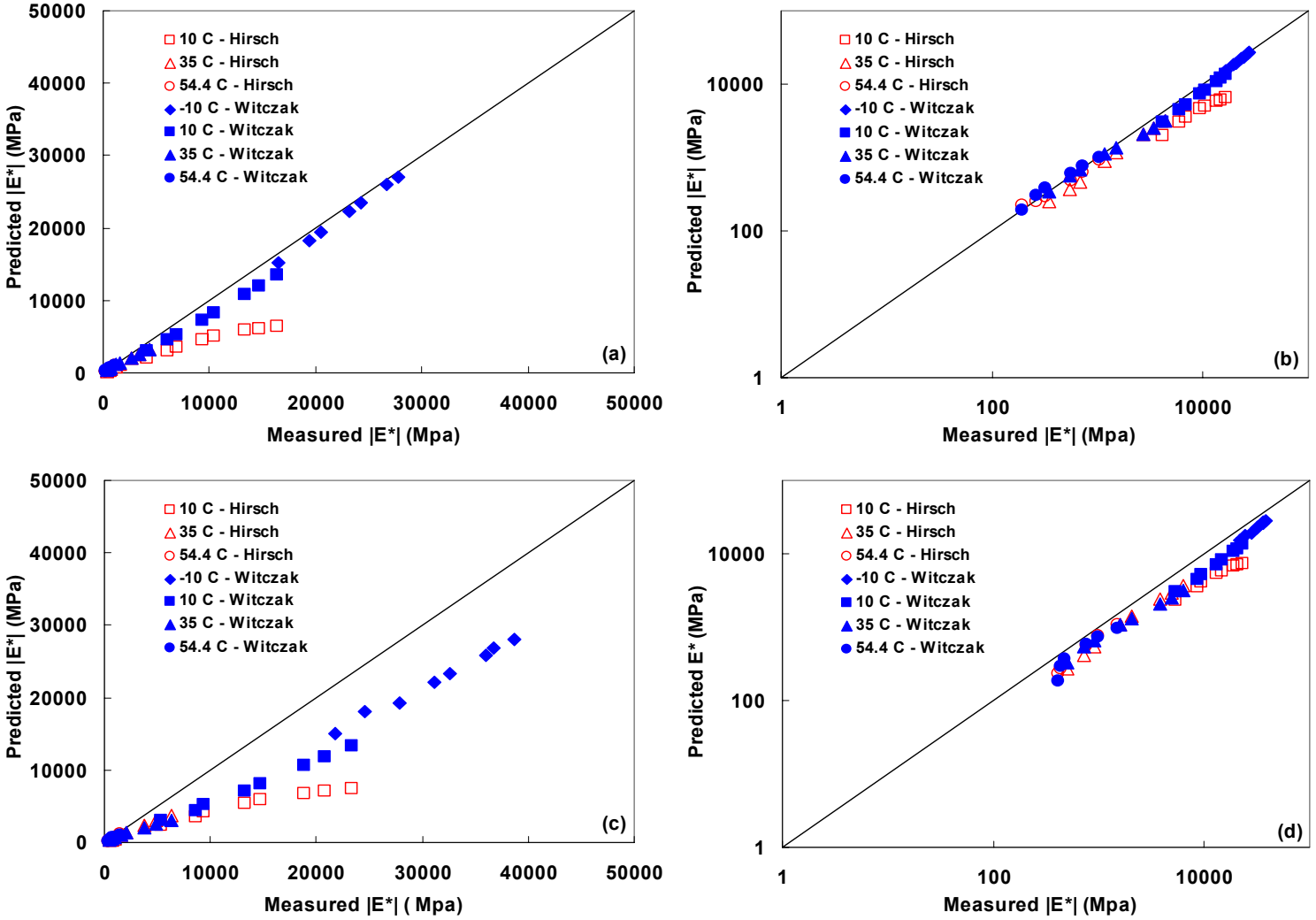

Figure 4.16 – Line of equality of predicted moduli vs. measured moduli yielding a relatively good prediction for S9.5B–Fine replicate 3 in figures (a) and (b) and a relatively poor prediction for I19.0B–Fine replicate 1 in figures (c) and (d).

4.3.2 Effects of Predictive Errors on Pavement Performance

Simply stating the % error in the |E*| prediction is not what matters most to pavement engineers. The true consequences of these errors show up in performance predictions. To evaluate the effect of the errors involved in predicting the dynamic modulus of asphalt mixtures, three pavement scenarios were selected. Table 4.2 shows the critical components of the pavement structures and asphalt mixtures. Moduli of aggregate base and subgrade used in the analysis were 414 and 105 MPa, respectively. These cases were used to predict performance in both fatigue cracking and permanent deformation using the measured dynamic modulus as well as using the predicted values from the Hirsch and Witczak models.

It would have been preferable if the NCHRP 1-37A Design Guide software could have been used for this evaluation; however, its release was too recent to be implemented in this analysis. The performance prediction analysis that was adopted in this research employed the Asphalt Institute fatigue life prediction model (23) and the rutting model presented in the NCHRP 1-37A Design Guide (24). Even though the analysis, without all the design components (i.e., traffic, climate, etc.), is not as comprehensive as the one presented in the NCHRP 1-37A Design Guide, it will yield some indications of the effects of prediction inaccuracy on the pavement design.

Table 4.2 – Summary of Performance Prediction Scenarios

Case	H_{AC}[a] (mm)	H_{Agg}[b] (mm)	Surface Course	Intermediate Course
#1	75	300	75 mm of S9.5B–Fine (Limestone) with poor prediction	-
#2	150	450	75 mm of S9.5B–Fine replicate 3 with good prediction	75 mm of I19.0B–Fine replicate 1 with poor prediction
#3	150	450	75 mm of S9.5–Fine (Limestone) with poor prediction	75 mm of I19.0B–Fine replicate 1 with poor prediction

Note:
[a]thickness of the asphalt layer; and [b]thickness of the aggregate base

4.3.2.1 Fatigue Life

The Asphalt Institute model presented in Eq. 4.1 was used to calculate the fatigue life of the three pavements described in Table 4.2. EverStress, a multilayered elastic analysis program, was used to calculate tensile strain at the bottom of the asphalt layer. The dynamic modulus of the asphalt layer was determined at 25°C and a frequency of 10Hz.

$$N_f = 0.00432 * C\left(\frac{1}{\varepsilon_t}\right)^{3.921}\left(\frac{1}{E*}\right)^{0.854} \quad (4.1)$$

where $C = 10^M$;

$$M = 4.84\left(\frac{V_b}{V_a + V_b} - 0.69\right);$$

V_b = effective binder content (%);

V_a = air voids (%);

N_f = number of repetitions to fatigue cracking;

ε_t = tensile strain at the critical location; and

$E*$ = dynamic modulus of asphalt concrete (psi).

In this analysis, it was assumed that the surface and intermediate courses have the same fatigue characteristics. That is, the fatigue model coefficients and the dynamic modulus of the intermediate course were used in Eq. 4.1 to calculate the fatigue life of pavement Cases 2 and 3.

Table 4.3 presents the fatigue lives predicted from Eq. 4.1 using the measured dynamic modulus and the dynamic moduli predicted from the Witczak and Hirsch models. Also presented in Table 4.3 are % errors, N_f (%), that are calculated between the predicted fatigue life using the measured dynamic modulus and the predicted fatigue life using the predicted dynamic modulus.

For Case 1 it is interesting to note that the error in the modulus prediction is about 50% for both Hirsch and Witczak models but there is only a reduction of 25 to 30% in predicted fatigue life. Case 2 was constructed to evaluate the effect of inaccurate prediction of dynamic modulus in an intermediate course assuming that the surface course prediction was relatively accurate. From Table 4.3 it is shown that the predicted modulus for the surface layer was relatively accurate and the prediction error for the modulus of the intermediate course is about 50%. It is shown through the fatigue analysis that a 50% error in dynamic modulus of intermediate layer causes about a 40% error in the fatigue performance prediction even though the dynamic modulus of the surface layer is accurate.

Case 3 shows a combination of a poor prediction of the surface course coupled with a poor prediction of the intermediate course. The modulus prediction errors in Case 3 are about 50% for both of the surface and intermediate courses. The error in the fatigue life prediction is over 50%. In Cases 1 and 2, the % error in the fatigue prediction was not as large as the % error in the modulus prediction. It is apparent that there are some

compounding effects of prediction errors in the surface and intermediate courses on the fatigue performance prediction.

In summary, an approximately 50% error in the dynamic modulus predicted from the predictive models causes about 25 to 50% error in the fatigue life prediction. The magnitude of the fatigue life prediction error may change depending on the performance prediction analysis method used, pavement structures, and mixture types for different layers.

Table 4.3 – Performance Prediction Results

	Fatigue Data – 25°C, 10Hz			Rutting Data – 54.4°C, 10Hz – 12.5mm failure		
Case 1	**N_f (in thousands)**	**N_f, % error**	**Modulus (MPa) top/bottom**	**N_f (in thousands)**	**N_f, % error**	**Modulus (MPa) top/bottom**
Measured	580	-	8542/ -	152	-	1303/ -
Hirsch	422	27.3	4316/ -	53	65.2	676/ -
Witczak	430	25.8	4640/ -	61	60.1	731/ -
Case 2						
Measured	3398	-	5240/9928	70	-	731/1000
Hirsch	1906	43.9	4095/4785	41	41.3	641/752
Witczak	2051	39.6	4868/4771	56	20.2	758/731
Case 3						
Measured	4360	-	8542/9928	230	-	1303/1000
Hirsch	1949	55.3	4316/4785	46	80.0	676/752
Witczak	2008	53.9	4640/4771	52	77.3	731/731

4.3.2.2 Rutting

The rutting model used in the analysis is shown in Eq. 4.2. The sublayering method adopted in the NCHRP 1-37A Design Guide was used. EverStress was used to calculate the resilient strains at three points within the asphalt layer. The analysis was performed assuming the temperature of 54.4°C and 10 Hz loading. The number of cycles to failure was determined based on the failure criterion of 12.5 mm surface rut depth.

$$\frac{\varepsilon_p}{\varepsilon_r} = k_1 * 10^{-3.4488} T^{1.5606} N^{0.479244} \quad (4.2)$$

where $k_1 = (C_1 + C_2 * depth) * 0.328196^{depth}$;

$C_1 = -0.1039 * h_{ac}^2 + 2.4868 * h_{ac} - 17.342$;

$C_2 = 0.0172 * h_{ac}^2 - 1.7331 * h_{ac} 27.428$;

$depth =$ distance to computational point (in.);

$h_{ac} =$ total asphalt layer thickness (in.);

$T =$ temperature (°F);

$N =$ number of load repetitions;

$\varepsilon_p =$ accumulated plastic strain at N repetitions of load; and

$\varepsilon_r =$ resilient strain

Table 4.3 also represents the summary of the rutting predictions. The three pavement cases provide some insight to how modulus affects permanent deformation. The first case is only comprised of a thin surface layer. The modulus prediction error is less than 50%, whereas the % error in the number of cycles to failure is over 60%. Case 2 has a surface layer with relatively good modulus prediction on top of an intermediate layer with poor modulus prediction (about 25% error). It resulted in about 20 to 40% error depending on the predictive model type. The third case yields very poor prediction due to the compounding effect of two poor predictions from the surface and intermediate courses.

In summary, the prediction errors in dynamic modulus have a significant effect on the rutting performance prediction. In the worst case scenario investigated in this research, up to 80% error in the pavement service life prediction was found.

4.4 Effect of Mixture Variables on Dynamic Modulus

Since dynamic modulus is one of the most important material properties, it is important to know how this property varies with differing mix designs. The large database of mixtures from North Carolina provides an opportunity to look at one aspect of this variability. NCDOT Superpave mixtures in Table 3.1 are classified depending on factors such as traffic level and gradation that allow grouping of similar mixtures. There were several mixtures that fell into the same classification. These classifications were S9.5B–Fine gradation, S9.5C–Fine gradation, and I19.0B–Fine gradation. Refer to Table 3.1 for more information on these designations. What is important to note is that the mixtures in each classification meet the same aggregate gradation and traffic design requirements. There were five mixtures classified S9.5B–Fine, four mixtures classified S9.5C–Fine, and four mixtures classified I19.0B–Fine. The mastercurves are presented in Figures 4.17 through 4.19 to illustrate the variability between mixtures of the same classification. Each of the mastercurves is an average of three replicate specimens.

Fortunately, many of the replicate mixtures had the same aggregate source, PG grade, and asphalt source. As a result, this allows for further evaluation of these mixtures. For example, in Figure 4.17(a) for S9.5B–Fine mixtures, replicates 2, 3, and 4 have identical sources for component materials and they have the closest mastercurves. Replicate 1 has a different aggregate source but the same binder grade and source and its mastercurve is close to the other replicates. Replicate 0 is the least like the other replicates. This mixture has different aggregate and asphalt sources but the PG grade is the same. Considering that replicate 1 had a different aggregate source and the curve was similar to replicates 2, 3, and 4 may indicate that the aggregate source has less impact on |E*|. However, replicate 0 having a

slightly different curve than replicates 1, 2, 3, and 4 may indicate binder source has a greater impact on |E*| even considering the PG grade was the same. However, the effect of binder source is not significant compared to effects of other binder variables that will be discussed below.

Another note comes from the S9.5C–Fine mixtures presented in Figures 4.18(a) and 4.18(b). All four mixtures have identical sources for binder and aggregate. The only difference is that replicate 3 has a PG grade of 64-22 whereas the other mixtures have a grade of PG 70-22. Replicate 3 has the most deviation at lower reduced frequencies. This trend makes sense because the difference in these two binders is in the high temperature grade, which affects the material behavior at the low reduced frequencies. Also, replicates 1, 2, and 3 have similar asphalt content, whereas slightly higher asphalt content is used in replicate 3. The difference in the dynamic modulus mastercurve could be from the binder grade or asphalt content, but is likely a combination of both.

Finally, Figures 4.19(a) and 4.19(b) show the I19.0B–Fine mixtures. The binder source and grade is the same for all four mixtures. The only differences are aggregate source and asphalt content. However, from the investigation of S9.5B–Fine mixtures, it was found that the aggregate source did not seem to impact the modulus value. It seems that a significantly higher asphalt content in I19.0B–Fine replicate 0 (5.4%) than in the rest of the I19.0B mixtures (4.3 to 4.5%) is the main reason for the lower modulus at the low reduced frequencies.

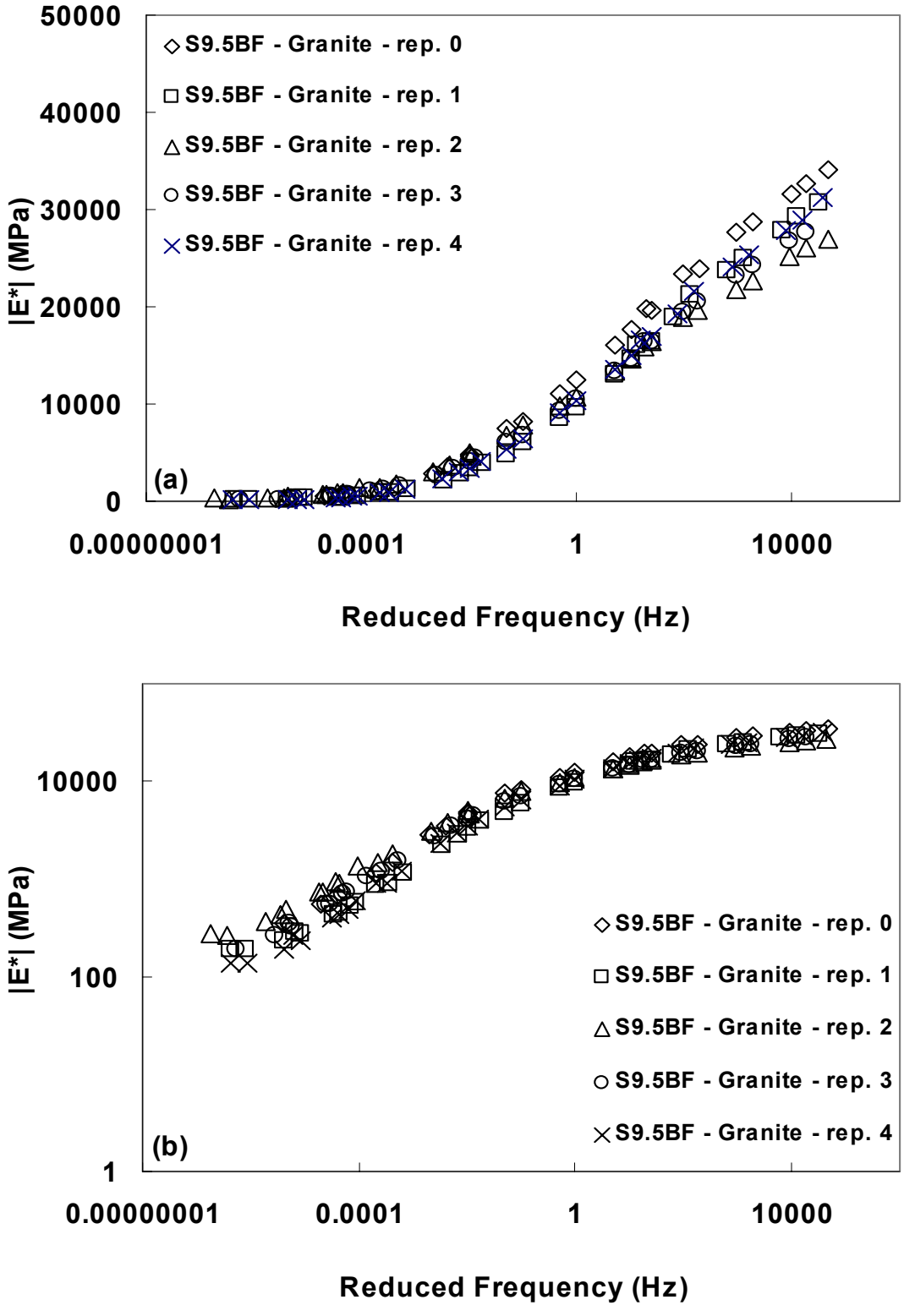

Figure 4.17 Mastercurves for S9.5B–Fine mixtures: (a) semi-log scale; (b) log-log scale

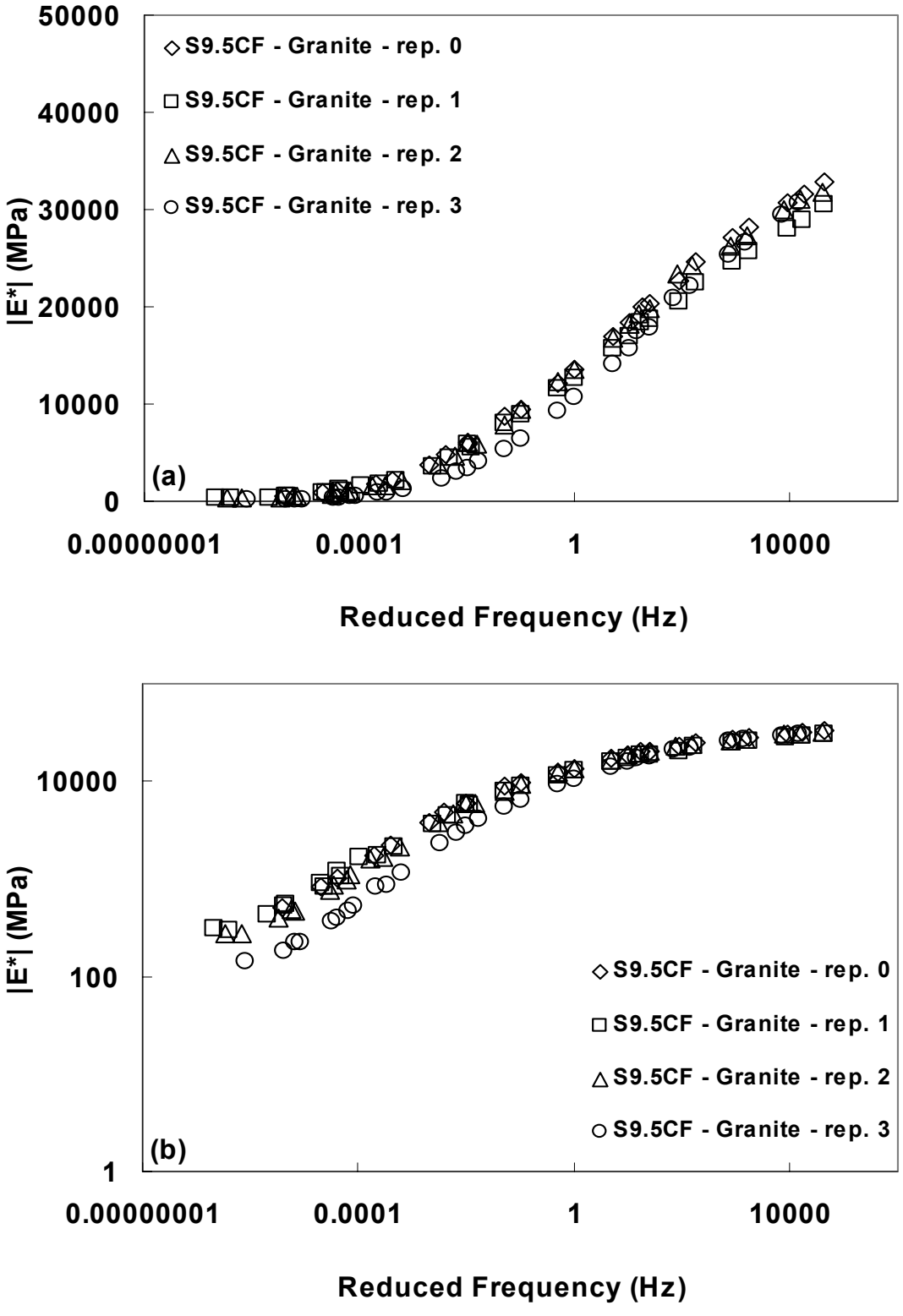

Figure 4.18 Mastercurves for S9.5C–Fine mixtures: (a) semi-log scale; (b) log-log scale

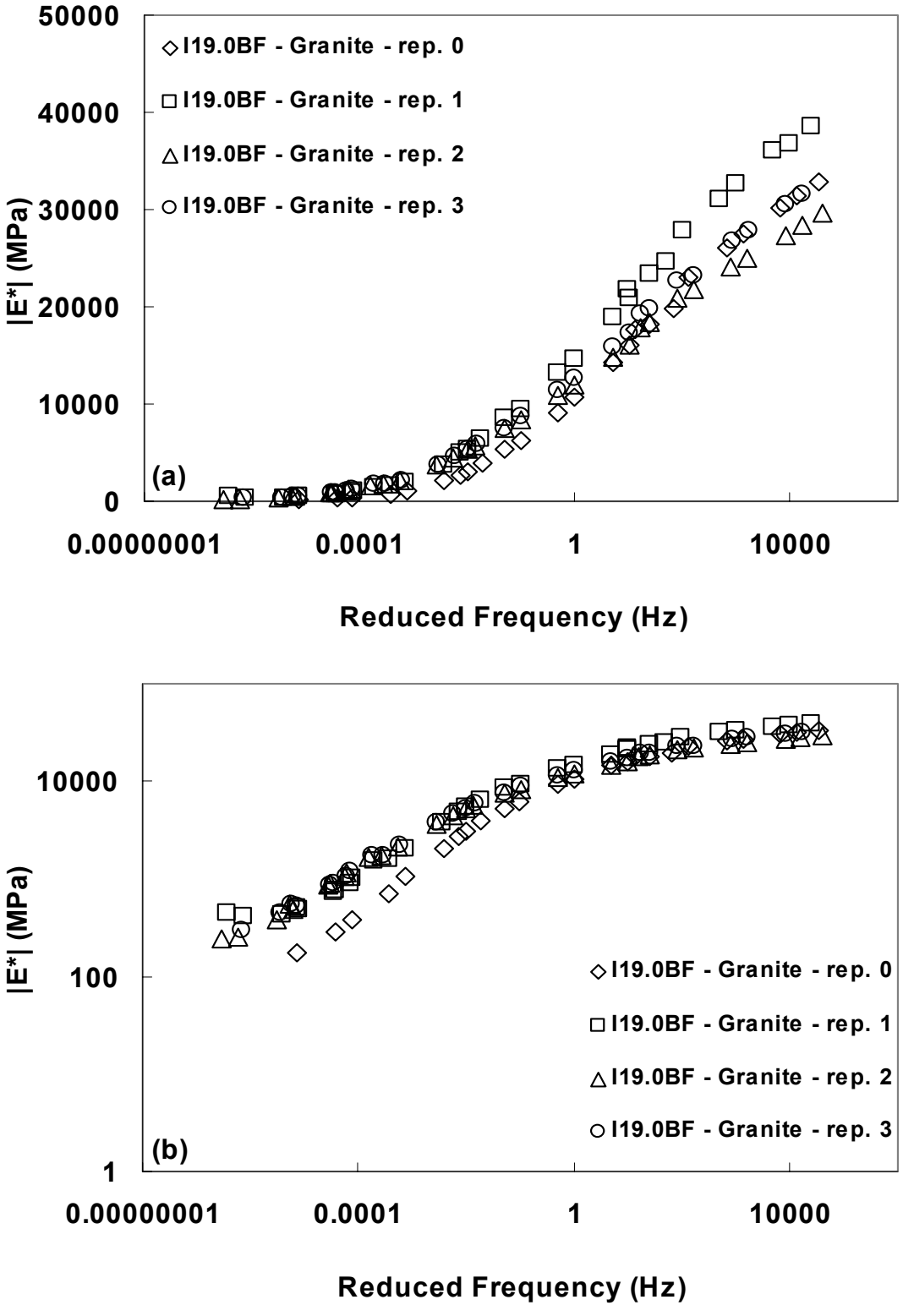

Figure 4.19 Mastercurves for I19.0B–Fine mixtures: (a) semi-log scale; (b) log-log scale

5. CONCLUSIONS

The dynamic modulus testing of Superpave mixtures commonly used in North Carolina resulted in a large database that can be used for various purposes. A total of 42 mixtures were tested in uniaxial compression.

The comparison of uniaxial and triaxial test results shows that there seems to be minimal effect of confining pressure at low temperatures but significant effect at high temperatures.

The investigation into reducing the number of testing temperatures for dynamic modulus suggests:

1. The mastercurves obtained from five temperature and three temperature test protocols are statistically the same.
2. However, the three-temperature protocol requires the extrapolation of the shift factor for temperatures higher than 35°C, which was the highest temperature in the three-temperature protocol. It was found that this extrapolation did not yield accurate enough dynamic moduli values at temperatures higher than 35°C. After considering these issues, a four-temperature protocol was developed.

The investigation of the effects of predictive errors in the dynamic modulus on the pavement performance was conducted by applying phenomenological pavement performance models and the multilayered elastic analysis to three pavement cases. The findings are summarized below:

1. About 50% error in the dynamic modulus predicted from the predictive models causes about 25 to 50% error in the fatigue life prediction.

2. In the rutting analysis, a much greater effect of the dynamic modulus predictive errors was found. In the worst case scenario investigated in this research, up to 80% error in the pavement service life was found.

The parametric study of the effects of mixture variables on the dynamic modulus revealed the following conclusions:

1. Aggregate source and gradation, within the same NCDOT Superpave classification, do not seem to have a significant effect on dynamic modulus.
2. Binder source, binder PG grade, and asphalt content seem to affect the dynamic modulus of asphalt mixtures.

6. REFERENCES

1. Shook, J.F., B.F. Kallas, and B.F. McLeod. Factors Influencing Dynamic Modulus of Asphalt Concrete. *Journal of Association of Asphalt Paving Technologists*, Vol. 38, 1969.

2. Kallas, B.F. Dynamic Modulus of Asphalt Concrete in Tension and Tension-Compression. *Journal of Association of Asphalt Paving Technologists*, Vol. 39, 1970.

3. Bohn, A.O., P. Ullidtz, and R. Stubstad. The Dynamic Modulus of Asphalt Concrete Surfaces. *Dansk Vejtidsskrift*, Vol. 47, 1970.

4. Cragg, R. and P.S. Pell. The Dynamic Stiffness of Bituminous Road Materials. *Journal of Association of Asphalt Paving Technologists*, Vol. 40, 1971.

5. Yeager L.L. and L.E. Wood. Recommended Procedure for Determining the Dynamic Modulus of Asphalt Mixtures. In *Transportation Research Record: Journal of the Transportation Research Board, No. 549*, TRB, National Research Council, Washington, D.C., 1975.

6. Majidzadeh, K., S. Khedr, and M. El-Mojarrush. Evaluation of Permanent Deformation in Asphalt Concrete Pavements. In *Transportation Research Record: Journal of the Transportation Research Board, No. 715*, TRB, National Research Council, Washington, D.C., 1979.

7. Akhter, G.F. and M.W. Witczak. Sensitivity of Flexible Pavement Performance to Bituminous Mix Properties. In *Transportation Research Record: Journal of the Transportation Research Board, No. 1036*, TRB, National Research Council, Washington, D.C., 1985.

8. Miller J.S., J. Uzan, and M.W. Witczak. Modification of the Asphalt Institute Bituminous Mix Modulus Predictive Equation. In *Transportation Research Record: Journal of the Transportation Research Board, No. 911*, TRB, National Research Council, Washington, D.C., 1983.

9. Kim, Y.R. and Y.C. Lee. Interrelationships among Stiffnesses of Asphalt-Aggregate Mixtures. *Journal of Association of Asphalt Paving Technologists*, Vol. 64, 1995, pp. 575-609.

10. Witczak, M.W. and O.A. Fonseca. Revised Predictive Model for Dynamic Modulus of Asphalt Mixtures. In *Transportation Research Record: Journal of the Transportation Research Board, No. 1540*, TRB, National Research Council, Washington, D.C., 1996.

11. Daniel, J.S. and Y.R. Kim. Relationships among Rate-Dependent Stiffnesses of Asphalt Concrete Using Laboratory and Field Test Methods. In *Transportation Research Record: Journal of the Transportation Research Board, No. 1630*, TRB, National Research Council, Washington, D.C., 1998, pp. 3-9.

12. Lee, H.J., J.S. Daniel, and Y.R. Kim. Laboratory Performance Evaluation of Modified Asphalt Mixtures for Inchon Airport Pavements. *International Journal of Pavement Engineering*, Vol. 1, No. 2, 2000.

13. Lee, H.J., J.Y. Choi, Y. Zhao, and Y.R. Kim. Laboratory Evaluation of the Effects of Aggregate Gradation and Binder Type on Performance of Asphalt Mixtures. *International Conference of Asphalt Pavements*, 2001.

14. Chehab, G.R., Y.R. Kim, R.A. Schapery, M.W. Witczak, R. Bonaquist, B. Huang, R. Roque, R. Davis, J. Penia, A. Molenaar, and E. Masad. Characterization of Asphalt Concrete in Uniaxial Tension using a Viscoelastoplastic Continuum Damage Model. *Journal of Association of Asphalt Paving Technologists*, Vol. 72, 2003, pp. 315-355.

15. Kim, Y.R., Y. Seo, M. King, and M. Momen. Dynamic Modulus Testing of Asphalt Concrete in Indirect Tension Mode. In *Transportation Research Record: Journal of the Transportation Research Board,* TRB, National Research Council, Washington, D.C., 2004.

16. AASHTO. Standard Method of Test for Determining Dynamic Modulus of Hot-Mix Asphalt Concrete Mixtures. *American Association of State Highway and Transportation Officials*, TP 62-03, 2003.

17. Witczak, M.W. Simple Performance Test: Test Results and Recommendations. *NCHRP 9-19 Interim Task C Report, Privileged Document by Transportation Research Board,* 2000.

18. Christensen, D.W., Jr, T. Pellinen, and R.F. Bonaquist. Hirsch Model for Estimating the Modulus of Asphalt Concrete. *Journal of Association of Asphalt Paving Technologists*, Vol. 72, 2003, pp. 97-121.

19. AASHTO. Standard Method of Test for Determining Theoretical Maximum Specific Gravity and Density of Bituminous Paving Mixtures. *American Association of State Highway and Transportation Officials*, T209.

20. Chehab, G.R., E. O'Quinn, Y.R. Kim. Specimen Geometry Study for Direct Tension Test Based on Mechanical Tests and Air Void Variation in SGC-Compacted Asphalt Concrete Specimens. In *Transportation Research Record: Journal of the Transportation Research Board,* TRB, National Research Council, Washington, D.C., 2000.

21. ASTM. Standard Test Method for Bulk Specific Gravity and Density of Compacted Bituminous Mixtures Using Automatic Vacuum Sealing Method. *American Society for Testing and Materials*, D6752-03, 2003.

22. Connecticut Transportation Institute. E* - Dynamic Modulus Test Protocol – Problems and Solutions. Final Report, 2003.

23. Huang, Y.H. *Pavement Analysis and Design.* Pearson Prentice Hall, Upper Saddle River, 2004.

24. Guide for Mechanistic-Empirical Design of New and Rehabilitated Pavement Structures. Final Report. *NCHRP*, ARA, Inc. and ERES Consultants Division, March, 2004.

APPENDIX A: DATA TABLES FOR ASPHALT MIXTURES TESTED

Table A-1 – S9.5A–Coarse – Granite

Temp (°C)	Rep.	Parameters	Frequency (Hz)							
			0.01	0.05	0.1	0.5	1	5	10	25
-10	1	|E*| (MPa)	20510	24590	26113	29152	30291	33215	34483	36028
		Phase Angle, Φ (°)	8.8	0.0	3.6	5.1	5.4	4.1	3.5	3.7
		Average Peak Stress (MPa)	1.212	1.438	1.495	1.637	1.691	1.859	1.918	2.078
		Average Peak Strain (με)	59	58	57	56	56	56	56	58
	2	|E*| (MPa)	20399	22271	24169	28465	29611	32353	33721	35061
		Phase Angle, Φ (°)	8.5	11.9	5.4	5.1	5.3	3.8	3.3	2.9
		Average Peak Stress (MPa)	1.212	1.438	1.495	1.637	1.691	1.859	1.918	2.076
		Average Peak Strain (με)	59	65	62	58	57	57	57	59
	3	|E*| (MPa)	18507	23576	21705	25344	26454	28986	29832	31318
		Phase Angle, Φ (°)	7.4	2.5	4.8	5.0	4.2	3.1	2.5	3.1
		Average Peak Stress (MPa)	1.212	1.438	1.495	1.637	1.691	1.861	1.921	2.083
		Average Peak Strain (με)	65	61	69	65	64	64	64	66
	Avg.	|E*| Average	19805	23479	23996	27653	28785	31518	32679	34136
		Φ Average	8.2	4.8	4.6	5.0	5.0	3.7	3.1	3.2
		|E*| Coeff. of Variation	0.057	0.050	0.092	0.073	0.071	0.071	0.076	0.073
		Φ Coeff. of Variation	0.09	1.32	0.19	0.01	0.14	0.15	0.17	0.12
		|E*| Std. Dev.	1125.9	1162.7	2209.2	2029.5	2047.5	2235.0	2494.5	2487.6
		Φ Std. Dev.	0.765	6.289	0.882	0.040	0.678	0.546	0.525	0.396
10	1	|E*| (MPa)	4465	7315	7948	11191	12482	16115	17719	
		Phase Angle, Φ (°)	30.1	20.1	25.6	18.8	17.0	13.7	12.2	
		Average Peak Stress (MPa)	0.141	0.240	0.282	0.395	0.506	0.701	0.817	
		Average Peak Strain (με)	32	33	36	35	41	44	46	
	2	|E*| (MPa)	5087	8844	8939	12101	13487	17240	18987	21118
		Phase Angle, Φ (°)	27.2	25.1	24.1	17.0	15.5	12.2	10.7	9.3
		Average Peak Stress (MPa)	0.141	0.240	0.282	0.395	0.506	0.702	0.817	0.919
		Average Peak Strain (με)	28	27	32	33	38	41	43	43
	3	|E*| (MPa)	4314	6211	7809	10071	11557	14703	16197	18057
		Phase Angle, Φ (°)	27.2	27.9	21.7	17.2	15.1	11.6	10.7	9.7
		Average Peak Stress (MPa)	0.141	0.240	0.282	0.395	0.507	0.703	0.819	0.922
		Average Peak Strain (με)	33	39	36	39	44	48	51	51
	Avg.	|E*| Average	4622	7457	8232	11121	12508	16019	17634	19587
		Φ Average	28.2	24.3	23.8	17.7	15.8	12.5	11.2	9.5
		|E*| Coeff. of Variation	0.089	0.177	0.075	0.091	0.077	0.079	0.079	0.111
		Φ Coeff. of Variation	0.06	0.16	0.08	0.06	0.06	0.09	0.08	0.03
		|E*| Std. Dev.	409.7	1322.3	616.2	1016.6	965.4	1271.0	1396.5	2164.5
		Φ Std. Dev.	1.656	3.962	1.965	0.985	1.025	1.095	0.851	0.248
35	1	|E*| (MPa)	384	578	687	1172	1480	2727	3480	
		Phase Angle, Φ (°)	27.7	28.7	30.2	33.0	33.1	29.5	28.2	
		Average Peak Stress (MPa)	0.017	0.023	0.028	0.036	0.055	0.109	0.135	
		Average Peak Strain (με)	44	39	41	31	37	40	39	
	2	|E*| (MPa)	352	522	661	1163	1473	2861	3581	4782
		Phase Angle, Φ (°)	29.0	31.1	33.0	34.0	33.1	29.1	27.8	26.4
		Average Peak Stress (MPa)	0.017	0.023	0.028	0.037	0.055	0.109	0.135	0.246
		Average Peak Strain (με)	48	43	43	32	37	38	38	51
	3	|E*| (MPa)	335	522	654	1131	1478	2765	3531	4697
		Phase Angle, Φ (°)	28.9	31.0	31.4	34.2	33.0	28.8	27.3	25.3
		Average Peak Stress (MPa)	0.017	0.023	0.028	0.036	0.055	0.109	0.136	0.248
		Average Peak Strain (με)	50	43	43	32	37	40	38	53
	Avg.	|E*| Average	357	541	667	1156	1477	2784	3530	4739
		Φ Average	28.5	30.3	31.5	33.7	33.1	29.1	27.8	25.8
		|E*| Coeff. of Variation	0.070	0.060	0.026	0.019	0.002	0.025	0.014	0.013
		Φ Coeff. of Variation	0.02	0.04	0.04	0.02	0.00	0.01	0.02	0.03
		|E*| Std. Dev.	25.0	32.5	17.4	21.6	3.5	68.9	50.3	59.9
		Φ Std. Dev.	0.682	1.361	1.377	0.611	0.067	0.327	0.439	0.799

Table A-2 – S9.5A–Fine – Granite

Temp (°C)	Rep.	Parameters	Frequency (Hz)							
			0.01	0.05	0.1	0.5	1	5	10	25
-10	1	|E*| (MPa)	13885	18204	18946	21527	22778	25732	27016	28556
		Phase Angle, Φ (°)	11.1	12.8	9.5	6.5	5.9	4.4	3.7	3.3
		Average Peak Stress (MPa)	1.409	1.578	1.636	1.751	1.809	1.862	1.922	2.077
		Average Peak Strain (με)	101	87	86	81	79	72	71	73
	2	|E*| (MPa)	14848		20011	22979	24027	26758	27972	29526
		Phase Angle, Φ (°)	12.4		7.3	8.4	7.7	5.8	4.9	4.7
		Average Peak Stress (MPa)	1.185		1.468	1.584	1.640	1.810	1.868	2.025
		Average Peak Strain (με)	80		73	69	68	68	67	69
	3	|E*| (MPa)	13578	15502	18721	20763	22007	24942	26218	27754
		Phase Angle, Φ (°)	12.5	6.7	10.1	8.3	8.0	6.2	5.7	5.3
		Average Peak Stress (MPa)	1.072	1.298	1.411	1.527	1.583	1.752	1.809	1.901
		Average Peak Strain (με)	79	84	75	74	72	70	69	69
	Avg.	|E*| Average	14104	16853	19226	21756	22937	25810	27069	28612
		Φ Average	12.0	9.8	8.9	7.7	7.2	5.5	4.7	4.5
		|E*| Coeff. of Variation	0.047	0.113	0.036	0.052	0.044	0.035	0.032	0.031
		Φ Coeff. of Variation	0.06	0.44	0.16	0.14	0.16	0.17	0.21	0.23
		|E*| Std. Dev.	662.6	1910.3	689.2	1125.8	1019.3	910.4	877.9	887.3
		Φ Std. Dev.	0.766	4.302	1.454	1.065	1.121	0.943	1.001	1.019
10	1	|E*| (MPa)	2441	4156	4797	7076	8362	11448	12946	14916
		Phase Angle, Φ (°)	29.6	22.7	22.7	20.6	17.8	13.8	12.2	10.5
		Average Peak Stress (MPa)	0.183	0.268	0.310	0.453	0.722	0.889	1.296	1.440
		Average Peak Strain (με)	75	64	65	64	86	78	100	97
	2	|E*| (MPa)	2758	4291	5415	7493	8747	11713	13266	15143
		Phase Angle, Φ (°)	31.2	22.4	26.8	22.6	20.1	16.5	15.2	14.0
		Average Peak Stress (MPa)	0.141	0.240	0.282	0.397	0.510	0.706	0.822	0.923
		Average Peak Strain (με)	51	56	52	53	58	60	62	61
	3	|E*| (MPa)	2444	3744	4756	6893	8034	10976	12375	14350
		Phase Angle, Φ (°)	30.9	28.1	23.9	22.3	20.0	15.9	14.5	13.7
		Average Peak Stress (MPa)	0.169	0.268	0.311	0.453	0.566	0.761	0.876	0.979
		Average Peak Strain (με)	69	72	65	66	70	69	71	68
	Avg.	|E*| Average	2548	4064	4989	7154	8381	11379	12862	14803
		Φ Average	30.6	24.4	24.5	21.8	19.3	15.4	14.0	12.7
		|E*| Coeff. of Variation	0.072	0.070	0.074	0.043	0.043	0.033	0.035	0.028
		Φ Coeff. of Variation	0.03	0.13	0.09	0.05	0.07	0.09	0.11	0.15
		|E*| Std. Dev.	182.2	284.8	369.3	307.3	356.7	373.1	451.3	408.5
		Φ Std. Dev.	0.895	3.200	2.146	1.080	1.316	1.408	1.582	1.956
35	1	|E*| (MPa)	221	321	393	646	885	1738	2288	3204
		Phase Angle, Φ (°)	22.1	26.9	29.3	34.2	32.7	30.2	28.2	27.0
		Average Peak Stress (MPa)	0.011	0.013	0.017	0.029	0.045	0.076	0.107	0.165
		Average Peak Strain (με)	51	42	43	44	51	44	47	52
	2	|E*| (MPa)	206	315	391	650	902	1799	2310	3243
		Phase Angle, Φ (°)	23.5	27.2	28.4	34.2	32.5	29.7	28.1	26.6
		Average Peak Stress (MPa)	0.017	0.023	0.028	0.037	0.057	0.109	0.135	0.243
		Average Peak Strain (με)	82	72	72	57	63	61	58	75
	3	|E*| (MPa)	246	342	412	673	912	1760	2267	3138
		Phase Angle, Φ (°)	23.1	27.2	29.0	34.6	32.6	30.0	29.0	27.3
		Average Peak Stress (MPa)	0.017	0.023	0.028	0.037	0.057	0.110	0.135	0.244
		Average Peak Strain (με)	69	66	68	55	62	62	60	78
	Avg.	|E*| Average	224	326	399	656	900	1766	2289	3195
		Φ Average	22.9	27.1	28.9	34.3	32.6	30.0	28.4	27.0
		|E*| Coeff. of Variation	0.090	0.043	0.030	0.022	0.015	0.018	0.009	0.017
		Φ Coeff. of Variation	0.03	0.01	0.02	0.01	0.00	0.01	0.02	0.01
		|E*| Std. Dev.	20.2	14.1	11.8	14.4	13.8	31.0	21.5	52.9
		Φ Std. Dev.	0.735	0.180	0.437	0.248	0.068	0.267	0.503	0.363

Table A-3 – S9.5A–Fine – Limestone

Temp (°C)	Rep.	Parameters	Frequency (Hz)							
			0.01	0.05	0.1	0.5	1	5	10	25
-10	1	|E*| (MPa)	13975	17037	16762	19260	20195	22021	22865	23847
		Phase Angle, Φ (°)	8.3	7.7	6.5	5.5	4.8	3.5	3.0	2.8
		Average Peak Stress (MPa)	1.083	1.264	1.309	1.401	1.446	1.579	1.627	1.754
		Average Peak Strain (με)	77	74	78	73	72	72	71	74
	2	|E*| (MPa)	15199	17842	18323	21279	22325	24204	25180	26321
		Phase Angle, Φ (°)	8.4	10.9	6.6	5.3	5.0	3.9	3.2	3.3
		Average Peak Stress (MPa)	1.082	1.263	1.308	1.398	1.443	1.577	1.625	1.754
		Average Peak Strain (με)	71	71	71	66	65	65	65	67
	3	|E*| (MPa)	14887	18558	17509	20380	21382	23459	24321	25398
		Phase Angle, Φ (°)	7.9	9.8	5.6	4.7	4.6	3.0	2.5	2.3
		Average Peak Stress (MPa)	1.084	1.264	1.310	1.401	1.446	1.580	1.628	1.757
		Average Peak Strain (με)	73	68	75	69	68	67	67	69
	Avg.	|E*| Average	14687	17813	17531	20307	21300	23228	24122	25189
		Φ Average	8.2	9.5	6.3	5.2	4.8	3.5	2.9	2.8
		|E*| Coeff. of Variation	0.043	0.043	0.045	0.050	0.050	0.048	0.049	0.050
		Φ Coeff. of Variation	0.03	0.17	0.09	0.08	0.04	0.12	0.12	0.18
		|E*| Std. Dev.	635.9	761.1	781.2	1011.4	1067.4	1109.9	1170.4	1250.1
		Φ Std. Dev.	0.249	1.627	0.546	0.390	0.186	0.436	0.340	0.491
10	1	|E*| (MPa)	3239	4665	5507	7630	8647	11154	12285	13806
		Phase Angle, Φ (°)	25.3	20.7	19.3	16.4	14.8	11.2	10.0	9.5
		Average Peak Stress (MPa)	0.212	0.296	0.360	0.466	0.551	0.761	0.867	0.947
		Average Peak Strain (με)	65	64	65	61	64	68	71	69
	2	|E*| (MPa)	3417	5076	5993	8032	9217	11812	13006	14758
		Phase Angle, Φ (°)	26.2	24.6	20.0	17.2	15.8	12.7	10.7	10.2
		Average Peak Stress (MPa)	0.225	0.316	0.383	0.497	0.586	0.811	0.923	1.008
		Average Peak Strain (με)	66	62	64	62	64	69	71	68
	3	|E*| (MPa)	3875	5680	6282	8596	9628	12192	13485	15002
		Phase Angle, Φ (°)	24.2	17.7	18.2	15.3	14.0	10.6	9.5	8.5
		Average Peak Stress (MPa)	0.226	0.316	0.384	0.498	0.588	0.812	0.924	1.011
		Average Peak Strain (με)	58	56	61	58	61	67	69	67
	Avg.	|E*| Average	3510	5140	5927	8086	9164	11720	12925	14522
		Φ Average	25.2	21.0	19.2	16.3	14.9	11.5	10.1	9.4
		|E*| Coeff. of Variation	0.093	0.099	0.066	0.060	0.054	0.045	0.047	0.044
		Φ Coeff. of Variation	0.04	0.16	0.05	0.06	0.06	0.09	0.06	0.09
		|E*| Std. Dev.	327.8	510.2	391.8	485.2	492.9	525.1	604.3	631.9
		Φ Std. Dev.	0.968	3.445	0.894	0.946	0.901	1.069	0.595	0.846
35	1	|E*| (MPa)	307	458	568	955	1237	2266	0	3696
		Phase Angle, Φ (°)	27.5	29.3	30.7	32.2	31.6	28.3	-6.6	25.0
		Average Peak Stress (MPa)	0.011	0.021	0.028	0.049	0.073	0.101	0.000	0.282
		Average Peak Strain (με)	35	46	48	51	59	45	0	76
	2	|E*| (MPa)	360	478	589	945	1226	2227	2852	3630
		Phase Angle, Φ (°)	22.6	28.4	29.9	31.9	31.8	28.0	24.8	25.1
		Average Peak Stress (MPa)	0.011	0.022	0.029	0.052	0.077	0.108	0.173	0.301
		Average Peak Strain (με)	32	47	50	55	63	48	61	83
	3	|E*| (MPa)	348	523	655	1107	1456	2622	3325	4302
		Phase Angle, Φ (°)	27.3	29.6	29.6	30.9	30.8	26.3	23.7	22.9
		Average Peak Stress (MPa)	0.011	0.022	0.029	0.052	0.077	0.108	0.174	0.304
		Average Peak Strain (με)	33	43	45	47	53	41	52	71
	Avg.	|E*| Average	338	486	604	1002	1306	2372	2059	3876
		Φ Average	25.8	29.1	30.1	31.7	31.4	27.5	14.0	24.3
		|E*| Coeff. of Variation	0.083	0.068	0.075	0.090	0.099	0.092	0.874	0.096
		Φ Coeff. of Variation	0.11	0.02	0.02	0.02	0.02	0.04	1.28	0.05
		|E*| Std. Dev.	28.1	33.1	45.6	90.4	129.5	217.4	1798.7	370.4
		Φ Std. Dev.	2.759	0.600	0.573	0.686	0.536	1.048	17.827	1.257
54.4	1	|E*| (MPa)	0	223	199	250	300	534	0	1043
		Phase Angle, Φ (°)	0.0	19.7	19.9	25.2	26.4	27.3	0.0	30.6
		Average Peak Stress (MPa)	0.000	0.006	0.011	0.021	0.027	0.044	0.000	0.082
		Average Peak Strain (με)	0	29	54	85	91	83	0	79
	2	|E*| (MPa)	149	155	169	233	283	516	0	1010
		Phase Angle, Φ (°)	14.1	16.9	18.9	23.7	25.7	26.4	-6.6	28.9
		Average Peak Stress (MPa)	0.004	0.007	0.011	0.023	0.029	0.048	0.000	0.087
		Average Peak Strain (με)	28	44	68	97	103	92	0	86
	3	|E*| (MPa)	158	161	184	261	325	602	811	1195
		Phase Angle, Φ (°)	16.3	18.2	19.3	23.5	25.0	25.3	24.8	26.7
		Average Peak Stress (MPa)	0.006	0.009	0.014	0.028	0.036	0.060	0.088	0.117
		Average Peak Strain (με)	36	53	78	109	112	100	108	97
	Avg.	|E*| Average	102	179	184	248	303	551	270	1083
		Φ Average	10.1	18.3	19.4	24.1	25.7	26.3	6.1	28.7
		|E*| Coeff. of Variation	0.867	0.209	0.080	0.056	0.069	0.082	1.732	0.091
		Φ Coeff. of Variation	0.87	0.08	0.03	0.04	0.03	0.04	2.73	0.07
		|E*| Std. Dev.	88.5	37.4	14.7	13.9	20.8	45.3	468.2	98.8
		Φ Std. Dev.	8.851	1.429	0.485	0.968	0.673	1.030	16.568	1.960

Table A-4 – S9.5B–Coarse – Granite

Temp (°C)	Rep.	Parameters	Frequency (Hz)							
			0.01	0.05	0.1	0.5	1	5	10	25
-10	1	|E*| (MPa)	16718		23110	25887	27253	30146	31629	33125
		Phase Angle, Φ (°)	10.2		6.7	5.7	5.1	4.0	2.1	2.1
		Average Peak Stress (MPa)	1.241		1.552	1.666	1.693	1.859	1.919	2.077
		Average Peak Strain (με)	74		67	64	62	62	61	63
	2	|E*| (MPa)	13924	18201	18042	21696	23079	25955	27305	28654
		Phase Angle, Φ (°)	13.6	9.6	11.8	9.4	8.8	7.4	6.8	6.1
		Average Peak Stress (MPa)	1.241	1.465	1.551	1.666	1.693	1.858	1.919	2.077
		Average Peak Strain (με)	89	80	86	77	73	72	70	72
	3	|E*| (MPa)	14142	18586	18929	21809	23207	26247	27363	28876
		Phase Angle, Φ (°)	10.7	6.6	5.8	6.6	5.6	3.7	3.4	3.1
		Average Peak Stress (MPa)	1.241	1.467	1.552	1.666	1.694	1.858	1.920	2.077
		Average Peak Strain (με)	88	79	82	76	73	71	70	72
	Avg.	|E*| Average	14928	18393	20027	23131	24513	27449	28766	30218
		Φ Average	11.5	8.1	8.1	7.3	6.5	5.0	4.1	3.8
		|E*| Coeff. of Variation	0.104	0.015	0.135	0.103	0.097	0.085	0.086	0.083
		Φ Coeff. of Variation	0.16	0.26	0.40	0.27	0.31	0.40	0.59	0.55
		|E*| Std. Dev.	1553.9	272.3	2706.5	2387.5	2373.9	2339.8	2479.8	2519.7
		Φ Std. Dev.	1.817	2.088	3.222	1.925	2.031	2.038	2.407	2.063
10	1	|E*| (MPa)	2359	4188	5071	7909	9272	12926	14622	17148
		Phase Angle, Φ (°)	31.1	29.2	24.7	21.2	19.3	14.3	12.8	12.1
		Average Peak Stress (MPa)	0.254	0.395	0.508	0.622	0.733	1.014	1.154	1.263
		Average Peak Strain (με)	108	94	100	79	79	78	79	74
	2	|E*| (MPa)	2605	4524	5334	7674	8945	12400	14043	15994
		Phase Angle, Φ (°)	33.8	27.0	27.6	22.6	20.6	16.4	15.0	13.6
		Average Peak Stress (MPa)	0.169	0.311	0.423	0.622	0.734	1.011	1.153	1.262
		Average Peak Strain (με)	65	69	79	81	82	82	82	79
	3	|E*| (MPa)	2337	4212	4913	7374	8630	11931	13433	15450
		Phase Angle, Φ (°)	30.8	25.9	23.2	20.0	18.0	13.9	12.4	11.3
		Average Peak Stress (MPa)	0.170	0.310	0.423	0.621	0.733	1.015	1.155	1.264
		Average Peak Strain (με)	73	74	86	84	85	85	86	82
	Avg.	|E*| Average	2434	4308	5106	7652	8949	12419	14033	16197
		Φ Average	31.9	27.4	25.2	21.3	19.3	14.9	13.4	12.3
		|E*| Coeff. of Variation	0.061	0.044	0.042	0.035	0.036	0.040	0.042	0.054
		Φ Coeff. of Variation	0.05	0.06	0.09	0.06	0.07	0.09	0.10	0.10
		|E*| Std. Dev.	149.0	187.6	212.5	268.4	321.0	497.9	594.8	867.1
		Φ Std. Dev.	1.634	1.663	2.247	1.287	1.295	1.362	1.378	1.175
35	1	|E*| (MPa)		328	411	763	1067	2149	2815	3966
		Phase Angle, Φ (°)		30.5	31.7	34.7	33.0	30.8	28.9	27.3
		Average Peak Stress (MPa)		0.023	0.028	0.051	0.097	0.164	0.217	0.356
		Average Peak Strain (με)		70	69	67	91	77	77	90
	2	|E*| (MPa)	237	368	454	811	1082	2216	2853	3982
		Phase Angle, Φ (°)	27.3	31.7	33.4	37.1	36.2	32.4	30.8	29.0
		Average Peak Stress (MPa)	0.013	0.022	0.028	0.045	0.070	0.138	0.189	0.299
		Average Peak Strain (με)	56	61	62	56	64	62	66	75
	3	|E*| (MPa)	180	281	364	681	927	1899	2518	3557
		Phase Angle, Φ (°)	24.3	28.2	29.7	33.4	33.1	29.1	28.5	27.2
		Average Peak Stress (MPa)	0.014	0.022	0.028	0.045	0.070	0.135	0.190	0.299
		Average Peak Strain (με)	81	79	77	66	75	71	75	84
	Avg.	|E*| Average	208	326	410	752	1025	2088	2729	3835
		Φ Average	25.8	30.1	31.6	35.1	34.1	30.8	29.4	27.8
		|E*| Coeff. of Variation	0.194	0.134	0.110	0.087	0.083	0.080	0.067	0.063
		Φ Coeff. of Variation	0.08	0.06	0.06	0.05	0.05	0.05	0.04	0.04
		|E*| Std. Dev.	40.3	43.8	45.0	65.6	85.2	167.2	183.4	241.0
		Φ Std. Dev.	2.096	1.746	1.887	1.864	1.798	1.684	1.261	0.979

Table A-5 – S9.5B0–Fine – Granite

Temp (°C)	Rep.	Parameters	Frequency (Hz)							
			0.01	0.05	0.1	0.5	1	5	10	25
-10	1	|E*| (MPa)	14329	16304	18422	20193	21225	23377	24287	25375
		Phase Angle, Φ (°)	8.8	11.5	4.7	5.1	4.9	3.4	3.1	2.8
		Average Peak Stress (MPa)	1.212	1.438	1.495	1.637	1.691	1.861	1.921	2.082
		Average Peak Strain (με)	85	88	81	81	80	80	79	82
	2	|E*| (MPa)	13313	15130	16051	18875	19790	22059	23042	24160
		Phase Angle, Φ (°)	9.5	12.6	8.9	5.6	6.1	4.6	4.3	3.6
		Average Peak Stress (MPa)	1.212	1.438	1.495	1.637	1.692	1.861	1.922	2.082
		Average Peak Strain (με)	91	95	93	87	85	84	83	86
	3	|E*| (MPa)	14570	15961	17733	20645	21634	23881	24764	26020
		Phase Angle, Φ (°)	8.0	8.4	4.1	4.3	4.0	2.7	2.2	2.2
		Average Peak Stress (MPa)	1.212	1.438	1.495	1.637	1.691	1.860	1.919	2.077
		Average Peak Strain (με)	83	90	84	79	78	78	77	80
	Avg.	|E*| Average	14071	15798	17402	19904	20883	23106	24031	25185
		Φ Average	8.8	10.8	5.9	5.0	5.0	3.6	3.2	2.9
		|E*| Coeff. of Variation	0.047	0.038	0.070	0.046	0.046	0.041	0.037	0.038
		Φ Coeff. of Variation	0.09	0.20	0.44	0.14	0.20	0.26	0.33	0.25
		|E*| Std. Dev.	667.3	603.6	1219.5	919.7	968.7	940.7	889.0	944.6
		Φ Std. Dev.	0.753	2.181	2.623	0.695	1.022	0.938	1.055	0.714
10	1	|E*| (MPa)	3150	4699	5629	7659	8670	11262	12433	14003
		Phase Angle, Φ (°)	26.7	26.8	18.0	17.2	15.5	12.4	11.1	10.5
		Average Peak Stress (MPa)	0.141	0.240	0.282	0.395	0.507	0.703	0.819	0.921
		Average Peak Strain (με)	45	51	50	52	58	62	66	66
	2	|E*| (MPa)	3299	4538	5605	7751	8683	11161	12349	13905
		Phase Angle, Φ (°)	28.0	24.7	18.9	17.9	16.3	13.2	11.6	11.1
		Average Peak Stress (MPa)	0.141	0.240	0.282	0.395	0.507	0.703	0.819	0.921
		Average Peak Strain (με)	43	53	50	51	58	63	66	66
	3	|E*| (MPa)	3288	5227	5905	7827	8865			
		Phase Angle, Φ (°)	26.2	24.2	19.4	16.0	14.7			
		Average Peak Stress (MPa)	0.141	0.240	0.282	0.395	0.506			
		Average Peak Strain (με)	43	46	48	50	57			
	Avg.	|E*| Average	3246	4821	5713	7746	8739	11211	12391	13954
		Φ Average	27.0	25.2	18.8	17.0	15.5	12.8	11.4	10.8
		|E*| Coeff. of Variation	0.026	0.075	0.029	0.011	0.012	0.006	0.005	0.005
		Φ Coeff. of Variation	0.03	0.05	0.04	0.06	0.05	0.05	0.03	0.04
		|E*| Std. Dev.	82.9	360.4	166.5	84.5	109.0	71.5	59.3	69.2
		Φ Std. Dev.	0.911	1.379	0.710	0.966	0.804	0.597	0.333	0.472
35	1	|E*| (MPa)	220	345	445	778	1019	1928	2461	3284
		Phase Angle, Φ (°)	31.1	33.4	33.7	34.1	33.5	29.4	27.9	26.2
		Average Peak Stress (MPa)	0.017	0.023	0.028	0.036	0.056	0.109	0.135	0.245
		Average Peak Strain (με)	77	65	63	47	54	56	55	75
	2	|E*| (MPa)	261	416	521	891	1153	2104	2658	3474
		Phase Angle, Φ (°)	31.5	31.8	33.3	34.5	33.3	29.5	27.5	25.9
		Average Peak Stress (MPa)	0.017	0.023	0.028	0.036	0.055	0.109	0.136	0.247
		Average Peak Strain (με)	65	54	54	41	48	52	51	71
	3	|E*| (MPa)	243	393	489	842	1078	1966	2467	3240
		Phase Angle, Φ (°)	29.8	30.5	31.6	32.5	32.0	27.9	26.4	25.3
		Average Peak Stress (MPa)	0.017	0.023	0.028	0.036	0.055	0.108	0.135	0.244
		Average Peak Strain (με)	69	57	58	43	51	55	55	75
	Avg.	|E*| Average	241	385	485	837	1083	2000	2529	3332
		Φ Average	30.8	31.9	32.9	33.7	32.9	28.9	27.3	25.8
		|E*| Coeff. of Variation	0.085	0.095	0.078	0.068	0.062	0.046	0.044	0.037
		Φ Coeff. of Variation	0.03	0.04	0.03	0.03	0.03	0.03	0.03	0.02
		|E*| Std. Dev.	20.5	36.4	38.0	56.8	67.4	92.9	112.0	124.4
		Φ Std. Dev.	0.900	1.433	1.093	1.081	0.838	0.918	0.765	0.433

Table A-6 – S9.5B1–Fine – Granite

Temp (°C)	Rep.	Parameters	Frequency (Hz)							
			0.01	0.05	0.1	0.5	1	5	10	25
-10	1	|E*| (MPa)	16441	19860	21429	24373	25802	28989	30300	31887
		Phase Angle, Φ (°)	14.5	7.4	14.9	11.1	11.1	10.0	9.3	9.0
		Average Peak Stress (MPa)	1.213	1.439	1.496	1.638	1.692	1.862	1.921	2.080
		Average Peak Strain (με)	74	72	70	67	66	64	63	65
	2	|E*| (MPa)	15704	17301	20771	22883	24169	27015	28138	29511
		Phase Angle, Φ (°)	9.7	10.4	10.0	6.7	5.7	4.6	4.2	4.1
		Average Peak Stress (MPa)	1.213	1.439	1.496	1.638	1.692	1.862	1.920	2.080
		Average Peak Strain (με)	77	83	72	72	70	69	68	70
	3	|E*| (MPa)	16173	19630	21306	23846	24799	27784		
		Phase Angle, Φ (°)	10.0	13.9	8.0	6.4	6.6	5.0		
		Average Peak Stress (MPa)	1.213	1.439	1.496	1.638	1.693	1.862		
		Average Peak Strain (με)	75	73	70	69	68	67		
	Avg.	|E*| Average	16106	18930	21169	23701	24924	27929	29219	30699
		Φ Average	11.4	10.6	11.0	8.1	7.8	6.6	6.8	6.6
		|E*| Coeff. of Variation	0.023	0.075	0.017	0.032	0.033	0.036	0.052	0.055
		Φ Coeff. of Variation	0.23	0.31	0.32	0.33	0.37	0.46	0.54	0.54
		|E*| Std. Dev.	372.8	1415.8	349.7	755.7	823.5	994.9	1529.1	1680.3
		Φ Std. Dev.	2.678	3.263	3.550	2.643	2.866	3.012	3.630	3.510
10	1	|E*| (MPa)	3550	5033	6532	8838	10046	13676	15452	17359
		Phase Angle, Φ (°)	36.3	28.0	28.1	26.0	24.1	20.9	19.0	17.8
		Average Peak Stress (MPa)	0.141	0.240	0.282	0.395	0.507	0.703	0.818	0.918
		Average Peak Strain (με)	40	48	43	45	50	51	53	53
	2	|E*| (MPa)	3176	4689	5582	8185	9323	12440	13892	15713
		Phase Angle, Φ (°)	28.3	20.7	22.9	19.3	17.4	14.4	12.9	12.4
		Average Peak Stress (MPa)	0.141	0.240	0.282	0.395	0.507	0.703	0.818	0.918
		Average Peak Strain (με)	44	51	51	48	54	57	59	58
	3	|E*| (MPa)	3266	4677	5972	8509	9676	12928	14453	16438
		Phase Angle, Φ (°)	27.8	25.9	24.9	19.6	18.0	14.6	13.4	12.4
		Average Peak Stress (MPa)	0.141	0.240	0.282	0.395	0.507	0.703	0.818	0.917
		Average Peak Strain (με)	43	51	47	46	52	54	57	56
	Avg.	|E*| Average	3331	4800	6029	8511	9681	13015	14599	16503
		Φ Average	30.8	24.9	25.3	21.6	19.8	16.6	15.1	14.2
		|E*| Coeff. of Variation	0.059	0.042	0.079	0.038	0.037	0.048	0.054	0.050
		Φ Coeff. of Variation	0.16	0.15	0.10	0.18	0.19	0.22	0.23	0.22
		|E*| Std. Dev.	195.2	201.8	477.3	326.6	361.2	622.3	790.1	825.0
		Φ Std. Dev.	4.778	3.799	2.607	3.782	3.687	3.678	3.415	3.139
35	1	|E*| (MPa)	312	453	559	938	1211	2271	2891	3890
		Phase Angle, Φ (°)	27.7	30.4	31.4	35.2	34.1	30.8	29.1	27.3
		Average Peak Stress (MPa)	0.017	0.023	0.028	0.036	0.055	0.109	0.135	0.243
		Average Peak Strain (με)	54	50	50	39	46	48	47	62
	2	|E*| (MPa)	266	401	489	840	1105	2109	2712	3720
		Phase Angle, Φ (°)	23.7	28.4	28.2	32.2	31.6	28.7	27.2	25.5
		Average Peak Stress (MPa)	0.017	0.023	0.028	0.036	0.055	0.109	0.135	0.243
		Average Peak Strain (με)	63	56	58	43	50	52	50	65
	3	|E*| (MPa)	269	420	526	906	1189	2269	2933	3971
		Phase Angle, Φ (°)	25.1	27.7	29.7	33.0	32.8	29.3	27.2	25.2
		Average Peak Stress (MPa)	0.017	0.023	0.028	0.036	0.055	0.109	0.135	0.243
		Average Peak Strain (με)	63	54	54	40	47	48	46	61
	Avg.	|E*| Average	282	425	525	895	1169	2216	2845	3860
		Φ Average	25.5	28.8	29.8	33.5	32.8	29.6	27.8	26.0
		|E*| Coeff. of Variation	0.091	0.061	0.066	0.056	0.048	0.042	0.041	0.033
		Φ Coeff. of Variation	0.08	0.05	0.06	0.05	0.04	0.04	0.04	0.04
		|E*| Std. Dev.	25.7	26.0	34.7	50.0	56.1	93.2	117.2	127.9
		Φ Std. Dev.	2.020	1.408	1.640	1.532	1.224	1.108	1.089	1.131
54.4	1	|E*| (MPa)		246	211	254	295	473	618	917
		Phase Angle, Φ (°)		17.6	12.6	19.5	21.6	27.2	29.2	32.2
		Average Peak Stress (MPa)		0.006	0.009	0.011	0.016	0.020	0.023	0.026
		Average Peak Strain (με)		23	41	44	56	43	38	28
	2	|E*| (MPa)		173	189	224	262	420	551	815
		Phase Angle, Φ (°)		16.6	15.2	20.4	21.7	27.0	28.6	31.2
		Average Peak Stress (MPa)		0.006	0.009	0.011	0.017	0.020	0.023	0.026
		Average Peak Strain (με)		32	45	50	63	48	42	32
	3	|E*| (MPa)		143	160	209	256	441	581	889
		Phase Angle, Φ (°)		13.3	14.8	21.1	23.2	27.0	29.0	31.7
		Average Peak Stress (MPa)		0.006	0.008	0.011	0.017	0.020	0.023	0.026
		Average Peak Strain (με)		39	53	54	65	46	40	29
	Avg.	|E*| Average		187	187	229	271	444	583	873
		Φ Average		15.8	14.2	20.3	22.2	27.1	28.9	31.7
		|E*| Coeff. of Variation		0.281	0.138	0.100	0.077	0.060	0.057	0.060
		Φ Coeff. of Variation		0.14	0.10	0.04	0.04	0.00	0.01	0.02
		|E*| Std. Dev.		52.6	25.7	22.9	20.9	26.6	33.2	52.8
		Φ Std. Dev.		2.261	1.371	0.783	0.869	0.124	0.322	0.507

Table A-7 – S9.5B2–Fine – Granite

Temp (°C)	Rep.	Parameters	Frequency (Hz)							
			0.01	0.05	0.1	0.5	1	5	10	25
-10	1	|E*| (MPa)	16190	17892	19428	22276	23172	25738	26679	0
		Phase Angle, Φ (°)	11.0	5.5	7.0	7.2	7.4	6.1	5.7	0.0
		Average Peak Stress (MPa)	1.214	1.440	1.497	1.639	1.694	1.863	1.922	0.000
		Average Peak Strain (με)	75	81	77	74	73	72	72	0
	2	|E*| (MPa)	15879	20026	20114	21949	22740	25170	26066	27224
		Phase Angle, Φ (°)	10.7	9.3	9.0	7.3	6.9	5.9	5.3	4.9
		Average Peak Stress (MPa)	1.214	1.440	1.497	1.639	1.694	1.863	1.922	2.079
		Average Peak Strain (με)	76	72	74	75	74	74	74	76
	3	|E*| (MPa)	15421	18913	19168	21383	22179	24491	25348	26589
		Phase Angle, Φ (°)	9.5	4.9	6.0	6.0	5.9	4.4	4.0	3.8
		Average Peak Stress (MPa)	1.214	1.440	1.497	1.640	1.694	1.863	1.922	2.077
		Average Peak Strain (με)	79	76	78	77	76	76	76	78
	Avg.	|E*| Average	15830	18944	19570	21869	22697	25133	26031	17938
		Φ Average	10.4	6.6	7.3	6.8	6.7	5.5	5.0	2.9
		|E*| Coeff. of Variation	0.024	0.056	0.025	0.021	0.022	0.025	0.026	0.866
		Φ Coeff. of Variation	0.08	0.36	0.21	0.11	0.12	0.17	0.18	0.88
		|E*| Std. Dev.	387.2	1067.4	489.1	452.0	498.3	624.3	666.0	15537.7
		Φ Std. Dev.	0.814	2.374	1.510	0.746	0.776	0.932	0.919	2.563
10	1	|E*| (MPa)	5397	7947	8434	10300	11117	13655	14940	16724
		Phase Angle, Φ (°)	29.7	24.5	23.3	18.7	17.5	14.4	12.9	11.3
		Average Peak Stress (MPa)	0.141	0.240	0.282	0.395	0.507	0.703	0.819	0.918
		Average Peak Strain (με)	26	30	33	38	46	51	55	55
	2	|E*| (MPa)	4816	6079	7793	9800	10713	13373	14543	16228
		Phase Angle, Φ (°)	28.8	21.8	24.0	19.4	17.4	14.6	13.3	12.3
		Average Peak Stress (MPa)	0.141	0.240	0.283	0.395	0.507	0.703	0.819	0.918
		Average Peak Strain (με)	29	40	36	40	47	53	56	57
	3	|E*| (MPa)	4685	6181	7149	9485	10443	13073	14337	16089
		Phase Angle, Φ (°)	26.7	25.9	18.6	17.7	16.0	13.2	12.5	11.9
		Average Peak Stress (MPa)	0.141	0.240	0.283	0.396	0.508	0.703	0.817	0.917
		Average Peak Strain (με)	30	39	40	42	49	54	57	57
	Avg.	|E*| Average	4966	6736	7792	9862	10758	13367	14607	16347
		Φ Average	28.4	24.1	21.9	18.6	17.0	14.1	12.9	11.8
		|E*| Coeff. of Variation	0.076	0.156	0.082	0.042	0.032	0.022	0.021	0.020
		Φ Coeff. of Variation	0.05	0.09	0.13	0.05	0.05	0.05	0.03	0.04
		|E*| Std. Dev.	379.0	1050.2	642.1	411.0	339.2	291.1	306.7	333.7
		Φ Std. Dev.	1.558	2.096	2.947	0.859	0.845	0.740	0.438	0.492
35	1	|E*| (MPa)	476	724	904	1480	1851	3172	3856	4795
		Phase Angle, Φ (°)	36.3	35.2	35.5	35.3	33.6	27.9	26.3	23.7
		Average Peak Stress (MPa)	0.017	0.023	0.028	0.037	0.055	0.109	0.136	0.245
		Average Peak Strain (με)	36	31	31	25	30	34	35	51
	2	|E*| (MPa)	451	715	856	1414	1736	3014	3762	4658
		Phase Angle, Φ (°)	34.8	35.1	36.3	37.6	35.7	30.3	28.9	25.7
		Average Peak Stress (MPa)	0.017	0.023	0.028	0.037	0.055	0.110	0.136	0.246
		Average Peak Strain (με)	38	32	33	26	32	36	36	53
	3	|E*| (MPa)	526	791	932	1522	1829	3039	3756	4670
		Phase Angle, Φ (°)	34.7	34.2	34.7	35.7	33.5	28.6	26.6	24.0
		Average Peak Stress (MPa)	0.017	0.023	0.028	0.037	0.056	0.110	0.136	0.245
		Average Peak Strain (με)	32	29	30	24	30	36	36	52
	Avg.	|E*| Average	484	743	897	1472	1805	3075	3791	4708
		Φ Average	35.3	34.8	35.5	36.2	34.3	28.9	27.3	24.5
		|E*| Coeff. of Variation	0.079	0.056	0.043	0.037	0.034	0.028	0.015	0.016
		Φ Coeff. of Variation	0.02	0.02	0.02	0.03	0.04	0.04	0.05	0.04
		|E*| Std. Dev.	38.4	41.9	38.4	54.6	61.3	85.1	55.9	76.1
		Φ Std. Dev.	0.879	0.548	0.827	1.251	1.260	1.236	1.427	1.072
54.4	1	|E*| (MPa)		219	248	349	425	747	973	1369
		Phase Angle, Φ (°)		22.5	25.0	29.0	29.9	31.0	31.2	32.6
		Average Peak Stress (MPa)		0.006	0.009	0.011	0.017	0.021	0.024	0.027
		Average Peak Strain (με)		26	35	32	39	28	25	20
	2	|E*| (MPa)		255	256	335	395	697	897	1328
		Phase Angle, Φ (°)		33.5	26.4	30.5	31.3	32.7	33.0	35.8
		Average Peak Stress (MPa)		0.006	0.009	0.011	0.017	0.021	0.025	0.029
		Average Peak Strain (με)		22	34	34	42	30	28	22
	3	|E*| (MPa)		334	297	398	467	777	982	1345
		Phase Angle, Φ (°)		23.5	21.6	26.3	28.5	29.3	30.0	32.7
		Average Peak Stress (MPa)		0.006	0.009	0.011	0.017	0.021	0.024	0.028
		Average Peak Strain (με)		17	29	28	36	27	25	21
	Avg.	|E*| Average		269	267	360	429	740	950	1347
		Φ Average		26.5	24.3	28.6	29.9	31.0	31.4	33.7
		|E*| Coeff. of Variation		0.219	0.099	0.091	0.085	0.055	0.049	0.015
		Φ Coeff. of Variation		0.23	0.10	0.07	0.05	0.06	0.05	0.05
		|E*| Std. Dev.		59.1	26.5	32.8	36.2	40.7	46.8	20.6
		Φ Std. Dev.		6.057	2.464	2.091	1.374	1.717	1.510	1.841

Table A-8 – S9.5B3–Fine – Granite

Temp (°C)	Rep.	Parameters	Frequency (Hz)							
			0.01	0.05	0.1	0.5	1	5	10	25
-10	1	|E*| (MPa)	16924	19704	20490	23895	25075	27547	28568	
		Phase Angle, Φ (°)	8.0	11.2	4.2	4.6	3.7	2.6	1.9	
		Average Peak Stress (MPa)	1.240	1.494	1.579	1.637	1.691	1.859	1.919	
		Average Peak Strain (με)	73	76	77	69	67	67	67	
	2	|E*| (MPa)	15643	17188	19974	22179	23315	25783	26767	
		Phase Angle, Φ (°)	8.1	6.5	6.7	4.7	4.7	3.1	2.2	
		Average Peak Stress (MPa)	1.241	1.494	1.579	1.637	1.691	1.859	1.919	
		Average Peak Strain (με)	79	87	79	74	73	72	72	
	3	|E*| (MPa)	16974	21501	21215	23529	24561	26895	27920	
		Phase Angle, Φ (°)	9.8	5.3	9.3	6.3	6.0	4.2	3.6	
		Average Peak Stress (MPa)	1.240	1.494	1.579	1.637	1.691	1.860	1.919	
		Average Peak Strain (με)	73	69	74	70	69	69	69	
	Avg.	|E*| Average	16514	19464	20560	23201	24317	26742	27752	
		Φ Average	8.6	7.7	6.7	5.2	4.8	3.3	2.6	
		|E*| Coeff. of Variation	0.046	0.111	0.030	0.039	0.037	0.033	0.033	
		Φ Coeff. of Variation	0.12	0.41	0.38	0.19	0.24	0.25	0.35	
		|E*| Std. Dev.	754.4	2166.5	623.5	903.8	904.7	892.1	912.5	
		Φ Std. Dev.	1.028	3.138	2.529	0.997	1.146	0.818	0.922	
10	1	|E*| (MPa)	3872	5790	6590	9251	10446	13443	14811	
		Phase Angle, Φ (°)	24.3	23.8	19.2	16.4	14.8	11.5	10.1	
		Average Peak Stress (MPa)	0.310	0.395	0.479	0.621	0.733	1.013	1.154	
		Average Peak Strain (με)	80	68	73	67	70	75	78	
	2	|E*| (MPa)	3992	6075	6862	9051	10243	13021	14310	16088
		Phase Angle, Φ (°)	23.6	18.2	17.6	15.1	13.9	10.8	9.6	8.5
		Average Peak Stress (MPa)	0.310	0.395	0.479	0.621	0.733	1.013	1.155	1.264
		Average Peak Strain (με)	78	65	70	69	72	78	81	79
	3	|E*| (MPa)	4446	6265	7121	9712	10797	13634	14994	16767
		Phase Angle, Φ (°)	24.4	24.5	18.8	16.1	14.9	11.8	10.6	10.0
		Average Peak Stress (MPa)	0.310	0.395	0.479	0.621	0.733	1.013	1.155	1.264
		Average Peak Strain (με)	70	63	67	64	68	74	77	75
	Avg.	|E*| Average	4103	6043	6858	9338	10495	13366	14705	16427
		Φ Average	24.1	22.2	18.5	15.9	14.5	11.4	10.1	9.3
		|E*| Coeff. of Variation	0.074	0.040	0.039	0.036	0.027	0.023	0.024	0.029
		Φ Coeff. of Variation	0.02	0.16	0.05	0.04	0.04	0.04	0.05	0.11
		|E*| Std. Dev.	303.0	239.1	265.3	339.1	280.3	313.9	354.4	480.5
		Φ Std. Dev.	0.434	3.461	0.862	0.680	0.555	0.500	0.496	1.031
35	1	|E*| (MPa)	305	495	627	1097	1441	2628	3299	4332
		Phase Angle, Φ (°)	26.4	29.0	29.8	31.0	29.9	25.9	23.9	22.6
		Average Peak Stress (MPa)	0.025	0.034	0.042	0.078	0.111	0.165	0.248	0.388
		Average Peak Strain (με)	83	68	68	71	77	63	75	90
	2	|E*| (MPa)	340	550	683	1169	1498	2670	3309	4317
		Phase Angle, Φ (°)	29.3	29.4	30.7	31.8	30.4	26.3	24.3	22.4
		Average Peak Stress (MPa)	0.020	0.034	0.042	0.078	0.111	0.165	0.248	0.389
		Average Peak Strain (με)	58	61	62	67	74	62	75	90
	3	|E*| (MPa)	398	615	759	1272	1633	2869	3609	4604
		Phase Angle, Φ (°)	29.4	30.1	30.7	31.3	30.5	26.4	24.1	22.9
		Average Peak Stress (MPa)	0.020	0.034	0.042	0.078	0.111	0.166	0.249	0.390
		Average Peak Strain (με)	50	55	56	61	68	58	69	85
	Avg.	|E*| Average	348	554	690	1179	1524	2722	3406	4418
		Φ Average	28.4	29.5	30.4	31.4	30.3	26.2	24.1	22.6
		|E*| Coeff. of Variation	0.136	0.108	0.096	0.074	0.065	0.047	0.052	0.037
		Φ Coeff. of Variation	0.06	0.02	0.02	0.01	0.01	0.01	0.01	0.01
		|E*| Std. Dev.	47.4	60.0	66.2	87.7	98.5	129.1	176.1	161.4
		Φ Std. Dev.	1.706	0.557	0.490	0.389	0.312	0.259	0.232	0.252
54.4	1	|E*| (MPa)		162	170	236	287	492	660	966
		Phase Angle, Φ (°)		14.1	19.0	23.8	25.5	28.5	29.1	33.0
		Average Peak Stress (MPa)		0.006	0.009	0.011	0.017	0.020	0.024	0.027
		Average Peak Strain (με)		34	50	48	58	42	36	28
	2	|E*| (MPa)		184	186	264	320	571	739	1077
		Phase Angle, Φ (°)		18.4	20.7	24.9	27.0	29.8	30.2	32.9
		Average Peak Stress (MPa)		0.006	0.009	0.011	0.017	0.021	0.024	0.028
		Average Peak Strain (με)		30	46	43	52	36	33	26
	3	|E*| (MPa)		217	217	296	352	607	793	1138
		Phase Angle, Φ (°)		25.4	22.1	24.8	26.0	29.6	30.2	34.0
		Average Peak Stress (MPa)		0.006	0.009	0.011	0.017	0.021	0.024	0.028
		Average Peak Strain (με)		26	39	38	47	34	31	25
	Avg.	|E*| Average		187	191	265	320	557	731	1061
		Φ Average		19.3	20.6	24.5	26.1	29.3	29.8	33.3
		|E*| Coeff. of Variation		0.147	0.124	0.113	0.101	0.106	0.092	0.082
		Φ Coeff. of Variation		0.30	0.08	0.03	0.03	0.02	0.02	0.02
		|E*| Std. Dev.		27.6	23.8	29.9	32.4	58.7	66.9	87.2
		Φ Std. Dev.		5.699	1.549	0.643	0.763	0.712	0.667	0.601

Table A-9 – S9.5B4–Fine – Granite

Temp (°C)	Rep.	Parameters	Frequency (Hz)							
			0.01	0.05	0.1	0.5	1	5	10	25
-10	1	|E*| (MPa)	16683	18364	22529	24721	25907	28540	29498	
		Phase Angle, Φ (°)	13.5	9.8	10.6	9.3	9.1	7.3	6.6	
		Average Peak Stress (MPa)	1.355	1.582	1.639	1.752	1.808	1.975	2.035	
		Average Peak Strain (με)	81	86	73	71	70	69	69	
	2	|E*| (MPa)	17117	21920	22534	24733	26028	28795	29947	31256
		Phase Angle, Φ (°)	10.0	12.6	9.6	6.1	5.6	4.3	3.6	2.5
		Average Peak Stress (MPa)	1.355	1.582	1.639	1.752	1.808	1.975	2.036	2.197
		Average Peak Strain (με)	79	72	73	71	69	69	68	70
	3	|E*| (MPa)	16011	17555	19929	23027	24065	26434	27391	
		Phase Angle, Φ (°)	9.5	7.2	8.4	6.1	5.2	3.6	2.8	
		Average Peak Stress (MPa)	1.355	1.582	1.639	1.752	1.808	1.976	2.036	
		Average Peak Strain (με)	85	90	82	76	75	75	74	
	Avg.	|E*| Average	16604	19279	21664	24160	25333	27923	28945	31256
		Φ Average	11.0	9.9	9.5	7.2	6.7	5.1	4.3	2.5
		|E*| Coeff. of Variation	0.034	0.120	0.069	0.041	0.043	0.046	0.047	
		Φ Coeff. of Variation	0.20	0.27	0.12	0.26	0.33	0.39	0.46	
		|E*| Std. Dev.	557.1	2322.3	1502.7	981.2	1100.1	1295.7	1364.5	
		Φ Std. Dev.	2.164	2.683	1.099	1.842	2.175	1.966	1.982	
10	1	|E*| (MPa)	3543	5825	6614	9250	10630	13946	15297	17301
		Phase Angle, Φ (°)	32.8	30.0	27.2	22.0	20.7	16.6	14.8	
		Average Peak Stress (MPa)	0.283	0.395	0.480	0.622	0.735	1.016	1.158	1.264
		Average Peak Strain (με)	80	68	73	67	69	73	76	73
	2	|E*| (MPa)	3522	5247	6700	9343	10604	13882	15434	17524
		Phase Angle, Φ (°)	28.2	23.5	21.4	18.3	16.9	12.9	11.5	10.6
		Average Peak Stress (MPa)	0.282	0.395	0.480	0.622	0.735	1.015	1.157	1.270
		Average Peak Strain (με)	80	75	72	67	69	73	75	72
	3	|E*| (MPa)	3375	5085	6039	8572	9783	12750	14126	15996
		Phase Angle, Φ (°)	27.3	26.4	20.6	17.7	16.2	12.4	10.9	10.0
		Average Peak Stress (MPa)	0.282	0.395	0.480	0.622	0.735	1.016	1.157	1.267
		Average Peak Strain (με)	84	78	80	73	75	80	82	79
	Avg.	|E*| Average	3480	5385	6451	9055	10339	13526	14953	16941
		Φ Average	29.4	26.6	23.0	19.4	17.9	14.0	12.4	10.3
		|E*| Coeff. of Variation	0.026	0.072	0.056	0.046	0.047	0.050	0.048	0.049
		Φ Coeff. of Variation	0.10	0.12	0.16	0.12	0.13	0.16	0.17	0.04
		|E*| Std. Dev.	91.9	389.0	359.5	420.7	481.8	672.7	718.8	825.7
		Φ Std. Dev.	2.937	3.241	3.631	2.337	2.405	2.303	2.066	0.457
35	1	|E*| (MPa)	281	406	512	915	1241	2382	3098	4208
		Phase Angle, Φ (°)	27.4	30.2	31.6	34.2	33.0	30.5	28.3	25.9
		Average Peak Stress (MPa)	0.014	0.028	0.037	0.065	0.097	0.137	0.219	0.388
		Average Peak Strain (με)	51	69	72	71	78	58	71	92
	2	|E*| (MPa)	244	378	483	882	1195	2288	2980	4096
		Phase Angle, Φ (°)	27.0	29.9	31.0	33.5	32.5	29.3	26.9	24.8
		Average Peak Stress (MPa)	0.014	0.028	0.037	0.064	0.097	0.137	0.219	0.388
		Average Peak Strain (με)	58	74	76	73	81	60	74	95
	3	|E*| (MPa)	253	388	490	883	1178	2217	2847	3872
		Phase Angle, Φ (°)	25.4	28.5	30.0	32.8	31.8	29.1	26.5	24.5
		Average Peak Stress (MPa)	0.014	0.028	0.037	0.064	0.097	0.137	0.220	0.387
		Average Peak Strain (με)	56	72	75	73	82	62	77	100
	Avg.	|E*| Average	259	391	495	893	1205	2296	2975	4059
		Φ Average	26.6	29.6	30.9	33.5	32.4	29.6	27.2	25.1
		|E*| Coeff. of Variation	0.074	0.037	0.030	0.021	0.027	0.036	0.042	0.042
		Φ Coeff. of Variation	0.04	0.03	0.03	0.02	0.02	0.03	0.04	0.03
		|E*| Std. Dev.	19.2	14.3	14.9	18.8	32.7	82.9	125.7	171.1
		Φ Std. Dev.	1.070	0.901	0.811	0.718	0.602	0.755	0.965	0.727
54.4	1	|E*| (MPa)		138	143	195	244	455	629	965
		Phase Angle, Φ (°)		18.6	16.4	22.0	23.9	27.0	27.5	29.3
		Average Peak Stress (MPa)		0.009	0.014	0.028	0.036	0.059	0.086	0.114
		Average Peak Strain (με)		62	100	146	148	131	136	118
	2	|E*| (MPa)		125	130	181	226	423	581	904
		Phase Angle, Φ (°)		16.0	17.4	22.4	24.4	26.7	27.1	29.2
		Average Peak Stress (MPa)		0.009	0.014	0.028	0.036	0.059	0.085	0.113
		Average Peak Strain (με)		68	110	157	160	139	147	125
	3	|E*| (MPa)		151	143	189	230	420	571	875
		Phase Angle, Φ (°)		15.9	16.5	20.6	22.7	26.0	26.5	28.6
		Average Peak Stress (MPa)		0.009	0.014	0.028	0.036	0.059	0.085	0.113
		Average Peak Strain (με)		56	100	150	157	140	149	129
	Avg.	|E*| Average		138	139	188	233	433	594	915
		Φ Average		16.9	16.8	21.7	23.7	26.5	27.0	29.0
		|E*| Coeff. of Variation		0.096	0.053	0.038	0.040	0.045	0.052	0.050
		Φ Coeff. of Variation		0.09	0.03	0.04	0.04	0.02	0.02	0.01
		|E*| Std. Dev.		13.2	7.4	7.2	9.3	19.5	30.7	45.6
		Φ Std. Dev.		1.544	0.528	0.961	0.891	0.522	0.479	0.386

Table A-10 – S9.5B–Fine – Limestone

Temp (°C)	Rep.	Parameters	Frequency (Hz)							
			0.01	0.05	0.1	0.5	1	5	10	25
-10	1	|E*| (MPa)	17764	21823	21583	23926	24801	26983	27905	
		Phase Angle, Φ (°)	11.0	7.0	7.0	7.6	7.4	6.2	5.9	
		Average Peak Stress (MPa)	1.355	1.582	1.639	1.752	1.808	1.977	2.037	
		Average Peak Strain (με)	76	72	76	73	73	73	73	
	2	|E*| (MPa)	17096	20233	19997	22643	23472	25139	25917	27022
		Phase Angle, Φ (°)	7.6	10.0	4.8	5.4	4.9	3.2	2.7	2.3
		Average Peak Stress (MPa)	1.151	1.343	1.391	1.487	1.535	1.678	1.728	1.872
		Average Peak Strain (με)	67	66	70	66	65	67	67	69
	3	|E*| (MPa)	17684	22033	21034	23589	24404	26565	27505	28570
		Phase Angle, Φ (°)	10.5	13.8	8.0	8.6	8.8	7.6	6.8	6.4
		Average Peak Stress (MPa)	1.151	1.343	1.391	1.488	1.536	1.678	1.730	1.872
		Average Peak Strain (με)	65	61	66	63	63	63	63	66
	Avg.	|E*| Average	17515	21363	20871	23386	24226	26229	27109	27796
		Φ Average	9.7	10.3	6.6	7.2	7.0	5.7	5.1	4.4
		|E*| Coeff. of Variation	0.021	0.046	0.039	0.028	0.028	0.037	0.039	0.039
		Φ Coeff. of Variation	0.19	0.33	0.25	0.23	0.28	0.39	0.42	0.66
		|E*| Std. Dev.	364.7	984.5	805.3	665.2	682.5	966.6	1051.2	1095.1
		Φ Std. Dev.	1.846	3.405	1.657	1.640	1.969	2.218	2.147	2.873
10	1	|E*| (MPa)	5219	7353	8162	10838	12017	15034	16359	17851
		Phase Angle, Φ (°)	28.2	26.7	22.1	18.7	16.9	13.5	11.9	11.2
		Average Peak Stress (MPa)	0.282	0.395	0.480	0.622	0.735	1.016	1.159	1.271
		Average Peak Strain (με)	54	54	59	57	61	68	71	71
	2	|E*| (MPa)	5777	7588	8943	11528	12522	15266	16437	18133
		Phase Angle, Φ (°)	24.9	22.9	18.7	15.0	14.0	11.1	10.0	9.6
		Average Peak Stress (MPa)	0.240	0.336	0.408	0.528	0.624	0.862	0.983	1.075
		Average Peak Strain (με)	41	44	46	46	50	56	60	59
	3	|E*| (MPa)	5820	7806	8823	11443	12452	15068	16336	18030
		Phase Angle, Φ (°)	25.7	18.3	20.2	17.7	16.2	13.2	12.2	11.5
		Average Peak Stress (MPa)	0.240	0.336	0.408	0.528	0.624	0.862	0.983	1.078
		Average Peak Strain (με)	41	43	46	46	50	57	60	60
	Avg.	|E*| Average	5606	7582	8643	11270	12330	15123	16377	18005
		Φ Average	26.2	22.6	20.3	17.1	15.7	12.6	11.4	10.8
		|E*| Coeff. of Variation	0.060	0.030	0.049	0.033	0.022	0.008	0.003	0.008
		Φ Coeff. of Variation	0.07	0.18	0.08	0.11	0.10	0.10	0.11	0.10
		|E*| Std. Dev.	335.3	226.7	420.7	375.9	273.7	125.0	53.4	143.0
		Φ Std. Dev.	1.710	4.178	1.689	1.935	1.508	1.320	1.207	1.058
35	1	|E*| (MPa)	808	946	1110	1741	2148	3872	4677	5830
		Phase Angle, Φ (°)	30.2	36.3	35.6	36.2	35.0	30.6	26.5	24.3
		Average Peak Stress (MPa)	0.014	0.028	0.037	0.064	0.097	0.138	0.221	0.392
		Average Peak Strain (με)	18	30	33	37	45	36	47	67
	2	|E*| (MPa)	785	1075	1247	1962	2430	4193	4969	6009
		Phase Angle, Φ (°)	29.6	32.8	35.3	35.4	33.5	29.1	25.3	23.1
		Average Peak Stress (MPa)	0.012	0.024	0.031	0.055	0.082	0.115	0.186	0.331
		Average Peak Strain (με)	15	22	25	28	34	28	37	55
	3	|E*| (MPa)	1077	1197	1385	2084	2484	4069	4812	5782
		Phase Angle, Φ (°)	35.2	36.1	35.7	35.3	32.2	28.0	24.8	22.1
		Average Peak Stress (MPa)	0.012	0.024	0.031	0.055	0.082	0.116	0.187	0.331
		Average Peak Strain (με)	11	20	22	26	33	29	39	57
	Avg.	|E*| Average	890	1073	1247	1929	2354	4045	4820	5874
		Φ Average	31.7	35.1	35.6	35.6	33.6	29.2	25.5	23.2
		|E*| Coeff. of Variation	0.182	0.117	0.110	0.090	0.077	0.040	0.030	0.020
		Φ Coeff. of Variation	0.10	0.06	0.01	0.01	0.04	0.04	0.04	0.05
		|E*| Std. Dev.	162.3	125.6	137.5	173.8	180.6	161.7	146.2	119.6
		Φ Std. Dev.	3.099	1.946	0.208	0.500	1.368	1.270	0.896	1.066
54.4	1	|E*| (MPa)	373	388	377	456	531	929	1198	1714
		Phase Angle, Φ (°)	26.0	20.2	23.8	29.8	31.1	30.7	29.3	30.1
		Average Peak Stress (MPa)	0.006	0.009	0.014	0.028	0.036	0.061	0.090	0.124
		Average Peak Strain (με)	15	22	38	62	68	66	75	72
	2	|E*| (MPa)	277	282	343	480	584	1083	1395	1928
		Phase Angle, Φ (°)	18.6	19.6	23.6	30.2	31.2	31.2	29.6	29.7
		Average Peak Stress (MPa)	0.005	0.007	0.012	0.024	0.031	0.052	0.076	0.103
		Average Peak Strain (με)	17	26	35	50	53	48	54	53
	3	|E*| (MPa)	419	330	349	484	585	1011	1309	1838
		Phase Angle, Φ (°)	28.4	22.5	23.2	25.9	27.0	27.5	26.3	26.8
		Average Peak Stress (MPa)	0.005	0.007	0.012	0.024	0.031	0.052	0.077	0.104
		Average Peak Strain (με)	11	22	35	50	53	51	59	57
	Avg.	|E*| Average	356	333	357	473	567	1008	1301	1827
		Φ Average	24.3	20.8	23.5	28.7	29.7	29.8	28.4	28.9
		|E*| Coeff. of Variation	0.203	0.159	0.050	0.033	0.055	0.076	0.076	0.059
		Φ Coeff. of Variation	0.21	0.07	0.01	0.08	0.08	0.07	0.06	0.06
		|E*| Std. Dev.	72.2	53.0	17.9	15.4	30.9	76.9	98.7	107.6
		Φ Std. Dev.	5.092	1.520	0.321	2.373	2.413	1.993	1.810	1.798

Table A-11 – S9.5C–Coarse – Granite

Temp (°C)	Rep.	Parameters	Frequency (Hz)							
			0.01	0.05	0.1	0.5	1	5	10	25
-10	1	|E*| (MPa)	17530	19120	22228	23719	24726	27021	28189	28566
		Phase Angle, Φ (°)	6.9	10.0	5.6	4.3	2.6	3.0	2.6	0.0
		Average Peak Stress (MPa)	1.354	1.580	1.637	1.751	1.806	1.974	2.035	2.201
		Average Peak Strain (με)	77	83	74	74	73	73	72	77
	2	|E*| (MPa)	18615		21988	25581	26360	28884	30241	31646
		Phase Angle, Φ (°)	10.0		6.4	7.6	6.3	5.7	5.7	5.4
		Average Peak Stress (MPa)	1.242		1.581	1.640	1.694	1.860	1.728	1.871
		Average Peak Strain (με)	67		72	64	64	64	57	59
	3	|E*| (MPa)	18056	19554	22899	24162	25330	27685	28663	29740
		Phase Angle, Φ (°)	8.2	2.8	5.6	6.4	4.6	4.1	3.5	3.2
		Average Peak Stress (MPa)	1.242	1.496	1.581	1.640	1.694	1.865	1.923	2.083
		Average Peak Strain (με)	69	77	69	68	67	67	67	70
	Avg.	|E*| Average	18067	19337	22372	24487	25472	27863	29031	29984
		Φ Average	8.4	6.4	5.9	6.1	4.5	4.3	3.9	2.9
		|E*| Coeff. of Variation	0.030	0.016	0.021	0.040	0.032	0.034	0.037	0.052
		Φ Coeff. of Variation	0.19	0.80	0.08	0.28	0.41	0.32	0.40	0.94
		|E*| Std. Dev.	542.7	307.5	472.0	973.0	826.0	943.8	1074.3	1554.3
		Φ Std. Dev.	1.600	5.088	0.457	1.703	1.843	1.385	1.585	2.699
10	1	|E*| (MPa)	5527	7883	9015	11378	12516	15346	16839	18509
		Phase Angle, Φ (°)	21.2	13.1	15.2	13.3	11.4	10.0	8.9	6.4
		Average Peak Stress (MPa)	0.254	0.355	0.432	0.559	0.661	0.911	1.157	1.267
		Average Peak Strain (με)	46	45	48	49	53	59	69	68
	2	|E*| (MPa)	5983	8037	9665	12038	13356	16185	17452	19493
		Phase Angle, Φ (°)	24.3	16.4	20.6	16.7	14.1	12.5	11.1	10.7
		Average Peak Stress (MPa)	0.282	0.396	0.480	0.622	0.734	1.015	1.158	1.269
		Average Peak Strain (με)	47	49	50	52	55	63	66	65
	3	|E*| (MPa)	5515	8080	8690	11393	12608	15536	16719	18725
		Phase Angle, Φ (°)	22.8	15.1	19.9	14.5	12.4	10.6	9.6	9.0
		Average Peak Stress (MPa)	0.311	0.395	0.480	0.622	0.734	1.014	1.156	1.268
		Average Peak Strain (με)	56	49	55	55	58	65	69	68
	Avg.	|E*| Average	5675	8000	9124	11603	12827	15689	17003	18909
		Φ Average	22.7	14.9	18.6	14.9	12.7	11.0	9.9	8.7
		|E*| Coeff. of Variation	0.047	0.013	0.054	0.032	0.036	0.028	0.023	0.027
		Φ Coeff. of Variation	0.07	0.11	0.16	0.12	0.11	0.11	0.12	0.25
		|E*| Std. Dev.	267.2	103.7	496.5	376.6	460.5	439.9	393.0	517.3
		Φ Std. Dev.	1.562	1.628	2.902	1.725	1.370	1.264	1.150	2.175
35	1	|E*| (MPa)	453	732	923	1592	2025	3564	4349	5534
		Phase Angle, Φ (°)	30.1	31.2	30.7	31.1	28.3	25.9	23.5	21.3
		Average Peak Stress (MPa)	0.013	0.025	0.033	0.058	0.088	0.125	0.198	0.353
		Average Peak Strain (με)	29	34	36	37	44	35	45	64
	2	|E*| (MPa)	550	817	1019	1708	2154	3791	4514	5683
		Phase Angle, Φ (°)	35.7	34.0	33.5	33.3	30.0	28.5	25.5	23.0
		Average Peak Stress (MPa)	0.014	0.028	0.037	0.065	0.098	0.140	0.221	0.393
		Average Peak Strain (με)	26	35	36	38	46	37	49	69
	3	|E*| (MPa)	498	776	934	1595	2047	3516	4381	5565
		Phase Angle, Φ (°)	30.7	29.6	30.5	31.0	29.1	26.7	23.9	22.1
		Average Peak Stress (MPa)	0.020	0.033	0.042	0.079	0.111	0.166	0.249	0.393
		Average Peak Strain (με)	40	43	45	50	54	47	57	71
	Avg.	|E*| Average	500	775	958	1632	2076	3624	4415	5594
		Φ Average	32.2	31.6	31.6	31.8	29.1	27.0	24.3	22.1
		|E*| Coeff. of Variation	0.097	0.055	0.055	0.041	0.033	0.040	0.020	0.014
		Φ Coeff. of Variation	0.10	0.07	0.05	0.04	0.03	0.05	0.04	0.04
		|E*| Std. Dev.	48.5	42.8	52.6	66.4	69.1	146.7	87.7	78.4
		Φ Std. Dev.	3.059	2.208	1.699	1.290	0.870	1.351	1.047	0.842

Table A-12 – S9.5C0–Fine – Granite

Temp (°C)	Rep.	Parameters	Frequency (Hz)							
			0.01	0.05	0.1	0.5	1	5	10	25
-10	1	|E*| (MPa)	20546	21227	23751	27519	28751	31026	31956	33053
		Phase Angle, Φ (°)	7.7	8.2	6.7	5.5	5.0	3.9	3.5	2.9
		Average Peak Stress (MPa)	1.412	1.582	1.639	1.755	1.814	1.873	1.932	2.083
		Average Peak Strain (με)	69	75	69	64	63	60	60	63
	2	|E*| (MPa)	18853	23966	23602	25533	26620	28987	29878	31102
		Phase Angle, Φ (°)	8.1	9.5	7.6	5.3	4.6	3.5	3.1	2.8
		Average Peak Stress (MPa)	1.412	1.582	1.639	1.755	1.814	1.871	1.932	2.096
		Average Peak Strain (με)	75	66	69	69	68	65	65	67
	3	|E*| (MPa)	20640		26388	28111	29379	32012	33140	34435
		Phase Angle, Φ (°)	8.6		5.4	6.7	5.9	4.1	3.4	3.8
		Average Peak Stress (MPa)	1.412		1.636	1.755	1.814	1.873	1.931	2.094
		Average Peak Strain (με)	68		62	62	62	59	58	61
	Avg.	|E*| Average	20013	22597	24580	27054	28250	30675	31658	32863
		Φ Average	8.1	8.9	6.6	5.8	5.2	3.8	3.3	3.1
		|E*| Coeff. of Variation	0.050	0.086	0.064	0.050	0.051	0.050	0.052	0.051
		Φ Coeff. of Variation	0.05	0.10	0.17	0.12	0.13	0.08	0.06	0.17
		|E*| Std. Dev.	1005.6	1936.9	1566.8	1350.2	1446.2	1542.5	1651.7	1674.5
		Φ Std. Dev.	0.445	0.918	1.105	0.720	0.662	0.298	0.205	0.532
10	1	|E*| (MPa)	6165	9168	9702	12752	14095	17376	18752	20796
		Phase Angle, Φ (°)	21.4	19.7	14.5	13.1	11.8	9.3	8.3	7.1
		Average Peak Stress (MPa)	0.367	0.537	0.622	0.907	0.965	1.192	1.305	1.452
		Average Peak Strain (με)	60	59	64	71	68	69	70	70
	2	|E*| (MPa)	5673	8367	9072	11472	12800	16040	17442	19292
		Phase Angle, Φ (°)	22.3	17.3	17.3	13.9	12.9	10.0	9.4	8.4
		Average Peak Stress (MPa)	0.367	0.537	0.622	0.907	0.965	1.193	1.305	1.451
		Average Peak Strain (με)	65	64	69	79	75	74	75	75
	3	|E*| (MPa)	5765	8878	9685	12457	13909	17438	18951	21126
		Phase Angle, Φ (°)	23.5	18.6	16.8	15.1	13.6	11.3	10.1	9.4
		Average Peak Stress (MPa)	0.367	0.537	0.623	0.907	0.965	1.193	1.304	1.448
		Average Peak Strain (με)	64	60	64	73	69	68	69	69
	Avg.	|E*| Average	5868	8804	9486	12227	13601	16951	18381	20404
		Φ Average	22.4	18.5	16.2	14.0	12.8	10.2	9.3	8.3
		|E*| Coeff. of Variation	0.045	0.046	0.038	0.055	0.052	0.047	0.045	0.048
		Φ Coeff. of Variation	0.05	0.06	0.09	0.07	0.07	0.10	0.10	0.14
		|E*| Std. Dev.	261.5	405.7	358.8	670.2	700.5	790.1	819.9	977.4
		Φ Std. Dev.	1.047	1.201	1.516	1.037	0.907	1.013	0.937	1.170
35	1	|E*| (MPa)	566	916	1138	1898	2383	4066	4948	6233
		Phase Angle, Φ (°)	30.8	31.7	32.3	32.0	29.8	25.0	22.6	20.7
		Average Peak Stress (MPa)	0.023	0.034	0.042	0.071	0.114	0.195	0.280	0.453
		Average Peak Strain (με)	40	37	37	37	48	48	56	73
	2	|E*| (MPa)	469	782	990	1671	2143	3785	4743	6001
		Phase Angle, Φ (°)	30.9	32.8	34.6	32.8	31.0	26.1	23.4	21.8
		Average Peak Stress (MPa)	0.022	0.034	0.043	0.071	0.114	0.196	0.279	0.451
		Average Peak Strain (με)	48	43	43	43	53	52	59	75
	3	|E*| (MPa)	466	754	948	1592	2049	3641	4535	5829
		Phase Angle, Φ (°)	33.0	33.8	40.9	35.0	32.8	26.7	24.6	22.7
		Average Peak Stress (MPa)	0.023	0.034	0.044	0.071	0.114	0.195	0.279	0.451
		Average Peak Strain (με)	48	45	46	45	56	54	61	77
	Avg.	|E*| Average	500	817	1025	1720	2192	3831	4742	6021
		Φ Average	31.6	32.8	36.0	33.3	31.2	25.9	23.6	21.7
		|E*| Coeff. of Variation	0.114	0.106	0.097	0.092	0.079	0.056	0.044	0.034
		Φ Coeff. of Variation	0.04	0.03	0.12	0.05	0.05	0.03	0.04	0.05
		|E*| Std. Dev.	57.0	86.8	99.8	159.0	172.4	216.1	206.4	202.6
		Φ Std. Dev.	1.208	1.065	4.454	1.569	1.512	0.862	0.992	1.001

Table A-13 – S9.5C1–Fine – Granite

Temp (°C)	Rep.	Parameters	Frequency (Hz)							
			0.01	0.05	0.1	0.5	1	5	10	25
-10	1	|E*| (MPa)	18465	23352	21716	24796	25814	28144	29177	30285
		Phase Angle, Φ (°)	9.9	6.6	6.9	6.9	6.5	5.1	4.7	4.4
		Average Peak Stress (MPa)	1.240	1.494	1.578	1.636	1.690	1.857	1.916	2.070
		Average Peak Strain (με)	67	64	73	66	65	66	66	68
	2	|E*| (MPa)	19247	19781	23913	25646	26553	28836	29775	30921
		Phase Angle, Φ (°)	5.9	5.9	4.8	3.5	3.1	2.2	1.6	1.3
		Average Peak Stress (MPa)	1.240	1.494	1.578	1.636	1.690	1.858	1.916	2.068
		Average Peak Strain (με)	64	76	66	64	64	64	64	67
	3	|E*| (MPa)	17484	18606	21881	23480	24615	26877	27726	
		Phase Angle, Φ (°)	7.4	3.9	7.2	4.8	4.8	3.2	2.9	
		Average Peak Stress (MPa)	1.240	1.494	1.578	1.636	1.690	1.857	1.917	
		Average Peak Strain (με)	71	80	72	70	69	69	69	
	Avg.	|E*| Average	18399	20580	22503	24641	25660	27952	28893	30603
		Φ Average	7.7	5.5	6.3	5.1	4.8	3.5	3.0	2.8
		|E*| Coeff. of Variation	0.048	0.120	0.054	0.044	0.038	0.036	0.036	0.015
		Φ Coeff. of Variation	0.26	0.25	0.21	0.34	0.35	0.42	0.51	0.78
		|E*| Std. Dev.	883.4	2471.7	1223.5	1091.2	978.0	993.5	1054.2	450.0
		Φ Std. Dev.	1.996	1.385	1.291	1.748	1.698	1.491	1.546	2.210
10	1	|E*| (MPa)	6126	9101	9191	11883	13067	15992	17346	19145
		Phase Angle, Φ (°)	23.5	19.5	17.4	15.8	14.3	11.6	10.6	9.7
		Average Peak Stress (MPa)	0.310	0.395	0.479	0.620	0.732	1.012	1.153	1.260
		Average Peak Strain (με)	51	43	52	52	56	63	66	66
	2	|E*| (MPa)	6139	7866	9253	11957	13165	16012	17299	19149
		Phase Angle, Φ (°)	18.6	12.6	15.4	11.9	10.8	8.8	7.9	7.6
		Average Peak Stress (MPa)	0.310	0.395	0.479	0.620	0.732	1.012	1.153	1.260
		Average Peak Strain (με)	51	50	52	52	56	63	67	66
	3	|E*| (MPa)	5411	7034	8609	10950	12013	14895	16190	17810
		Phase Angle, Φ (°)	21.1	15.3	16.7	13.5	12.2	9.6	8.8	8.3
		Average Peak Stress (MPa)	0.310	0.395	0.479	0.620	0.732	1.012	1.153	1.260
		Average Peak Strain (με)	57	56	56	57	61	68	71	71
	Avg.	|E*| Average	5892	8001	9017	11597	12748	15633	16945	18701
		Φ Average	21.1	15.8	16.5	13.7	12.5	10.0	9.1	8.5
		|E*| Coeff. of Variation	0.071	0.130	0.039	0.048	0.050	0.041	0.039	0.041
		Φ Coeff. of Variation	0.12	0.22	0.06	0.14	0.14	0.15	0.15	0.13
		|E*| Std. Dev.	416.5	1040.2	355.4	561.5	638.5	639.1	654.6	771.6
		Φ Std. Dev.	2.471	3.459	1.042	1.987	1.752	1.468	1.395	1.084
35	1	|E*| (MPa)	615	895	1103	1765	2188	3699	4436	5600
		Phase Angle, Φ (°)	34.8	34.5	34.3	32.7	30.6	26.6	24.2	22.2
		Average Peak Stress (MPa)	0.020	0.034	0.042	0.078	0.111	0.166	0.248	0.390
		Average Peak Strain (με)	32	38	38	44	51	45	56	70
	2	|E*| (MPa)	530	842	1088	1805	2280	3835	4686	5893
		Phase Angle, Φ (°)	31.1	31.2	31.0	29.9	28.0	23.6	21.6	20.1
		Average Peak Stress (MPa)	0.020	0.034	0.042	0.078	0.111	0.166	0.249	0.390
		Average Peak Strain (με)	37	40	39	43	49	43	53	66
	3	|E*| (MPa)	529	782	971	1581	1955	3356	4150	5254
		Phase Angle, Φ (°)	30.0	30.7	30.9	30.6	28.8	25.0	22.3	21.1
		Average Peak Stress (MPa)	0.020	0.034	0.042	0.078	0.111	0.165	0.248	0.388
		Average Peak Strain (με)	38	43	44	49	57	49	60	74
	Avg.	|E*| Average	558	840	1054	1717	2141	3630	4424	5582
		Φ Average	32.0	32.1	32.0	31.1	29.1	25.1	22.7	21.2
		|E*| Coeff. of Variation	0.088	0.067	0.068	0.070	0.078	0.068	0.061	0.057
		Φ Coeff. of Variation	0.08	0.07	0.06	0.05	0.05	0.06	0.06	0.05
		|E*| Std. Dev.	49.2	56.1	72.2	119.4	167.5	247.0	268.3	320.0
		Φ Std. Dev.	2.503	2.095	1.915	1.441	1.320	1.531	1.303	1.074
54.4	1	|E*| (MPa)		403	326	467	556	963	1247	1745
		Phase Angle, Φ (°)		28.5	27.7	29.5	30.4	31.3	31.7	32.9
		Average Peak Stress (MPa)		0.006	0.009	0.011	0.017	0.021	0.025	0.030
		Average Peak Strain (με)		14	26	24	30	22	20	17
	2	|E*| (MPa)		285	289	439	542	934	1196	1707
		Phase Angle, Φ (°)		26.2	23.4	26.1	27.4	28.3	27.7	27.2
		Average Peak Stress (MPa)		0.006	0.009	0.011	0.017	0.021	0.025	0.030
		Average Peak Strain (με)		20	30	26	31	23	21	18
	3	|E*| (MPa)		226	266	395	489	833	1078	1505
		Phase Angle, Φ (°)		18.6	19.9	24.8	25.9	27.8	27.9	30.0
		Average Peak Stress (MPa)		0.006	0.009	0.011	0.017	0.021	0.025	0.030
		Average Peak Strain (με)		25	32	28	34	25	23	20
	Avg.	|E*| Average		305	294	434	529	910	1174	1652
		Φ Average		24.5	23.7	26.8	27.9	29.1	29.1	30.0
		|E*| Coeff. of Variation		0.296	0.104	0.085	0.066	0.075	0.074	0.078
		Φ Coeff. of Variation		0.21	0.16	0.09	0.08	0.07	0.08	0.10
		|E*| Std. Dev.		90.2	30.5	36.7	35.0	68.1	86.8	128.7
		Φ Std. Dev.		5.169	3.878	2.411	2.294	1.930	2.265	2.854

Table A-14 – S9.5C2–Fine – Granite

Temp (°C)	Rep.	Parameters	Frequency (Hz)							
			0.01	0.05	0.1	0.5	1	5	10	25
-10	1	|E*| (MPa)	19553	25402	24454	26578	27798	30536	31908	
		Phase Angle, Φ (°)	9.0	8.0	4.4	5.9	5.4	4.3	4.1	
		Average Peak Stress (MPa)	1.240	1.494	1.578	1.636	1.690	1.858	1.916	
		Average Peak Strain (με)	63	59	65	62	61	61	60	
	2	|E*| (MPa)	19502	20558	24180	26293	27362	29685	30542	32016
		Phase Angle, Φ (°)	8.7	8.0	8.5	5.2	5.0	3.7	3.0	3.0
		Average Peak Stress (MPa)	1.240	1.494	1.579	1.636	1.690	1.857	1.915	2.068
		Average Peak Strain (με)	64	73	65	62	62	63	63	65
	3	|E*| (MPa)	19010	24090	24041	25714	27004	29585	30546	31718
		Phase Angle, Φ (°)	7.9	5.9	6.4	5.2	5.0	4.2	3.6	3.3
		Average Peak Stress (MPa)	1.240	1.494	1.579	1.636	1.690	1.857	1.916	2.066
		Average Peak Strain (με)	65	62	66	64	63	63	63	65
	Avg.	|E*| Average	19355	23350	24225	26195	27388	29935	30999	31867
		Φ Average	8.5	7.3	6.4	5.4	5.1	4.1	3.6	3.1
		|E*| Coeff. of Variation	0.016	0.107	0.009	0.017	0.015	0.017	0.025	0.007
		Φ Coeff. of Variation	0.06	0.17	0.32	0.07	0.05	0.09	0.14	0.06
		|E*| Std. Dev.	300.1	2505.4	210.1	440.2	397.7	522.4	787.2	210.4
		Φ Std. Dev.	0.533	1.239	2.055	0.387	0.247	0.348	0.514	0.199
10	1	|E*| (MPa)	6396	8245	9946	12835	14165	17408	18883	
		Phase Angle, Φ (°)	23.2	21.8	19.3	15.0	13.4	10.9	10.1	
		Average Peak Stress (MPa)	0.310	0.395	0.479	0.620	0.732	1.012	1.153	
		Average Peak Strain (με)	48	48	48	48	52	58	61	
	2	|E*| (MPa)	5849	7873	9169	12063	13258	16318	17753	19765
		Phase Angle, Φ (°)	24.0	16.7	16.9	15.0	13.2	10.7	9.5	8.7
		Average Peak Stress (MPa)	0.310	0.395	0.479	0.620	0.732	1.011	1.152	1.256
		Average Peak Strain (με)	53	50	52	51	55	62	65	64
	3	|E*| (MPa)	5724	7524	9140	11862	13256	16599	18253	20053
		Phase Angle, Φ (°)	22.8	17.0	19.2	14.5	13.3	11.0	10.4	9.5
		Average Peak Stress (MPa)	0.310	0.395	0.479	0.620	0.732	1.012	1.153	1.258
		Average Peak Strain (με)	54	52	52	52	55	61	63	63
	Avg.	|E*| Average	5990	7881	9418	12254	13560	16775	18296	19909
		Φ Average	23.4	18.5	18.5	14.8	13.3	10.8	10.0	9.1
		|E*| Coeff. of Variation	0.060	0.046	0.049	0.042	0.039	0.034	0.031	0.010
		Φ Coeff. of Variation	0.03	0.16	0.07	0.02	0.01	0.02	0.05	0.06
		|E*| Std. Dev.	357.1	360.9	457.3	513.7	524.3	566.2	566.6	203.5
		Φ Std. Dev.	0.596	2.898	1.363	0.312	0.094	0.174	0.471	0.561
35	1	|E*| (MPa)	523	825	1055	1809	2332	4096	5082	6402
		Phase Angle, Φ (°)	33.5	34.5	33.1	33.3	31.7	27.2	24.1	22.1
		Average Peak Stress (MPa)	0.020	0.034	0.042	0.078	0.111	0.166	0.249	0.391
		Average Peak Strain (με)	38	41	40	43	48	41	49	61
	2	|E*| (MPa)	485	770	928	1575	2011	3592	4444	5703
		Phase Angle, Φ (°)	33.5	33.3	34.6	33.1	31.8	27.1	24.8	22.6
		Average Peak Stress (MPa)	0.020	0.034	0.042	0.078	0.111	0.165	0.247	0.389
		Average Peak Strain (με)	41	44	46	49	55	46	56	68
	3	|E*| (MPa)	436	707	899	1544	2006	3584	4485	5730
		Phase Angle, Φ (°)	30.6	31.5	31.7	31.2	30.3	26.3	23.8	22.1
		Average Peak Stress (MPa)	0.020	0.034	0.042	0.078	0.111	0.166	0.249	0.390
		Average Peak Strain (με)	45	48	47	51	55	46	55	68
	Avg.	|E*| Average	481	767	961	1643	2117	3757	4671	5945
		Φ Average	32.6	33.1	33.2	32.5	31.3	26.9	24.2	22.3
		|E*| Coeff. of Variation	0.090	0.077	0.087	0.088	0.088	0.078	0.076	0.067
		Φ Coeff. of Variation	0.05	0.05	0.04	0.04	0.03	0.02	0.02	0.01
		|E*| Std. Dev.	43.5	59.3	83.2	145.0	186.7	293.3	357.1	395.9
		Φ Std. Dev.	1.680	1.499	1.416	1.148	0.832	0.464	0.531	0.284
54.4	1	|E*| (MPa)		314	309	436	514	920	1189	1676
		Phase Angle, Φ (°)		20.0	22.5	29.0	29.7	31.8	32.1	33.9
		Average Peak Stress (MPa)		0.006	0.009	0.011	0.017	0.021	0.025	0.030
		Average Peak Strain (με)		18	28	26	32	23	21	18
	2	|E*| (MPa)		265	253	362	447	810	1073	1528
		Phase Angle, Φ (°)		29.1	25.4	28.8	30.3	32.6	32.7	34.2
		Average Peak Stress (MPa)		0.006	0.009	0.011	0.017	0.021	0.025	0.029
		Average Peak Strain (με)		21	34	31	37	26	23	19
	3	|E*| (MPa)		234	268	385	465	830	1072	1552
		Phase Angle, Φ (°)		17.2	21.9	26.7	27.9	30.3	30.2	31.6
		Average Peak Stress (MPa)		0.006	0.009	0.011	0.017	0.021	0.025	0.030
		Average Peak Strain (με)		24	32	29	36	26	23	19
	Avg.	|E*| Average		271	277	394	475	853	1111	1585
		Φ Average		22.1	23.3	28.2	29.3	31.6	31.7	33.2
		|E*| Coeff. of Variation		0.148	0.104	0.096	0.073	0.069	0.061	0.050
		Φ Coeff. of Variation		0.28	0.08	0.05	0.04	0.04	0.04	0.04
		|E*| Std. Dev.		40.1	28.8	37.7	34.6	58.6	67.3	79.6
		Φ Std. Dev.		6.219	1.908	1.272	1.257	1.134	1.302	1.429

Table A-15 – S9.5C3–Fine – Granite

Temp (°C)	Rep.	Parameters	Frequency (Hz)							
			0.01	0.05	0.1	0.5	1	5	10	25
-10	1	|E*| (MPa)	18894	20468	24258	27222	28489	31624	33020	34607
		Phase Angle, Φ (°)	14.3	13.7	9.1	10.4	9.7	7.9	7.6	7.4
		Average Peak Stress (MPa)	1.241	1.495	1.580	1.638	1.692	1.861	1.920	2.077
		Average Peak Strain (με)	66	73	65	60	59	59	58	60
	2	|E*| (MPa)	16945	21414	20905	24734	25709	28566	29728	31029
		Phase Angle, Φ (°)	9.7	12.0	8.0	5.1	5.0	3.3	2.8	2.4
		Average Peak Stress (MPa)	1.241	1.495	1.580	1.638	1.692	1.861	1.920	2.078
		Average Peak Strain (με)	73	70	76	66	66	65	65	67
	3	|E*| (MPa)	16703	20769	21366	24281	25467	28393	29314	
		Phase Angle, Φ (°)	8.5	11.8	3.5	4.8	4.3	2.7	2.1	
		Average Peak Stress (MPa)	1.241	1.495	1.580	1.638	1.692	1.862	1.921	
		Average Peak Strain (με)	74	72	74	67	66	66	66	
	Avg.	|E*| Average	17514	20884	22176	25412	26555	29528	30688	32818
		Φ Average	10.8	12.5	6.9	6.8	6.4	4.6	4.2	4.9
		|E*| Coeff. of Variation	0.069	0.023	0.082	0.062	0.063	0.062	0.066	0.077
		Φ Coeff. of Variation	0.28	0.09	0.43	0.47	0.46	0.61	0.73	0.71
		|E*| Std. Dev.	1200.9	483.1	1817.7	1583.7	1679.3	1817.7	2030.7	2530.0
		Φ Std. Dev.	3.046	1.084	2.967	3.165	2.947	2.824	3.038	3.504
10	1	|E*| (MPa)	3955	6136	7241	10500	11970	15548	17229	19679
		Phase Angle, Φ (°)	33.0	25.3	26.5	22.4	20.7	16.8	15.7	14.6
		Average Peak Stress (MPa)	0.310	0.395	0.480	0.621	0.733	1.014	1.156	1.265
		Average Peak Strain (με)	78	64	66	59	61	65	67	64
	2	|E*| (MPa)	3123	4701	6056	8579	9909	13310	14877	16959
		Phase Angle, Φ (°)	29.3	25.3	24.1	18.8	17.1	13.0	11.7	10.6
		Average Peak Stress (MPa)	0.310	0.395	0.480	0.621	0.733	1.014	1.157	1.264
		Average Peak Strain (με)	99	84	79	72	74	76	78	75
	3	|E*| (MPa)	3351	5440	6230	8947	10244	13497	14994	17075
		Phase Angle, Φ (°)	27.2	22.2	22.0	17.3	15.6	11.7	10.4	9.5
		Average Peak Stress (MPa)	0.310	0.395	0.480	0.621	0.733	1.014	1.156	1.265
		Average Peak Strain (με)	93	73	77	69	72	75	77	74
	Avg.	|E*| Average	3476	5426	6509	9342	10708	14119	15700	17904
		Φ Average	29.8	24.3	24.2	19.5	17.8	13.8	12.6	11.6
		|E*| Coeff. of Variation	0.124	0.132	0.098	0.109	0.103	0.088	0.084	0.086
		Φ Coeff. of Variation	0.10	0.07	0.09	0.13	0.15	0.19	0.22	0.23
		|E*| Std. Dev.	430.2	717.2	640.2	1019.8	1105.8	1241.5	1325.6	1537.9
		Φ Std. Dev.	2.923	1.820	2.277	2.609	2.627	2.654	2.768	2.656
35	1	|E*| (MPa)	250	395	504	927	1260	2502	3262	4399
		Phase Angle, Φ (°)	28.2	31.4	32.9	35.4	34.4	31.7	29.3	27.1
		Average Peak Stress (MPa)	0.020	0.034	0.042	0.078	0.111	0.166	0.248	0.389
		Average Peak Strain (με)	79	85	84	84	88	66	76	89
	2	|E*| (MPa)	220	346	440	806	1088	2120	2807	3910
		Phase Angle, Φ (°)	24.2	27.4	28.7	32.1	31.4	28.6	26.8	25.6
		Average Peak Stress (MPa)	0.020	0.034	0.042	0.078	0.111	0.165	0.246	0.387
		Average Peak Strain (με)	90	97	96	97	102	78	88	99
	3	|E*| (MPa)	213	352	455	845	1137	2184	2837	3931
		Phase Angle, Φ (°)	24.8	28.0	29.1	32.1	31.2	27.7	25.5	24.7
		Average Peak Stress (MPa)	0.020	0.034	0.042	0.078	0.111	0.165	0.247	0.388
		Average Peak Strain (με)	93	96	93	92	98	76	87	99
	Avg.	|E*| Average	228	364	466	859	1162	2269	2969	4080
		Φ Average	25.7	28.9	30.2	33.2	32.3	29.3	27.2	25.8
		|E*| Coeff. of Variation	0.086	0.074	0.072	0.072	0.076	0.090	0.086	0.068
		Φ Coeff. of Variation	0.08	0.07	0.08	0.06	0.06	0.07	0.07	0.05
		|E*| Std. Dev.	19.6	26.8	33.4	62.1	88.7	204.9	253.9	276.5
		Φ Std. Dev.	2.146	2.166	2.322	1.916	1.826	2.097	1.904	1.216
54.4	1	|E*| (MPa)		167	166	206	244	434	585	922
		Phase Angle, Φ (°)		13.3	19.2	25.1	26.7	32.1	33.5	36.0
		Average Peak Stress (MPa)		0.006	0.009	0.011	0.017	0.020	0.024	0.027
		Average Peak Strain (με)		33	52	55	68	47	40	29
	2	|E*| (MPa)		142	141	183	222	388	530	816
		Phase Angle, Φ (°)		17.2	15.9	22.1	23.9	28.5	30.4	32.7
		Average Peak Stress (MPa)		0.006	0.009	0.011	0.017	0.020	0.023	0.026
		Average Peak Strain (με)		39	61	62	74	52	44	32
	3	|E*| (MPa)		109	120	166	209	367	494	754
		Phase Angle, Φ (°)		10.5	14.3	21.9	23.8	27.7	28.7	32.6
		Average Peak Stress (MPa)		0.006	0.009	0.011	0.017	0.020	0.024	0.027
		Average Peak Strain (με)		51	71	68	79	55	48	36
	Avg.	|E*| Average		139	142	185	225	396	536	831
		Φ Average		13.7	16.5	23.0	24.8	29.4	30.9	33.8
		|E*| Coeff. of Variation		0.209	0.160	0.109	0.079	0.086	0.086	0.103
		Φ Coeff. of Variation		0.24	0.15	0.08	0.07	0.08	0.08	0.06
		|E*| Std. Dev.		29.1	22.7	20.2	17.7	34.2	46.0	85.1
		Φ Std. Dev.		3.333	2.454	1.773	1.614	2.360	2.462	1.975

Table A-16 – S9.5C–Fine – Limestone

Temp (°C)	Rep.	Parameters	Frequency (Hz)							
			0.01	0.05	0.1	0.5	1	5	10	25
-10	1	|E*| (MPa)	16617	19935	19186	21850	22535	24289	25006	25935
		Phase Angle, Φ (°)	5.6	2.2	3.0	3.4	3.0	2.0	1.5	1.6
		Average Peak Stress (MPa)	1.083	1.264	1.309	1.400	1.444	1.579	1.625	1.757
		Average Peak Strain (με)	65	63	68	64	64	65	65	68
	2	|E*| (MPa)	17247	20306	21020	22426	23324	25190	25936	26799
		Phase Angle, Φ (°)	7.0	3.8	5.3	4.5	4.3	3.6	3.0	2.8
		Average Peak Stress (MPa)	1.354	1.579	1.636	1.750	1.806	1.975	2.035	2.202
		Average Peak Strain (με)	78	78	78	78	77	78	78	82
	3	|E*| (MPa)	15163	17282	17542	19801	20415	22359	23008	23862
		Phase Angle, Φ (°)	7.4	2.6	5.0	4.8	4.7	3.8	3.3	3.2
		Average Peak Stress (MPa)	1.082	1.263	1.309	1.400	1.445	1.579	1.628	1.757
		Average Peak Strain (με)	71	73	75	71	71	71	71	74
	Avg.	|E*| Average	16342	19174	19249	21359	22091	23946	24650	25532
		Φ Average	6.7	2.8	4.4	4.3	4.0	3.1	2.6	2.5
		|E*| Coeff. of Variation	0.065	0.086	0.090	0.065	0.068	0.060	0.061	0.059
		Φ Coeff. of Variation	0.14	0.29	0.27	0.17	0.22	0.32	0.38	0.34
		|E*| Std. Dev.	1068.6	1649.0	1739.6	1379.8	1504.5	1446.4	1496.3	1509.3
		Φ Std. Dev.	0.955	0.823	1.220	0.712	0.888	0.991	0.967	0.869
10	1	|E*| (MPa)	5748	7511	8789	11248	12309	14836	16054	17452
		Phase Angle, Φ (°)	19.4	14.0	15.7	12.3	11.1	8.7	7.4	6.7
		Average Peak Stress (MPa)	0.226	0.316	0.383	0.497	0.587	0.812	0.925	1.014
		Average Peak Strain (με)	39	42	44	44	48	55	58	58
	2	|E*| (MPa)	6067	8555	9201	11597	12579	15037	16041	17643
		Phase Angle, Φ (°)	22.2	20.4	15.0	13.7	12.6	9.9	8.7	8.0
		Average Peak Stress (MPa)	0.282	0.395	0.480	0.621	0.734	1.015	1.157	1.270
		Average Peak Strain (με)	46	46	52	54	58	68	72	72
	3	|E*| (MPa)	5498	7672	8066	10215	11131	13574	14774	16057
		Phase Angle, Φ (°)	21.4	19.7	17.0	13.7	12.6	10.4	9.5	10.1
		Average Peak Stress (MPa)	0.226	0.316	0.384	0.497	0.588	0.811	0.924	1.010
		Average Peak Strain (με)	41	41	48	49	53	60	63	63
	Avg.	|E*| Average	5771	7913	8685	11020	12006	14482	15623	17051
		Φ Average	21.0	18.1	15.9	13.3	12.1	9.7	8.5	8.3
		|E*| Coeff. of Variation	0.049	0.071	0.066	0.065	0.064	0.055	0.047	0.051
		Φ Coeff. of Variation	0.07	0.19	0.06	0.06	0.07	0.09	0.13	0.20
		|E*| Std. Dev.	285.0	562.2	574.4	718.5	769.7	793.0	735.6	865.5
		Φ Std. Dev.	1.453	3.510	1.018	0.801	0.834	0.834	1.075	1.690
35	1	|E*| (MPa)	613	858	1046	1687	2147	3620	4402	5484
		Phase Angle, Φ (°)	29.9	31.9	30.6	31.9	29.5	24.7	22.0	19.6
		Average Peak Stress (MPa)	0.011	0.022	0.029	0.052	0.077	0.109	0.176	0.308
		Average Peak Strain (με)	19	26	28	31	36	30	40	56
	2	|E*| (MPa)	671	967	1176	1901	2370	3967	4717	5777
		Phase Angle, Φ (°)	35.3	34.1	33.8	33.0	30.6	25.9	22.6	20.4
		Average Peak Stress (MPa)	0.014	0.028	0.037	0.064	0.097	0.137	0.221	0.391
		Average Peak Strain (με)	21	29	31	34	41	35	47	68
	3	|E*| (MPa)	617	966	1173	1869	2325	3906	4668	5664
		Phase Angle, Φ (°)	26.4	30.2	31.7	32.7	30.5	26.2	22.7	20.6
		Average Peak Stress (MPa)	0.014	0.028	0.037	0.064	0.097	0.137	0.220	0.389
		Average Peak Strain (με)	23	29	31	34	42	35	47	69
	Avg.	|E*| Average	634	930	1132	1819	2281	3831	4596	5642
		Φ Average	30.5	32.0	32.0	32.5	30.2	25.6	22.4	20.2
		|E*| Coeff. of Variation	0.051	0.067	0.066	0.063	0.052	0.048	0.037	0.026
		Φ Coeff. of Variation	0.15	0.06	0.05	0.02	0.02	0.03	0.02	0.03
		|E*| Std. Dev.	32.2	62.4	74.3	115.2	118.1	185.1	169.2	148.1
		Φ Std. Dev.	4.488	1.975	1.636	0.550	0.589	0.799	0.382	0.560
54.4	1	|E*| (MPa)	276	286	302	438	547	981	1298	1788
		Phase Angle, Φ (°)	18.5	25.6	23.7	26.9	27.3	26.3	25.2	25.7
		Average Peak Stress (MPa)	0.006	0.009	0.014	0.028	0.036	0.061	0.091	0.124
		Average Peak Strain (με)	20	30	47	64	66	62	70	70
	2	|E*| (MPa)	272	301	309	450	567	1028	1338	1879
		Phase Angle, Φ (°)	27.3	24.8	27.2	28.4	28.5	27.3	26.2	26.2
		Average Peak Stress (MPa)	0.006	0.009	0.014	0.028	0.036	0.061	0.091	0.124
		Average Peak Strain (με)	21	28	46	63	64	60	68	66
	3	|E*| (MPa)	300	335	336	460	573	1010	1315	1795
		Phase Angle, Φ (°)	13.9	22.0	22.4	26.3	27.1	27.2	25.6	25.8
		Average Peak Stress (MPa)	0.006	0.008	0.014	0.028	0.036	0.061	0.090	0.122
		Average Peak Strain (με)	19	25	42	62	63	60	68	68
	Avg.	|E*| Average	283	308	316	449	562	1006	1317	1821
		Φ Average	19.9	24.1	24.4	27.2	27.6	26.9	25.7	25.9
		|E*| Coeff. of Variation	0.053	0.082	0.056	0.023	0.024	0.024	0.016	0.028
		Φ Coeff. of Variation	0.34	0.08	0.10	0.04	0.03	0.02	0.02	0.01
		|E*| Std. Dev.	15.1	25.1	17.7	10.5	13.7	23.8	20.4	50.8
		Φ Std. Dev.	6.813	1.925	2.459	1.045	0.773	0.545	0.539	0.251

Table A-17 – S12.5B–Coarse – Granite

Temp (°C)	Rep.	Parameters	Frequency (Hz)							
			0.01	0.05	0.1	0.5	1	5	10	25
-10	1	|E*| (MPa)	17425	22872	23478	25710	27007	29979	31180	32744
		Phase Angle, Φ (°)	9.8	5.8	6.7	5.6	4.6	4.5	3.9	3.2
		Average Peak Stress (MPa)	1.241	1.467	1.552	1.666	1.694	1.862	1.919	2.077
		Average Peak Strain (με)	71	64	66	65	63	62	62	63
	2	|E*| (MPa)	16092	21453	21700	23896	25179	27874	29043	30522
		Phase Angle, Φ (°)	11.9	7.9	7.4	7.0	5.6	5.1	4.6	4.3
		Average Peak Stress (MPa)	1.241	1.467	1.552	1.666	1.693	1.862	1.920	2.077
		Average Peak Strain (με)	77	68	72	70	67	67	66	68
	3	|E*| (MPa)	16977	22516	21588	24791	25990	28772	29914	31346
		Phase Angle, Φ (°)	10.5	9.8	5.1	6.9	5.0	4.5	4.0	3.5
		Average Peak Stress (MPa)	1.240	1.466	1.551	1.666	1.693	1.862	1.921	2.082
		Average Peak Strain (με)	73	65	72	67	65	65	64	66
	Avg.	|E*| Average	16831	22280	22255	24799	26059	28875	30046	31537
		Φ Average	10.7	7.8	6.4	6.5	5.1	4.7	4.1	3.6
		|E*| Coeff. of Variation	0.040	0.033	0.048	0.037	0.035	0.037	0.036	0.036
		Φ Coeff. of Variation	0.10	0.25	0.19	0.12	0.10	0.07	0.09	0.15
		|E*| Std. Dev.	678.5	738.2	1060.3	906.7	915.7	1056.3	1074.5	1123.0
		Φ Std. Dev.	1.046	1.999	1.182	0.759	0.509	0.319	0.369	0.548
10	1	|E*| (MPa)	2869	5054	5691	8579	9986	13681	15345	17636
		Phase Angle, Φ (°)	31.3	24.9	24.3	20.6	17.8	14.7	12.8	11.9
		Average Peak Stress (MPa)	0.169	0.310	0.423	0.622	0.734	1.014	1.155	1.260
		Average Peak Strain (με)	59	61	74	72	74	74	75	71
	2	|E*| (MPa)	2699	4551	5482	8285	9649	13113	14839	17125
		Phase Angle, Φ (°)	32.7	24.9	26.0	21.6	18.6	14.9	13.0	13.0
		Average Peak Stress (MPa)	0.169	0.310	0.423	0.622	0.734	1.014	1.155	1.262
		Average Peak Strain (με)	63	68	77	75	76	77	78	74
	3	|E*| (MPa)	3181	4892	6421	9036	10404	13983	15558	17621
		Phase Angle, Φ (°)	30.4	28.0	24.6	19.2	16.2	14.0	12.3	10.9
		Average Peak Stress (MPa)	0.169	0.310	0.423	0.622	0.734	0.986	1.155	1.265
		Average Peak Strain (με)	53	63	66	69	71	70	74	72
	Avg.	|E*| Average	2917	4832	5865	8633	10013	13593	15248	17461
		Φ Average	31.4	25.9	25.0	20.5	17.5	14.6	12.7	11.9
		|E*| Coeff. of Variation	0.084	0.053	0.084	0.044	0.038	0.032	0.024	0.017
		Φ Coeff. of Variation	0.04	0.07	0.04	0.06	0.07	0.03	0.03	0.09
		|E*| Std. Dev.	244.6	256.5	493.2	378.2	378.1	441.7	369.2	290.9
		Φ Std. Dev.	1.149	1.781	0.877	1.209	1.250	0.489	0.371	1.080
35	1	|E*| (MPa)	216	350	447	846	1141	2316	3030	4216
		Phase Angle, Φ (°)	27.0	30.0	31.3	34.8	33.1	30.8	29.1	27.6
		Average Peak Stress (MPa)	0.014	0.023	0.028	0.045	0.070	0.136	0.189	0.298
		Average Peak Strain (με)	66	65	63	53	61	59	62	71
	2	|E*| (MPa)	191	313	402	742	1023	2118	2807	3982
		Phase Angle, Φ (°)	24.1	26.4	28.7	33.1	31.8	30.5	29.4	27.8
		Average Peak Stress (MPa)	0.014	0.023	0.028	0.045	0.069	0.135	0.189	0.298
		Average Peak Strain (με)	74	72	70	61	68	64	67	75
	3	|E*| (MPa)	260	393	498	894	1214	2382	3120	4293
		Phase Angle, Φ (°)	25.1	28.8	30.0	34.1	31.6	29.8	28.3	26.7
		Average Peak Stress (MPa)	0.014	0.022	0.028	0.045	0.070	0.136	0.189	0.300
		Average Peak Strain (με)	55	57	56	50	57	57	61	70
	Avg.	|E*| Average	223	352	449	827	1126	2272	2986	4164
		Φ Average	25.4	28.4	30.0	34.0	32.2	30.4	28.9	27.3
		|E*| Coeff. of Variation	0.157	0.114	0.107	0.094	0.086	0.060	0.054	0.039
		Φ Coeff. of Variation	0.06	0.07	0.04	0.03	0.03	0.02	0.02	0.02
		|E*| Std. Dev.	34.8	40.2	48.2	77.5	96.5	137.3	160.9	161.6
		Φ Std. Dev.	1.477	1.848	1.258	0.853	0.825	0.505	0.532	0.579

Table A-18 – S12.5B–Fine – Granite

Temp (°C)	Rep.	Parameters	Frequency (Hz)							
			0.01	0.05	0.1	0.5	1	5	10	25
-10	1	|E*| (MPa)	16442	21370	21706	23599	24858	27280	28352	29497
		Phase Angle, Φ (°)	9.9	6.7	6.6	6.5	5.1	5.0	4.0	3.6
		Average Peak Stress (MPa)	1.354	1.580	1.637	1.751	1.806	1.969	2.031	2.191
		Average Peak Strain (με)	82	74	75	74	73	72	72	74
	2	|E*| (MPa)	17306		20612	24494	25585	28208	29032	30464
		Phase Angle, Φ (°)	8.6		6.8	5.4	4.0	3.9	3.1	3.5
		Average Peak Stress (MPa)	1.354		1.637	1.750	1.806	1.975	2.032	2.196
		Average Peak Strain (με)	78		79	71	71	70	70	72
	3	|E*| (MPa)	17315	18594	21742	24545	25700	28349	29123	30436
		Phase Angle, Φ (°)	9.1	4.7	4.1	5.2	4.0	3.3	2.9	2.5
		Average Peak Stress (MPa)	1.354	1.580	1.637	1.751	1.806	1.972	2.033	2.193
		Average Peak Strain (με)	78	85	75	71	70	70	70	72
	Avg.	|E*| Average	17021	19982	21353	24213	25381	27946	28836	30132
		Φ Average	9.2	5.7	5.8	5.7	4.4	4.1	3.3	3.2
		|E*| Coeff. of Variation	0.029	0.098	0.030	0.022	0.018	0.021	0.015	0.018
		Φ Coeff. of Variation	0.07	0.25	0.26	0.13	0.15	0.22	0.18	0.19
		|E*| Std. Dev.	501.2	1963.3	642.3	531.9	456.4	580.5	421.3	550.3
		Φ Std. Dev.	0.678	1.393	1.488	0.722	0.642	0.897	0.586	0.599
10	1	|E*| (MPa)	3485	5708	6584	9069	10273	13366	14816	16925
		Phase Angle, Φ (°)	27.5	24.0	22.1	17.9	15.6	12.9	11.1	10.9
		Average Peak Stress (MPa)	0.367	0.480	0.565	0.707	0.819	1.098	1.265	1.373
		Average Peak Strain (με)	105	84	86	78	80	82	85	81
	2	|E*| (MPa)	3981	6090	7056	9864	11099	14338	15801	17990
		Phase Angle, Φ (°)	25.9	18.9	21.6	17.2	14.4	12.3	11.1	10.5
		Average Peak Stress (MPa)	0.367	0.480	0.565	0.706	0.819	1.098	1.267	1.380
		Average Peak Strain (με)	92	79	80	72	74	77	80	77
	3	|E*| (MPa)	3567	5643	6511	9187	10486	13778	15146	17202
		Phase Angle, Φ (°)	26.3	20.1	22.2	17.2	14.8	11.7	10.5	9.8
		Average Peak Stress (MPa)	0.367	0.479	0.564	0.707	0.819	1.097	1.268	1.380
		Average Peak Strain (με)	103	85	87	77	78	80	84	80
	Avg.	|E*| Average	3678	5814	6717	9373	10620	13827	15254	17372
		Φ Average	26.6	21.0	22.0	17.5	14.9	12.3	10.9	10.4
		|E*| Coeff. of Variation	0.072	0.042	0.044	0.046	0.040	0.035	0.033	0.032
		Φ Coeff. of Variation	0.03	0.13	0.01	0.02	0.04	0.05	0.03	0.05
		|E*| Std. Dev.	266.0	241.7	296.1	429.0	429.0	487.7	501.4	552.8
		Φ Std. Dev.	0.800	2.690	0.311	0.421	0.603	0.582	0.363	0.562
35	1	|E*| (MPa)	261	434	542	987	1332	2475	3173	4339
		Phase Angle, Φ (°)	29.2	32.2	32.2	32.9	29.5	28.4	26.0	24.5
		Average Peak Stress (MPa)	0.020	0.034	0.042	0.079	0.140	0.218	0.301	0.442
		Average Peak Strain (με)	76	77	78	80	105	88	95	102
	2	|E*| (MPa)	277	487	617	1138	1557	2855	3620	4784
		Phase Angle, Φ (°)	27.1	29.7	30.4	31.9	28.5	27.1	24.6	23.2
		Average Peak Stress (MPa)	0.020	0.034	0.042	0.079	0.140	0.219	0.303	0.446
		Average Peak Strain (με)	71	71	69	69	90	77	84	93
	3	|E*| (MPa)	251	424	525	991	1375	2576	3333	4589
		Phase Angle, Φ (°)	26.0	26.1	30.1	31.7	28.7	26.6	25.7	24.4
		Average Peak Stress (MPa)	0.020	0.034	0.042	0.079	0.140	0.219	0.303	0.445
		Average Peak Strain (με)	79	81	81	80	102	85	91	97
	Avg.	|E*| Average	263	448	561	1039	1421	2635	3375	4571
		Φ Average	27.4	29.3	30.9	32.2	28.9	27.4	25.4	24.0
		|E*| Coeff. of Variation	0.051	0.075	0.087	0.083	0.084	0.075	0.067	0.049
		Φ Coeff. of Variation	0.06	0.10	0.04	0.02	0.02	0.03	0.03	0.03
		|E*| Std. Dev.	13.5	33.6	49.1	86.1	119.6	197.0	226.7	223.2
		Φ Std. Dev.	1.630	3.038	1.154	0.637	0.503	0.898	0.742	0.720

Table A-19 – S12.5C–Coarse – Granite

Temp (°C)	Rep.	Parameters	Frequency (Hz)							
			0.01	0.05	0.1	0.5	1	5	10	25
-10	1	|E*| (MPa)	20510	24590	26113	29152	30291	33215	34483	36028
		Phase Angle, Φ (°)	8.8	0.0	3.6	5.1	5.4	4.1	3.5	3.7
		Average Peak Stress (MPa)	1.212	1.438	1.495	1.637	1.691	1.859	1.918	2.078
		Average Peak Strain (με)	59	58	57	56	56	56	56	58
	2	|E*| (MPa)	20399	22271	24169	28465	29611	32353	33721	35061
		Phase Angle, Φ (°)	8.5	11.9	5.4	5.1	5.3	3.8	3.3	2.9
		Average Peak Stress (MPa)	1.212	1.438	1.495	1.637	1.691	1.859	1.918	2.076
		Average Peak Strain (με)	59	65	62	58	57	57	57	59
	3	|E*| (MPa)	18507	23576	21705	25344	26454	28986	29832	31318
		Phase Angle, Φ (°)	7.4	2.5	4.8	5.0	4.2	3.1	2.5	3.1
		Average Peak Stress (MPa)	1.212	1.438	1.495	1.637	1.691	1.861	1.921	2.083
		Average Peak Strain (με)	65	61	69	65	64	64	64	66
	Avg.	|E*| Average	19805	23479	23996	27653	28785	31518	32679	34136
		Φ Average	8.2	4.8	4.6	5.0	5.0	3.7	3.1	3.2
		|E*| Coeff. of Variation	0.057	0.050	0.092	0.073	0.071	0.071	0.076	0.073
		Φ Coeff. of Variation	0.09	1.32	0.19	0.01	0.14	0.15	0.17	0.12
		|E*| Std. Dev.	1125.9	1162.7	2209.2	2029.5	2047.5	2235.0	2494.5	2487.6
		Φ Std. Dev.	0.765	6.289	0.882	0.040	0.678	0.546	0.525	0.396
10	1	|E*| (MPa)	4465	7315	7948	11191	12482	16115	17719	
		Phase Angle, Φ (°)	30.1	20.1	25.6	18.8	17.0	13.7	12.2	
		Average Peak Stress (MPa)	0.141	0.240	0.282	0.395	0.506	0.701	0.817	
		Average Peak Strain (με)	32	33	36	35	41	44	46	
	2	|E*| (MPa)	5087	8844	8939	12101	13487	17240	18987	21118
		Phase Angle, Φ (°)	27.2	25.1	24.1	17.0	15.5	12.2	10.7	9.3
		Average Peak Stress (MPa)	0.141	0.240	0.282	0.395	0.506	0.702	0.817	0.919
		Average Peak Strain (με)	28	27	32	33	38	41	43	43
	3	|E*| (MPa)	4314	6211	7809	10071	11557	14703	16197	18057
		Phase Angle, Φ (°)	27.2	27.9	21.7	17.2	15.1	11.6	10.7	9.7
		Average Peak Stress (MPa)	0.141	0.240	0.282	0.395	0.507	0.703	0.819	0.922
		Average Peak Strain (με)	33	39	36	39	44	48	51	51
	Avg.	|E*| Average	4622	7457	8232	11121	12508	16019	17634	19587
		Φ Average	28.2	24.3	23.8	17.7	15.8	12.5	11.2	9.5
		|E*| Coeff. of Variation	0.089	0.177	0.075	0.091	0.077	0.079	0.079	0.111
		Φ Coeff. of Variation	0.06	0.16	0.08	0.06	0.06	0.09	0.08	0.03
		|E*| Std. Dev.	409.7	1322.3	616.2	1016.6	965.4	1271.0	1396.5	2164.5
		Φ Std. Dev.	1.656	3.962	1.965	0.985	1.025	1.095	0.851	0.248
35	1	|E*| (MPa)	384	578	687	1172	1480	2727	3480	
		Phase Angle, Φ (°)	27.7	28.7	30.2	33.0	33.1	29.5	28.2	
		Average Peak Stress (MPa)	0.017	0.023	0.028	0.036	0.055	0.109	0.135	
		Average Peak Strain (με)	44	39	41	31	37	40	39	
	2	|E*| (MPa)	352	522	661	1163	1473	2861	3581	4782
		Phase Angle, Φ (°)	29.0	31.1	33.0	34.0	33.1	29.1	27.8	26.4
		Average Peak Stress (MPa)	0.017	0.023	0.028	0.037	0.055	0.109	0.135	0.246
		Average Peak Strain (με)	48	43	43	32	37	38	38	51
	3	|E*| (MPa)	335	522	654	1131	1478	2765	3531	4697
		Phase Angle, Φ (°)	28.9	31.0	31.4	34.2	33.0	28.8	27.3	25.3
		Average Peak Stress (MPa)	0.017	0.023	0.028	0.036	0.055	0.109	0.136	0.248
		Average Peak Strain (με)	50	43	43	32	37	40	38	53
	Avg.	|E*| Average	357	541	667	1156	1477	2784	3530	4739
		Φ Average	28.5	30.3	31.5	33.7	33.1	29.1	27.8	25.8
		|E*| Coeff. of Variation	0.070	0.060	0.026	0.019	0.002	0.025	0.014	0.013
		Φ Coeff. of Variation	0.02	0.04	0.04	0.02	0.00	0.01	0.02	0.03
		|E*| Std. Dev.	25.0	32.5	17.4	21.6	3.5	68.9	50.3	59.9
		Φ Std. Dev.	0.682	1.361	1.377	0.611	0.067	0.327	0.439	0.799

Table A-20 – S12.5C–Fine – Granite

Temp (°C)	Rep.	Parameters	Frequency (Hz)							
			0.01	0.05	0.1	0.5	1	5	10	25
-10	1	|E*| (MPa)	22539		25985	29425	30824	33479	34825	36061
		Phase Angle, Φ (°)	11.1		6.9	8.2	8.2	8.2	8.8	12.3
		Average Peak Stress (MPa)	1.212		1.468	1.640	1.750	1.863	1.953	2.082
		Average Peak Strain (με)	54		56	56	57	56	56	58
	2	|E*| (MPa)	20229	21630	25149	28083	29294	32103	33078	34344
		Phase Angle, Φ (°)	16.1	10.9	10.9	12.8	12.4	12.5	13.4	16.4
		Average Peak Stress (MPa)	1.356	1.525	1.582	1.753	1.808	1.975	2.034	2.200
		Average Peak Strain (με)	67	71	63	62	62	62	61	64
	3	|E*| (MPa)	22679	26985	27808	30896	31868	34691	35951	37288
		Phase Angle, Φ (°)	13.7	6.0	14.8	11.1	10.7	10.6	11.2	13.9
		Average Peak Stress (MPa)	1.356	1.525	1.582	1.753	1.809	1.973	2.033	2.191
		Average Peak Strain (με)	60	57	57	57	57	57	57	59
	Avg.	|E*| Average	21815	24307	26314	29468	30662	33424	34618	35898
		Φ Average	13.6	8.5	10.9	10.7	10.4	10.4	11.1	14.2
		|E*| Coeff. of Variation	0.063	0.156	0.052	0.048	0.042	0.039	0.042	0.041
		Φ Coeff. of Variation	0.18	0.42	0.36	0.22	0.20	0.21	0.20	0.14
		|E*| Std. Dev.	1375.5	3786.2	1359.9	1407.2	1294.5	1295.1	1447.8	1478.7
		Φ Std. Dev.	2.493	3.519	3.967	2.306	2.114	2.152	2.258	2.039
10	1	|E*| (MPa)	6662	8445	10798	13906	15072	18516	20024	22163
		Phase Angle, Φ (°)	25.3	21.8	22.3	17.6	16.2	15.0	15.3	18.4
		Average Peak Stress (MPa)	0.310	0.395	0.452	0.594	0.706	0.931	1.073	1.151
		Average Peak Strain (με)	47	47	42	43	47	50	54	52
	2	|E*| (MPa)	6242	8211	9710	13195	14654	18295	19859	22313
		Phase Angle, Φ (°)	31.2	26.2	23.8	22.1	20.1	19.0	19.5	22.2
		Average Peak Stress (MPa)	0.367	0.480	0.565	0.707	0.820	1.099	1.213	1.324
		Average Peak Strain (με)	59	58	58	54	56	60	61	59
	3	|E*| (MPa)	6866	9942	11508	14655	16135	19436	21251	23557
		Phase Angle, Φ (°)	29.3	28.5	24.1	20.3	19.2	17.7	18.6	21.6
		Average Peak Stress (MPa)	0.367	0.480	0.565	0.708	0.820	1.099	1.209	1.322
		Average Peak Strain (με)	54	48	49	48	51	57	57	56
	Avg.	|E*| Average	6590	8866	10672	13919	15287	18749	20378	22678
		Φ Average	28.6	25.5	23.4	20.0	18.5	17.3	17.8	20.7
		|E*| Coeff. of Variation	0.048	0.106	0.085	0.052	0.050	0.032	0.037	0.034
		Φ Coeff. of Variation	0.11	0.14	0.04	0.11	0.11	0.12	0.12	0.10
		|E*| Std. Dev.	318.3	939.5	905.8	729.6	763.7	605.0	760.2	765.3
		Φ Std. Dev.	3.015	3.444	0.980	2.263	2.072	2.028	2.205	2.029
35	1	|E*| (MPa)	558	949	1199	1885	2491	4238	5106	6481
		Phase Angle, Φ (°)	31.7	32.2	32.5	34.8	31.7	29.1	29.0	31.0
		Average Peak Stress (MPa)	0.028	0.057	0.085	0.113	0.169	0.250	0.305	0.392
		Average Peak Strain (με)	50	60	71	60	68	59	60	60
	2	|E*| (MPa)	695	974	1159	1802	2426	4154	5050	6332
		Phase Angle, Φ (°)	37.1	39.7	36.1	38.5	33.6	31.7	31.0	32.9
		Average Peak Stress (MPa)	0.025	0.034	0.051	0.079	0.169	0.223	0.305	0.448
		Average Peak Strain (με)	37	35	44	44	70	54	60	71
	3	|E*| (MPa)	646	1017	1261	2054	2810	4732	5868	7399
		Phase Angle, Φ (°)	34.1	33.7	35.5	37.0	33.0	30.9	30.0	31.8
		Average Peak Stress (MPa)	0.034	0.042	0.057	0.085	0.168	0.219	0.302	0.443
		Average Peak Strain (με)	52	41	45	41	60	46	51	60
	Avg.	|E*| Average	633	980	1206	1914	2576	4375	5341	6737
		Φ Average	34.3	35.2	34.7	36.8	32.8	30.6	30.0	31.9
		|E*| Coeff. of Variation	0.109	0.035	0.043	0.067	0.080	0.071	0.086	0.086
		Φ Coeff. of Variation	0.08	0.11	0.06	0.05	0.03	0.04	0.03	0.03
		|E*| Std. Dev.	69.2	34.4	51.5	128.5	205.2	312.6	457.0	577.9
		Φ Std. Dev.	2.691	3.967	1.927	1.888	0.959	1.324	0.968	0.928

Table A-21 – S12.5C–Fine – Limestone

Temp (°C)	Rep.	Parameters	Frequency (Hz)							
			0.01	0.05	0.1	0.5	1	5	10	25
-10	1	|E*| (MPa)	16085	19423	18827	21101	21971	23583	24343	25208
		Phase Angle, Φ (°)	5.5	4.6	2.9	3.8	3.0	2.4	1.7	1.9
		Average Peak Stress (MPa)	1.351	1.577	1.634	1.747	1.802	1.970	2.031	2.195
		Average Peak Strain (με)	84	81	87	83	82	84	83	87
	2	|E*| (MPa)	17149	18331	20053	22556	23324	25149	25879	26425
		Phase Angle, Φ (°)	8.4	9.7	4.5	5.6	5.2	4.4	3.8	3.7
		Average Peak Stress (MPa)	1.083	1.264	1.309	1.400	1.445	1.579	1.627	1.758
		Average Peak Strain (με)	63	69	65	62	62	63	63	67
	3	|E*| (MPa)	13243	17068	19071	21580	22773	24708	25437	26260
		Phase Angle, Φ (°)	12.4	9.2	8.0	7.6	7.0	6.1	5.1	4.6
		Average Peak Stress (MPa)	1.083	1.264	1.309	1.400	1.444	1.578	1.629	1.756
		Average Peak Strain (με)	82	74	69	65	63	64	64	67
	Avg.	|E*| Average	15492	18274	19317	21746	22690	24480	25220	25964
		Φ Average	8.8	7.8	5.1	5.7	5.1	4.3	3.6	3.4
		|E*| Coeff. of Variation	0.130	0.065	0.034	0.034	0.030	0.033	0.031	0.025
		Φ Coeff. of Variation	0.39	0.36	0.51	0.33	0.39	0.43	0.48	0.39
		|E*| Std. Dev.	2018.9	1179.0	648.7	741.7	680.3	807.6	790.7	660.2
		Φ Std. Dev.	3.443	2.830	2.620	1.882	1.993	1.854	1.700	1.339
10	1	|E*| (MPa)	5228	7027	8125	10395	11312	13806	15039	16427
		Phase Angle, Φ (°)	20.4	19.7	13.4	12.4	10.9	8.8	7.8	7.6
		Average Peak Stress (MPa)	0.226	0.316	0.384	0.497	0.587	0.811	0.924	1.010
		Average Peak Strain (με)	43	45	47	48	52	59	61	61
	2	|E*| (MPa)	5511	8188	8819	10954	12125	14957	16063	17474
		Phase Angle, Φ (°)	22.8	19.1	18.8	14.4	13.3	11.2	10.2	9.6
		Average Peak Stress (MPa)	0.226	0.316	0.384	0.497	0.587	0.812	0.924	1.014
		Average Peak Strain (με)	41	39	43	45	48	54	58	58
	3	|E*| (MPa)	5609	8147	8983	11257	12282	14796	15977	17450
		Phase Angle, Φ (°)	28.6	27.1	19.9	18.4	15.9	12.9	11.8	11.3
		Average Peak Stress (MPa)	0.226	0.316	0.384	0.497	0.587	0.811	0.925	1.012
		Average Peak Strain (με)	40	39	43	44	48	55	58	58
	Avg.	|E*| Average	5450	7787	8642	10869	11906	14520	15693	17117
		Φ Average	24.0	22.0	17.4	15.1	13.3	11.0	10.0	9.5
		|E*| Coeff. of Variation	0.036	0.085	0.053	0.040	0.044	0.043	0.036	0.035
		Φ Coeff. of Variation	0.18	0.20	0.20	0.20	0.19	0.19	0.20	0.19
		|E*| Std. Dev.	197.9	658.8	455.1	437.1	520.9	623.4	568.1	597.7
		Φ Std. Dev.	4.234	4.447	3.469	3.031	2.537	2.036	2.036	1.828
35	1	|E*| (MPa)	524	830	1047	1706	2173	3741	4599	5658
		Phase Angle, Φ (°)	26.2	28.1	28.5	29.8	27.6	22.4	20.5	19.9
		Average Peak Stress (MPa)	0.022	0.034	0.059	0.090	0.134	0.222	0.310	0.353
		Average Peak Strain (με)	43	41	56	53	62	59	67	62
	2	|E*| (MPa)	729	987	1140	1734	2205	3811	4613	5691
		Phase Angle, Φ (°)	23.5	27.5	30.1	31.9	29.6	25.7	22.9	22.4
		Average Peak Stress (MPa)	0.022	0.034	0.056	0.090	0.134	0.222	0.311	0.355
		Average Peak Strain (με)	31	34	50	52	61	58	67	62
	3	|E*| (MPa)	716	955	1135	1729	2196	3752	4570	5617
		Phase Angle, Φ (°)	31.5	31.8	30.1	32.2	30.1	25.6	23.1	22.1
		Average Peak Stress (MPa)	0.023	0.034	0.059	0.090	0.134	0.222	0.311	0.355
		Average Peak Strain (με)	32	35	52	52	61	59	68	63
	Avg.	|E*| Average	656	924	1107	1723	2191	3768	4594	5655
		Φ Average	27.1	29.1	29.6	31.3	29.1	24.6	22.1	21.5
		|E*| Coeff. of Variation	0.174	0.090	0.047	0.009	0.008	0.010	0.005	0.007
		Φ Coeff. of Variation	0.15	0.08	0.03	0.04	0.05	0.08	0.07	0.06
		|E*| Std. Dev.	114.4	83.0	52.2	15.2	16.6	37.4	21.8	37.4
		Φ Std. Dev.	4.083	2.311	0.900	1.305	1.332	1.855	1.454	1.350
54.4	1	|E*| (MPa)	247	296	320	447	551	976	1278	1798
		Phase Angle, Φ (°)	10.5	11.5	20.8	23.8	25.0	25.9	25.0	25.9
		Average Peak Stress (MPa)	0.004	0.007	0.011	0.023	0.029	0.049	0.071	0.095
		Average Peak Strain (με)	18	23	36	51	53	50	56	53
	2	|E*| (MPa)		448	489	556	641	1049	1325	1800
		Phase Angle, Φ (°)		14.7	15.4	22.0	24.9	27.1	26.2	27.3
		Average Peak Stress (MPa)		0.007	0.011	0.023	0.029	0.049	0.071	0.095
		Average Peak Strain (με)		15	23	41	46	47	54	53
	3	|E*| (MPa)	516	473	416	511	603	998	1316	1815
		Phase Angle, Φ (°)	20.0	25.4	24.2	26.3	27.1	28.1	26.6	28.2
		Average Peak Stress (MPa)	0.005	0.007	0.011	0.023	0.029	0.049	0.072	0.094
		Average Peak Strain (με)	9	14	27	44	48	49	54	52
	Avg.	|E*| Average	382	406	408	505	598	1008	1306	1804
		Φ Average	15.3	17.2	20.1	24.0	25.7	27.0	26.0	27.1
		|E*| Coeff. of Variation	0.498	0.237	0.208	0.109	0.075	0.037	0.019	0.005
		Φ Coeff. of Variation	0.44	0.42	0.22	0.09	0.05	0.04	0.03	0.04
		|E*| Std. Dev.	190.1	96.0	84.8	54.9	45.0	37.1	24.9	9.6
		Φ Std. Dev.	6.731	7.292	4.434	2.160	1.270	1.079	0.827	1.175

Table A-22 – S12.5D–Coarse – Granite

Temp (°C)	Rep.	Parameters	Frequency (Hz)							
			0.01	0.05	0.1	0.5	1	5	10	25
-10	1	|E*| (MPa)	20674	21519	27178	29179	30302	32928	34041	35616
		Phase Angle, Φ (°)	16.1	17.4	15.8	12.6	12.0	11.8	12.8	16.1
		Average Peak Stress (MPa)	1.270	1.467	1.524	1.696	1.806	1.918	2.004	2.134
		Average Peak Strain (με)	61	68	56	58	60	58	59	60
	2	|E*| (MPa)	20772	22398	25808	29546	31089	33935	35201	36661
		Phase Angle, Φ (°)	12.3	8.3	9.7	9.6	9.1	9.1	10.3	13.8
		Average Peak Stress (MPa)	1.213	1.411	1.468	1.639	1.748	1.859	1.948	2.072
		Average Peak Strain (με)	58	63	57	55	56	55	55	57
	3	|E*| (MPa)	21144		24997	29721	30696	34081	35283	36758
		Phase Angle, Φ (°)	11.8		10.3	8.9	8.3	8.5	9.2	13.0
		Average Peak Stress (MPa)	1.269		1.524	1.696	1.805	1.917	2.005	2.134
		Average Peak Strain (με)	60		61	57	59	56	57	58
	Avg.	|E*| Average	20863	21958	25994	29482	30695	33648	34842	36345
		Φ Average	13.4	12.9	11.9	10.4	9.8	9.8	10.8	14.3
		|E*| Coeff. of Variation	0.012	0.028	0.042	0.009	0.013	0.019	0.020	0.017
		Φ Coeff. of Variation	0.17	0.50	0.28	0.19	0.20	0.18	0.17	0.11
		|E*| Std. Dev.	247.9	621.6	1102.2	276.8	393.5	627.8	694.8	633.3
		Φ Std. Dev.	2.345	6.439	3.361	1.963	1.978	1.775	1.814	1.615
10	1	|E*| (MPa)	5360	7877	9248	12440	13835	17138	18871	19845
		Phase Angle, Φ (°)	30.9	22.0	22.6	21.8	20.0	17.9	18.2	19.7
		Average Peak Stress (MPa)	0.367	0.480	0.565	0.706	0.818	1.071	1.241	1.325
		Average Peak Strain (με)	68	61	61	57	59	62	66	67
	2	|E*| (MPa)	5841	9157	10405	13350	14682	18209	19830	22215
		Phase Angle, Φ (°)	27.3	27.2	22.8	19.3	18.4	16.5	17.2	20.2
		Average Peak Stress (MPa)	0.310	0.395	0.452	0.593	0.705	0.929	1.071	1.150
		Average Peak Strain (με)	53	43	43	44	48	51	54	52
	3	|E*| (MPa)								
		Phase Angle, Φ (°)								
		Average Peak Stress (MPa)								
		Average Peak Strain (με)								
	Avg.	|E*| Average	5600	8517	9827	12895	14258	17674	19351	21030
		Φ Average	29.1	24.6	22.7	20.5	19.2	17.2	17.7	19.9
		|E*| Coeff. of Variation	0.061	0.106	0.083	0.050	0.042	0.043	0.035	0.080
		Φ Coeff. of Variation	0.09	0.15	0.01	0.09	0.06	0.06	0.04	0.02
		|E*| Std. Dev.	340.3	905.7	818.0	643.4	598.8	757.6	678.1	1675.4
		Φ Std. Dev.	2.529	3.662	0.161	1.796	1.139	0.959	0.693	0.399
35	1	|E*| (MPa)	524	827	1067	1586	2186	3773	4719	6154
		Phase Angle, Φ (°)	29.0	29.3	30.1	35.7	32.2	31.2	31.3	33.7
		Average Peak Stress (MPa)	0.071	0.113	0.169	0.198	0.281	0.390	0.446	0.565
		Average Peak Strain (με)	135	136	159	125	128	103	94	92
	2	|E*| (MPa)	472	747	947	1481	2034	3635	4570	6001
		Phase Angle, Φ (°)	29.0	30.5	30.3	34.9	32.2	30.0	30.2	32.8
		Average Peak Stress (MPa)	0.042	0.071	0.113	0.141	0.196	0.305	0.361	0.450
		Average Peak Strain (με)	89	94	119	95	97	84	79	75
	3	|E*| (MPa)	505	818	1076	1655	2290	3951	4941	6457
		Phase Angle, Φ (°)	27.8	29.1	29.2	34.5	31.0	29.4	29.7	32.4
		Average Peak Stress (MPa)	0.070	0.113	0.169	0.198	0.281	0.390	0.445	0.563
		Average Peak Strain (με)	140	138	157	119	123	99	90	87
	Avg.	|E*| Average	500	797	1030	1574	2170	3786	4743	6204
		Φ Average	28.6	29.6	29.9	35.0	31.8	30.2	30.4	33.0
		|E*| Coeff. of Variation	0.053	0.055	0.070	0.056	0.059	0.042	0.039	0.037
		Φ Coeff. of Variation	0.02	0.03	0.02	0.02	0.02	0.03	0.03	0.02
		|E*| Std. Dev.	26.4	43.9	72.3	87.9	129.1	158.7	186.6	232.2
		Φ Std. Dev.	0.697	0.754	0.586	0.598	0.694	0.931	0.790	0.696

Table A-23 – S12.5D–Fine – Granite

Temp (°C)	Rep.	Parameters	Frequency (Hz)							
			0.01	0.05	0.1	0.5	1	5	10	25
-10	1	|E*| (MPa)	21274	23784	24782	28509	29395	31576	32765	34053
		Phase Angle, Φ (°)	9.8	1.0	5.1	7.2	7.4	6.1	5.4	5.4
		Average Peak Stress (MPa)	1.214	1.440	1.497	1.640	1.694	1.863	1.921	2.079
		Average Peak Strain (με)	57	61	60	58	58	59	59	61
	2	|E*| (MPa)		20914	23869	28057	29116	31507	32542	
		Phase Angle, Φ (°)		5.7	6.9	4.8	4.9	3.9	4.0	
		Average Peak Stress (MPa)		1.440	1.497	1.639	1.693	1.863	1.918	
		Average Peak Strain (με)		69	63	58	58	59	59	
	3	|E*| (MPa)	20390	21438	24408	26198	27289	29516	30370	
		Phase Angle, Φ (°)	6.8	1.2	2.8	4.9	4.8	3.6	3.3	
		Average Peak Stress (MPa)	1.214	1.440	1.497	1.640	1.694	1.863	1.924	
		Average Peak Strain (με)	60	67	61	63	62	63	63	
	Avg.	|E*| Average	20832	22045	24353	27588	28600	30866	31892	34053
		Φ Average	8.3	2.6	4.9	5.6	5.7	4.5	4.2	5.4
		|E*| Coeff. of Variation	0.030	0.069	0.019	0.044	0.040	0.038	0.041	
		Φ Coeff. of Variation	0.25	1.01	0.42	0.25	0.25	0.31	0.26	
		|E*| Std. Dev.	625.0	1528.2	459.2	1225.1	1144.2	1169.6	1323.3	
		Φ Std. Dev.	2.108	2.664	2.055	1.403	1.435	1.387	1.096	
10	1	|E*| (MPa)	7460	8894	10338	14074	15080	18097	19466	21420
		Phase Angle, Φ (°)	28.6	16.3	23.1	17.5	15.7	13.7	12.2	12.1
		Average Peak Stress (MPa)	0.141	0.240	0.282	0.395	0.507	0.704	0.819	0.919
		Average Peak Strain (με)	19	27	27	28	34	39	42	43
	2	|E*| (MPa)	7022	9168	11641	13661	15042	18138	19642	21599
		Phase Angle, Φ (°)	23.8	28.0	15.6	14.0	13.3	10.5	9.1	8.6
		Average Peak Stress (MPa)	0.141	0.240	0.282	0.395	0.507	0.703	0.819	0.919
		Average Peak Strain (με)	20	26	24	29	34	39	42	43
	3	|E*| (MPa)	7775	11148	10855	13845	14851	17582	18963	20573
		Phase Angle, Φ (°)	23.1	27.6	13.5	14.8	12.7	10.0	9.3	8.8
		Average Peak Stress (MPa)	0.141	0.240	0.283	0.396	0.508	0.703	0.820	0.921
		Average Peak Strain (με)	18	22	26	29	34	40	43	45
	Avg.	|E*| Average	7419	9737	10945	13860	14991	17939	19357	21197
		Φ Average	25.2	24.0	17.4	15.4	13.9	11.4	10.2	9.8
		|E*| Coeff. of Variation	0.051	0.126	0.060	0.015	0.008	0.017	0.018	0.026
		Φ Coeff. of Variation	0.12	0.28	0.29	0.12	0.11	0.18	0.17	0.20
		|E*| Std. Dev.	378.2	1229.9	656.1	206.7	122.8	309.4	352.4	547.9
		Φ Std. Dev.	2.960	6.656	5.043	1.850	1.570	2.009	1.749	1.977
35	1	|E*| (MPa)	628	1027	1257	2136	2602	4259	5344	6505
		Phase Angle, Φ (°)	35.9	37.2	37.9	37.4	35.2	29.9	28.1	24.8
		Average Peak Stress (MPa)	0.017	0.023	0.028	0.037	0.056	0.110	0.137	0.249
		Average Peak Strain (με)	27	22	22	17	21	26	26	38
	2	|E*| (MPa)	608	953	1156	1905	2349	4077	5003	6231
		Phase Angle, Φ (°)	32.7	32.1	34.9	34.4	33.1	27.6	26.3	23.0
		Average Peak Stress (MPa)	0.017	0.023	0.028	0.036	0.055	0.110	0.136	0.247
		Average Peak Strain (με)	28	24	24	19	24	27	27	40
	3	|E*| (MPa)	670	1072	1343	2261	2721	4452	5394	6580
		Phase Angle, Φ (°)	34.7	34.8	34.6	34.4	32.4	26.5	24.5	22.1
		Average Peak Stress (MPa)	0.017	0.023	0.028	0.037	0.056	0.110	0.137	0.249
		Average Peak Strain (με)	25	21	21	16	21	25	25	38
	Avg.	|E*| Average	636	1018	1252	2101	2557	4263	5247	6439
		Φ Average	34.4	34.7	35.8	35.4	33.6	28.0	26.3	23.3
		|E*| Coeff. of Variation	0.050	0.059	0.075	0.086	0.074	0.044	0.041	0.029
		Φ Coeff. of Variation	0.05	0.07	0.05	0.05	0.04	0.06	0.07	0.06
		|E*| Std. Dev.	31.6	60.2	93.4	180.5	189.9	187.3	212.9	183.7
		Φ Std. Dev.	1.653	2.528	1.813	1.773	1.462	1.729	1.792	1.390

Table A-24 – I19.0B–Coarse – Granite

Temp (°C)	Rep.	Parameters	Frequency (Hz)							
			0.01	0.05	0.1	0.5	1	5	10	25
-10	1	|E*| (MPa)	15957	17773	19485	23351	24588	27439	28730	30202
		Phase Angle, Φ (°)	10.5	11.9	7.5	6.8	6.3	5.3	4.9	4.6
		Average Peak Stress (MPa)	1.353	1.579	1.636	1.749	1.804	1.970	2.029	2.190
		Average Peak Strain (με)	85	89	84	75	73	72	71	73
	2	|E*| (MPa)	15141	19635	19685	22179	23379	26174	27318	28733
		Phase Angle, Φ (°)	8.9	5.0	4.2	4.7	4.3	3.2	2.4	2.4
		Average Peak Stress (MPa)	1.353	1.579	1.636	1.749	1.804	1.970	2.030	2.191
		Average Peak Strain (με)	89	80	83	79	77	75	74	76
	3	|E*| (MPa)	17376	23261	21816	26005	27572	30807	32332	34190
		Phase Angle, Φ (°)	11.7	10.8	10.4	8.0	7.2	6.0	5.4	5.6
		Average Peak Stress (MPa)	1.353	1.579	1.636	1.749	1.804	1.970	2.030	2.193
		Average Peak Strain (με)	78	68	75	67	65	64	63	64
	Avg.	|E*| Average	16158	20223	20328	23845	25180	28140	29460	31042
		Φ Average	10.4	9.2	7.4	6.5	6.0	4.8	4.2	4.2
		|E*| Coeff. of Variation	0.070	0.138	0.064	0.082	0.086	0.085	0.088	0.091
		Φ Coeff. of Variation	0.14	0.40	0.43	0.26	0.25	0.30	0.37	0.39
		|E*| Std. Dev.	1130.8	2790.9	1292.3	1960.4	2158.3	2394.6	2585.3	2823.6
		Φ Std. Dev.	1.415	3.700	3.146	1.675	1.477	1.462	1.576	1.616
10	1	|E*| (MPa)	3315	5307	6153	8556	9846	13154	14698	16783
		Phase Angle, Φ (°)	27.0	22.9	21.9	19.0	17.5	14.0	12.6	11.8
		Average Peak Stress (MPa)	0.367	0.479	0.564	0.706	0.817	1.097	1.208	1.319
		Average Peak Strain (με)	111	90	92	82	83	83	82	79
	2	|E*| (MPa)	2888	4385	5381	7744	8974	12185	13717	15580
		Phase Angle, Φ (°)	26.6	25.1	20.7	18.3	16.6	12.8	11.5	10.5
		Average Peak Stress (MPa)	0.367	0.479	0.564	0.706	0.817	1.097	1.208	1.320
		Average Peak Strain (με)	127	109	105	91	91	90	88	85
	3	|E*| (MPa)	3527	5512	6697	9387	10765	14396	16188	18624
		Phase Angle, Φ (°)	28.0	27.4	23.0	20.2	18.6	14.9	13.5	12.5
		Average Peak Stress (MPa)	0.367	0.479	0.564	0.705	0.817	1.097	1.208	1.321
		Average Peak Strain (με)	104	87	84	75	76	76	75	71
	Avg.	|E*| Average	3244	5068	6077	8562	9862	13245	14868	16996
		Φ Average	27.2	25.1	21.9	19.2	17.5	13.9	12.5	11.6
		|E*| Coeff. of Variation	0.100	0.118	0.109	0.096	0.091	0.084	0.084	0.090
		Φ Coeff. of Variation	0.03	0.09	0.05	0.05	0.06	0.08	0.08	0.08
		|E*| Std. Dev.	325.5	600.1	661.1	821.1	895.6	1108.4	1244.3	1532.9
		Φ Std. Dev.	0.717	2.290	1.175	0.976	1.008	1.048	1.015	0.974
35	1	|E*| (MPa)	298	449	563	971	1370	2438	3108	4220
		Phase Angle, Φ (°)	26.3	29.5	28.7	31.7	28.5	27.8	26.4	25.5
		Average Peak Stress (MPa)	0.025	0.034	0.051	0.078	0.168	0.221	0.302	0.441
		Average Peak Strain (με)	85	75	90	81	122	90	97	104
	2	|E*| (MPa)	253	390	494	850	1209	2123	2738	3744
		Phase Angle, Φ (°)	22.3	25.1	25.5	29.1	26.8	26.4	25.2	24.8
		Average Peak Stress (MPa)	0.025	0.034	0.051	0.079	0.168	0.220	0.302	0.440
		Average Peak Strain (με)	100	87	103	92	139	104	110	117
	3	|E*| (MPa)	327	490	590	989	1363	2400	3080	4185
		Phase Angle, Φ (°)	26.6	28.8	29.1	31.5	28.3	27.6	26.8	25.5
		Average Peak Stress (MPa)	0.025	0.034	0.051	0.078	0.168	0.220	0.302	0.440
		Average Peak Strain (με)	78	69	86	79	123	92	98	105
	Avg.	|E*| Average	293	443	549	937	1314	2320	2976	4050
		Φ Average	25.1	27.8	27.8	30.8	27.9	27.2	26.1	25.3
		|E*| Coeff. of Variation	0.127	0.113	0.091	0.081	0.070	0.074	0.069	0.065
		Φ Coeff. of Variation	0.10	0.08	0.07	0.05	0.03	0.03	0.03	0.02
		|E*| Std. Dev.	37.2	50.2	49.8	75.7	91.3	171.8	205.9	265.0
		Φ Std. Dev.	2.433	2.360	1.984	1.461	0.945	0.779	0.821	0.384

Table A-25 – I19.0B–Coarse – Limestone

Temp (°C)	Rep.	Parameters	Frequency (Hz)							
			0.01	0.05	0.1	0.5	1	5	10	25
-10	1	|E*| (MPa)	22909	25635	27922	29251	29794	31626	32320	33399
		Phase Angle, Φ (°)	8.4	13.3	5.8	6.2	5.6	3.8	2.9	3.1
		Average Peak Stress (MPa)	1.353	1.578	1.635	1.748	1.803	1.970	2.031	2.192
		Average Peak Strain (με)	59	62	59	60	61	62	63	66
	2	|E*| (MPa)	19329	20766	23867	25990	26833	28871	29730	30791
		Phase Angle, Φ (°)	9.0	8.9	9.0	5.6	5.0	4.4	3.9	3.8
		Average Peak Stress (MPa)	1.353	1.578	1.635	1.748	1.803	1.970	2.030	2.192
		Average Peak Strain (με)	70	76	69	67	67	68	68	71
	3	|E*| (MPa)	20059	24242	24683	25912	26839	29023	29851	30691
		Phase Angle, Φ (°)	7.5	10.5	6.2	4.7	4.4	2.9	2.4	2.8
		Average Peak Stress (MPa)	1.353	1.579	1.635	1.748	1.803	1.970	2.031	2.194
		Average Peak Strain (με)	67	65	66	67	67	68	68	71
	Avg.	|E*| Average	20766	23548	25491	27051	27822	29840	30634	31627
		Φ Average	8.3	10.9	7.0	5.5	5.0	3.7	3.1	3.2
		|E*| Coeff. of Variation	0.091	0.106	0.084	0.070	0.061	0.052	0.048	0.049
		Φ Coeff. of Variation	0.09	0.20	0.25	0.14	0.13	0.21	0.24	0.16
		|E*| Std. Dev.	1891.5	2507.6	2144.4	1905.4	1708.0	1548.3	1461.6	1535.6
		Φ Std. Dev.	0.764	2.224	1.733	0.759	0.642	0.779	0.743	0.521
10	1	|E*| (MPa)	5733	8094	9598	13010	14469	17732	19239	21424
		Phase Angle, Φ (°)	29.4	26.6	23.2	18.7	16.5	12.3	11.0	10.3
		Average Peak Stress (MPa)	0.282	0.395	0.480	0.620	0.733	1.011	1.154	1.264
		Average Peak Strain (με)	49	49	50	48	51	57	60	59
	2	|E*| (MPa)	5400	8241	8531	11508	12553	15812	17560	19447
		Phase Angle, Φ (°)	26.8	20.9	19.9	17.1	15.3	11.6	10.9	9.9
		Average Peak Stress (MPa)	0.282	0.395	0.479	0.620	0.733	1.013	1.153	1.263
		Average Peak Strain (με)	52	48	56	54	58	64	66	65
	3	|E*| (MPa)	5692	7680	9438	12395	13668	16938	18399	20251
		Phase Angle, Φ (°)	26.7	20.6	17.5	16.0	13.7	10.5	9.1	8.5
		Average Peak Stress (MPa)	0.282	0.395	0.479	0.620	0.733	1.012	1.155	1.267
		Average Peak Strain (με)	50	51	51	50	54	60	63	63
	Avg.	|E*| Average	5608	8005	9189	12304	13563	16827	18400	20374
		Φ Average	27.6	22.7	20.2	17.3	15.2	11.5	10.3	9.6
		|E*| Coeff. of Variation	0.032	0.036	0.063	0.061	0.071	0.057	0.046	0.049
		Φ Coeff. of Variation	0.05	0.15	0.14	0.08	0.09	0.08	0.10	0.10
		|E*| Std. Dev.	181.3	290.9	575.7	754.9	962.1	964.8	839.4	994.0
		Φ Std. Dev.	1.508	3.358	2.864	1.351	1.415	0.900	1.048	0.974
35	1	|E*| (MPa)	503	772	997	1780	2400	4367	5443	6999
		Phase Angle, Φ (°)	31.4	33.0	33.0	36.1	33.6	29.9	26.4	24.1
		Average Peak Stress (MPa)	0.014	0.028	0.037	0.064	0.097	0.137	0.221	0.393
		Average Peak Strain (με)	28	36	37	36	41	31	41	56
	2	|E*| (MPa)	478	751	961	1703	2276	4052	5118	6514
		Phase Angle, Φ (°)	29.3	31.2	31.7	33.6	30.9	27.8	24.4	22.0
		Average Peak Stress (MPa)	0.014	0.028	0.037	0.064	0.097	0.137	0.221	0.394
		Average Peak Strain (με)	30	37	38	38	43	34	43	60
	3	|E*| (MPa)	503	787	984	1741	2302	4046	5140	6660
		Phase Angle, Φ (°)	29.9	32.2	31.9	33.5	31.2	28.4	24.4	21.8
		Average Peak Stress (MPa)	0.014	0.028	0.037	0.064	0.097	0.137	0.221	0.395
		Average Peak Strain (με)	28	36	37	37	42	34	43	59
	Avg.	|E*| Average	494	770	980	1741	2326	4155	5234	6724
		Φ Average	30.2	32.1	32.2	34.4	31.9	28.7	25.1	22.6
		|E*| Coeff. of Variation	0.029	0.023	0.019	0.022	0.028	0.044	0.035	0.037
		Φ Coeff. of Variation	0.04	0.03	0.02	0.04	0.05	0.04	0.05	0.06
		|E*| Std. Dev.	14.1	18.0	18.2	38.1	65.6	183.7	181.4	248.7
		Φ Std. Dev.	1.097	0.910	0.743	1.469	1.504	1.078	1.172	1.247
54.4	1	|E*| (MPa)	290	284	260	369	463	871	1218	1831
		Phase Angle, Φ (°)	17.4	19.4	21.0	23.9	25.3	27.6	26.6	27.4
		Average Peak Stress (MPa)	0.006	0.009	0.014	0.028	0.036	0.061	0.092	0.128
		Average Peak Strain (με)	20	30	54	76	78	70	75	70
	2	|E*| (MPa)	259	260	269	378	472	873	1211	1818
		Phase Angle, Φ (°)	15.2	17.6	21.6	24.8	26.0	28.1	27.0	27.9
		Average Peak Stress (MPa)	0.006	0.009	0.014	0.028	0.036	0.061	0.091	0.127
		Average Peak Strain (με)	22	33	53	74	76	70	75	70
	3	|E*| (MPa)	231	268	285	400	496	920	1257	1890
		Phase Angle, Φ (°)	13.4	19.0	19.5	23.5	24.7	26.9	26.6	27.8
		Average Peak Stress (MPa)	0.006	0.008	0.014	0.028	0.036	0.062	0.091	0.127
		Average Peak Strain (με)	24	32	50	70	73	67	73	67
	Avg.	|E*| Average	260	271	272	382	477	888	1229	1846
		Φ Average	15.3	18.6	20.7	24.1	25.3	27.6	26.8	27.7
		|E*| Coeff. of Variation	0.113	0.046	0.047	0.042	0.035	0.031	0.020	0.021
		Φ Coeff. of Variation	0.13	0.05	0.05	0.03	0.03	0.02	0.01	0.01
		|E*| Std. Dev.	29.5	12.5	12.9	16.1	16.6	27.8	25.1	38.4
		Φ Std. Dev.	2.037	0.949	1.077	0.658	0.640	0.617	0.241	0.233

Table A-26 – I19.0B0–Fine – Granite

Temp (°C)	Rep.	Parameters	Frequency (Hz)							
			0.01	0.05	0.1	0.5	1	5	10	25
-10	1	|E*| (MPa)	16608	21479	21280	24785	26011	28798	29930	31413
		Phase Angle, Φ (°)	11.3	4.5	9.9	6.5	5.2	4.1	3.6	3.6
		Average Peak Stress (MPa)	1.355	1.582	1.639	1.752	1.808	1.976	2.034	2.196
		Average Peak Strain (με)	82	74	77	71	69	69	68	70
	2	|E*| (MPa)	19383		26073	28731	30061	33060	34365	35949
		Phase Angle, Φ (°)	12.1		6.4	7.1	5.5	5.6	3.9	4.0
		Average Peak Stress (MPa)	1.218		1.473	1.575	1.624	1.773	1.826	1.969
		Average Peak Strain (με)	63		56	55	54	54	53	55
	3	|E*| (MPa)	16943	18102	21600	24902	26275	28823	29731	30942
		Phase Angle, Φ (°)	9.7	11.2	3.1	4.9	4.6	3.2	2.7	2.8
		Average Peak Stress (MPa)	0.947	1.105	1.145	1.225	1.263	1.378	1.420	1.530
		Average Peak Strain (με)	56	61	53	49	48	48	48	49
	Avg.	|E*| Average	17645	19791	22984	26139	27449	30227	31342	32768
		Φ Average	11.0	7.9	6.5	6.2	5.1	4.3	3.4	3.5
		|E*| Coeff. of Variation	0.086	0.121	0.117	0.086	0.083	0.081	0.084	0.084
		Φ Coeff. of Variation	0.11	0.60	0.52	0.18	0.09	0.29	0.19	0.18
		|E*| Std. Dev.	1514.7	2388.1	2679.6	2245.6	2266.0	2453.7	2619.5	2764.9
		Φ Std. Dev.	1.225	4.685	3.396	1.111	0.465	1.243	0.636	0.623
10	1	|E*| (MPa)	2767	4529	5642	8417	9822	13556	15331	17274
		Phase Angle, Φ (°)	31.7	28.7	25.3	21.8	18.4	15.2	15.3	12.2
		Average Peak Stress (MPa)	0.257	0.336	0.395	0.494	0.573	0.767	0.844	1.322
		Average Peak Strain (με)	93	74	70	59	58	57	55	77
	2	|E*| (MPa)	3454	6158	6820	10217	11787	15577	17247	19541
		Phase Angle, Φ (°)	31.6	25.9	25.7	21.4	18.4	14.9	13.2	12.4
		Average Peak Stress (MPa)	0.257	0.334	0.395	0.495	0.573	0.767	0.883	0.961
		Average Peak Strain (με)	74	54	58	48	49	49	51	49
	3	|E*| (MPa)	3002	5125	6056	8926	10368	13828	15434	17597
		Phase Angle, Φ (°)	31.0	24.0	24.9	19.1	15.9	13.2	11.6	10.8
		Average Peak Stress (MPa)	0.257	0.335	0.395	0.495	0.574	0.767	0.885	0.962
		Average Peak Strain (με)	85	65	65	55	55	55	57	55
	Avg.	|E*| Average	3074	5270	6173	9187	10659	14320	16004	18137
		Φ Average	31.4	26.2	25.3	20.7	17.6	14.5	13.4	11.8
		|E*| Coeff. of Variation	0.114	0.156	0.097	0.101	0.095	0.077	0.067	0.068
		Φ Coeff. of Variation	0.01	0.09	0.01	0.07	0.08	0.07	0.14	0.08
		|E*| Std. Dev.	349.4	824.2	597.5	927.6	1014.0	1096.3	1077.5	1226.1
		Φ Std. Dev.	0.407	2.355	0.372	1.458	1.462	1.074	1.851	0.890
35	1	|E*| (MPa)	188		353	676	1012	1960	2662	3833
		Phase Angle, Φ (°)	19.3		30.7	35.3	31.3	31.4	29.9	28.8
		Average Peak Stress (MPa)	0.016		0.031	0.047	0.100	0.128	0.178	0.259
		Average Peak Strain (με)	86		87	70	99	65	67	68
	2	|E*| (MPa)		311	416	790	1123	2194	2964	4243
		Phase Angle, Φ (°)		30.0	30.6	33.8	31.2	31.3	28.8	27.5
		Average Peak Stress (MPa)		0.023	0.030	0.055	0.098	0.151	0.208	0.305
		Average Peak Strain (με)		73	71	70	87	69	70	72
	3	|E*| (MPa)	168	262	349	674	984	2031	2653	3773
		Phase Angle, Φ (°)	26.1	28.1	30.2	33.9	31.1	30.1	28.6	27.2
		Average Peak Stress (MPa)	0.014	0.023	0.030	0.055	0.097	0.155	0.208	0.305
		Average Peak Strain (με)	86	89	85	82	99	76	78	81
	Avg.	|E*| Average	178	287	373	713	1040	2062	2759	3950
		Φ Average	22.7	29.0	30.5	34.3	31.2	30.9	29.1	27.8
		|E*| Coeff. of Variation	0.078	0.120	0.102	0.093	0.070	0.058	0.064	0.065
		Φ Coeff. of Variation	0.21	0.05	0.01	0.02	0.00	0.02	0.02	0.03
		|E*| Std. Dev.	13.9	34.4	38.0	66.6	73.1	119.9	176.8	255.9
		Φ Std. Dev.	4.817	1.347	0.241	0.802	0.126	0.697	0.661	0.865

Table A-27 – I19.0B1–Fine – Granite

Temp (°C)	Rep.	Parameters	Frequency (Hz)							
			0.01	0.05	0.1	0.5	1	5	10	25
-10	1	|E*| (MPa)	21830	26843	25994	30727	32256	35426	36482	38083
		Phase Angle, Φ (°)	7.4	-1.2	2.5	3.7	3.3	2.4	1.9	2.0
		Average Peak Stress (MPa)	1.214	1.440	1.497	1.640	1.695	1.863	1.922	2.078
		Average Peak Strain (με)	56	54	58	53	53	53	53	55
	2	|E*| (MPa)	21336	23309	29176	31219	32658	36331		
		Phase Angle, Φ (°)	13.7	7.5	9.0	9.9	10.0	9.1		
		Average Peak Stress (MPa)	1.214	1.440	1.497	1.640	1.694	1.863		
		Average Peak Strain (με)	57	62	51	53	52	51		
	3	|E*| (MPa)	22319	23547	28243	31443	32955	36356	37115	39189
		Phase Angle, Φ (°)	11.9	11.4	13.4	9.1	8.6	7.9	6.8	6.7
		Average Peak Stress (MPa)	1.214	1.440	1.497	1.640	1.694	1.862	1.921	2.076
		Average Peak Strain (με)	54	61	53	52	51	51	52	53
	Avg.	|E*| Average	21828	24567	27804	31130	32623	36038	36798	38636
		Φ Average	11.0	5.9	8.3	7.6	7.3	6.5	4.4	4.3
		|E*| Coeff. of Variation	0.023	0.080	0.059	0.012	0.011	0.015	0.012	0.020
		Φ Coeff. of Variation	0.29	1.09	0.66	0.44	0.49	0.55	0.79	0.77
		|E*| Std. Dev.	491.6	1975.5	1636.1	366.4	350.5	529.9	447.8	782.0
		Φ Std. Dev.	3.239	6.450	5.481	3.352	3.566	3.526	3.466	3.331
10	1	|E*| (MPa)	5100	8578	9059	12710	14249	18437	20257	22823
		Phase Angle, Φ (°)	26.8	29.6	23.7	17.5	14.8	11.7	10.4	9.5
		Average Peak Stress (MPa)	0.141	0.240	0.283	0.395	0.508	0.704	0.819	0.919
		Average Peak Strain (με)	28	28	31	31	36	38	40	40
	2	|E*| (MPa)	5290	9538	8901	13391	14709	19086	21129	23643
		Phase Angle, Φ (°)	35.2	28.4	27.7	24.4	22.6	18.7	17.5	16.0
		Average Peak Stress (MPa)	0.141	0.240	0.283	0.395	0.508	0.704	0.820	0.921
		Average Peak Strain (με)	27	25	32	30	35	37	39	39
	3	|E*| (MPa)	5816	7865	10293	13724	15033	19219	21163	23764
		Phase Angle, Φ (°)	34.9	33.1	29.7	22.7	21.6	17.8	17.0	15.2
		Average Peak Stress (MPa)	0.141	0.240	0.283	0.395	0.507	0.704	0.819	0.918
		Average Peak Strain (με)	24	31	27	29	34	37	39	39
	Avg.	|E*| Average	5402	8660	9418	13275	14664	18914	20850	23410
		Φ Average	32.3	30.4	27.0	21.6	19.7	16.1	15.0	13.6
		|E*| Coeff. of Variation	0.069	0.097	0.081	0.039	0.027	0.022	0.025	0.022
		Φ Coeff. of Variation	0.15	0.08	0.11	0.17	0.22	0.24	0.26	0.26
		|E*| Std. Dev.	371.1	839.7	762.2	516.9	394.4	418.6	513.6	512.1
		Φ Std. Dev.	4.758	2.435	3.082	3.608	4.244	3.804	3.961	3.509
35	1	|E*| (MPa)	357	603	763	1403	1863	3575	4509	6053
		Phase Angle, Φ (°)	25.3	29.3	30.6	33.3	32.4	27.7	25.9	23.8
		Average Peak Stress (MPa)	0.017	0.023	0.028	0.037	0.056	0.110	0.136	0.247
		Average Peak Strain (με)	47	37	37	26	30	31	30	41
	2	|E*| (MPa)	551	753	921	1577	1980	3661		
		Phase Angle, Φ (°)	30.2	32.1	34.0	38.1	36.1	33.5		
		Average Peak Stress (MPa)	0.017	0.023	0.028	0.037	0.056	0.110		
		Average Peak Strain (με)	31	30	31	23	28	30		
	3	|E*| (MPa)	586	842	1066	1874	2309	4080	5330	6674
		Phase Angle, Φ (°)	31.0	33.8	36.2	40.3	37.9	33.9	33.0	29.2
		Average Peak Stress (MPa)	0.017	0.023	0.028	0.037	0.056	0.110	0.137	0.247
		Average Peak Strain (με)	29	27	26	20	24	27	26	37
	Avg.	|E*| Average	498	733	917	1618	2051	3772	4920	6364
		Φ Average	28.8	31.7	33.6	37.2	35.5	31.7	29.5	26.5
		|E*| Coeff. of Variation	0.248	0.165	0.165	0.147	0.113	0.072	0.118	0.069
		Φ Coeff. of Variation	0.11	0.07	0.08	0.10	0.08	0.11	0.17	0.14
		|E*| Std. Dev.	123.4	120.9	151.7	237.8	231.2	270.6	580.6	438.9
		Φ Std. Dev.	3.122	2.252	2.818	3.564	2.807	3.485	4.971	3.807
54.4	1	|E*| (MPa)		197	212	295	362	658	867	1302
		Phase Angle, Φ (°)		19.1	17.2	22.0	24.4	29.4	30.7	32.1
		Average Peak Stress (MPa)		0.006	0.009	0.011	0.017	0.021	0.024	0.028
		Average Peak Strain (με)		28	40	38	46	32	28	21
	2	|E*| (MPa)		535	521	499	520	777	1002	1508
		Phase Angle, Φ (°)		6.7	12.6	21.8	24.2	30.3	32.3	35.5
		Average Peak Stress (MPa)		0.006	0.009	0.011	0.017	0.021	0.024	0.027
		Average Peak Strain (με)		10	16	22	32	27	24	18
	3	|E*| (MPa)		611	501	514	550	870	1137	1698
		Phase Angle, Φ (°)		21.2	13.8	22.5	24.1	31.8	32.6	35.7
		Average Peak Stress (MPa)		0.006	0.009	0.011	0.017	0.021	0.024	0.028
		Average Peak Strain (με)		9	17	22	30	24	21	16
	Avg.	|E*| Average		448	411	436	478	768	1002	1503
		Φ Average		15.7	14.5	22.1	24.2	30.5	31.9	34.5
		|E*| Coeff. of Variation		0.492	0.421	0.280	0.211	0.138	0.135	0.132
		Φ Coeff. of Variation		0.50	0.16	0.02	0.01	0.04	0.03	0.06
		|E*| Std. Dev.		220.6	173.0	122.1	100.9	106.3	134.8	198.1
		Φ Std. Dev.		7.853	2.378	0.362	0.176	1.204	1.011	2.025

Table A-28 – I19.0B2–Fine – Granite

Temp (°C)	Rep.	Parameters	Frequency (Hz)							
			0.01	0.05	0.1	0.5	1	5	10	25
-10	1	|E*| (MPa)	17253	18971	21945	23616	24612	26910	27822	28992
		Phase Angle, Φ (°)	7.5	10.6	5.9	5.1	4.8	3.5	3.0	2.7
		Average Peak Stress (MPa)	1.214	1.440	1.497	1.640	1.694	1.862	1.920	2.078
		Average Peak Strain (με)	70	76	68	69	69	69	69	72
	2	|E*| (MPa)	18197	22739	22714	24634	25591	27965	28846	30155
		Phase Angle, Φ (°)	7.8	9.7	7.7	5.1	4.7	3.8	3.2	3.0
		Average Peak Stress (MPa)	1.355	1.581	1.638	1.750	1.806	1.975	2.034	2.195
		Average Peak Strain (με)	74	70	72	71	71	71	71	73
	3	|E*| (MPa)	17891	20888	20925	23871	24994	27238	28705	29638
		Phase Angle, Φ (°)	8.0	11.4	6.3	5.1	4.9	3.7	3.5	2.8
		Average Peak Stress (MPa)	1.355	1.581	1.638	1.751	1.806	1.974	2.034	2.195
		Average Peak Strain (με)	76	76	78	73	72	72	71	74
	Avg.	|E*| Average	17780	20866	21861	24040	25066	27371	28458	29595
		Φ Average	7.8	10.6	6.6	5.1	4.8	3.6	3.3	2.9
		|E*| Coeff. of Variation	0.027	0.090	0.041	0.022	0.020	0.020	0.019	0.020
		Φ Coeff. of Variation	0.03	0.08	0.15	0.01	0.02	0.05	0.08	0.05
		|E*| Std. Dev.	481.9	1884.1	897.4	529.5	493.3	540.0	554.8	582.6
		Φ Std. Dev.	0.236	0.851	0.989	0.043	0.097	0.179	0.267	0.134
10	1	|E*| (MPa)	4865	7416	7706	10253	11448	14226	15584	0
		Phase Angle, Φ (°)	22.1	18.8	18.3	14.3	13.6	10.5	9.6	0.0
		Average Peak Stress (MPa)	0.282	0.395	0.480	0.621	0.734	1.014	1.156	0.000
		Average Peak Strain (με)	58	53	62	61	64	71	74	0
	2	|E*| (MPa)	5434	7996	8404	11223	12425	15258	16536	18479
		Phase Angle, Φ (°)	22.5	16.9	16.1	14.5	13.4	11.1	10.1	9.4
		Average Peak Stress (MPa)	0.282	0.395	0.480	0.621	0.734	1.014	1.156	1.264
		Average Peak Strain (με)	52	49	57	55	59	66	70	68
	3	|E*| (MPa)	5524	7118	8882	11159	12229	15025	16311	18134
		Phase Angle, Φ (°)	21.8	19.3	16.6	14.3	12.8	10.5	9.5	8.9
		Average Peak Stress (MPa)	0.282	0.395	0.480	0.621	0.734	1.014	1.156	1.264
		Average Peak Strain (με)	51	56	54	56	60	68	71	70
	Avg.	|E*| Average	5275	7510	8330	10879	12034	14836	16143	12204
		Φ Average	22.1	18.3	17.0	14.4	13.3	10.7	9.7	6.1
		|E*| Coeff. of Variation	0.068	0.059	0.071	0.050	0.043	0.036	0.031	0.866
		Φ Coeff. of Variation	0.02	0.07	0.07	0.01	0.03	0.03	0.03	0.87
		|E*| Std. Dev.	357.3	446.3	591.6	542.5	517.1	540.9	497.6	10570.6
		Φ Std. Dev.	0.358	1.280	1.166	0.137	0.402	0.347	0.305	5.299
35	1	|E*| (MPa)	470	748	942	1590	2028	3504	4311	5474
		Phase Angle, Φ (°)	32.7	33.1	32.1	31.5	29.8	25.5	23.1	20.9
		Average Peak Stress (MPa)	0.014	0.028	0.037	0.064	0.098	0.138	0.220	0.389
		Average Peak Strain (με)	30	38	39	40	48	39	51	71
	2	|E*| (MPa)	544	835	1040	1729	2160	3685	4523	5654
		Phase Angle, Φ (°)	32.7	32.2	32.5	32.2	30.2	26.5	23.7	21.5
		Average Peak Stress (MPa)	0.014	0.028	0.037	0.064	0.098	0.138	0.220	0.390
		Average Peak Strain (με)	26	34	35	37	45	37	49	69
	3	|E*| (MPa)	659	989	1172	1868	2282	3842	4604	5781
		Phase Angle, Φ (°)	35.7	33.7	33.5	31.5	29.7	26.0	22.5	21.5
		Average Peak Stress (MPa)	0.014	0.028	0.037	0.064	0.098	0.138	0.220	0.389
		Average Peak Strain (με)	22	28	31	34	43	36	48	67
	Avg.	|E*| Average	558	858	1051	1729	2157	3677	4479	5636
		Φ Average	33.7	33.0	32.7	31.8	29.9	26.0	23.1	21.3
		|E*| Coeff. of Variation	0.171	0.142	0.110	0.080	0.059	0.046	0.034	0.027
		Φ Coeff. of Variation	0.05	0.02	0.02	0.01	0.01	0.02	0.03	0.02
		|E*| Std. Dev.	95.6	121.9	115.4	138.8	126.9	168.9	151.1	154.3
		Φ Std. Dev.	1.691	0.738	0.724	0.392	0.293	0.524	0.589	0.364
54.4	1	|E*| (MPa)	151	191	217	343	444	824	1101	1587
		Phase Angle, Φ (°)	20.2	24.9	23.0	25.7	27.0	27.1	26.4	27.2
		Average Peak Stress (MPa)	0.006	0.009	0.014	0.028	0.036	0.061	0.091	0.124
		Average Peak Strain (με)	37	45	66	81	81	74	82	78
	2	|E*| (MPa)	174		231	367	465	853	1131	1628
		Phase Angle, Φ (°)	23.4		23.2	25.6	26.8	26.9	26.3	27.3
		Average Peak Stress (MPa)	0.006		0.014	0.028	0.036	0.061	0.091	0.125
		Average Peak Strain (με)	32		62	76	77	71	80	77
	3	|E*| (MPa)	276	287	295	437	546	977	1275	1790
		Phase Angle, Φ (°)	28.2	26.1	27.1	28.8	29.3	29.1	28.1	28.2
		Average Peak Stress (MPa)	0.006	0.009	0.014	0.028	0.036	0.061	0.091	0.125
		Average Peak Strain (με)	20	30	48	64	66	63	72	70
	Avg.	|E*| Average	201	239	248	382	485	885	1169	1668
		Φ Average	23.9	25.5	24.4	26.7	27.7	27.7	26.9	27.5
		|E*| Coeff. of Variation	0.331	0.285	0.168	0.127	0.112	0.092	0.079	0.064
		Φ Coeff. of Variation	0.17	0.03	0.09	0.07	0.05	0.04	0.04	0.02
		|E*| Std. Dev.	66.4	68.1	41.7	48.6	54.1	81.1	92.7	107.3
		Φ Std. Dev.	4.036	0.813	2.305	1.824	1.361	1.236	1.000	0.538

Table A-29 – I19.0B3–Fine – Granite

Temp (°C)	Rep.	Parameters	Frequency (Hz)							
			0.01	0.05	0.1	0.5	1	5	10	25
-10	1	|E*| (MPa)	20586	22194	24879	28506	29891	32684	33962	
		Phase Angle, Φ (°)	7.1	10.3	7.6	3.8	4.1	2.7	2.3	
		Average Peak Stress (MPa)	1.241	1.495	1.580	1.638	1.692	1.859	1.917	
		Average Peak Strain (με)	60	67	63	57	57	57	56	
	2	|E*| (MPa)	18537	23573	22168	25487	26404	28985	29930	
		Phase Angle, Φ (°)	8.2	6.1	3.9	5.4	5.0	3.6	3.0	
		Average Peak Stress (MPa)	1.241	1.495	1.580	1.638	1.692	1.859	1.918	
		Average Peak Strain (με)	67	63	71	64	64	64	64	
	3	|E*| (MPa)	18618	22091	22821	26097	27393	30003	31142	32534
		Phase Angle, Φ (°)	8.2	12.0	8.2	4.6	4.4	3.1	2.2	2.3
		Average Peak Stress (MPa)	1.241	1.495	1.580	1.638	1.692	1.860	1.918	2.077
		Average Peak Strain (με)	67	68	69	63	62	62	62	64
	Avg.	|E*| Average	19247	22619	23289	26697	27896	30557	31678	32534
		Φ Average	7.8	9.5	6.6	4.6	4.5	3.1	2.5	2.3
		|E*| Coeff. of Variation	0.060	0.037	0.061	0.060	0.064	0.063	0.065	
		Φ Coeff. of Variation	0.08	0.32	0.36	0.17	0.10	0.14	0.18	
		|E*| Std. Dev.	1160.7	827.7	1414.8	1596.3	1796.9	1910.8	2069.0	
		Φ Std. Dev.	0.627	3.057	2.371	0.810	0.442	0.452	0.463	
10	1	|E*| (MPa)	5748	8341	9488	12349	13771	17127	18748	20933
		Phase Angle, Φ (°)	21.7	21.9	15.1	13.7	12.5	10.1	9.1	8.6
		Average Peak Stress (MPa)	0.310	0.395	0.480	0.621	0.733	1.013	1.154	1.260
		Average Peak Strain (με)	54	47	51	50	53	59	62	60
	2	|E*| (MPa)	5247	7366	8673	11107	12290	15399	16759	18690
		Phase Angle, Φ (°)	22.3	21.9	17.6	14.5	13.4	10.6	9.3	8.8
		Average Peak Stress (MPa)	0.310	0.395	0.480	0.621	0.733	1.012	1.154	1.261
		Average Peak Strain (με)	59	54	55	56	60	66	69	67
	3	|E*| (MPa)	4872	6576	8049	10626	11930	15208	16719	
		Phase Angle, Φ (°)	23.0	19.8	16.8	15.0	13.8	10.8	9.7	
		Average Peak Stress (MPa)	0.310	0.395	0.480	0.621	0.733	1.014	1.154	
		Average Peak Strain (με)	64	60	60	58	61	67	69	
	Avg.	|E*| Average	5289	7428	8737	11361	12664	15911	17409	19812
		Φ Average	22.3	21.2	16.5	14.4	13.2	10.5	9.4	8.7
		|E*| Coeff. of Variation	0.083	0.119	0.083	0.078	0.077	0.066	0.067	0.080
		Φ Coeff. of Variation	0.03	0.06	0.08	0.04	0.05	0.04	0.04	0.02
		|E*| Std. Dev.	439.3	884.1	721.3	888.9	976.0	1057.3	1160.4	1586.1
		Φ Std. Dev.	0.642	1.256	1.241	0.641	0.671	0.375	0.328	0.166
35	1	|E*| (MPa)	572	882	1103	1818	2299	3918	4829	6148
		Phase Angle, Φ (°)	27.8	27.7	29.1	29.7	28.3	24.3	22.2	20.9
		Average Peak Stress (MPa)	0.020	0.034	0.042	0.078	0.111	0.166	0.248	0.388
		Average Peak Strain (με)	35	38	38	43	48	42	51	63
	2	|E*| (MPa)	559	878	1089	1792	2246	3847	4701	5863
		Phase Angle, Φ (°)	33.5	31.8	32.4	31.7	30.0	25.7	23.2	21.5
		Average Peak Stress (MPa)	0.020	0.034	0.042	0.078	0.111	0.166	0.248	0.389
		Average Peak Strain (με)	35	38	39	44	50	43	53	66
	3	|E*| (MPa)	529	789	963	1605	2022	3474	4255	5451
		Phase Angle, Φ (°)	29.8	30.1	30.9	30.6	29.3	25.1	23.0	21.8
		Average Peak Stress (MPa)	0.020	0.034	0.042	0.078	0.111	0.165	0.248	0.390
		Average Peak Strain (με)	37	43	44	49	55	48	58	71
	Avg.	|E*| Average	553	850	1052	1738	2189	3746	4595	5820
		Φ Average	30.4	29.9	30.8	30.7	29.2	25.1	22.8	21.4
		|E*| Coeff. of Variation	0.040	0.062	0.073	0.067	0.067	0.064	0.066	0.060
		Φ Coeff. of Variation	0.10	0.07	0.05	0.03	0.03	0.03	0.02	0.02
		|E*| Std. Dev.	22.1	52.6	77.1	116.3	147.1	238.4	301.4	350.5
		Φ Std. Dev.	2.938	2.031	1.666	1.036	0.855	0.680	0.520	0.457
54.4	1	|E*| (MPa)		272	319	457	556	942	1240	1750
		Phase Angle, Φ (°)		26.0	19.8	24.7	25.9	27.3	27.8	29.6
		Average Peak Stress (MPa)		0.005	0.008	0.011	0.017	0.021	0.025	0.028
		Average Peak Strain (με)		20	27	25	30	22	20	16
	2	|E*| (MPa)		455		463	546	965	1267	1799
		Phase Angle, Φ (°)		30.4		29.3	31.1	32.4	32.4	32.6
		Average Peak Stress (MPa)		0.007		0.011	0.017	0.021	0.025	0.028
		Average Peak Strain (με)		15		24	31	22	20	16
	3	|E*| (MPa)		259	283	396	483	828	1085	1554
		Phase Angle, Φ (°)		16.0	21.2	26.5	27.1	29.0	29.2	30.9
		Average Peak Stress (MPa)		0.006	0.009	0.011	0.017	0.021	0.025	0.028
		Average Peak Strain (με)		22	30	29	35	25	23	18
	Avg.	|E*| Average		329	301	439	528	912	1197	1701
		Φ Average		24.2	20.5	26.8	28.0	29.6	29.8	31.0
		|E*| Coeff. of Variation		0.333	0.086	0.085	0.075	0.081	0.082	0.076
		Φ Coeff. of Variation		0.31	0.05	0.09	0.10	0.09	0.08	0.05
		|E*| Std. Dev.		109.5	25.8	37.2	39.8	73.6	98.5	129.4
		Φ Std. Dev.		7.378	1.013	2.345	2.746	2.573	2.352	1.481

Table A-30 – I19.0B–Fine – Limestone

Temp (°C)	Rep.	Parameters	Frequency (Hz)							
			0.01	0.05	0.1	0.5	1	5	10	25
-10	1	|E*| (MPa)	17827	20329	20807	23640	24402	26360	27153	28187
		Phase Angle, Φ (°)	8.4	11.9	5.6	5.9	5.4	4.1	3.5	3.2
		Average Peak Stress (MPa)	1.355	1.582	1.639	1.752	1.808	1.976	2.037	2.207
		Average Peak Strain (με)	76	78	79	74	74	75	75	78
	2	|E*| (MPa)	18756	19803	22730	25122	25850	28155	29220	29734
		Phase Angle, Φ (°)	7.8	5.9	7.6	5.1	4.9	3.6	3.2	2.9
		Average Peak Stress (MPa)	1.355	1.582	1.639	1.753	1.808	1.977	2.037	2.203
		Average Peak Strain (με)	72	80	72	70	70	70	70	74
	3	|E*| (MPa)	18564	22298	22275	24441	25513	27533	28339	29502
		Phase Angle, Φ (°)	10.3	5.0	6.3	7.3	7.2	6.1	5.8	5.0
		Average Peak Stress (MPa)	1.355	1.582	1.638	1.752	1.808	1.976	2.036	2.200
		Average Peak Strain (με)	73	71	74	72	71	72	72	75
	Avg.	|E*| Average	18382	20810	21937	24401	25255	27350	28238	29141
		Φ Average	8.8	7.6	6.5	6.1	5.8	4.6	4.2	3.7
		|E*| Coeff. of Variation	0.027	0.063	0.046	0.030	0.030	0.033	0.037	0.029
		Φ Coeff. of Variation	0.15	0.49	0.16	0.18	0.20	0.29	0.33	0.30
		|E*| Std. Dev.	490.7	1314.9	1005.0	741.8	757.7	911.4	1037.3	834.4
		Φ Std. Dev.	1.314	3.745	1.043	1.111	1.178	1.311	1.383	1.136
10	1	|E*| (MPa)	5358	7978	8344	11146	12225	15021	16330	18038
		Phase Angle, Φ (°)	25.5	20.3	18.8	16.4	15.0	11.1	10.0	9.3
		Average Peak Stress (MPa)	0.282	0.395	0.480	0.622	0.735	1.016	1.158	1.267
		Average Peak Strain (με)	53	50	58	56	60	68	71	70
	2	|E*| (MPa)	5586	7468	8701	11556	12789	15859	17168	18899
		Phase Angle, Φ (°)	25.3	17.6	18.3	15.5	14.3	11.0	9.7	8.7
		Average Peak Stress (MPa)	0.282	0.395	0.480	0.622	0.735	1.016	1.158	1.269
		Average Peak Strain (με)	51	53	55	54	57	64	67	67
	3	|E*| (MPa)	5940	7921	8906	11761	12933	15779	16949	18671
		Phase Angle, Φ (°)	27.7	26.6	20.8	17.8	16.2	13.3	11.8	11.0
		Average Peak Stress (MPa)	0.282	0.395	0.480	0.622	0.735	1.016	1.158	1.264
		Average Peak Strain (με)	48	50	54	53	57	64	68	68
	Avg.	|E*| Average	5628	7789	8650	11488	12649	15553	16816	18536
		Φ Average	26.2	21.5	19.3	16.6	15.2	11.8	10.5	9.7
		|E*| Coeff. of Variation	0.052	0.036	0.033	0.027	0.030	0.030	0.026	0.024
		Φ Coeff. of Variation	0.05	0.21	0.07	0.07	0.06	0.11	0.11	0.12
		|E*| Std. Dev.	293.3	279.2	284.8	313.0	374.2	462.2	434.9	446.3
		Φ Std. Dev.	1.299	4.583	1.362	1.153	0.964	1.275	1.130	1.186
35	1	|E*| (MPa)	570	865	1073	1779	2287	3862	4777	5946
		Phase Angle, Φ (°)	32.4	33.2	32.0	32.5	30.2	27.0	24.1	21.8
		Average Peak Stress (MPa)	0.014	0.028	0.037	0.065	0.097	0.137	0.221	0.392
		Average Peak Strain (με)	25	33	34	36	43	36	46	66
	2	|E*| (MPa)	616	852	1061	1745	2255	3924	4796	6070
		Phase Angle, Φ (°)	33.1	35.6	33.6	34.3	31.9	28.6	24.6	22.4
		Average Peak Stress (MPa)	0.014	0.028	0.037	0.065	0.097	0.138	0.221	0.391
		Average Peak Strain (με)	23	33	35	37	43	35	46	64
	3	|E*| (MPa)	777	1054	1270	1992	2484	4335	5263	6285
		Phase Angle, Φ (°)	34.3	34.5	36.1	36.0	34.4	29.9	25.8	23.5
		Average Peak Stress (MPa)	0.014	0.028	0.037	0.064	0.097	0.138	0.220	0.388
		Average Peak Strain (με)	18	27	29	32	39	32	42	62
	Avg.	|E*| Average	654	923	1135	1838	2342	4040	4945	6101
		Φ Average	33.3	34.4	33.9	34.3	32.2	28.5	24.9	22.6
		|E*| Coeff. of Variation	0.166	0.122	0.103	0.073	0.053	0.064	0.056	0.028
		Φ Coeff. of Variation	0.03	0.04	0.06	0.05	0.07	0.05	0.03	0.04
		|E*| Std. Dev.	108.9	113.0	117.4	133.9	124.3	256.8	275.3	171.6
		Φ Std. Dev.	1.000	1.247	2.034	1.780	2.097	1.441	0.868	0.891
54.4	1	|E*| (MPa)	250	250	262	387	484	885	1201	1799
		Phase Angle, Φ (°)	20.4	19.2	21.4	25.4	26.1	26.8	25.8	27.0
		Average Peak Stress (MPa)	0.006	0.009	0.014	0.028	0.036	0.061	0.090	0.121
		Average Peak Strain (με)	22	34	54	73	75	69	75	67
	2	|E*| (MPa)	491	547	504	678	839	1526	1902	2576
		Phase Angle, Φ (°)	16.7	17.2	25.6	27.9	28.3	30.0	32.1	34.3
		Average Peak Stress (MPa)	0.006	0.009	0.014	0.028	0.036	0.061	0.090	0.123
		Average Peak Strain (με)	11	16	28	42	43	40	47	48
	3	|E*| (MPa)	322	319	324	445	557	1046	1393	1997
		Phase Angle, Φ (°)	25.3	27.9	26.7	30.3	30.2	30.1	28.6	29.1
		Average Peak Stress (MPa)	0.006	0.009	0.014	0.028	0.036	0.061	0.090	0.122
		Average Peak Strain (με)	17	27	44	63	65	58	65	61
	Avg.	|E*| Average	354	372	364	503	626	1152	1499	2124
		Φ Average	20.8	21.4	24.6	27.8	28.2	29.0	28.8	30.2
		|E*| Coeff. of Variation	0.350	0.418	0.346	0.306	0.300	0.289	0.242	0.190
		Φ Coeff. of Variation	0.21	0.27	0.11	0.09	0.07	0.06	0.11	0.12
		|E*| Std. Dev.	123.9	155.5	125.8	153.9	187.6	333.4	362.4	403.5
		Φ Std. Dev.	4.313	5.717	2.766	2.426	2.058	1.877	3.164	3.745

Table A-31 – I19.0C–Coarse – Granite

Temp (°C)	Rep.	Parameters	Frequency (Hz)							
			0.01	0.05	0.1	0.5	1	5	10	25
-10	1	|E*| (MPa)	16802	19690	20536	25223	26535	30216	32261	34042
		Phase Angle, Φ (°)	17.6	8.3	16.6	14.6	14.9	15.5	15.7	18.6
		Average Peak Stress (MPa)	0.956	0.984	1.012	1.040	1.068	1.065	1.064	1.084
		Average Peak Strain (με)	57	50	49	41	40	35	33	32
	2	|E*| (MPa)	16941	19366	21247	25193	26277	29555	31013	33354
		Phase Angle, Φ (°)	18.7	11.3	19.7	16.3	16.8	17.2	16.9	20.4
		Average Peak Stress (MPa)	0.844	0.928	0.985	1.012	1.039	1.063	1.063	1.082
		Average Peak Strain (με)	50	48	46	40	40	36	34	32
	3	|E*| (MPa)	16255		19430	23746	25087	27895	29246	30798
		Phase Angle, Φ (°)	15.1		11.9	12.3	11.9	11.7	12.9	16.3
		Average Peak Stress (MPa)	0.844		0.985	1.012	1.039	1.064	1.063	1.085
		Average Peak Strain (με)	52		51	43	41	38	36	35
	Avg.	|E*| Average	16666	19528	20404	24720	25967	29222	30840	32732
		Φ Average	17.1	9.8	16.1	14.4	14.5	14.8	15.2	18.4
		|E*| Coeff. of Variation	0.022	0.012	0.045	0.034	0.030	0.041	0.049	0.052
		Φ Coeff. of Variation	0.11	0.21	0.24	0.14	0.17	0.19	0.13	0.11
		|E*| Std. Dev.	363.0	229.1	915.6	844.3	772.2	1195.8	1515.0	1709.5
		Φ Std. Dev.	1.827	2.086	3.923	2.018	2.479	2.792	2.042	2.026
10	1	|E*| (MPa)	3441	5191	6400	9264	10484	14156	15818	18030
		Phase Angle, Φ (°)	35.9	28.2	31.4	26.0	24.7	22.3	22.6	24.9
		Average Peak Stress (MPa)	0.169	0.309	0.365	0.506	0.589	0.729	0.812	0.911
		Average Peak Strain (με)	49	59	57	55	56	51	51	51
	2	|E*| (MPa)	3977	5721	7098	9602	10869	14292	15761	17828
		Phase Angle, Φ (°)	37.5	29.3	28.8	26.3	24.8	23.0	22.7	24.8
		Average Peak Stress (MPa)	0.169	0.309	0.366	0.506	0.589	0.728	0.810	0.905
		Average Peak Strain (με)	42	54	52	53	54	51	51	51
	3	|E*| (MPa)	3451	5664	6532	9097	10290	13706	15149	17115
		Phase Angle, Φ (°)	33.5	33.2	29.1	23.4	22.3	19.9	19.9	22.2
		Average Peak Stress (MPa)	0.168	0.309	0.365	0.506	0.589	0.728	0.812	0.913
		Average Peak Strain (με)	49	55	56	56	57	53	54	53
	Avg.	|E*| Average	3623	5525	6677	9321	10548	14051	15576	17657
		Φ Average	35.6	30.2	29.8	25.2	23.9	21.7	21.8	24.0
		|E*| Coeff. of Variation	0.085	0.053	0.056	0.028	0.028	0.022	0.024	0.027
		Φ Coeff. of Variation	0.06	0.09	0.05	0.06	0.06	0.08	0.07	0.06
		|E*| Std. Dev.	306.6	291.2	370.6	257.1	294.3	306.4	371.3	480.7
		Φ Std. Dev.	1.980	2.638	1.414	1.584	1.428	1.646	1.585	1.493
35	1	|E*| (MPa)	384			1172		2727	3480	
		Phase Angle, Φ (°)	32.6			37.2		35.3	35.8	
		Average Peak Stress (MPa)	0.017			0.056		0.135	0.161	
		Average Peak Strain (με)	60			63		63	57	
	2	|E*| (MPa)	430	575	664	1088	1398	2509	3187	4211
		Phase Angle, Φ (°)	36.4	39.1	37.8	38.3	37.9	35.7	36.4	38.2
		Average Peak Stress (MPa)	0.017	0.022	0.028	0.056	0.069	0.134	0.157	0.227
		Average Peak Strain (με)	39	39	42	51	49	53	49	54
	3	|E*| (MPa)	290	418	521	923	1212	2362	3065	4209
		Phase Angle, Φ (°)	31.1	32.2	35.1	36.6	37.0	35.3	35.2	36.8
		Average Peak Stress (MPa)	0.017	0.022	0.028	0.056	0.069	0.134	0.160	0.235
		Average Peak Strain (με)	58	53	53	60	57	57	52	56
	Avg.	|E*| Average	368	496	593	1061	1305	2532	3244	4210
		Φ Average	33.4	35.6	36.4	37.4	37.4	35.4	35.8	37.5
		|E*| Coeff. of Variation	0.194	0.224	0.171	0.119	0.101	0.073	0.066	0.000
		Φ Coeff. of Variation	0.08	0.14	0.05	0.02	0.02	0.01	0.02	0.03
		|E*| Std. Dev.	71.4	111.0	101.1	126.4	131.8	183.8	213.2	0.9
		Φ Std. Dev.	2.740	4.929	1.901	0.859	0.630	0.262	0.598	0.996

Table A-32 – I19.0C–Fine – Granite

Temp (°C)	Rep.	Parameters	Frequency (Hz)							
			0.01	0.05	0.1	0.5	1	5	10	25
-10	1	|E*| (MPa)	14571	18376	17432	20489	21469	23755	24680	25799
		Phase Angle, Φ (°)	7.5	6.0	4.5	4.1	3.8	2.6	2.1	2.0
		Average Peak Stress (MPa)	1.355	1.582	1.639	1.751	1.807	1.975	2.035	2.197
		Average Peak Strain (με)	93	86	94	85	84	83	82	85
	2	|E*| (MPa)	15440	19738	19402	22139	23231			
		Phase Angle, Φ (°)	9.2	5.8	9.4	5.9	5.5			
		Average Peak Stress (MPa)	1.355	1.582	1.639	1.751	1.807			
		Average Peak Strain (με)	88	80	84	79	78			
	3	|E*| (MPa)	17465	18618	20580	24261	25300	28045	29208	30704
		Phase Angle, Φ (°)	8.6	9.5	7.3	5.4	5.9	4.6	4.3	4.0
		Average Peak Stress (MPa)	1.355	1.582	1.639	1.751	1.807	1.975	2.035	2.198
		Average Peak Strain (με)	78	85	80	72	71	70	70	72
	Avg.	|E*| Average	15825	18910	19138	22296	23333	25900	26944	28251
		Φ Average	8.4	7.1	7.1	5.1	5.1	3.6	3.2	3.0
		|E*| Coeff. of Variation	0.094	0.038	0.083	0.085	0.082	0.117	0.119	0.123
		Φ Coeff. of Variation	0.10	0.29	0.35	0.18	0.22	0.40	0.49	0.47
		|E*| Std. Dev.	1485.0	726.6	1590.3	1891.2	1917.9	3033.4	3202.0	3468.1
		Φ Std. Dev.	0.853	2.093	2.471	0.940	1.107	1.445	1.566	1.414
10	1	|E*| (MPa)	3778	5630	6485	8483	9568	12204	13444	15074
		Phase Angle, Φ (°)	22.2	22.0	16.5	14.6	12.9	10.3	9.1	8.4
		Average Peak Stress (MPa)	0.282	0.367	0.424	0.565	0.677	0.930	1.043	1.149
		Average Peak Strain (με)	75	65	65	67	71	76	78	76
	2	|E*| (MPa)	3760	5718	6301	8795	9815	12606	13944	15826
		Phase Angle, Φ (°)	24.8	24.2	18.5	16.4	15.0	12.1	10.9	10.3
		Average Peak Stress (MPa)	0.282	0.367	0.424	0.565	0.677	0.930	1.043	1.150
		Average Peak Strain (με)	75	64	67	64	69	74	75	73
	3	|E*| (MPa)	5039	7507	8338	10758	11933	14787	16334	18269
		Phase Angle, Φ (°)	23.4	24.3	17.3	15.9	14.3	11.8	10.7	10.1
		Average Peak Stress (MPa)	0.282	0.367	0.424	0.565	0.677	0.931	1.043	1.150
		Average Peak Strain (με)	56	49	51	53	57	63	64	63
	Avg.	|E*| Average	4192	6285	7041	9345	10439	13199	14574	16390
		Φ Average	23.5	23.5	17.4	15.6	14.1	11.4	10.2	9.6
		|E*| Coeff. of Variation	0.175	0.169	0.160	0.132	0.125	0.105	0.106	0.102
		Φ Coeff. of Variation	0.05	0.06	0.06	0.06	0.08	0.08	0.10	0.11
		|E*| Std. Dev.	733.1	1059.2	1126.6	1233.1	1299.8	1390.0	1544.5	1670.3
		Φ Std. Dev.	1.284	1.307	0.998	0.971	1.089	0.941	0.999	1.031
35	1	|E*| (MPa)	374	602	752	1266	1664	2834	3455	4371
		Phase Angle, Φ (°)	26.9	28.0	28.6	28.7	26.6	23.1	21.4	20.7
		Average Peak Stress (MPa)	0.021	0.028	0.042	0.070	0.140	0.207	0.275	0.416
		Average Peak Strain (με)	57	47	56	55	84	73	80	95
	2	|E*| (MPa)	388	588	727	1199	1564	2679	3286	4201
		Phase Angle, Φ (°)	29.3	30.6	29.7	30.4	27.5	24.3	22.8	21.9
		Average Peak Stress (MPa)	0.021	0.028	0.042	0.070	0.140	0.207	0.275	0.415
		Average Peak Strain (με)	54	48	58	58	90	77	84	99
	3	|E*| (MPa)	554	818	1006	1599	2081	3517		
		Phase Angle, Φ (°)	27.0	29.7	29.6	30.7	27.8	25.5		
		Average Peak Stress (MPa)	0.021	0.028	0.042	0.070	0.140	0.208		
		Average Peak Strain (με)	38	34	42	44	67	59		
	Avg.	|E*| Average	439	669	828	1355	1769	3010	3370	4286
		Φ Average	27.7	29.4	29.3	29.9	27.3	24.3	22.1	21.3
		|E*| Coeff. of Variation	0.229	0.192	0.186	0.158	0.155	0.148	0.035	0.028
		Φ Coeff. of Variation	0.05	0.05	0.02	0.04	0.02	0.05	0.05	0.04
		|E*| Std. Dev.	100.3	128.7	154.1	214.2	274.2	445.9	119.4	119.9
		Φ Std. Dev.	1.369	1.351	0.623	1.102	0.585	1.204	1.004	0.811

Table A-33 – I19.0C–Fine – Limestone

Temp (°C)	Rep.	Parameters	Frequency (Hz)							
			0.01	0.05	0.1	0.5	1	5	10	25
-10	1	|E*| (MPa)	19764	21931	22494	25521	26555	28528	29351	30499
		Phase Angle, Φ (°)	8.1	1.4	7.5	5.3	5.3	3.8	3.1	3.1
		Average Peak Stress (MPa)	1.218	1.422	1.473	1.575	1.625	1.776	1.829	1.977
		Average Peak Strain (με)	62	65	65	62	61	62	62	65
	2	|E*| (MPa)	18986	19828	22631	24553	25271	27294	27979	28606
		Phase Angle, Φ (°)	10.8	8.8	10.8	7.9	7.5	6.5	6.0	5.4
		Average Peak Stress (MPa)	1.351	1.577	1.634	1.747	1.803	1.971	2.030	2.195
		Average Peak Strain (με)	71	80	72	71	71	72	73	77
	3	|E*| (MPa)	19595	23353	23292	25179	26068	28035	28608	29631
		Phase Angle, Φ (°)	12.0	13.5	11.0	8.9	8.3	6.9	6.5	6.1
		Average Peak Stress (MPa)	1.351	1.577	1.634	1.747	1.803	1.970	2.029	2.193
		Average Peak Strain (με)	69	68	70	69	69	70	71	74
	Avg.	|E*| Average	19448	21704	22805	25084	25965	27952	28646	29578
		Φ Average	10.3	7.9	9.8	7.4	7.0	5.8	5.2	4.9
		|E*| Coeff. of Variation	0.021	0.082	0.019	0.020	0.025	0.022	0.024	0.032
		Φ Coeff. of Variation	0.19	0.77	0.20	0.25	0.22	0.30	0.36	0.32
		|E*| Std. Dev.	409.3	1773.1	426.6	490.6	648.3	621.4	687.3	947.7
		Φ Std. Dev.	1.991	6.100	1.972	1.866	1.520	1.709	1.851	1.549
10	1	|E*| (MPa)	6749	8654	10251	13206	14425	17388	18649	20623
		Phase Angle, Φ (°)	24.1	20.5	19.9	15.6	13.6	10.8	9.4	8.7
		Average Peak Stress (MPa)	0.254	0.355	0.432	0.559	0.661	0.913	1.040	1.138
		Average Peak Strain (με)	38	41	42	42	46	52	56	55
	2	|E*| (MPa)	6780	8765	9975	12857	14071	16689	17927	19428
		Phase Angle, Φ (°)	28.0	21.0	22.3	18.4	17.7	14.1	12.8	11.9
		Average Peak Stress (MPa)	0.281	0.394	0.479	0.621	0.733	1.013	1.154	1.262
		Average Peak Strain (με)	42	45	48	48	52	61	64	65
	3	|E*| (MPa)	7551	10805	10938	14095	15136	17749	18838	20544
		Phase Angle, Φ (°)	28.8	26.8	21.5	19.4	18.2	14.8	13.3	12.5
		Average Peak Stress (MPa)	0.282	0.394	0.479	0.620	0.733	1.013	1.154	1.264
		Average Peak Strain (με)	37	36	44	44	48	57	61	62
	Avg.	|E*| Average	7026	9408	10388	13386	14544	17275	18471	20198
		Φ Average	27.0	22.8	21.2	17.8	16.5	13.2	11.8	11.0
		|E*| Coeff. of Variation	0.065	0.129	0.048	0.048	0.037	0.031	0.026	0.033
		Φ Coeff. of Variation	0.09	0.15	0.06	0.11	0.15	0.16	0.18	0.18
		|E*| Std. Dev.	454.3	1210.9	495.9	638.5	542.6	538.9	481.2	668.5
		Φ Std. Dev.	2.549	3.487	1.267	1.956	2.522	2.089	2.095	2.009
35	1	|E*| (MPa)	869	1254	1486	2337	2837	4763	5712	6949
		Phase Angle, Φ (°)	38.0	36.1	34.6	35.3	32.7	28.5	24.5	21.5
		Average Peak Stress (MPa)	0.014	0.028	0.037	0.058	0.088	0.123	0.198	0.348
		Average Peak Strain (με)	16	22	25	25	31	26	35	50
	2	|E*| (MPa)	843	1184	1429	2323	2840	4949	5923	6961
		Phase Angle, Φ (°)	43.4	40.3	39.0	37.7	35.8	29.4	27.2	24.6
		Average Peak Stress (MPa)	0.014	0.028	0.037	0.064	0.097	0.166	0.220	0.387
		Average Peak Strain (με)	17	24	26	28	34	34	37	56
	3	|E*| (MPa)	711	1078	1327	2124	2694	4568	5556	6907
		Phase Angle, Φ (°)	34.8	36.1	33.6	33.5	31.9	26.1	23.5	23.5
		Average Peak Stress (MPa)	0.028	0.042	0.074	0.112	0.168	0.279	0.390	0.448
		Average Peak Strain (με)	39	39	55	53	62	61	70	65
	Avg.	|E*| Average	808	1172	1414	2261	2790	4760	5730	6939
		Φ Average	38.7	37.5	35.7	35.5	33.5	28.0	25.1	23.2
		|E*| Coeff. of Variation	0.105	0.076	0.057	0.053	0.030	0.040	0.032	0.004
		Φ Coeff. of Variation	0.11	0.06	0.08	0.06	0.06	0.06	0.08	0.07
		|E*| Std. Dev.	84.6	88.5	80.4	119.4	83.5	190.6	184.0	28.2
		Φ Std. Dev.	4.330	2.399	2.854	2.084	2.094	1.672	1.933	1.569
54.4	1	|E*| (MPa)	311	345	368	548	721	1187	1550	2182
		Phase Angle, Φ (°)	24.2	23.0	21.7	25.2	24.3	26.2	25.6	26.2
		Average Peak Stress (MPa)	0.009	0.011	0.023	0.042	0.069	0.079	0.104	0.152
		Average Peak Strain (με)	27	32	61	77	96	67	67	70
	2	|E*| (MPa)	198	248	282	461	639	1136	1506	2144
		Phase Angle, Φ (°)	28.6	32.8	27.9	30.2	28.2	29.3	28.0	28.4
		Average Peak Stress (MPa)	0.008	0.011	0.023	0.042	0.069	0.079	0.103	0.151
		Average Peak Strain (με)	43	45	80	92	108	69	68	70
	3	|E*| (MPa)	294	354	388	574	774	1277	1658	2299
		Phase Angle, Φ (°)	23.3	26.7	24.1	26.6	25.8	27.4	26.5	27.3
		Average Peak Stress (MPa)	0.008	0.011	0.023	0.042	0.069	0.079	0.104	0.153
		Average Peak Strain (με)	29	32	58	74	89	62	63	67
	Avg.	|E*| Average	268	316	346	528	711	1200	1572	2208
		Φ Average	25.3	27.5	24.6	27.3	26.1	27.6	26.7	27.3
		|E*| Coeff. of Variation	0.227	0.186	0.162	0.113	0.095	0.059	0.050	0.037
		Φ Coeff. of Variation	0.11	0.18	0.13	0.09	0.08	0.06	0.05	0.04
		|E*| Std. Dev.	60.7	58.6	56.2	59.4	67.8	71.2	78.2	81.1
		Φ Std. Dev.	2.841	4.928	3.152	2.560	1.970	1.595	1.235	1.087

Table A-34 – I19.0D–Coarse – Granite

Temp (°C)	Rep.	Parameters	Frequency (Hz)							
			0.01	0.05	0.1	0.5	1	5	10	25
-10	1	|E*| (MPa)	21059		25227	29058	30236	32848	33889	35390
		Phase Angle, Φ (°)	12.4		8.1	9.5	8.2	8.0	9.0	12.5
		Average Peak Stress (MPa)	1.356		1.639	1.753	1.808	1.976	2.035	2.137
		Average Peak Strain (με)	64		65	60	60	60	60	60
	2	|E*| (MPa)	20280	22479	24606	27996	29274	31892	32994	34433
		Phase Angle, Φ (°)	11.5		12.9	8.8	8.6	8.4	9.2	12.7
		Average Peak Stress (MPa)	1.355	1.582	1.639	1.753	1.809	1.976	2.033	2.195
		Average Peak Strain (με)	67	70	67	63	62	62	62	64
	3	|E*| (MPa)	18926	22364	24436	26171	27566	30365	31453	33018
		Phase Angle, Φ (°)	12.0		10.7	8.7	8.7	8.3	9.7	13.2
		Average Peak Stress (MPa)	1.355	1.582	1.639	1.753	1.808	1.974	2.030	2.194
		Average Peak Strain (με)	72	71	67	67	66	65	65	66
	Avg.	|E*| Average	20088	22422	24756	27741	29025	31702	32779	34280
		Φ Average	11.9		10.6	9.0	8.5	8.2	9.3	12.8
		|E*| Coeff. of Variation	0.054	0.004	0.017	0.053	0.047	0.039	0.038	0.035
		Φ Coeff. of Variation	0.04		0.22	0.05	0.03	0.03	0.04	0.03
		|E*| Std. Dev.	1079.2	81.0	416.3	1460.3	1352.6	1252.2	1232.0	1193.2
		Φ Std. Dev.	0.437		2.373	0.427	0.272	0.234	0.337	0.385
10	1	|E*| (MPa)	5336	7609	9442	12463	13975	17696	19414	21459
		Phase Angle, Φ (°)	28.1	22.1	22.9	19.5	18.5	16.0	16.4	19.4
		Average Peak Stress (MPa)	0.367	0.480	0.565	0.707	0.820	1.100	1.185	1.323
		Average Peak Strain (με)	69	63	60	57	59	62	61	62
	2	|E*| (MPa)	5456	8122	9060	12282	13757	17389	19099	21172
		Phase Angle, Φ (°)	27.0		23.1	18.7	17.1	15.5	16.1	19.0
		Average Peak Stress (MPa)	0.367	0.480	0.565	0.708	0.820	1.099	1.209	1.317
		Average Peak Strain (με)	67	59	62	58	60	63	63	62
	3	|E*| (MPa)	4829	7129	8095	11005	12422	16144	17880	20007
		Phase Angle, Φ (°)	27.3		23.4	19.9	17.9	16.3	16.6	19.4
		Average Peak Stress (MPa)	0.367	0.480	0.565	0.708	0.820	1.097	1.209	1.317
		Average Peak Strain (με)	76	67	70	64	66	68	68	66
	Avg.	|E*| Average	5207	7620	8866	11917	13385	17076	18798	20879
		Φ Average	27.4	22.1	23.2	19.4	17.9	15.9	16.4	19.3
		|E*| Coeff. of Variation	0.064	0.065	0.078	0.067	0.063	0.048	0.043	0.037
		Φ Coeff. of Variation	0.02		0.01	0.03	0.04	0.03	0.01	0.01
		|E*| Std. Dev.	332.7	496.5	694.0	794.7	841.0	821.8	810.3	769.1
		Φ Std. Dev.	0.583		0.250	0.583	0.674	0.401	0.230	0.241
35	1	|E*| (MPa)	651	903	1077	1736	2347	3957	5000	6414
		Phase Angle, Φ (°)	33.6	34.3	34.7	38.8	33.3	31.8	30.7	33.5
		Average Peak Stress (MPa)	0.034	0.042	0.057	0.085	0.169	0.220	0.303	0.445
		Average Peak Strain (με)	52	47	53	49	72	56	61	69
	2	|E*| (MPa)	543	861	1080	1709	2350	4042	4990	6443
		Phase Angle, Φ (°)	33.6	34.2	35.0	36.7	31.9	30.7	29.8	32.1
		Average Peak Stress (MPa)	0.025	0.034	0.051	0.079	0.169	0.219	0.301	0.440
		Average Peak Strain (με)	47	39	47	46	72	54	60	68
	3	|E*| (MPa)	441	689	892	1457	2121	3662	4607	5979
		Phase Angle, Φ (°)	31.5	32.5	33.4	36.7	31.7	30.6	30.0	32.6
		Average Peak Stress (MPa)	0.026	0.033	0.051	0.079	0.169	0.219	0.303	0.443
		Average Peak Strain (με)	58	48	57	54	80	60	66	74
	Avg.	|E*| Average	545	817	1016	1634	2273	3887	4865	6279
		Φ Average	32.9	33.7	34.4	37.4	32.3	31.0	30.1	32.8
		|E*| Coeff. of Variation	0.193	0.139	0.106	0.094	0.058	0.051	0.046	0.041
		Φ Coeff. of Variation	0.04	0.03	0.02	0.03	0.03	0.02	0.02	0.02
		|E*| Std. Dev.	105.0	113.4	107.7	153.5	131.2	199.6	224.2	259.8
		Φ Std. Dev.	1.163	1.022	0.851	1.241	0.872	0.647	0.467	0.721

Table A-35 – I19.0D–Fine – Granite

Temp (°C)	Rep.	Parameters	Frequency (Hz)							
			0.01	0.05	0.1	0.5	1	5	10	25
-10	1	|E*| (MPa)	24186	27130	27813	31805	32404	35446	36371	37796
		Phase Angle, Φ (°)	10.1	0.8	11.8	7.6	6.9	7.3	8.0	11.9
		Average Peak Stress (MPa)	1.354	1.580	1.637	1.751	1.806	1.973	2.031	2.194
		Average Peak Strain (με)	56	58	59	55	56	56	56	58
	2	|E*| (MPa)	21146	26191	26432	27898	29241	31695	32340	33854
		Phase Angle, Φ (°)	11.1	9.5	8.2	6.7	7.0	8.0	8.8	12.5
		Average Peak Stress (MPa)	1.354	1.580	1.637	1.751	1.806	1.972	2.031	2.193
		Average Peak Strain (με)	64	60	62	63	62	62	63	65
	3	|E*| (MPa)	20867	25153	25850	27393	28623	31094	31971	33241
		Phase Angle, Φ (°)	12.1	14.1	11.8	8.9	9.2	9.6	10.6	14.0
		Average Peak Stress (MPa)	1.354	1.580	1.637	1.750	1.806	1.970	2.028	2.190
		Average Peak Strain (με)	65	63	63	64	63	63	63	66
	Avg.	|E*| Average	22066	26158	26698	29032	30089	32745	33561	34963
		Φ Average	11.1	8.1	10.6	7.7	7.7	8.3	9.2	12.8
		|E*| Coeff. of Variation	0.083	0.038	0.038	0.083	0.067	0.072	0.073	0.071
		Φ Coeff. of Variation	0.09	0.83	0.20	0.14	0.17	0.14	0.15	0.09
		|E*| Std. Dev.	1841.0	988.7	1008.1	2415.2	2028.3	2358.4	2440.9	2472.0
		Φ Std. Dev.	1.024	6.788	2.090	1.091	1.305	1.176	1.330	1.109
10	1	|E*| (MPa)	7706	11878	12494	15729	17255	20842	22331	24575
		Phase Angle, Φ (°)	24.6	19.1	17.2	16.1	15.6	13.6	14.4	17.1
		Average Peak Stress (MPa)	0.367	0.480	0.564	0.707	0.819	1.099	1.211	1.325
		Average Peak Strain (με)	48	40	45	45	47	53	54	54
	2	|E*| (MPa)	6909	10456	11250	13883	15325	18606	20082	22074
		Phase Angle, Φ (°)	24.8	19.9	18.6	16.5	15.7	14.3	14.8	17.8
		Average Peak Stress (MPa)	0.367	0.479	0.565	0.707	0.819	1.099	1.210	1.320
		Average Peak Strain (με)	53	46	50	51	53	59	60	60
	3	|E*| (MPa)	6839	9851	10519	13579	14870	18088	19514	21382
		Phase Angle, Φ (°)	25.8	24.7	21.0	17.8	17.2	15.5	16.3	19.2
		Average Peak Stress (MPa)	0.367	0.480	0.564	0.707	0.819	1.097	1.207	1.314
		Average Peak Strain (με)	54	49	54	52	55	61	62	61
	Avg.	|E*| Average	7151	10728	11421	14397	15817	19179	20642	22677
		Φ Average	25.1	21.3	18.9	16.8	16.2	14.4	15.2	18.0
		|E*| Coeff. of Variation	0.067	0.097	0.087	0.081	0.080	0.076	0.072	0.074
		Φ Coeff. of Variation	0.02	0.14	0.10	0.05	0.05	0.07	0.07	0.06
		|E*| Std. Dev.	481.7	1040.7	998.8	1163.6	1266.3	1463.6	1490.0	1679.8
		Φ Std. Dev.	0.615	3.005	1.909	0.869	0.874	0.988	1.023	1.061
35	1	|E*| (MPa)	647	1079	1344	2172	2987	5078	6086	7686
		Phase Angle, Φ (°)	34.1	36.7	35.0	36.5	31.9	29.6	27.7	30.2
		Average Peak Stress (MPa)	0.025	0.034	0.051	0.079	0.168	0.221	0.304	0.447
		Average Peak Strain (με)	39	31	38	36	56	44	50	58
	2	|E*| (MPa)	639	1076	1317	2091	2798	4674	5688	7128
		Phase Angle, Φ (°)	36.6	37.7	35.5	36.5	32.0	29.5	28.6	30.7
		Average Peak Stress (MPa)	0.025	0.034	0.051	0.079	0.169	0.222	0.304	0.448
		Average Peak Strain (με)	40	31	39	38	60	47	54	63
	3	|E*| (MPa)	689	1107	1375	2152	2898	4806	5807	7115
		Phase Angle, Φ (°)	35.8	35.9	34.8	36.6	32.1	29.9	29.7	31.8
		Average Peak Stress (MPa)	0.025	0.034	0.051	0.079	0.169	0.222	0.303	0.441
		Average Peak Strain (με)	37	30	37	37	58	46	52	62
	Avg.	|E*| Average	658	1087	1345	2138	2894	4853	5860	7310
		Φ Average	35.5	36.8	35.1	36.5	32.0	29.6	28.7	30.9
		|E*| Coeff. of Variation	0.041	0.016	0.022	0.020	0.033	0.042	0.035	0.045
		Φ Coeff. of Variation	0.04	0.02	0.01	0.00	0.00	0.01	0.03	0.02
		|E*| Std. Dev.	26.7	17.0	29.0	42.2	94.8	206.1	204.2	325.8
		Φ Std. Dev.	1.307	0.912	0.372	0.072	0.083	0.209	1.003	0.768

Table A-36 – B25.0B–Coarse – Granite

Temp (°C)	Rep.	Parameters	Frequency (Hz)							
			0.01	0.05	0.1	0.5	1	5	10	25
-10	1	|E*| (MPa)	18408		22873	27145	28297	31426	32493	33614
		Phase Angle, Φ (°)	13.9		8.6	10.1	8.3	7.8	7.0	6.4
		Average Peak Stress (MPa)	1.354		1.638	1.752	1.807	1.977	2.035	2.200
		Average Peak Strain (με)	74		72	65	64	63	63	65
	2	|E*| (MPa)	15914	19459	20983	22540	23644	25863	26724	27728
		Phase Angle, Φ (°)	7.5	10.9	5.1	3.9	2.0	1.8	1.1	1.3
		Average Peak Stress (MPa)	1.242	1.468	1.553	1.667	1.695	1.861	1.921	2.083
		Average Peak Strain (με)	78	75	74	74	72	72	72	75
	3	|E*| (MPa)	14142	18586	18929	21809	23207	26247	27363	28876
		Phase Angle, Φ (°)	10.7	6.6	5.8	6.6	5.6	3.7	3.4	3.1
		Average Peak Stress (MPa)	1.241	1.467	1.552	1.666	1.694	1.858	1.920	2.077
		Average Peak Strain (με)	88	79	82	76	73	71	70	72
	Avg.	|E*| Average	16155	19022	20928	23831	25049	27845	28860	30072
		Φ Average	10.7	8.8	6.5	6.9	5.3	4.4	3.8	3.6
		|E*| Coeff. of Variation	0.133	0.032	0.094	0.121	0.113	0.112	0.110	0.104
		Φ Coeff. of Variation	0.30	0.35	0.28	0.45	0.59	0.69	0.77	0.71
		|E*| Std. Dev.	2143.3	617.3	1972.8	2892.7	2820.9	3106.9	3162.5	3120.3
		Φ Std. Dev.	3.239	3.043	1.811	3.128	3.149	3.048	2.930	2.552
10	1	|E*| (MPa)	3417	5467	6558	9440	10868	14662	16111	18480
		Phase Angle, Φ (°)	29.1	23.0	26.3	21.1	18.1	14.8	12.9	12.1
		Average Peak Stress (MPa)	0.367	0.480	0.565	0.707	0.820	1.100	1.269	1.382
		Average Peak Strain (με)	107	88	86	75	75	75	79	75
	2	|E*| (MPa)	3119	4912	6138	8667	9957	13138	14517	16291
		Phase Angle, Φ (°)	25.6	19.1	19.3	16.5	13.8	10.7	9.3	8.4
		Average Peak Stress (MPa)	0.254	0.395	0.508	0.622	0.735	1.014	1.156	1.265
		Average Peak Strain (με)	81	80	83	72	74	77	80	78
	3	|E*| (MPa)	2337	4212	4913	7374	8630	11931	13433	15450
		Phase Angle, Φ (°)	30.8	25.9	23.2	20.0	18.0	13.9	12.4	11.3
		Average Peak Stress (MPa)	0.170	0.310	0.423	0.621	0.733	1.015	1.155	1.264
		Average Peak Strain (με)	73	74	86	84	85	85	86	82
	Avg.	|E*| Average	2958	4864	5870	8494	9818	13244	14687	16740
		Φ Average	28.5	22.6	23.0	19.2	16.6	13.1	11.5	10.6
		|E*| Coeff. of Variation	0.189	0.129	0.146	0.123	0.115	0.103	0.092	0.093
		Φ Coeff. of Variation	0.09	0.15	0.15	0.12	0.15	0.16	0.17	0.18
		|E*| Std. Dev.	557.6	628.9	854.7	1044.1	1125.7	1368.2	1346.9	1564.3
		Φ Std. Dev.	2.674	3.429	3.477	2.377	2.467	2.146	1.949	1.952
35	1	|E*| (MPa)	263	416	517	962	1326	2523	3257	4527
		Phase Angle, Φ (°)	23.1	28.1	29.3	32.2	29.2	29.5	27.6	25.7
		Average Peak Stress (MPa)	0.020	0.034	0.042	0.079	0.140	0.220	0.303	0.444
		Average Peak Strain (με)	76	81	82	82	105	87	93	98
	2	|E*| (MPa)	240	377	474	881	1256	2458	3144	4414
		Phase Angle, Φ (°)	24.0	28.6	29.2	31.8	29.1	28.0	25.6	24.3
		Average Peak Stress (MPa)	0.014	0.023	0.028	0.051	0.098	0.165	0.218	0.359
		Average Peak Strain (με)	59	60	59	58	78	67	69	81
	3	|E*| (MPa)	180	281	364	681	927	1899	2518	3557
		Phase Angle, Φ (°)	24.3	28.2	29.7	33.4	33.1	29.1	28.5	27.2
		Average Peak Stress (MPa)	0.014	0.022	0.028	0.045	0.070	0.135	0.190	0.299
		Average Peak Strain (με)	81	79	77	66	75	71	75	84
	Avg.	|E*| Average	227	358	452	841	1170	2293	2973	4166
		Φ Average	23.8	28.3	29.4	32.5	30.5	28.9	27.2	25.8
		|E*| Coeff. of Variation	0.189	0.195	0.174	0.172	0.182	0.150	0.134	0.127
		Φ Coeff. of Variation	0.03	0.01	0.01	0.03	0.08	0.03	0.05	0.06
		|E*| Std. Dev.	43.0	69.7	78.7	144.7	212.9	343.1	398.2	530.6
		Φ Std. Dev.	0.631	0.275	0.239	0.827	2.299	0.767	1.460	1.459

Table A-37 – B25.0B–Coarse – Limestone

Temp (°C)	Rep.	Parameters	Frequency (Hz)							
			0.01	0.05	0.1	0.5	1	5	10	25
-10	1	|E*| (MPa)	24483	27088	27680	31248	32093	34154	35104	36086
		Phase Angle, Φ (°)	11.7	15.4	9.4	8.2	7.9	6.2	5.6	5.2
		Average Peak Stress (MPa)	1.219	1.422	1.474	1.576	1.626	1.778	1.831	1.975
		Average Peak Strain (με)	50	53	53	50	51	52	52	55
	2	|E*| (MPa)	21239	24997	24022	26898	27853	29381	30087	31106
		Phase Angle, Φ (°)	6.8	0.4	2.8	3.8	3.0	1.9	2.1	1.6
		Average Peak Stress (MPa)	1.219	1.422	1.474	1.577	1.627	1.777	1.831	1.985
		Average Peak Strain (με)	57	57	61	59	58	60	61	64
	3	|E*| (MPa)	22971	28571	25660	29372	30091	31784	32574	33646
		Phase Angle, Φ (°)	7.5	5.9	5.2	4.4	4.1	2.7	2.3	2.3
		Average Peak Stress (MPa)	1.219	1.422	1.474	1.576	1.627	1.778	1.831	1.978
		Average Peak Strain (με)	53	50	57	54	54	56	56	59
	Avg.	|E*| Average	22898	26885	25787	29173	30012	31773	32588	33613
		Φ Average	8.7	7.2	5.8	5.5	5.0	3.6	3.3	3.0
		|E*| Coeff. of Variation	0.071	0.067	0.071	0.075	0.071	0.075	0.077	0.074
		Φ Coeff. of Variation	0.31	1.05	0.58	0.44	0.52	0.63	0.60	0.63
		|E*| Std. Dev.	1623.3	1795.4	1832.1	2181.6	2121.2	2386.5	2508.4	2490.0
		Φ Std. Dev.	2.674	7.594	3.358	2.405	2.583	2.267	1.990	1.913
10	1	|E*| (MPa)	7796	12528	13030	16219	17661	21036	22610	24998
		Phase Angle, Φ (°)	32.7	28.7	25.8	20.1	18.1	13.6	12.6	11.8
		Average Peak Stress (MPa)	0.254	0.356	0.432	0.560	0.661	0.914	1.041	1.137
		Average Peak Strain (με)	33	28	33	35	37	43	46	45
	2	|E*| (MPa)	6704	8835	11145	13951	15211	18239	19582	21406
		Phase Angle, Φ (°)	24.6	20.5	17.1	14.1	12.4	9.2	7.7	7.1
		Average Peak Stress (MPa)	0.254	0.356	0.432	0.560	0.661	0.914	1.041	1.141
		Average Peak Strain (με)	38	40	39	40	43	50	53	53
	3	|E*| (MPa)	7709	10089	11912	15621	17123	20239	21646	23522
		Phase Angle, Φ (°)	26.2	16.8	20.5	15.0	13.4	10.2	9.4	8.5
		Average Peak Stress (MPa)	0.254	0.356	0.432	0.560	0.661	0.914	1.041	1.142
		Average Peak Strain (με)	33	35	36	36	39	45	48	49
	Avg.	|E*| Average	7403	10484	12029	15264	16665	19838	21280	23309
		Φ Average	27.8	22.0	21.1	16.4	14.6	11.0	9.9	9.1
		|E*| Coeff. of Variation	0.082	0.179	0.079	0.077	0.077	0.073	0.073	0.077
		Φ Coeff. of Variation	0.15	0.28	0.21	0.20	0.21	0.21	0.25	0.27
		|E*| Std. Dev.	607.0	1877.5	948.0	1175.3	1287.8	1440.9	1546.9	1805.2
		Φ Std. Dev.	4.286	6.093	4.356	3.219	3.006	2.341	2.501	2.428
35	1	|E*| (MPa)	862	1141	1424	2372	3028	5716	6880	8523
		Phase Angle, Φ (°)	36.1	37.3	40.1	41.7	37.9	33.9	29.9	25.8
		Average Peak Stress (MPa)	0.013	0.025	0.033	0.058	0.088	0.123	0.197	0.353
		Average Peak Strain (με)	15	22	23	24	29	22	29	41
	2	|E*| (MPa)	614	974	1247	2150	2813	4949	6060	7723
		Phase Angle, Φ (°)	27.9	29.1	31.0	31.6	30.1	25.9	22.5	20.3
		Average Peak Stress (MPa)	0.013	0.025	0.033	0.058	0.088	0.123	0.197	0.350
		Average Peak Strain (με)	21	26	26	27	31	25	33	45
	3	|E*| (MPa)	661	1010	1258	2223	2919	5217	6383	7990
		Phase Angle, Φ (°)	33.4	33.1	33.8	34.6	31.9	27.6	23.5	20.9
		Average Peak Stress (MPa)	0.013	0.025	0.033	0.058	0.088	0.124	0.199	0.352
		Average Peak Strain (με)	19	25	26	26	30	24	31	44
	Avg.	|E*| Average	712	1042	1310	2248	2920	5294	6441	8079
		Φ Average	32.5	33.2	35.0	36.0	33.3	29.1	25.3	22.3
		|E*| Coeff. of Variation	0.185	0.084	0.076	0.050	0.037	0.074	0.064	0.050
		Φ Coeff. of Variation	0.13	0.12	0.13	0.14	0.12	0.14	0.16	0.13
		|E*| Std. Dev.	131.8	87.6	98.9	113.3	108.0	389.3	413.1	407.0
		Φ Std. Dev.	4.151	4.086	4.636	5.175	4.118	4.189	4.048	3.006
54.4	1	|E*| (MPa)	629	546	441	543	649	1167	1566	2359
		Phase Angle, Φ (°)	25.3	31.6	26.3	31.0	31.8	32.9	32.4	32.5
		Average Peak Stress (MPa)	0.005	0.008	0.013	0.025	0.033	0.054	0.080	0.111
		Average Peak Strain (με)	8	14	29	47	50	47	51	47
	2	|E*| (MPa)	252	302	289	446	566	1056	1447	2176
		Phase Angle, Φ (°)	19.8	21.1	21.0	25.0	26.1	26.7	26.3	26.9
		Average Peak Stress (MPa)	0.005	0.008	0.013	0.026	0.033	0.055	0.081	0.109
		Average Peak Strain (με)	20	25	45	57	58	52	56	50
	3	|E*| (MPa)	219	251	283	446	572	1094	1501	2279
		Phase Angle, Φ (°)	18.3	19.4	22.4	26.4	27.8	28.2	27.9	27.5
		Average Peak Stress (MPa)	0.005	0.008	0.013	0.025	0.033	0.055	0.081	0.111
		Average Peak Strain (με)	23	31	45	57	57	50	54	49
	Avg.	|E*| Average	367	366	337	479	596	1106	1505	2272
		Φ Average	21.1	24.1	23.2	27.5	28.6	29.3	28.8	29.0
		|E*| Coeff. of Variation	0.622	0.430	0.266	0.117	0.077	0.051	0.040	0.040
		Φ Coeff. of Variation	0.17	0.27	0.12	0.11	0.10	0.11	0.11	0.11
		|E*| Std. Dev.	227.9	157.6	89.7	56.0	46.1	56.3	59.7	91.7
		Φ Std. Dev.	3.654	6.599	2.761	3.145	2.912	3.269	3.187	3.052

Table A-38 – B25.0B–Fine – Granite

Temp (°C)	Rep.	Parameters	Frequency (Hz)							
			0.01	0.05	0.1	0.5	1	5	10	25
-10	1	|E*| (MPa)	22800	24140	27215	32658	33727	36471	37766	39099
		Phase Angle, Φ (°)	12.7	7.4	9.9	9.4	8.3	6.6	6.4	5.7
		Average Peak Stress (MPa)	1.353	1.579	1.636	1.752	1.811	1.980	2.041	2.208
		Average Peak Strain (με)	59	65	60	54	54	54	54	56
	2	|E*| (MPa)	23059	26454	27067	31951	33312	35665	36807	
		Phase Angle, Φ (°)	9.6	0.0	6.5	6.5	6.0	4.9	4.0	
		Average Peak Stress (MPa)	1.353	1.579	1.636	1.752	1.810	1.980	2.041	
		Average Peak Strain (με)	59	60	60	55	54	56	55	
	3	|E*| (MPa)	19365	25535	24360	26956	28056	30406	31214	32463
		Phase Angle, Φ (°)	8.9	6.3	4.0	5.8	5.2	3.6	3.1	2.8
		Average Peak Stress (MPa)	1.354	1.580	1.637	1.751	1.807	1.975	2.034	2.196
		Average Peak Strain (με)	70	62	67	65	64	65	65	68
	Avg.	|E*| Average	21741	25376	26214	30522	31698	34181	35262	35781
		Φ Average	10.4	4.6	6.8	7.2	6.5	5.1	4.5	4.2
		|E*| Coeff. of Variation	0.095	0.046	0.061	0.102	0.100	0.096	0.100	0.131
		Φ Coeff. of Variation	0.20	0.87	0.44	0.26	0.25	0.30	0.38	0.50
		|E*| Std. Dev.	2062.2	1165.2	1607.3	3107.9	3161.5	3293.8	3538.5	4692.2
		Φ Std. Dev.	2.030	3.981	2.968	1.876	1.609	1.506	1.711	2.109
10	1	|E*| (MPa)	5265	9347	10081	13580	15450	19479	21307	24084
		Phase Angle, Φ (°)	31.8	24.2	27.9	20.5	18.7	14.9	13.4	12.3
		Average Peak Stress (MPa)	0.282	0.367	0.423	0.566	0.679	0.934	1.048	1.159
		Average Peak Strain (με)	54	39	42	42	44	48	49	48
	2	|E*| (MPa)	5123	8841	9872	13293	14727	18501	20201	
		Phase Angle, Φ (°)	29.5	25.5	21.4	18.7	16.4	12.2	11.3	
		Average Peak Stress (MPa)	0.367	0.479	0.564	0.707	0.821	1.103	1.217	
		Average Peak Strain (με)	72	54	57	53	56	60	60	
	3	|E*| (MPa)	4013	6756	7821	10556	12191	15890	17455	19499
		Phase Angle, Φ (°)	28.1	24.8	21.6	17.7	15.8	11.9	10.3	9.3
		Average Peak Stress (MPa)	0.367	0.480	0.564	0.707	0.819	1.100	1.211	1.323
		Average Peak Strain (με)	91	71	72	67	67	69	69	68
	Avg.	|E*| Average	4800	8315	9258	12476	14123	17957	19654	21792
		Φ Average	29.8	24.8	23.6	19.0	16.9	13.0	11.7	10.8
		|E*| Coeff. of Variation	0.143	0.165	0.135	0.134	0.121	0.103	0.101	0.149
		Φ Coeff. of Variation	0.06	0.02	0.16	0.08	0.09	0.13	0.14	0.20
		|E*| Std. Dev.	685.2	1373.2	1248.7	1669.7	1711.1	1855.7	1983.5	3242.3
		Φ Std. Dev.	1.855	0.616	3.711	1.435	1.567	1.647	1.602	2.153
35	1	|E*| (MPa)	368	588	752	1380	1925	3666	4683	6304
		Phase Angle, Φ (°)	32.6	36.2	36.4	38.9	34.7	31.4	29.0	26.7
		Average Peak Stress (MPa)	0.021	0.028	0.042	0.071	0.142	0.209	0.278	0.421
		Average Peak Strain (με)	57	48	56	51	74	57	59	67
	2	|E*| (MPa)	341	539	1604	1355	1991	3757	5377	6557
		Phase Angle, Φ (°)	26.2	31.8	32.5	35.4	31.8	29.1	22.9	24.7
		Average Peak Stress (MPa)	0.025	0.034	0.001	0.079	0.170	0.222	0.074	0.448
		Average Peak Strain (με)	74	63	1	59	85	59	14	68
	3	|E*| (MPa)	251	371	487	877	1399	2718	3622	5144
		Phase Angle, Φ (°)	24.4	26.4	28.7	35.4	30.2	29.2	27.3	25.4
		Average Peak Stress (MPa)	0.025	0.034	0.051	0.079	0.169	0.219	0.301	0.437
		Average Peak Strain (με)	101	91	104	90	121	81	83	85
	Avg.	|E*| Average	320	499	948	1204	1772	3380	4561	6002
		Φ Average	27.7	31.5	32.5	36.6	32.2	29.9	26.4	25.6
		|E*| Coeff. of Variation	0.191	0.227	0.616	0.235	0.183	0.170	0.194	0.126
		Φ Coeff. of Variation	0.16	0.16	0.12	0.05	0.07	0.04	0.12	0.04
		|E*| Std. Dev.	61.0	113.6	583.4	283.5	324.4	575.5	884.0	753.5
		Φ Std. Dev.	4.346	4.905	3.834	2.007	2.247	1.320	3.144	0.988

Table A-39 – B25.0B–Fine – Limestone

Temp (°C)	Rep.	Parameters	Frequency (Hz)							
			0.01	0.05	0.1	0.5	1	5	10	25
-10	1	|E*| (MPa)	18875	20572	23908	25466	26198	28475	29339	30320
		Phase Angle, Φ (°)	9.7	12.0	6.3	6.8	6.7	5.2	4.5	4.2
		Average Peak Stress (MPa)	1.151	1.343	1.391	1.488	1.535	1.677	1.727	1.864
		Average Peak Strain (με)	61	65	58	58	59	59	59	61
	2	|E*| (MPa)	18826	20566	22965	25675	26411	28497	29367	30704
		Phase Angle, Φ (°)	9.5	5.2	9.5	7.7	6.1	5.5	4.9	4.6
		Average Peak Stress (MPa)	1.151	1.343	1.391	1.488	1.535	1.678	1.729	1.866
		Average Peak Strain (με)	61	65	61	58	58	59	59	61
	3	|E*| (MPa)	22625	26835	26816	30391	31636	33643	36808	
		Phase Angle, Φ (°)	8.5	1.0	8.6	5.8	4.6	4.0	5.3	
		Average Peak Stress (MPa)	1.016	1.184	1.227	1.312	1.354	1.479	1.524	
		Average Peak Strain (με)	45	44	46	43	43	44	41	
	Avg.	|E*| Average	20108	22658	24563	27177	28082	30205	31838	30512
		Φ Average	9.2	6.1	8.1	6.8	5.8	4.9	4.9	4.4
		|E*| Coeff. of Variation	0.108	0.160	0.082	0.102	0.110	0.099	0.135	0.009
		Φ Coeff. of Variation	0.07	0.92	0.21	0.14	0.18	0.16	0.08	0.07
		|E*| Std. Dev.	2179.3	3617.5	2007.1	2784.9	3080.0	2977.5	4303.9	271.3
		Φ Std. Dev.	0.620	5.559	1.676	0.963	1.070	0.794	0.380	0.291
10	1	|E*| (MPa)	5618	8586	9143	11798	13109	16038	17341	19154
		Phase Angle, Φ (°)	27.8	23.1	22.6	17.6	16.2	12.7	11.4	10.2
		Average Peak Stress (MPa)	0.240	0.336	0.408	0.528	0.624	0.862	0.978	1.070
		Average Peak Strain (με)	43	39	45	45	48	54	56	56
	2	|E*| (MPa)	5461	7464	8838	11843	13072	15949	17265	19071
		Phase Angle, Φ (°)	28.2	24.4	22.0	18.6	16.5	12.8	11.5	10.7
		Average Peak Stress (MPa)	0.210	0.296	0.359	0.466	0.550	0.760	0.869	0.953
		Average Peak Strain (με)	38	40	41	39	42	48	50	50
	3	|E*| (MPa)	7037	10346	10709	14475	15855	19169	20558	22694
		Phase Angle, Φ (°)	26.8	18.0	19.0	16.2	14.8	11.2	10.1	9.2
		Average Peak Stress (MPa)	0.212	0.296	0.360	0.466	0.550	0.759	0.865	0.939
		Average Peak Strain (με)	30	29	34	32	35	40	42	41
	Avg.	|E*| Average	6039	8799	9563	12705	14012	17052	18388	20306
		Φ Average	27.6	21.9	21.2	17.4	15.8	12.2	11.0	10.0
		|E*| Coeff. of Variation	0.144	0.165	0.105	0.121	0.114	0.108	0.102	0.102
		Φ Coeff. of Variation	0.03	0.15	0.09	0.07	0.06	0.08	0.07	0.07
		|E*| Std. Dev.	868.3	1452.9	1003.8	1532.8	1596.2	1834.0	1879.6	2068.4
		Φ Std. Dev.	0.726	3.351	1.936	1.199	0.919	0.921	0.773	0.730
35	1	|E*| (MPa)	678	912	1073	1756	2243	3997	4923	6136
		Phase Angle, Φ (°)	34.6	36.8	36.5	37.2	34.7	30.8	26.2	23.5
		Average Peak Stress (MPa)	0.012	0.024	0.031	0.055	0.082	0.116	0.185	0.327
		Average Peak Strain (με)	18	26	29	31	37	29	38	53
	2	|E*| (MPa)	686	870	1042	1683	2149	3736	4873	5844
		Phase Angle, Φ (°)	34.7	31.6	32.8	32.8	31.3	27.4	22.3	22.5
		Average Peak Stress (MPa)	0.011	0.021	0.028	0.049	0.072	0.102	0.163	0.286
		Average Peak Strain (με)	16	24	26	29	34	27	33	49
	3	|E*| (MPa)	793	1174	1432	2294	2919	4913	5867	7275
		Phase Angle, Φ (°)	31.8	31.4	33.2	34.0	32.3	26.8	24.4	22.0
		Average Peak Stress (MPa)	0.014	0.028	0.027	0.048	0.072	0.101	0.162	0.283
		Average Peak Strain (με)	18	24	19	21	25	21	28	39
	Avg.	|E*| Average	719	986	1182	1911	2437	4215	5221	6419
		Φ Average	33.7	33.2	34.2	34.7	32.8	28.3	24.3	22.7
		|E*| Coeff. of Variation	0.089	0.167	0.183	0.175	0.172	0.147	0.107	0.118
		Φ Coeff. of Variation	0.05	0.09	0.06	0.07	0.05	0.08	0.08	0.04
		|E*| Std. Dev.	63.9	164.7	216.8	333.8	420.2	618.2	559.7	755.9
		Φ Std. Dev.	1.624	3.084	2.063	2.287	1.765	2.156	1.906	0.795
54.4	1	|E*| (MPa)	352	366	322	422	519	951	1274	1849
		Phase Angle, Φ (°)	18.0	27.5	25.1	28.7	29.2	29.4	28.4	28.7
		Average Peak Stress (MPa)	0.005	0.007	0.012	0.024	0.031	0.051	0.074	0.099
		Average Peak Strain (με)	13	20	38	57	59	54	58	54
	2	|E*| (MPa)	368	447	344	405	487	864	1146	1667
		Phase Angle, Φ (°)	24.6	23.5	25.9	26.6	27.3	27.6	26.8	27.5
		Average Peak Stress (MPa)	0.004	0.006	0.011	0.021	0.027	0.045	0.066	0.087
		Average Peak Strain (με)	11	14	31	52	56	53	58	52
	3	|E*| (MPa)	0	328	355	491	602	1074	1420	2072
		Phase Angle, Φ (°)	0.0	17.1	19.6	23.9	25.3	26.1	25.6	27.1
		Average Peak Stress (MPa)	0.000	0.009	0.014	0.028	0.036	0.060	0.088	0.117
		Average Peak Strain (με)	0	26	40	57	60	56	62	56
	Avg.	|E*| Average	240	380	340	439	536	963	1280	1863
		Φ Average	14.2	22.7	23.5	26.4	27.2	27.7	26.9	27.8
		|E*| Coeff. of Variation	0.867	0.160	0.050	0.103	0.110	0.110	0.107	0.109
		Φ Coeff. of Variation	0.90	0.23	0.14	0.09	0.07	0.06	0.05	0.03
		|E*| Std. Dev.	208.1	60.8	16.9	45.4	59.1	105.6	137.2	202.9
		Φ Std. Dev.	12.729	5.237	3.405	2.408	1.954	1.662	1.411	0.853

Table A-40 – B25.0C–Coarse – Granite

Temp (°C)	Rep.	Parameters	Frequency (Hz)							
			0.01	0.05	0.1	0.5	1	5	10	25
-10	1	|E*| (MPa)	24759	32712	32133	36206	37831	41047	42879	44709
		Phase Angle, Φ (°)	12.7	3.4	6.5	7.8	7.9	6.6	5.9	6.0
		Average Peak Stress (MPa)	1.241	1.466	1.551	1.664	1.691	1.859	1.918	2.079
		Average Peak Strain (με)	50	45	48	46	45	45	45	46
	2	|E*| (MPa)	20435	24681	24493	28671	30043	33227	34011	35288
		Phase Angle, Φ (°)	9.9	14.7	6.3	5.7	4.5	3.3	2.5	2.1
		Average Peak Stress (MPa)	1.269	1.495	1.579	1.694	1.746	1.916	1.975	2.197
		Average Peak Strain (με)	62	61	64	59	58	58	58	62
	3	|E*| (MPa)	21173	27689	26787	32148	33333	37056	38202	39337
		Phase Angle, Φ (°)	14.1	16.4	11.9	8.2	7.9	5.8	5.6	5.1
		Average Peak Stress (MPa)	1.269	1.495	1.579	1.694	1.746	1.916	1.976	2.199
		Average Peak Strain (με)	60	54	59	53	52	52	52	56
	Avg.	|E*| Average	22122	28361	27805	32342	33736	37110	38364	39778
		Φ Average	12.2	11.5	8.3	7.2	6.8	5.3	4.7	4.4
		|E*| Coeff. of Variation	0.105	0.143	0.141	0.117	0.116	0.105	0.116	0.119
		Φ Coeff. of Variation	0.17	0.61	0.38	0.19	0.29	0.33	0.40	0.46
		|E*| Std. Dev.	2312.9	4057.4	3920.0	3771.1	3909.9	3910.0	4436.3	4726.2
		Φ Std. Dev.	2.128	7.077	3.180	1.371	1.949	1.714	1.879	2.044
10	1	|E*| (MPa)	4428	7019	8888	13517	15596	20519	22889	25961
		Phase Angle, Φ (°)	32.9	28.1	27.6	22.1	20.5	15.7	13.9	12.9
		Average Peak Stress (MPa)	0.282	0.451	0.564	0.705	0.817	1.125	1.267	1.381
		Average Peak Strain (με)	64	64	63	52	52	55	55	53
	2	|E*| (MPa)	3657	6109	7568	11014	12817	17107	18927	21386
		Phase Angle, Φ (°)	29.6	22.8	25.4	19.3	17.0	12.7	11.1	10.0
		Average Peak Stress (MPa)	0.282	0.451	0.564	0.705	0.817	1.125	1.266	1.381
		Average Peak Strain (με)	77	74	75	64	64	66	67	65
	3	|E*| (MPa)	3605	6852	7927	11732	13553	18531	20499	23421
		Phase Angle, Φ (°)	34.5	29.3	27.1	23.9	21.8	16.7	14.7	13.2
		Average Peak Stress (MPa)	0.282	0.451	0.564	0.705	0.817	1.125	1.267	1.382
		Average Peak Strain (με)	78	66	71	60	60	61	62	59
	Avg.	|E*| Average	3897	6660	8128	12088	13989	18719	20772	23589
		Φ Average	32.3	26.7	26.7	21.8	19.8	15.0	13.3	12.0
		|E*| Coeff. of Variation	0.118	0.073	0.084	0.107	0.103	0.092	0.096	0.097
		Φ Coeff. of Variation	0.08	0.13	0.04	0.11	0.13	0.14	0.14	0.15
		|E*| Std. Dev.	461.0	484.0	682.5	1288.9	1439.8	1713.9	1994.7	2291.9
		Φ Std. Dev.	2.526	3.469	1.194	2.303	2.521	2.100	1.912	1.787
35	1	|E*| (MPa)	358	495	600	1084	1531	3093	4143	5979
		Phase Angle, Φ (°)	25.1	30.1	30.7	35.7	33.6	33.3	31.8	29.6
		Average Peak Stress (MPa)	0.017	0.025	0.034	0.056	0.111	0.178	0.246	0.413
		Average Peak Strain (με)	47	51	56	52	73	57	59	69
	2	|E*| (MPa)	329	442	522	925	1326	2670	3603	5248
		Phase Angle, Φ (°)	22.1	26.5	27.3	32.7	31.4	31.6	30.2	27.8
		Average Peak Stress (MPa)	0.017	0.025	0.034	0.056	0.111	0.177	0.245	0.412
		Average Peak Strain (με)	51	58	65	61	84	66	68	79
	3	|E*| (MPa)	289	410	511	905	1274	2586	3456	5104
		Phase Angle, Φ (°)	25.1	29.1	30.3	35.4	33.8	34.1	32.9	31.2
		Average Peak Stress (MPa)	0.017	0.025	0.034	0.056	0.111	0.178	0.245	0.412
		Average Peak Strain (με)	58	62	66	62	87	69	71	81
	Avg.	|E*| Average	325	449	544	972	1377	2783	3734	5444
		Φ Average	24.1	28.5	29.4	34.6	32.9	33.0	31.6	29.5
		|E*| Coeff. of Variation	0.107	0.096	0.089	0.101	0.099	0.098	0.097	0.086
		Φ Coeff. of Variation	0.07	0.07	0.06	0.05	0.04	0.04	0.04	0.06
		|E*| Std. Dev.	34.9	43.1	48.4	97.9	136.0	271.8	361.8	469.1
		Φ Std. Dev.	1.714	1.858	1.828	1.656	1.309	1.247	1.360	1.714

Table A-41 – B25.0C–Fine – Granite

Temp (°C)	Rep.	Parameters	Frequency (Hz)							
			0.01	0.05	0.1	0.5	1	5	10	25
-10	1	|E*| (MPa)	16536	18902	21164	22946	23998	26301	27143	28419
		Phase Angle, Φ (°)	8.3	11.9	5.1	4.9	4.3	3.2	2.6	2.5
		Average Peak Stress (MPa)	1.356	1.582	1.639	1.751	1.806	1.974	2.034	2.197
		Average Peak Strain (με)	82	84	77	76	75	75	75	77
	2	|E*| (MPa)	17232	20922	22033	23798	25242	27824	28896	30075
		Phase Angle, Φ (°)	9.5	13.2	6.4	8.5	7.4	6.7	6.4	6.1
		Average Peak Stress (MPa)	1.356	1.582	1.639	1.751	1.807	1.973	2.033	2.196
		Average Peak Strain (με)	79	76	74	74	72	71	70	73
	3	|E*| (MPa)	16487	19811	21177	23012	23848	26459		
		Phase Angle, Φ (°)	10.8	13.8	8.5	7.1	7.3	6.7		
		Average Peak Stress (MPa)	1.355	1.582	1.639	1.751	1.806	1.974		
		Average Peak Strain (με)	82	80	77	76	76	75		
	Avg.	|E*| Average	16751	19878	21458	23252	24363	26861	28019	29247
		Φ Average	9.5	13.0	6.7	6.8	6.3	5.5	4.5	4.3
		|E*| Coeff. of Variation	0.025	0.051	0.023	0.020	0.031	0.031	0.044	0.040
		Φ Coeff. of Variation	0.13	0.08	0.26	0.26	0.28	0.37	0.59	0.61
		|E*| Std. Dev.	416.5	1011.5	498.0	474.1	765.5	837.3	1239.6	1171.3
		Φ Std. Dev.	1.239	1.001	1.749	1.794	1.756	2.048	2.676	2.611
10	1	|E*| (MPa)	4555	6770	7642	9752	10714	13507	14808	16547
		Phase Angle, Φ (°)	23.0	23.0	18.0	15.5	14.3	11.0	9.6	9.0
		Average Peak Stress (MPa)	0.282	0.367	0.424	0.565	0.677	0.930	1.043	1.150
		Average Peak Strain (με)	62	54	55	58	63	69	70	69
	2	|E*| (MPa)	4779	6811	8045	10263	11451	14375	15773	17584
		Phase Angle, Φ (°)	24.7	17.3	20.6	17.7	16.3	13.4	12.5	11.8
		Average Peak Stress (MPa)	0.282	0.367	0.424	0.565	0.677	0.930	1.042	1.147
		Average Peak Strain (με)	59	54	53	55	59	65	66	65
	3	|E*| (MPa)	4531	6918	7347	9866	10946	13887	15249	17117
		Phase Angle, Φ (°)	26.6	21.3	22.9	18.3	17.2	14.1	12.9	12.5
		Average Peak Stress (MPa)	0.282	0.367	0.424	0.565	0.677	0.930	1.043	1.149
		Average Peak Strain (με)	62	53	58	57	62	67	68	67
	Avg.	|E*| Average	4622	6833	7678	9960	11037	13923	15277	17083
		Φ Average	24.7	20.5	20.5	17.2	15.9	12.8	11.7	11.1
		|E*| Coeff. of Variation	0.030	0.011	0.046	0.027	0.034	0.031	0.032	0.030
		Φ Coeff. of Variation	0.07	0.14	0.12	0.09	0.10	0.13	0.15	0.17
		|E*| Std. Dev.	136.5	76.1	350.0	268.2	376.6	434.9	483.1	519.1
		Φ Std. Dev.	1.794	2.918	2.448	1.503	1.530	1.658	1.801	1.837
35	1	|E*| (MPa)	463	710	892	1496	1994	3366	4145	5297
		Phase Angle, Φ (°)	27.3	28.2	28.1	28.8	26.3	23.5	21.8	20.3
		Average Peak Stress (MPa)	0.022	0.028	0.042	0.070	0.140	0.208	0.277	0.420
		Average Peak Strain (με)	47	40	48	47	70	62	67	79
	2	|E*| (MPa)	511	769	912	1512	1951	3341	4080	5180
		Phase Angle, Φ (°)	28.2	32.5	30.2	30.8	28.3	24.9	23.5	22.1
		Average Peak Stress (MPa)	0.021	0.028	0.042	0.070	0.140	0.207	0.276	0.416
		Average Peak Strain (με)	41	37	46	46	72	62	68	80
	3	|E*| (MPa)	554	818	1006	1599	2081	3517	4293	5331
		Phase Angle, Φ (°)	27.0	29.7	29.6	30.7	27.8	25.5	24.0	22.7
		Average Peak Stress (MPa)	0.021	0.028	0.042	0.070	0.140	0.208	0.277	0.419
		Average Peak Strain (με)	38	34	42	44	67	59	64	79
	Avg.	|E*| Average	510	766	936	1536	2009	3408	4173	5269
		Φ Average	27.5	30.1	29.3	30.1	27.5	24.6	23.1	21.7
		|E*| Coeff. of Variation	0.089	0.071	0.065	0.036	0.033	0.028	0.026	0.015
		Φ Coeff. of Variation	0.02	0.07	0.04	0.04	0.04	0.04	0.05	0.06
		|E*| Std. Dev.	45.5	54.0	60.9	55.6	66.1	95.3	109.6	79.3
		Φ Std. Dev.	0.660	2.149	1.040	1.140	1.037	0.990	1.145	1.235

Table A-42 – B25.0C–Fine – Limestone

Temp (°C)	Rep.	Parameters	Frequency (Hz)							
			0.01	0.05	0.1	0.5	1	5	10	25
-10	1	|E*| (MPa)	17099	18323	19701	22218	23139	25076	25869	26804
		Phase Angle, Φ (°)	5.7	2.2	3.3	2.9	3.0	1.7	1.4	1.5
		Average Peak Stress (MPa)	1.353	1.579	1.636	1.750	1.806	1.975	2.034	2.197
		Average Peak Strain (με)	79	86	83	79	78	79	79	82
	2	|E*| (MPa)	18512	21170	22473	24461	25212	27050	27946	28874
		Phase Angle, Φ (°)	11.5	12.5	8.3	7.9	7.6	6.1	5.2	4.5
		Average Peak Stress (MPa)	1.353	1.579	1.636	1.749	1.805	1.974	2.033	2.195
		Average Peak Strain (με)	73	75	73	72	72	73	73	76
	3	|E*| (MPa)	16784	18608	20044	22556	23539	25469	26396	27282
		Phase Angle, Φ (°)	11.0	9.7	9.3	8.2	7.9	6.3	6.1	5.7
		Average Peak Stress (MPa)	1.353	1.579	1.636	1.750	1.805	1.973	2.031	2.197
		Average Peak Strain (με)	81	85	82	78	77	77	77	81
	Avg.	|E*| Average	17465	19367	20740	23078	23964	25865	26737	27653
		Φ Average	9.4	8.1	6.9	6.4	6.2	4.7	4.2	3.9
		|E*| Coeff. of Variation	0.053	0.081	0.073	0.052	0.046	0.040	0.040	0.039
		Φ Coeff. of Variation	0.34	0.65	0.46	0.47	0.45	0.56	0.59	0.55
		|E*| Std. Dev.	920.3	1568.2	1511.3	1209.1	1099.6	1044.8	1079.7	1084.1
		Φ Std. Dev.	3.209	5.316	3.213	2.990	2.779	2.622	2.496	2.168
10	1	|E*| (MPa)	4927	6845	7956	10531	11603	14245	15451	17138
		Phase Angle, Φ (°)	22.6	15.8	16.9	13.5	12.4	9.0	7.7	7.4
		Average Peak Stress (MPa)	0.282	0.395	0.479	0.622	0.734	1.015	1.158	1.263
		Average Peak Strain (με)	57	58	60	59	63	71	75	74
	2	|E*| (MPa)	5561	8232	8840	11586	12829	15462	16746	18454
		Phase Angle, Φ (°)	28.7	22.6	22.1	18.0	16.7	12.7	11.4	10.2
		Average Peak Stress (MPa)	0.282	0.395	0.480	0.621	0.734	1.014	1.156	1.263
		Average Peak Strain (με)	51	48	54	54	57	66	69	68
	3	|E*| (MPa)	4991	7139	7881	10479	11634	14567	15986	17454
		Phase Angle, Φ (°)	27.0	19.3	20.9	17.5	15.7	12.1	11.4	10.4
		Average Peak Stress (MPa)	0.282	0.395	0.479	0.621	0.734	1.014	1.156	1.264
		Average Peak Strain (με)	56	55	61	59	63	70	72	72
	Avg.	|E*| Average	5160	7405	8226	10865	12022	14758	16061	17682
		Φ Average	26.1	19.3	20.0	16.3	14.9	11.3	10.2	9.3
		|E*| Coeff. of Variation	0.068	0.099	0.065	0.058	0.058	0.043	0.041	0.039
		Φ Coeff. of Variation	0.12	0.18	0.14	0.15	0.15	0.17	0.21	0.18
		|E*| Std. Dev.	349.0	730.6	533.3	624.8	699.1	630.6	650.5	687.1
		Φ Std. Dev.	3.132	3.410	2.714	2.476	2.255	1.967	2.099	1.698
35	1	|E*| (MPa)	475	749	903	1533	1984	3481	4376	5599
		Phase Angle, Φ (°)	28.6	29.6	30.1	31.4	29.5	25.0	21.0	21.1
		Average Peak Stress (MPa)	0.014	0.028	0.037	0.064	0.097	0.137	0.220	0.389
		Average Peak Strain (με)	30	38	41	42	49	39	50	69
	2	|E*| (MPa)	590	853	1022	1671	2150	3841	4674	5752
		Phase Angle, Φ (°)	31.6	36.8	36.0	37.4	34.6	30.6	26.8	23.6
		Average Peak Stress (MPa)	0.014	0.028	0.037	0.064	0.097	0.137	0.220	0.387
		Average Peak Strain (με)	24	33	36	39	45	36	47	67
	3	|E*| (MPa)	602	856	1060	1766	2295	4024	4989	6242
		Phase Angle, Φ (°)	33.7	33.9	33.6	35.1	32.7	28.7	25.4	22.9
		Average Peak Stress (MPa)	0.014	0.028	0.037	0.064	0.097	0.137	0.219	0.387
		Average Peak Strain (με)	24	33	35	36	42	34	44	62
	Avg.	|E*| Average	556	819	995	1656	2143	3782	4680	5864
		Φ Average	31.3	33.4	33.2	34.6	32.3	28.1	24.4	22.6
		|E*| Coeff. of Variation	0.126	0.075	0.082	0.071	0.073	0.073	0.065	0.057
		Φ Coeff. of Variation	0.08	0.11	0.09	0.09	0.08	0.10	0.12	0.06
		|E*| Std. Dev.	70.1	61.0	81.8	117.2	155.5	276.4	306.3	335.9
		Φ Std. Dev.	2.547	3.625	2.962	3.034	2.561	2.846	2.994	1.308
54.4	1	|E*| (MPa)	157	197	218	345	441	842	1146	1694
		Phase Angle, Φ (°)	16.9	20.6	21.0	24.7	26.0	26.6	25.6	26.3
		Average Peak Stress (MPa)	0.006	0.008	0.014	0.028	0.036	0.061	0.090	0.121
		Average Peak Strain (με)	35	43	66	82	83	72	78	72
	2	|E*| (MPa)	485	414	373	445	536	960	1255	1785
		Phase Angle, Φ (°)	27.4	33.0	30.8	32.9	32.5	32.6	30.1	30.0
		Average Peak Stress (MPa)	0.006	0.009	0.014	0.028	0.036	0.060	0.089	0.120
		Average Peak Strain (με)	12	21	38	63	68	63	71	68
	3	|E*| (MPa)	418	338	319	434	528	962	1281	1887
		Phase Angle, Φ (°)	20.9	22.4	22.6	25.7	26.9	28.9	28.1	28.6
		Average Peak Stress (MPa)	0.006	0.009	0.014	0.028	0.036	0.060	0.088	0.118
		Average Peak Strain (με)	13	25	44	65	69	62	68	63
	Avg.	|E*| Average	353	316	303	408	501	921	1227	1789
		Φ Average	21.7	25.3	24.8	27.8	28.5	29.3	27.9	28.3
		|E*| Coeff. of Variation	0.490	0.349	0.260	0.134	0.105	0.074	0.059	0.054
		Φ Coeff. of Variation	0.24	0.27	0.21	0.16	0.12	0.10	0.08	0.07
		|E*| Std. Dev.	173.1	110.3	79.0	54.8	52.4	68.6	71.9	96.2
		Φ Std. Dev.	5.294	6.724	5.275	4.483	3.523	3.003	2.221	1.905

APPENDIX B – AASHTO TP 62-03

Standard Method of Test for

Determining Dynamic Modulus of Hot-Mix Asphalt Concrete Mixtures

AASHTO Designation: TP 62-03

American Association of State Highway and Transportation Officials
444 North Capitol Street N.W., Suite 249
Washington, D.C. 20001

Standard Method of Test for

Determining Dynamic Modulus of Hot-Mix Asphalt Concrete Mixtures

AASHTO Designation: TP 62-03

1. SCOPE

1.1. This test method covers procedures for preparing and testing asphalt concrete mixtures to determine the dynamic modulus and phase angle over a range of temperatures and loading frequencies.

1.2. This standard is applicable to laboratory prepared specimens of mixtures with nominal maximum size aggregate less than or equal to 37.5 mm (1.48 in.).

1.3. This standard may involve hazardous material, operations, and equipment. This standard does not purport to address all safety problems associated with its use. It is the responsibility of the user of this procedure to establish appropriate safety and health practices and to determine the applicability of regulatory limitations prior to use.

2. REFERENCED DOCUMENTS

2.1. *AASHTO Standards:*

- R 30, Practice for Mixture Conditioning of Hot Mix Asphalt (HMA)
- T 166, Bulk Specific Gravity of Compacted Asphalt Mixtures
- T 209, Maximum Specific Gravity of Bituminous Paving Mixtures
- T 269, Percent Air Voids in Compacted Dense and Open Bituminous Paving Mixtures
- T 312, Method for Preparing and Determining the Density of Hot Mix Asphalt (HMA) Specimens by Means of the Superpave Gyratory Compactor

3. DEFINITIONS

3.1. *complex modulus* (E*)—a complex number that defines the relationship between stress and strain for a linear viscoelastic material.

3.2. *dynamic modulus* (|E*|)—the absolute value of the complex modulus calculated by dividing the maximum (peak-to-peak) stress by the recoverable (peak-to-peak) axial strain for a material subjected to a sinusoidal loading.

3.3. *phase angle* (N)— the angle in degrees between a sinusoidal applied (peak-to-peak) stress and the resulting (peak-to-peak) strain in a controlled-stress test.

3.4. *linear viscoelastic*—within the context of this test, refers to behavior in which the dynamic modulus is independent of stress or strain amplitude.

4. SUMMARY OF METHOD

4.1. A sinusoidal (haversine) axial compressive stress is applied to a specimen of asphalt concrete at a given temperature and loading frequency. The applied stress and the resulting recoverable axial strain response of the specimen is measured and used to calculate the dynamic modulus and phase angle.

4.2. Figure 1 presents one schematic of the dynamic modulus test that is in use.

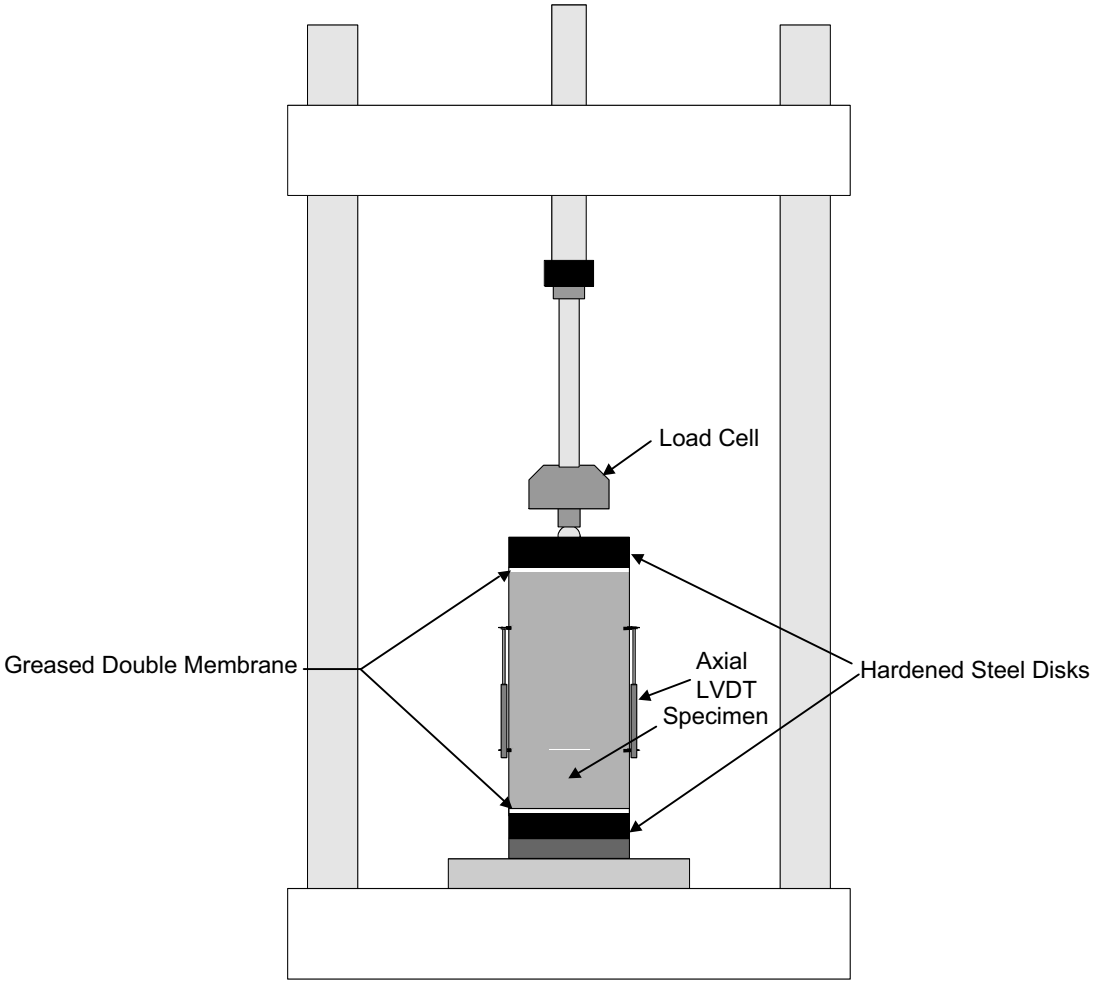

Figure 1—General Schematic of Dynamic Modulus Test

5. SIGNIFICANCE AND USE

5.1. Dynamic modulus values measured over a range of temperatures and frequencies of loading can be shifted into a master curve for characterizing asphalt concrete for pavement thickness design and performance analysis.

5.2. The values of dynamic modulus and phase angle can also be used as performance criteria for asphalt concrete mixture design.

6. APPARATUS

6.1. *Dynamic Modulus Test System*—A dynamic modulus test system consisting of a testing machine, environmental chamber, and measuring system.

6.1.1. *Testing Machine*—A servo-hydraulic testing machine capable of producing a controlled haversine compressive loading. The testing machine should have a capability of applying load over a range of frequencies from 0.1 to 25 Hz and stress level up to 2800 kPa (400 psi).

6.1.2. *Environmental Chamber*—A chamber for controlling the test specimen at the desired temperature. The environmental chamber shall be capable of controlling the temperature of the specimen over a temperature range from –10 to 60°C (14 to 140°F) to an accuracy of ± 0.5°C (1°F). The chamber shall be large enough to accommodate the test specimen and a dummy specimen with thermocouple mounted at the center for temperature verification.

6.1.3. *Measurement System*—The system shall be fully computer controlled capable of measuring and recording the time history of the applied load, and the axial deformations. The system shall be capable of measuring the period of the applied sinusoidal load and resulting deformations with a resolution of 0.5 percent.

6.1.3.1 *Load*—The load shall be measured with an electronic load cell in contact with one of the specimen caps. The load cell shall be calibrated in accordance with AASHTO T 67. The load measuring system shall have a minimum range of 0 to 25 kN (0 – 5600 lb) with a resolution of 5 N (1 lb).

6.1.3.2. *Axial Deformations*—Axial deformations shall be measured with linear variable differential transformers (LVDT) mounted between gauge points glued to the specimen as shown in Figure 2.

The deformations shall be measured at a minimum of two locations 180° apart; however, three locations located 120° apart is recommended to minimize the number of replicate specimens required for testing. The LVDTs shall have a range of ± 0.5 mm (0.02 in.). The deformation measuring system shall have auto zero and selecTable ranges as defined in Table 1.

Table 1—Deformation Measuring System Requirements

Range, mm (in)	Resolution, mm (in)
±0.5 (0.01969)	0.0100 (0.00039)
±0.25 (0.00984)	0.0050 (0.00020)
±0.125 (0.00492)	0.0025 (0.00010)
±0.0625 (0.00246)	0.0010 (0.00004)

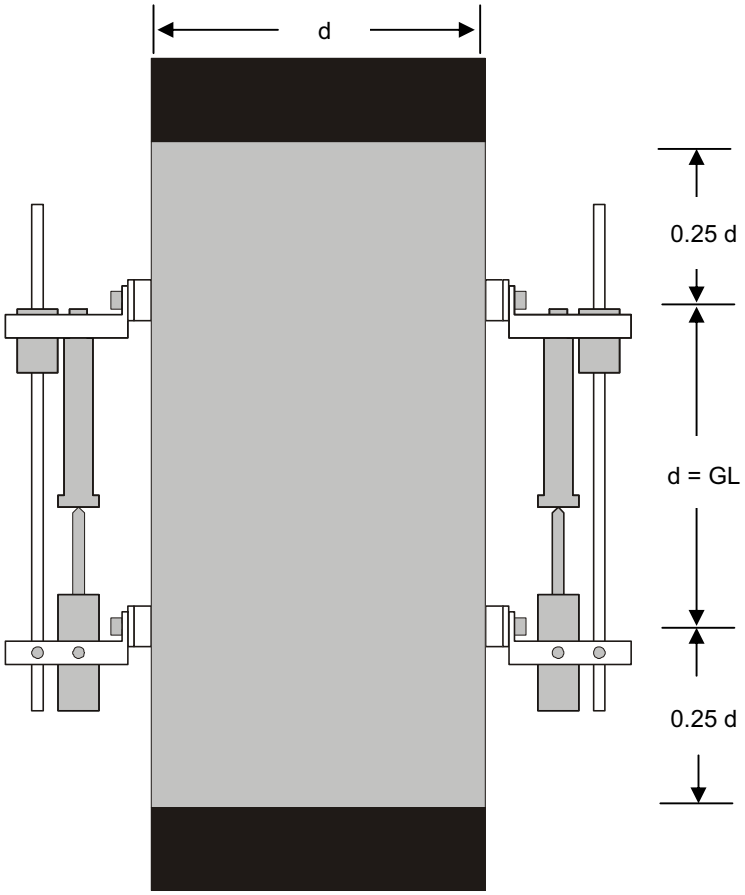

Figure 2—General Schematic of Gauge Points (Not to Scale)

6.1.4. *Loading Platens*—Platens, with a diameter equal to or greater than that of the test specimen are required above and below the specimen to transfer the load from the testing machine to the specimen. Generally, these platens should be made of hardened or plated steel, or anodized high strength aluminum. Softer materials will require more frequent replacement. Materials that have linear elastic modulus properties and hardness properties lower than that of 6061-T6 aluminum shall not be used.

6.1.5. *End Treatment*—Friction reducing end treatments shall be placed between the specimen ends and the loading platens. The end treatments shall consist of two 0.5 mm (0.02 in.) thick latex membranes separated with silicone grease.

6.2. *Superpave Gyratory Compactor*—A gyratory compactor and associated equipment for preparing laboratory specimens in accordance with AASHTO T 312. The compactor shall be capable of compacting 170 mm (6.69 in.) high specimen.

6.3. *Saw*—A machine for sawing test specimens ends to the appropriate length is required. The saw shall have a diamond cutting edge and shall be capable of cutting specimens to the prescribed dimensions without excessive heating or shock.

Note 1—A diamond masonry saw greatly facilitates the preparation of test specimens with smooth, parallel ends. Both single or double-bladed diamond saws should have feed mechanisms and speed controls of sufficient precision to ensure compliance with paragraphs 9.5 and 9.6 of this method. Adequate blade stiffness is also important to control flexing of the blade during thin cuts.

6.4. *Core Drill*—A coring machine with cooling system and a diamond bit for cutting nominal 101.6 mm (4.00 in.) diameter test specimens.

Note 2—A coring machine with adjusTable vertical feed and rotational speed is recommended. The variable feeds and speeds may be controlled by various methods. A vertical feed rate of approximately 0.05 mm/rev (0.002 in/rev) and a rotational speed of approximately 450 RPM has been found to be satisfactory for several Superpave mixtures.

7. HAZARDS

7.1. Observe standard laboratory safety precautions when preparing and testing HMA specimens.

8. TESTING EQUIPMENT CALIBRATION

8.1. The signal conditioning and data acquisition device of the testing system shall be checked to ensure that there is no excess phase shift between load and displacement channels.

8.2. The testing system shall be calibrated prior to initial use and at least once a year thereafter or per manufacturer requirements or per every 200 tests.

8.3. Verify the capability of the environmental chamber to maintain the required temperature within the accuracy specified.

8.4. Verify the calibration of all measurement components (such as load cell and specimen deformation measurement device) of the testing system.

8.5. If any of the verifications yield data that does not comply with the accuracy specified, correct the problem prior to proceeding with testing.

9. TEST SPECIMENS

9.1. *Size*—Dynamic modulus testing shall be performed on test specimens cored from gyratory compacted mixtures. The average diameter of the test specimens shall be between 100 and 104 mm (3.94 and 4.09 in.) with a standard deviation of 1.0 mm (0.04 in.). The average height of the test specimen shall be between 147.5 and 152.5 mm (5.81 and 6.00 in.).

9.2. *Aging*—Laboratory prepared mixtures shall be conditioned in accordance with the 4-hours short-term oven conditioning procedure in AASHTO R30. Field mixtures shall not be conditioned.

9.3. *Gyratory Specimens*—Prepare 170 mm (6.69 in.) high specimens to the required air void content in accordance with AASHTO T 312.

Note 3—Testing should be performed on test specimens (101.6 mm (4.00 in.) diameter) meeting specific air void tolerances. The gyratory specimen (152.4 mm (6.00 in.) diameter) air void content required to obtain a specified test specimen air void content must be determined by trial and error. Generally, the test specimen air void content is 1.5 to 2.5 percent lower than the air void content of the gyratory specimen when the test specimen is removed from the middle as specified in this test method.

9.4. *Coring*—Core the nominal 101.6 mm (4.00 in.) diameter test specimens from the center of the gyratory specimens. Both the core drill and the gyratory specimen should be adequately supported to ensure that the resulting test specimen is cylindrical with sides that are smooth, parallel, and free from steps, ridges, and grooves.

9.5. *Diameter*—Measure the diameter of the test specimen at the mid height and third points along axes that are 90 degrees apart. Record each of the six measurements to the nearest 1 mm (0.04 in.). Calculate the average and the standard deviation of the six measurements. If the standard deviation is greater than 2.5 mm (0.01 in.) discard the specimen. For accepTable specimens, the average diameter, reported to the nearest 1 mm (0.04 in.), shall be used in all material property calculations.

9.6. *End Preparation*—The ends of all test specimens shall be smooth and perpendicular to the axis of the specimen. Prepare the ends of the specimen by sawing with a single or double bladed saw. The prepared specimen ends shall meet the tolerances described below. Reject test specimens not meeting these tolerances.

9.6.1. The specimen ends shall have a cut surface waviness height within a tolerance of ± 0.05 mm (0.002 in.) across any diameter. This requirement shall be checked in a minimum of three positions at approximately 120° intervals using a straight edge and feeler gauges approximately
8–12.5 mm (0.32–0.49 in.) wide or an optical comparator.

9.6.2. The specimen end shall not depart from perpendicular to the axis of the specimen by more than 1 degree. This requirement shall be checked on each specimen using a machinists square and feeler gauges.

9.7. *Air Void Content*—Determine the air void content of the final test specimen in accordance with AASHTO T 269. Reject specimens with air voids that differ by more than 0.5 percent from the target air voids.

Note 4—Considerable time can be saved if the cored test specimens were treated as wet, and the weights in water and saturated surface dry were measured immediately or within a short time period after coring. The test specimens can then be left to dry overnight, the dry weight can be measured the next day, and then they can be immediately prepared for testing.

9.8. *Replicates*—The number of test specimens required depends on the number of axial strain measurements made per specimen and the desired accuracy of the average dynamic modulus. Table 2 summarizes the replicate number of specimens that should be tested to obtain a desired accuracy limit (e.g., less than ± 15 percent of the true dynamic modulus).

Table 2—Recommended Number of Specimens

LVDTs per Specimen	Number of Specimens	Estimated Limit of Accuracy
2	2	± 18.0 %
2	3	± 15.0 %
2	4	± 13.4 %
3	2	± 13.1 %
3	3	± 12.0 %
3	4	± 11.5 %

9.9. **Sample Storage**—If test specimens will not be tested within two days, wrap specimens in polyethylene and store in an environmentally protected storage area at temperatures between 5 and 26.7°C (40 and 80°F).

Note 5—To eliminate effects of aging on test results, it is recommended that specimens be stored no more than two weeks prior to testing.

10. TEST SPECIMEN INSTRUMENTATION

10.1. Attach mounting studs for the axial LVDTs to the sides of the specimen with epoxy cement. Figure 3 shows details of the mounting studs and LVDT mounting hardware.

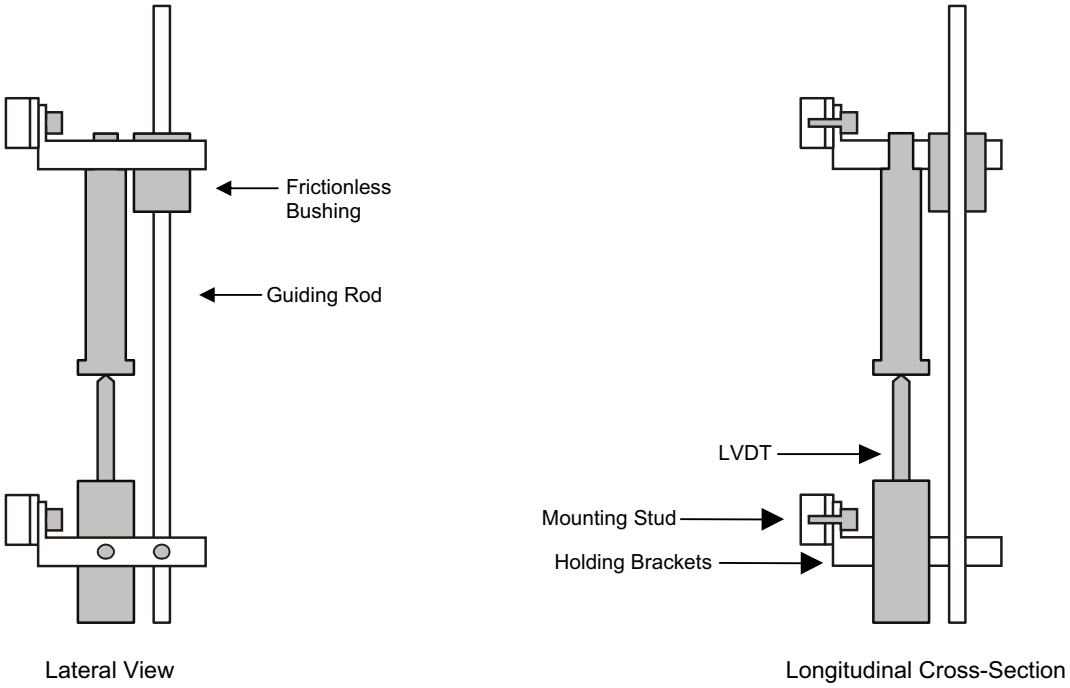

Figure 3—Mounting Hardware Details

Note 6—Quick setting epoxy such as Duro Master Mend Extra Strength Quick Set QM-50 has been found satisfactory for attaching studs.

10.2. The gauge length for measuring axial deformations shall be 101.6 mm ± 1 mm (4.00 in ± 0.04 in.). SuiTable alignment and spacing fixture shall be used to facilitate mounting of the axial deformation measuring hardware. The gauge length is measured between the stud centers.

11. PROCEDURE

11.1 The recommended test series for the development of master curves for use in pavement response and performance analysis consists of testing at –10, 4.4, 21.1, 37.8, and 54.4°C (14, 40, 70, 100, and 130°F) at loading frequencies of 0.1, 0.5, 1.0, 5, 10, an 25 Hz at each temperature. Each test specimen, individually instrumented with LVDT brackets, should be tested for each of the 30 combinations of temperature and frequency of loading starting with

the lowest temperature and proceeding to the highest. Testing at a given temperature should begin with the highest frequency of loading and proceed to the lowest.

11.2. Place the test specimen in the environmental chamber and allow it to equilibrate to the specified testing temperature ± 1°F. A dummy specimen with a thermocouple mounted at the center can be monitored to determine when the specimen reaches the specified test temperature. In the absence of the dummy specimen, minimum recommended equilibrium temperature times are provided as a guideline. Note that these guidelines/equilibrium times are recommended when testing 2 to 4 replicates at a time.

Table 3— Recommended Equilibrium Times

Specimen Temperature, °C (°F)	Time from Room Temperature, Hrs 25°C (77°F)	Time from Previous Test Temperature, Hrs
–10 (14)	Overnight	—
4.4 (40)	Overnight	4 hours or overnight
21.1 (70)	1	3
37.8 (100)	2	2
54.4 (130)	2	1

11.3. Place one of the friction reducing end treatments on top of the hardened steel disk at the bottom of the loading frame. Place the specimen on top of the lower end treatment, and mount the axial LVDTs to the hardware previously attached to the specimen. Adjust the LVDT to near the end of its linear range to allow the full range to be available for the accumulation of compressive permanent deformation.

11.4. Place the upper friction reducing end treatment and hardened steel disk on top of the specimen. Center the specimen with the hydraulic load actuator visually in order to avoid eccentric loading.

11.5. Apply a contact load (Pmin) equal to 5 percent of the dynamic load that will be applied to the specimen.

11.6. Adjust and balance the electronic measuring system as necessary.

11.7. Apply sinusoidal (haversine) loading ($P_{dynamic}$) to the specimen in a cyclic manner. The dynamic load should be adjusted to obtain axial strains between 50 and 150 microstrain.

Note 7—The dynamic load depends upon the specimen stiffness and generally ranges between 15 and 2800 kPa (2 and 400 psi). Higher load is needed at colder temperatures. Table 4 presents typical dynamic stress levels based on temperature.

Table 4—Typical Dynamic Stress Levels

Temperature, °C (°F)	Range, kPa	Range, psi
–10 (14)	1400–2800	200–400
4.4 (40)	700–1400	100–200
21.1 (70)	350–700	50–100
37.8 (100)	140–250	20–50
54.4 (130)	35–70	5–10

11.8. Test the specimens from lowest to highest temperature; that is from –10°C (14°F) to 54.4°C (130°F). At each temperature apply the loading from highest to lowest frequency; that is from

25 Hz to 0.1 Hz. At the beginning of testing, precondition the specimen with 200 cycles at 25 Hz at stress level corresponding to Table 4. Then load the specimen as specified in Table 5. A typical rest period between each frequency run is two minutes. This rest period shall not exceed 30 minutes for any two-frequency runs.

Table 5—Number of Cycles for the Test Sequence

Frequency (Hz)	Number of Cycles
25	200
10	200
5	100
1	20
0.5	15
0.1	15

11.9. It is recommended that the end of any testing series at each temperature period, if the cumulative un-recovered permanent strain was found to be greater than 1500 micro units of strain, reduce the maximum loading stress level to half. Keep the test data up to this last resting period, discard the specimen, and use a new specimen for the rest of testing periods under reduced load conditions.

12. CACULATIONS

12.1. Determine the average amplitude of the sinusoidal load from the load cell and deformation measured from each axial LVDT over the last five loading cycles for each test condition.

12.2. Determine the average lag time (t_l) between the peak load and the peak deformation from each LVDT over the last five loading cycles for each test condition.

Note 8—Different approaches are available to determine these. The approach is highly dependent upon the number of data points collected per cycle. Approaches that have been used include peak search algorithms, various curve fitting techniques, and Fourier Transform.

12.3. Over the last five loading cycles and for each test condition, calculate the loading stress, Φ_o, as follows:

$$\sigma_o = \frac{\overline{P}}{A} \quad (1)$$

Where:

P = average peak load,
A = area of specimen,
σ_o = average peak stress.

12.4. Over the last five loading cycles and for each test condition, calculate the recoverable axial strain individually for each LVDT, Φ_o, as follows:

$$\varepsilon_o = \frac{\overline{\Delta}}{GL} \quad (2)$$

Where:

$\overline{\Delta}$ = average peak deformation,
GL = gage length,
ε_o = average peak strain.

12.5. Over the last five loading cycles and for each test condition, calculate the dynamic modulus, |E*| individually for each LVDT as follows:

$$\text{Dynamic Modulus, } |E^*| = \frac{\sigma_0}{\varepsilon_0} \quad (3)$$

12.6. Over the last five loading cycles and for each test condition, calculate the phase angle individually for each LVDT:

$$\phi = \frac{t_i}{t_p} = *(360) \quad (4)$$

Where:

t_i = average lag time between a cycle of stress and strain (sec),
t_p = average time for a stress cycle (sec),
ϕ = phase angle (degree).

12.7. Calculate average dynamic modulus and phase angle from the results of each individual LVDT.

13. MASTER CURVE DEVELOPMENT

13.1. The mechanical behavior of viscoelastic materials such as asphalt mixtures is dependent on the temperature and time of load (frequency) at which the material is tested. In order to compare test results of various mixes, it is important to normalize one of these variables. Data collected at different temperatures can be "shifted" relative to the time of loading, so that the various curves can be aligned to form a single master curve.

13.2. The shift factor, a(T), defines the required shift (as log of time) at a given temperature, i.e., a constant by which the loading times must be divided to get a reduced time, tr, for the master curve:

$$t_r = \frac{t}{a(T)} \quad (5)$$

Where:

t_r = reduced time, time of loading at the reference temperature,
t = time of loading, the reciprocal of the loading frequency,
a(T) = shift factor as a function of temperature,

T = Temperature.

The master curve development can be found in numerous documents on pavement materials characterization. The concept is illustrated in Figure 4, which presents the shifting of laboratory measured dynamic modulus test data to the reference temperature T0 of 21.1°C (70°F). A sigmoidal fitting function is used to construct the master curve.

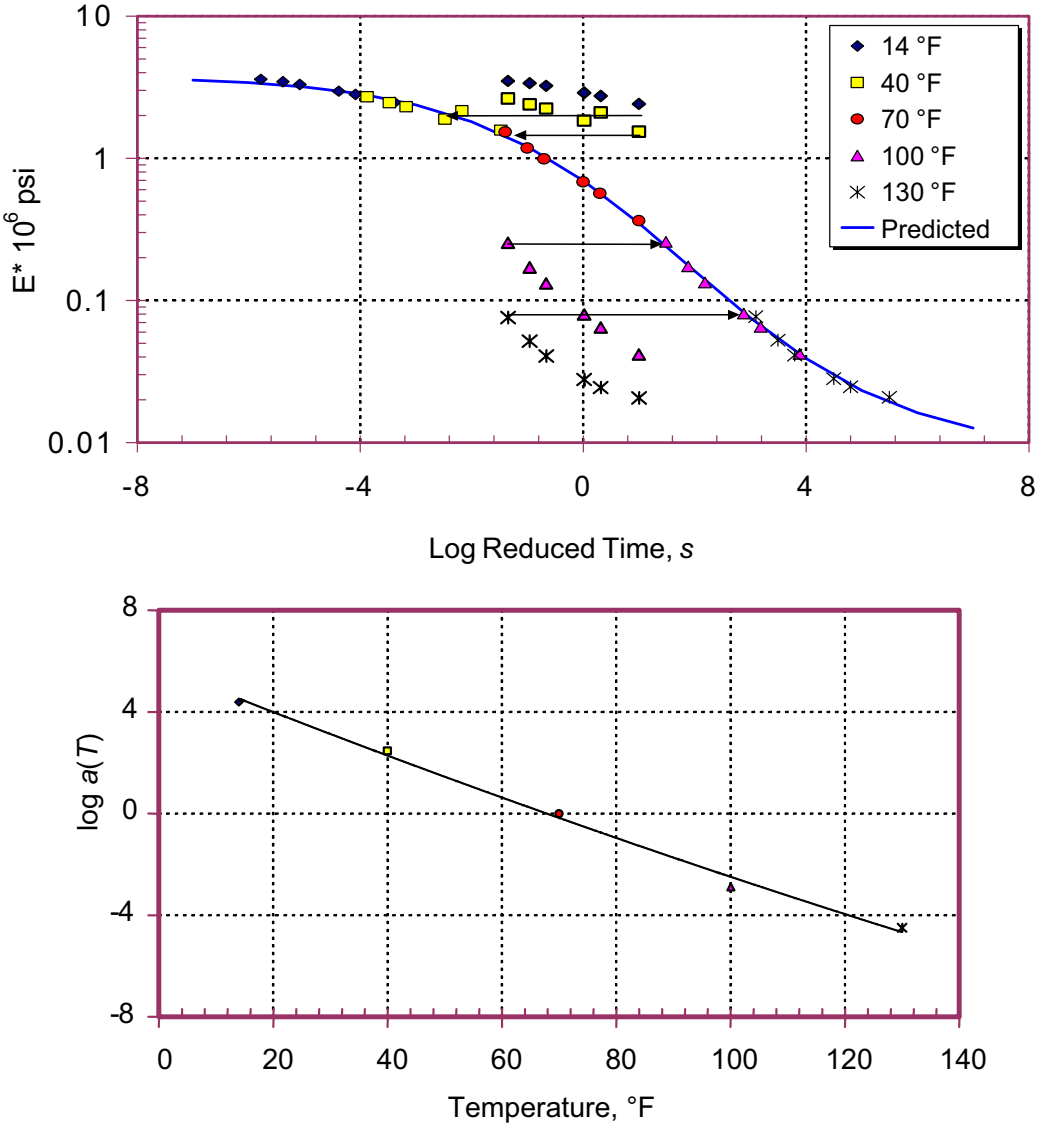

Figure 4—Example of Master Curve Construction

13.3. Using the shift factors, the master curve can be constructed using a selected reference temperature of 70°F to which all data are shifted.

13.4. Various computer programs can be used to define relationships with a(T) and temperature. One method is to use the numerical optimization (Solver) provided in the Microsoft Excel program.

13.5. Different functions are used to mathematically model the material response and create the master curve for asphalt mixtures. For time or frequency dependency, the generalized power law is most widely accepted at low to intermediate temperatures. As high temperature data is included, a polynomial and sigmoidal functions have been used. Caution should be exercised when employing polynomial fitting functions due to the polynomial swing in low and high temperatures, when extrapolating outside the range of data. The generalized power law and sigmoidal functions will approach asymptotically the limiting stiffness values, thus, allowing the prediction outside the measured range of data.

14. REPORT

14.1. For each individual LVDT report the dynamic modulus (|E*|) and phase angle (ϕ) for each temperature-frequency combination tested.

14.2. Report the average peak stress (Φ_o) and strain (ε_o) for each temperature-frequency combination tested per Section 12.1.

14.3. Report for each temperature-frequency combination tested, the dynamic modulus and phase angle for each replicate test specimen along with the average, standard deviation and coefficient of variation of the three replicates.

14.4. In addition, report the dynamic modulus replicate results in a format compatible with Table 6. This is the format of data entry required for the computer program "Asphalt Pavement Analysis and Design System" (APADS) that was developed under the 2002 Design Guide for the design of new and rehabilitated pavement structures.

14.5. Report the constructed master curve.

Table 6—Required Input Data for APADS 2002

Temperature, °F	Replicate	Mixture |E*|, psi (or MPa) at Frequency Noted					
		0.1	0.5	1	5	10	25
14	1						
	2						
	3						
	4						
40	1						
	2						
	3						
	4						
70	1						
	2						
	3						
	4						
100	1						
	2						
	3						
	4						
130	1						
	2						
	3						
	4						